
Lab Medicine

Relationship Between Gene Polymorphism of Methylenetetrahydrofolate Reductase C677T and Left Ventricular Hypertrophy in Chinese Patients with Chronic Kidney Disease

Xie Wu, MD,[1,2,#] Jing Lin, MD,[1,2,3,4,#] Ning Xue, MD,[1,3,4,#] Jie Teng, MD,[1,2,3,4] Yaqiong Wang, MD,[1,3,4] Yang Li, PhD,[1,2] Xunhui Xu, MD,[1,2] Ziyan Shen, MD,[1,3,4] Xiaoqiang Ding, MD,[1,2,3,4] Yi Fang, MD PhD,[1,2,3,4,]*

Laboratory Medicine 2021;52:519-527

DOI: 10.1093/labmed/lmab004

ABSTRACT

Objective: This study aimed to investigate the relationship between the gene polymorphism of methylenetetrahydrofolate reductase (*MTHFR*) C677T and left ventricular hypertrophy (LVH) in patients with chronic kidney disease (CKD).

Methods: A total of 763 Chinese patients with CKD undergoing genetic testing were included in the study. The association between the gene polymorphism of *MTHFR* C677T and echocardiographic parameters was analyzed through univariate and multivariate analyses.

Results: We found a remarkably positive association between *MTHFR* C677T gene polymorphism and LVH indexes, including interventricular septal thickness ($F = 3.8$; $P = .022$), left ventricular posterior wall thickness ($F = 3.0$; $P = .052$), left ventricular mass ($F = 3.9$; $P = .022$), and left ventricular mass index ($F = 2.6$; $P = .075$). After adjusting for the potential confounders linking the polymorphism,we found that the positive association between the polymorphism and LVH indexes still existed in patients with CKD in some multiple linear regression models ($P < .05$).

Conclusion: *MTHFR* C677T gene polymorphism may be a genetic susceptibility marker for the development of LVH in patients with CKD.

Keywords: methylenetetrahydrofolate reductase, gene polymorphism, homocysteine, left ventricular hypertrophy, chronic kidney disease

Abbreviations: *MTHFR,* methylenetetrahydrofolate reductase; LVH, left ventricular hypertrophy; CKD, chronic kidney disease; CVD, cardiovascular disease; HHcy, hyperhomocysteinemia; SAM, S-adenosyl methionine; SAH, S-adenosyl homocysteine; Hcy, homocysteine; LAD, inner diameter of left atrium; LVIDd, end-diastolic left ventricular internal dimension; LVPWT, left ventricular posterior wall thickness; AORD, inner diameter of aortic root; IVST, interventricular septal thickness; LVM, left ventricular mass; LVMI, left ventricular mass index; PCR, polymerase chain reaction; eGFR, estimated glomerular filtration rate.

[1]Department of Nephrology, Zhongshan Hospital, Fudan University, Shanghai, China, [2]Shanghai Key Laboratory of Kidney and Blood Purification, Zhongshan Hospital, Fudan University, Shanghai, China, [3]Shanghai Medical Center of Kidney Disease, Zhongshan Hospital, Fudan University, Shanghai, China, [4]Shanghai Institute of Kidney and Dialysis, Zhongshan Hospital, Fudan University, Shanghai, China

*To whom correspondence should be addressed.
fang.yi@zs-hospital.sh.cn

#These authors contributed equally to this work and should be considered as co-first authors on this work.

Cardiovascular disease (CVD) is the main cause of premature death in patients with chronic kidney disease (CKD),[1] a situation in which CKD and CVD are closely related. It is widely recognized that severe dysfunction in either the kidney or the heart seldom occurs in isolation.[2] Left ventricular hypertrophy (LVH), which is the most common cardiac abnormality, serves as a primary risk factor contributing to cardiovascular mortality in patients with CKD.[3, 4] In addition to these well-recognized traditional risk factors, hyperhomocysteinemia (HHcy), a novel cardiac risk factor, is regarded as an independent risk factor participating in the pathogenesis and development of CVD in patients with CKD.[5, 6]

Methylenetetrahydrofolate reductase (*MTHFR*) catalyzes the irreversible transition of 5,10-methylenetetrahydrofolate to 5-methyltetrahydrofolate, reduced S-adenosyl methionine

(SAM), increased S-adenosyl homocysteine (SAH), HHcy, and global DNA hypomethylation are observed in *MTHFR* knockout mice.[7] The gene polymorphism of *MTHFR* C677T is the most important genetic variation leading to HHcy; a C to T conversion at base pair 677 is the C677T polymorphism, which results in the amino acid conversion from Ala to Val and the subsequent decline of MTHFR activity.[8] Compared with the wild genotype (*MTHFR* 677CC genotype), the enzyme activity of the heterozygote (*MTHFR* 677CT genotype) and the mutation homozygote (*MTHFR* 677TT genotype) has been reported to decrease by 34% and 75%, respectively.[9] The total T allele frequency of the single nucleotide polymorphism was 45.2% in 15,357 healthy Chinese Han adults and 43.5% in 477 subjects from the southeastern province of Jiangsu in China.[10] Although many studies[11-17] have recently reported the relationship between *MTHFR* C677T gene polymorphism and the development of CVD, few studies[18-21] have focused on the relationship between *MTHFR* C677T gene polymorphism and LVH. In this study, the association between *MTHFR* C677T gene polymorphism and LVH was analyzed in hospitalized Chinese patients with CKD.

Materials and Methods

Study Population and Evaluation

The study was a cross-sectional survey approved by the clinical research ethical committee of Zhongshan Hospital, Fudan University, Shanghai, China (approval number: B2018-269). All procedures performed in studies involving human participants were in accordance with the Declaration of Helsinki, and all patients were provided informed consent. A total of 2522 patients with CKD who were admitted to the hospital from June 1, 2017, to June 1, 2019, were randomly recruited to this study, and 763 patients met the inclusion criterion and were free of the exclusion criteria. Patients enrolled were requested to have a routine test for the gene polymorphism of *MTHFR* C677T and plasma homocysteine (Hcy) level. The inclusion criterion was patients with CKD. The exclusion criteria included age ≥80 years or <18 years, acute kidney injury, a history of liver diseases, malignant tumor, active tuberculosis, acute infection or hemorrhage, a history of dialysis treatment, cardiac disease and CVD, difficulty cooperating with the requirements of the study, and refusal to participate. We defined CKD as abnormalities of the kidney structure or function, present for >3 months, with implications for health.[22] Patients with cardiac disease and CVD excluded from the study presented with any of the following: heart failure, arrhythmia, coronary heart disease, heart valve disease, cardiomyopathy, stroke, and peripheral artery disease.

Data on demographic characteristics and medical history were collected from electronic medical records. The potential confounders in the pathogenetic pathway linking the polymorphism with LVH, including a history of diabetes, hypertension, and hyperlipidemia, were collected along with age and sex. Conventional echocardiographic images of patients were obtained by an iE33 ultrasound machine (Philips Ultrasound, Andover, MA, USA) equipped with an S5-1 transducer (Philips Ultrasound, Andover, MA, USA). The inner diameter of left atrium (LAD), left ventricular ejection fraction, end-systolic left ventricular internal diameter, end-diastolic left ventricular internal dimension (LVIDd), left ventricular posterior wall thickness (LVPWT), inner diameter of aortic root (AORD), interventricular septal thickness (IVST), and pulmonary arterial systolic pressure were determined by an experienced echocardiologist. Left ventricular mass (LVM) and left ventricular mass index (LVMI) were calculated using the following formula: $LVM = 0.8 \times 1.04 \times \{(IVST + LVIDd + LVPWT)^3 - LVIDd^3\} + 0.6$ g, LVMI=LVM/ (height$^{2.7}$) g/m$^{2.7}$.[23]

Genetic Analysis

DNA Extraction, Polymerase Chain Reaction, and Chip Hybridization

The *MTHFR* C677T genotype was analyzed through polymerase chain reaction chip hybridization. Anticoagulated (EDTA) peripheral blood specimens were obtained via phlebotomy and stored at –20°C until extraction was completed. We extracted DNA from 200 μL of whole blood from patients using the DNA extraction and purification kit (BaiO, Shanghai, China) following manufacturer instructions. The DNA specimens were quantitated using the NanoDrop 1 spectrophotometer (Thermo Fisher Scientific, Waltham, MA).

We performed DNA amplification in a 25 μL volume containing 22 μL of *MTHFR* amplification solution, 1 μL of reaction solution A (*MTHFR* gene detection kit; BaiO), and 2 μL of DNA specimen. We performed PCR using a TC-XP PCR thermal cycler (BIOER, Hangzhou, China), following manufacturer instructions: 50°C, 5 minutes; 94°C, 5 minutes; 94°C, 25

seconds; denaturation, 56°C, 25 seconds; annealing, 72°C, 25 seconds; and extension, 35 cycles, 72°C, 5 minutes.

We performed chip hybridization with the hybridization kit (*MTHFR* gene detection kit; BaiO) using an automatic chip hybridization instrument (BaiO), following manufacturer instructions as follows: adding 10 μL reaction solution B to the hybridization buffer, then adding 190 μL hybridization buffer and 10 μL *MTHFR* amplification product to the corresponding position of the 8-strip tube, then respectively adding 200 μL of the antibody solution and 200 μL color-developing solution to the corresponding positions of the 8-strip tube, and respectively placing the 8-strip tube and the aldehyde-based chip into the corresponding positions of the automatic hybridization instrument to start hybridization.

We performed chip reading with a BE-2.0 biochip reader, gene chip image analysis software, and *MTHFR* genotyping software (BaiO), following manufacturer instructions; negative and positive control specimens were always used during the test.

Laboratory Assays

All tests were conducted in the hospital laboratory. Plasma total Hcy was measured by automatic biochemical analyzer (Hitachi 7600 P, Tokyo, Japan) using an enzymatic cycling method and homocysteine detection kit (DIASYS, Shanghai, China). Briefly, oxidized total Hcy was reduced to free Hcy. The free Hcy reacted with a cosubstrate, SAM, catalyzed by Hcy S-methyltransferase to form methionine and SAH. SAH was hydrolyzed into adenosine and Hcy by SAH-hydrolase. The formed Hcy was cycled into the Hcy conversion reaction by Hcy S-methyltransferase. The cycling reaction led to significant amplification of detection signals. The formed adenosine was immediately hydrolyzed into inosine and ammonia, which was processed by glutamate dehydrogenase with concomitant conversion of reduced nicotinamide adenine dinucleotide (NADH) to nicotinamide adenine dinucleotide (NAD+). The decrease in NADH was measured at 340 nm and was proportional to the homocysteine concentration in the specimen. Serum levels of creatinine and urea nitrogen were measured by the enzymatic method (Roche Cobas c702, Basel, Switzerland). The estimated glomerular filtration rate (eGFR) was calculated according to the CKD-Epidemiology Collaboration equation,[24] and CKD staging was based on the criteria of the kidney disease.[22]

Statistical Analyses

Values of continuous variables were expressed as mean ± SD. The age of the study population and the effect of *MTHFR* C677T polymorphism on renal function, plasma Hcy level, and echocardiographic parameters were analyzed by a 1-way analysis of variance test. Least-significant difference was adopted for pairwise comparisons between the TT, CT, and CC genotypes, and the ratio and genotype distribution for Hardy-Weinberg equilibrium were calculated using the χ^2 test. Taking LAD, IVST, LVPWT, LVM, and LVMI values as the dependent variables, we applied multiple linear regression to determine the relative importance of the C677T polymorphism with the potential confounders. In this analysis, the *MTHFR* genotype was designated by using a codominant model as follows: CC = 0, CT = 1, and TT = 2, respectively. Scatterplots were used to detect the correlation between the Hcy level and the values of LAD, IVST, LVPWT, LVM, and LVMI. A P value <.05 was considered significant. Statistical software (PAWS 18.0, SPSS, Chicago, IL), was adopted to analyze all data.

Results

Characteristics in Different *MTHFR* C677T Genotype Groups

There were 142 patients with two copies (*MTHFR* 677TT genotype) of the T allele, 351 with one copy (*MTHFR* 677CT genotype) of the T allele, and 270 with the wild-type allele (*MTHFR* 677CC genotype). The distribution of the *MTHFR* C677T genotype complied with the Hardy-Weinberg equilibrium (P >.05). **Table 1** showed that no significant difference was discovered between different genomic subgroups in terms of age, sex, eGFR, serum creatinine, urea nitrogen, hypertension, hyperlipidemia, and the proportion rate of CKD stage. However, the probability of diabetes was significantly different among different genotypes (χ^2 = 6.788; P =.034), and patients with the TT genotype had a higher probability of diabetes than those with the CT genotype and the CC genotype (26.1% vs 16.0%; 26.1% vs 18.5%; **Table 1**).

DOI: 10.1093/labmed/lmab004

Table 1. Demographic and Clinical Characteristics of Patients with CKD

	Total	TT Genotype	CT Genotype	CC Genotype	χ^2/F	*P* Value
	n = 763	n = 142	n = 351	n = 270		
Age, y	47.2 ± 14.8	45.8 ± 15.0	46.5 ± 14.5	48.9 ± 15.0	2.942	.053
Male, n (%)	436 (57.1)	94 (66.2)	192 (54.7)	150 (55.6)	5.886	.053
Hypertension, n (%)	457 (59.9)	96 (67.6)	200 (57.0)	161 (59.6)	4.764	.092
Diabetes, n (%)	143 (18.7)	37 (26.1)	56 (16.0)	50 (18.5)	6.788	.034
Hyperlipidemia, n (%)	73 (9.6)	17 (12.0)	30 (8.5)	26 (9.6)	1.372	.503
Total cholesterol (mmol/L)	5.4 ± 2.0	5.1 ± 1.9	5.4 ± 2.1	5.5 ± 2.1	1.245	.289
Triglycerides (mmol/L)	2.1 ± 1.6	2.0 ± 1.5	2.2 ± 1.6	2.1 ± 1.6	0.423	.655
Low-density lipoprotein (mmol/L)	3.3 ± 1.7	3.0 ± 1.6	3.3 ± 1.8	3.3 ± 1.8	1.085	.338
CKD stage 1, n (%)	205 (26.9)	40 (28.2)	93 (26.5)	72 (26.7)	0.153	.927
CKD stage 2, n (%)	179 (23.5)	24 (16.9)	86 (24.5)	69 (25.6)	4.274	.118
CKD stage 3a, n (%)	85 (11.1)	20 (14.1)	35 (10.0)	30 (11.1)	1.728	.421
CKD stage 3b, n (%)	85 (11.1)	16 (11.3)	44 (12.5)	25 (9.3)	1.658	.437
CKD stage 4, n (%)	85 (11.1)	19 (13.4)	40 (11.4)	26 (9.6)	1.365	.505
CKD stage 5, n (%)	124 (16.3)	23 (16.2)	53 (15.1)	48 (17.8)	0.805	.669
eGFR (mL/min/1.73 m^2)	60.6 ± 37.6	59.1 ± 38.0	60.9 ± 37.5	60.9 ± 37.5	0.140	.869
Serum creatinine (μmol/L)	202.1 ± 219.1	207.9 ± 207.7	199.7 ± 224.3	202.2 ± 218.7	0.071	.932
Serum urea nitrogen (mmol/L)	10.3 ± 7.8	10.5 ± 7.8	10.3 ± 7.7	10.2 ± 8.0	0.090	.914
Plasma Hcy (μmol/L)	20.3 ± 16.4	28.8 ± 25.0	19.4 ± 14.5	16.9 ± 10.7	27.063	<.001
Plasma vitamin B_{12} (pg/mL)	510.2 ± 297.9	495.5 ± 347.9	524.5 ± 335.4	503.3 ± 225.6	0.259	.772

CKD, chronic kidney disease; eGFR, estimated glomerular filtration rate; Hcy, homocysteine.

The Effect of *MTHFR* C677T Gene Polymorphism on Echocardiographic and LVH Indexes

The C677T polymorphism remarkably affected the values of LAD ($F = 4.8$; $P = .009$), IVST ($F = 3.8$; $P = .022$), LVPWT ($F = 3.0$; $P = .052$), LVM ($F = 3.9$; $P = .022$), and LVMI ($F = 2.6$; $P = .075$). Values of AORD (33.0 mm vs 32.2 mm; $P = .033$), LAD (37.7 mm vs 36.2 mm; $P = .002$), IVST (10.1 mm vs 9.7 mm; $P = .012$), LVPWT (9.8 mm vs 9.5 mm; $P = .041$), LVM (170.1 g vs 155.1 g; $P = .008$), and LVMI (42.5 g/$m^{2.7}$ vs 39.7 g/$m^{2.7}$; $P = .036$) in patients with the TT genotype were higher than in those with the CC genotype. The values of LAD (37.7 mm vs 36.6 mm; $P = .015$), IVST (10.1 mm vs 9.7 mm; $P = .011$), LVPWT (9.8 mm vs 9.4 mm; $P = .018$), LVM (170.1 g vs 157.0 g; $P = .016$), and LVMI (42.5 g/$m^{2.7}$ vs 39.9 g/$m^{2.7}$; $P = .038$) in patients with the TT genotype were also higher than in those with the CT genotype (**Table 2**).

Association Between *MTHFR* C677T Gene Polymorphism and Echocardiographic Values

After adjusting for several potential confounders including eGFR, sex, age, and history of hypertension and hyperlipidemia, we found that C677T polymorphism was significantly associated with the values of LAD (Model 1, $\beta = 0.104$, $P = .004$; Model 2, $\beta = 0.122$, $P < .001$; Model 3, $\beta = 0.114$, $P < .001$; Model 4, $\beta = 0.101$, $P = .001$), IVST (Model 1, $\beta = 0.080$, $P = .026$; Model 2, $\beta = 0.082$, $P = .016$; Model 3, $\beta = 0.072$, $P = .028$), LVM (Model 1, $\beta = 0.087$, $P = .016$; Model 2, $\beta = 0.078$, $P = .021$; Model 3, $\beta = 0.065$, $P = .039$), and LVMI (Model 2, $\beta = 0.083$, $P = .019$; Model 3, $\beta = 0.069$, $P = .035$; **Table 3**).

Correlation Analysis Between Hcy Level and Echocardiographic Values

Patients with the TT genotype had a higher plasma Hcy level compared with those with the CT or CC genotypes (28.8 μmol/L vs 19.4 μmol/L, $P < .001$; 28.8 vs 16.9 μmol/L, $P < .001$; **Table 1**). A previous article[25] reported that the level of plasma Hcy was remarkably higher in patients with CKD than in healthy patients, especially in end-stage renal disease, the Hcy level in patients with LVH was increased, and there was a positive association between LVM value and Hcy level in patients with CKD.[26] As shown in **Figure 1**, we identified a positive correlation between Hcy level and the values of LAD ($r = 0.131$; $P < .001$), IVST ($r = 0.191$; $P < .001$), LVPWT ($r = 0.197$; $P < .001$), LVM ($r = 0.231$; $P < .001$), and LVMI ($r = 0.214$; $P < .001$).

Discussion

The main finding of this study was that the gene polymorphism of *MTHFR* C677T was associated with LVH indexes (LVMI, LVM, IVST, and LVPWT) in patients with CKD. The C677T polymorphism seemed to increase the risk of the development of LVH independent of renal function.

In our study, patients with CKD with the TT genotype had higher IVST, LVPWT, LVM, and LVMI values than those with the CT and CC genotypes, which was similar to the results in Turkish patients with type II diabetes,[19] of whom patients with the TT genotype had a higher prevalence of LVH than patients with the CT and CC genotypes. However, most studies have not found an association between *MTHFR* C677T gene polymorphism and LVH,[20, 21] and some have even found the opposite effect.[18] For example, Maura et al.[20] reported that the prevalence of LVH was not different among different *MTHFR* C677T genotypes in Italian primary hypertension groups. In Italian patients without diabetes, Trovato et al[18] found that the *MTHFR* C677T gene polymorphism contributed to a lower probability of LVH. Obineche et al[21] found that the *MTHFR* C677T gene polymorphism was not a risk factor for LVH among patients from the United Arab Emirates.

From **Table 1**, we can see that the proportion of male patients with the TT genotype was relatively high, but in the multivariate analysis (**Table 3**), after adjusting for age and sex factors, *MTHFR* C677T was still correlated with LVH indexes; therefore, the effect of *MTHFR* C677T on LVH indexes was independent of age and sex. Our study also showed that patients with CKD with the TT genotype had a higher rate of diabetes compared with those with the CT and CC genotypes, which was consistent with the research of Zhu, Wu, et al [8] in a Han Chinese population. Those authors found that the *MTHFR* C677T gene polymorphism was significantly associated with type II diabetes in a random-effects model. In the multivariate analysis of our study, because of the significant correlation between

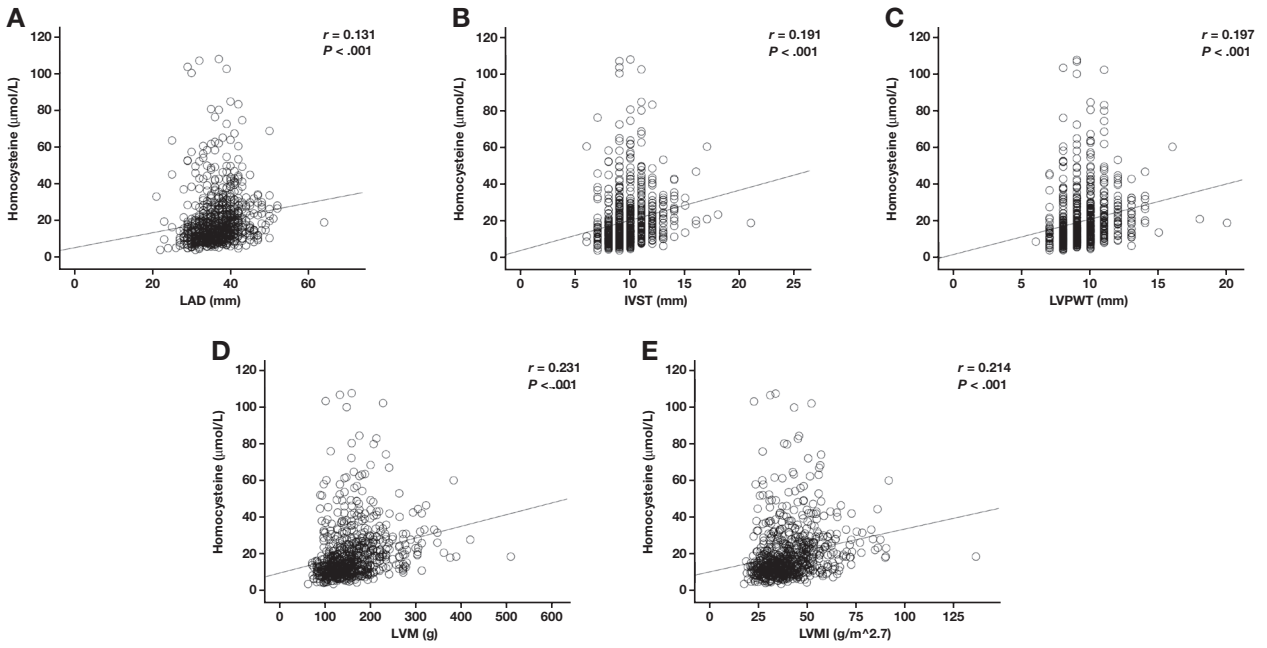

Figure 1

Correlation analysis between plasma Hcy level and the values of echocardiographic parameters. **A,** Correlation between plasma Hcy level and LAD ($r = 0.131$; $P < .001$); plasma Hcy level was expressed as micromolar per liter concentration. **B,** Correlation between plasma Hcy level and IVST ($r = 0.191$; $P < .001$). **C,** Correlation between plasma Hcy level and LVPWT ($r = 0.197$; $P < .001$). **D,** Correlation between plasma Hcy level and LVM ($r = 0.231$; $P < .001$); LVM was expressed in grams. **E,** Correlation between plasma Hcy level and LVMI ($r = 0.214$; $P < .001$); LVMI was expressed as gram per meter raised to the power of 2.7. Hcy, homocysteine; IVST, interventricular septal thickness; LAD, inner diameter of left atrium; LVM, left ventricular mass; LVMI, left ventricular mass index; LVPWT, left ventricular posterior wall thickness.

Lab Medicine 2021;52;519–527
DOI: 10.1093/labmed/lmab004

Table 2. Analysis of Echocardiographic and LVH Indexes in Different *MTHFR* C677T Genotype Groups

	TT Genotype (n = 142)	CT Genotype (n = 351)	CC Genotype (n = 270)	*P* Value
AORD (mm)	33.0 ± 3.6	32.4 ± 3.3	32.2 ± 3.5	.101
LAD (mm)	37.7 ± 5.3	36.6 ± 4.9	36.2 ± 4.7	.009
IVST (mm)	10.1 ± 2.0	9.7 ± 1.7	9.7 ± 1.6	.022
LVPWT (mm)	9.8 ± 1.8	9.4 ± 1.5	9.5 ± 1.4	.052
LVM (g)	170.1 ± 64.6	157.0 ± 54.2	155.1 ± 48.7	.022
LVMI ($g/m^{2.7}$)	42.5 ± 16.3	39.9 ± 12.8	39.7 ± 11.0	.075
LVIDs (mm)	30.0 ± 4.3	29.5 ± 3.5	29.3 ± 3.4	.189
LVIDd (mm)	47.0 ± 5.2	46.6 ± 4.5	46.2 ± 4.4	.223
LVEF (%)	65.6 ± 5.7	66.1 ± 4.1	66.2 ± 4.2	.413
PASP (mm Hg)	32.4 ± 5.1	32.0 ± 4.8	32.1 ± 4.8	.793

AORD, aortic root inside diameter; IVST, interventricular septal thickness; LAD, left atrial diameter; LVEF, left ventricular ejection fraction; LVH, left ventricular hypertrophy; LVIDd, end-diastolic left ventricular internal dimension; LVIDs, end-systolic left ventricular internal diameter; LVM, left ventricular mass; LVMI, left ventricular mass index; LVPWT, left ventricular posterior wall thickness; MTHFR, *methylenetetrahydrofolate reductase; PASP, pulmonary arterial systolic pressure.*

Table 3. Comparison of *MTHFR* C677T Gene Polymorphism for Role in LAD, IVST, LVPWT, LVM, and LVMI Values Based on Multiple Regression Analysis

	LAD		IVST		LVPWT		LVM		LVMI	
	β	*P*	β	*P*	β	*P*	β	*P*	β	*P*
Model 1	0.104	.004	0.080	.026	0.062	.088	0.087	.016	0.067	.064
Model 2	0.122	<.001	0.082	.016	0.060	.079	0.078	.021	0.083	.019
Model 3	0.114	<.001	0.072	.028	0.050	.131	0.065	.039	0.069	.035
Model 4	0.101	.001	0.055	.080	0.034	.283	0.050	.102	0.054	.088

eGFR, estimated glomerular filtration rate; IVST, interventricular septal thickness; LAD, left atrial diameter; LVM, left ventricular mass; LVMI, left ventricular mass index; LVPWT, left ventricular posterior wall thickness; MTHFR, *methylenetetrahydrofolate reductase.*
MTHFR *genotypes were designated by using a codominant model as follows: CC = 0, CT = 1, and TT = 2, respectively. Sex was defined as female: 0, male: 1. The history of hypertension or hyperlipidemia was defined as no: 0 and yes: 1. Variables of Model 1 included* MTHFR *genotype. Variables of Model 2 included* MTHFR *genotype, sex, and age. Variables of Model 3 included* MTHFR *genotype, sex, age, and eGFR. Variables of Model 4 included* MTHFR *genotype, sex, age, eGFR, and history of hypertension and hyperlipidemia.*

the *MTHFR* C677T gene polymorphism and the history of diabetes in patients with CKD and considering that collinearity between the 2 factors may be quite strong, we did not include the history of diabetes as an independent variable for analyzing.

Many studies[27-29] have reported the relationship between Hcy and ventricular hypertrophy to be that through damaged myocardial contractile function, oxidative reaction, and changed mitochondrial permeability, Hcy promotes myocardial fibrosis and hypertrophy induced by hypertension and can activate sympathetic nerves and aggravate myocardial hypertrophy.[27] Moreover, Hcy has direct detrimental effects on cardiac structure and function, which may represent a direct relationship between HHcy and LVH, regardless of other risk factors, such as hypertension. A latent mechanism for the cardiac remodeling triggered by HHcy may be attributed to the recruitment of inflammatory cells and an excessive immune response, resulting in cell death, cardiac fibrosis, or myocyte hypertrophy.[28] In addition, Hcy can promote adenosine triphosphate 7a protein expression, lower the copper content, and reduce Cytochrome C oxidase (COX) activity, finally resulting in cardiac hypertrophy.[29] Similarly, in our study, a positive relationship between Hcy level and the values of echocardiographic indexes was found; therefore, we speculated that the effect of *MTHFR* C677T gene polymorphism on LVH in this study could be partially caused by elevated Hcy.

Studies have also shown *MTHFR* C677T to be associated with essential hypertension,[30] which in turn can cause LVH; in our study, the demographics data (**Table 1**) showed that the rate of hypertension in patients with CKD with the TT genotype was relatively high, but it did not reach statistical significance. In patients with CKD, blood pressure levels are often elevated, the prevalence of hypertension and LVH increases with kidney disease progression, and CKD is one of the most important causes of secondary hypertension[31, 32];

the hypertension in these patients is mainly caused by water and sodium retention secondary to the long-term decline of kidney function. These conditions may have masked the effect of *MTHFR* C677T on blood pressure in our patients with CKD. Therefore, the hypertension in our study population may have been caused primarily by worsening kidney function rather than genetic polymorphism.

In addition, the rate of hypertension in our patients with CKD was 59.9% (457 patients; **Table 1**). To avoid the influence of cardiac disease and CVD on cardiac structure and function, we had excluded patients with these diseases; if hypertension was still listed as an exclusion criterion, then there would be too small of a sample size to maintain enough statistical power. Therefore, we enrolled those patients with hypertension without cardiac disease and CVD. The multivariate regression analysis (**Table 3**), adjusting for the history of hypertension that attenuated the relationship of *MTHFR* C677T to LVH indexes, suggested that this relationship seems to be partially mediated by hypertension. Finally, the view that diabetes was closely linked to LVH has been widely recognized,[33, 34] and there has been a significant relationship between Hcy and insulin resistance.[35, 36] Therefore, in patients with CKD, through HHcy, *MTHFR* C677T gene polymorphism could also be linked to a high probability of diabetes,[8,37] thereby affecting the structure and function of the left ventricle to some extent.

Apart from the positive association between the TT genotype of *MTHFR* C677T polymorphism and LVH, patients with CKD with the TT genotype had a higher value in LAD and in AORD. Similar to LVH, the left atrium enlargement could be also regarded as a marker of cardiac structure remodeling,[38, 39] and the increase in LAD in this study may have been associated with LVH.[40,41] Moreover, the high probability of diabetes may also play a role in the pathogenesis of left atrium dilatation in patients with the TT genotype.[42] The size of a normal aortic root is controversial, and the pathogenesis of aortic root dilatation is unclear.[43] An enlarged AORD in our patients with CKD was presumed to be the consequence of decreased cardiac diastolic function,[44] which may also be secondary to the development of LVH. Published literature[38, 43] has reported that increased LAD and AORD, along with LVH, could be used as predictors of cardiovascular events and poor prognosis.

The main differences between our study and other studies about the association of *MTHFR* C677T gene polymorphism with LVH were as follows. First, the sample size of our study was relatively larger. After screening for inclusion and exclusion criteria, we identified a total of 763 qualified patients with CKD; the number of enrolled patients may be much larger than those of other related studies.[18-21] Second, the patients in our study were patients with CKD. Published literature[45, 46] has reported that the TT genotype may account for a 40% to 100% increase in Hcy in patients with CKD, whereas in patients with normal renal function, the TT genotype only contributed to a 25% increase in Hcy level. The polymorphism seemed to play a more important role in the CKD population. In addition, because Turkish peoples[19] are descended from populations whose genetic traits are closer to those of central Asian peoples, the mutation may have ethnic discrepancy, and its effect may be stronger in Asian populations.[47, 48] For these reasons, it may be easier to identify the statistical differences between the *MTHFR* C677T polymorphism and LVH in a Chinese cohort with CKD.

Our study had some limitations: First, Hcy was dependent on dietary habits, but the serum levels of folate and vitamins B_{12} and B_6 in our patients were not acknowledged. Second, other genetic polymorphisms affecting folate and the methionine cycle such as *MTHFR* A1298C, methionine synthase A2756G, and methionine synthase reductase A66G[49] were not introduced in this study, leaving the genetic factors affecting the Hcy level not well controlled, which could affect our interpretation of the results of this study. Moreover, in addition to the Hcy level, the results may have other potential explanations such as study design and gene-specific methylations; further study will be needed to validate this hypothesis. Finally, because the study population had CKD, the results of this study may not be generalizable to the general population; confirmation in the general population would be helpful.

Conclusion

In conclusion, we suggest that *MTHFR* C677T gene polymorphism may be a genetic susceptibility marker for LVH in Chinese patients with CKD and that treatment to reduce plasma Hcy may contribute to delaying the development of LVH in these patients. **LM**

Lab Medicine 2021;52;519–527
DOI: 10.1093/labmed/lmab004

Acknowledgments

We thank the patients for their participation in the study. JL, YF, XW, NX, and YQW contributed to the study design. Data were collected by XHX. YL performed data analysis. XW and NX drafted the manuscript. JL, YF, JT, ZYS, and XQD edited the manuscript.

This work was supported by the Shanghai Municipal Commission of Health and Family Planning (2017ZZ01015, the project of Shanghai Clinical Medical Center), the Science and Technology Commission of Shanghai Municipality (14DZ2260200), and the project of Shanghai Key Laboratory of Kidney and Blood Purification (18411960800).

References

1. Fujii H, Kono K, Nishi S. Characteristics of coronary artery disease in chronic kidney disease. *Clin Exp Nephrol.* 2019;23(6):725–732.
2. Liu M, Li XC, Lu L, et al. Cardiovascular disease and its relationship with chronic kidney disease. *Eur Rev Med Pharmacol Sci.* 2014;18(19):2918–2926.
3. Leifheit-Nestler M, Große Siemer R, Flasbart K, et al. Induction of cardiac FGF23/FGFR4 expression is associated with left ventricular hypertrophy in patients with chronic kidney disease. *Nephrol Dial Transplant.* 2016; 31(7):1088–1099.
4. Gutiérrez OM, Januzzi JL, Isakova T, et al. Fibroblast growth factor 23 and left ventricular hypertrophy in chronic kidney disease. *Circulation.* 2009;119(19):2545–2552.
5. Harjai KJ. Potential new cardiovascular risk factors: left ventricular hypertrophy, homocysteine, lipoprotein(a), triglycerides, oxidative stress, and fibrinogen. *Ann Intern Med.* 1999;131(5):376–386.
6. Cianciolo G, De Pascalis A, Di Lullo L, Ronco C, Zannini C, La Manna G. Folic acid and homocysteine in chronic kidney disease and cardiovascular disease progression: which comes first? *Cardiorenal Med.* 2017;7(4):255–266.
7. Chen Z, Karaplis AC, Ackerman SL, et al. Mice deficient in methylenetetrahydrofolate reductase exhibit hyperhomocysteinemia and decreased methylation capacity, with neuropathology and aortic lipid deposition. *Hum Mol Genet.* 2001;10(5):433–443.
8. Zhu B, Wu X, Zhi X, Liu L, Zheng Q, Sun G. Methylenetetrahydrofolate reductase C677T polymorphism and type 2 diabetes mellitus in Chinese population: a meta-analysis of 29 case-control studies. *PLoS One.* 2014;9(7):e102443.
9. Wan L, Li Y, Zhang Z, Sun Z, He Y, Li R. Methylenetetrahydrofolate reductase and psychiatric diseases. *Transl Psychiatry.* 2018;8(1):242.
10. Yang B, Liu Y, Li Y, et al. Geographical distribution of MTHFR C677T, A1298C and MTRR A66G gene polymorphisms in China: findings from 15,357 adults of Han nationality. *PLoS One.* 2013;8(3):e57917.
11. Gao XH, Zhang GY, Wang Y, Zhang HY. Correlations of MTHFR 677C>T polymorphism with cardiovascular disease in patients with end-stage renal disease: a meta-analysis. *PLoS One.* 2014;9(7):e102323.
12. Morimoto K, Haneda T, Okamoto K, Ishida H, Kikuchi K. Methylenetetrahydrofolate reductase gene polymorphism, hyperhomocysteinemia, and cardiovascular diseases in chronic hemodialysis patients. *Nephron.* 2002;90(1):43–50.
13. Haviv YS, Shpichinetsky V, Goldschmidt N, Atta IA, Ben-Yehuda A, Friedman G. The common mutations C677T and A1298C in the human methylenetetrahydrofolate reductase gene are associated with hyperhomocysteinemia and cardiovascular disease in hemodialysis patients. *Nephron.* 2002;92(1):120–126.
14. Çetintaş VB, Gündüz C. Association between polymorphism of MTHFR c.677C>T and risk of cardiovascular disease in Turkish population: a meta-analysis for 2.780 cases and 3.022 controls. *Mol Biol Rep.* 2014; 41(1):397–409.
15. Wrone EM, Zehnder JL, Hornberger JM, McCann LM, Coplon NS, Fortmann SP. An MTHFR variant, homocysteine, and cardiovascular comorbidity in renal disease. *Kidney Int.* 2001;60(3):1106–1113.
16. Alam MA, Husain SA, Narang R, Chauhan SS, Kabra M, Vasisht S. Association of polymorphism in the thermolabile 5,10-methylene tetrahydrofolate reductase gene and hyperhomocysteinemia with coronary artery disease. *Mol Cell Biochem.* 2008;310(1-2):111–117.
17. Yang Q, Bailey L, Clarke R, et al. Prospective study of methylenetetrahydrofolate reductase (MTHFR) variant C677T and risk of all-cause and cardiovascular disease mortality among 6000 US adults. *Am J Clin Nutr.* 2012;95(5):1245–1253.
18. Trovato GM, Catalano D, Ragusa A, et al. Renal insufficiency in non-diabetic subjects: relationship of MTHFR C677t gene polymorphism and left ventricular hypertrophy. *Ren Fail.* 2013;35(5):615–623.
19. Yilmaz H, Agachan B, Ergen A, Karaalib ZE, Isbir T. Methylene tetrahydrofolate reductase C677T mutation and left ventricular hypertrophy in Turkish patients with type II diabetes mellitus. *J Biochem Mol Biol.* 2004;37(2):234–238.
20. Maura R, Francesca V, Valeria B, et al. 5,10-methylenetetrahydrof olate reductase polymorphism and early organ damage in primary hypertension. *Am J Hypertens.* 2001;14(4 Pt 1):371–376.
21. Obineche EN, Frossard PM, Bokhari AM. An association study of five genetic loci and left ventricular hypertrophy amongst Gulf Arabs. *Hypertens Res.* 2001;24(6):635–639.
22. Stevens PE, Levin A. Evaluation and management of chronic kidney disease: synopsis of the kidney disease: improving global outcomes 2012 clinical practice guideline. *Ann Intern Med.* 2013;158(11):825–830.
23. Zhang W, Zhou Y, Bai B, et al. Consistency of left ventricular hypertrophy diagnosed by electrocardiography and echocardiography: the Northern Shanghai Study. *Clin Interv Aging.* 2019;14:549–556.
24. Levey AS, Stevens LA, Schmid CH, et al.; CKD-EPI (Chronic Kidney Disease Epidemiology Collaboration). A new equation to estimate glomerular filtration rate. *Ann Intern Med.* 2009;150(9):604–612.
25. Wu CC, Zheng CM, Lin YF, Lo L, Liao MT, Lu KC. Role of homocysteine in end-stage renal disease. *Clin Biochem.* 2012;45(16-17):1286–1294.
26. Chien SJ, Lin IC, Hsu CN, Lo MH, Tain YL. Homocysteine and arginine-to-asymmetric dimethylarginine ratio associated with blood pressure abnormalities in children with early chronic kidney disease. *Circ J.* 2015;79(9):2031–2037.
27. Lin BY, Li P, Wu XD, Li H, Zeng ZY. The relationship between homocysteine, blood pressure variability, and left ventricular hypertrophy in patients with essential hypertension: an observational study. *Adv Ther.* 2020;37(1):381–389.
28. Joseph J, Joseph L, Shekhawat NS, et al. Hyperhomocysteinemia leads to pathological ventricular hypertrophy in normotensive rats. *Am J Physiol Heart Circ Physiol.* 2003;285(2):H679–H686.
29. Cao Z, Zhang Y, Sun T, Zhang S, Yu W, Zhu J. Homocysteine induces cardiac hypertrophy by up-regulating ATP7a expression. *Int J Clin Exp Pathol.* 2015;8(10):12829–12836.
30. Wu YL, Hu CY, Lu SS, et al. Association between methylenetetrahydrofolate reductase (MTHFR) C677T/A1298C polymorphisms and essential hypertension: a systematic review and meta-analysis. *Metabolism.* 2014;63(12):1503–1511.

31. Václav M. Hypertension and chronic kidney diseases. *Cor Et Vasa*. 2013;55(4):e397–e402.
32. Middleton RJ, Parfrey PS, Foley RN. Left ventricular hypertrophy in the renal patient. *J Am Soc Nephrol.* 2001;12(5):1079–1084.
33. Derosa G, Maffioli P. Assessment and management of left ventricular hypertrophy in type 2 diabetes patients with high blood pressure. *Expert Rev Cardiovasc Ther.* 2013;11(6):719–728.
34. Szwejkowski BR, Gandy SJ, Rekhraj S, et al. Allopurinol reduces left ventricular mass in patients with type 2 diabetes and left ventricular hypertrophy. *J Am Coll Cardiol.* 2013;62(24):2284–2293.
35. Zhang SY, Dong YQ, Wang P, et al. Adipocyte-derived lysophosphatidylcholine activates adipocyte and adipose tissue macrophage nod-like receptor protein 3 inflammasomes mediating homocysteine-induced insulin resistance. *EBioMedicine.* 2018;31:202–216.
36. Ala OA, Akintunde AA, Ikem RT, Kolawole BA, Ala OO, Adedeji TA. Association between insulin resistance and total plasma homocysteine levels in type 2 diabetes mellitus patients in south west Nigeria. *Diabetes Metab Syndr.* 2017;11 Suppl 2:S803–S809.
37. Al-Rubeaan K, Siddiqui K, Saeb AT, Nazir N, Al-Naqeb D, Al-Qasim S. ACE I/D and MTHFR C677T polymorphisms are significantly associated with type 2 diabetes in Arab ethnicity: a meta-analysis. *Gene.* 2013;520(2):166–177.
38. Zhu N, Chen H, Zhao X, Ye F, Jiang W, Wang Y. Left atrial diameter in heart failure with left ventricular preserved, mid-range, and reduced ejection fraction. *Medicine (Baltimore).* 2019;98(48):e18146.
39. de Cleva R, Araujo VA, Buchalla CCO, et al. Cardiac remodeling patterns in severe obesity according to arterial hypertension grade. *Obes Surg.* 2018;28(4):1047–1054.
40. Beach JM, Mihaljevic T, Rajeswaran J, et al. Ventricular hypertrophy and left atrial dilatation persist and are associated with reduced survival after valve replacement for aortic stenosis. *J Thorac Cardiovasc Surg.* 2014;147(1):362–369.e8.
41. Benjamin EJ, D'Agostino RB, Belanger AJ, Wolf PA, Levy D. Left atrial size and the risk of stroke and death. The Framingham Heart Study. *Circulation.* 1995;92(4):835–841.
42. Polovina MM, Coats A, Seferovic P. Is left atrium the best kept secret of the heart? Left atrial dilatation and cardiovascular outcomes. *Heart.* 2019;105(24):1848–1849.
43. Mulé G, Nardi E, Morreale M, et al. Relationship between aortic root size and glomerular filtration rate in hypertensive patients. *J Hypertens.* 2016;34(3):495–504.
44. Green D, Vassallo D, Handley K, et al. Cardiac structure and function after revascularization versus medical therapy for renal artery stenosis: the ASTRAL heart echocardiographic sub-study. *BMC Nephrol.* 2019;20(1):220.
45. Brattström L, Wilcken DE, Ohrvik J, Brudin L. Common methylenetetrahydrofolate reductase gene mutation leads to hyperhomocysteinemia but not to vascular disease: the result of a meta-analysis. *Circulation.* 1998;98(23):2520–2526.
46. Kimura H, Gejyo F, Suzuki S, Miyazaki R. The C677T methylenetetrahydrofolate reductase gene mutation in hemodialysis patients. *J Am Soc Nephrol.* 2000;11(5):885–893.
47. Balta G, Gurgey A, Kudayarov DK, Tunc B, Altay C. Evidence for the existence of the PAF acetylhydrolase mutation (Val279Phe) in non-Japanese populations: a preliminary study in Turkey, Azerbaijan, and Kyrgyzstan. *Thromb Res.* 2001;101(4):231–234.
48. Chen D, Wang J, Dan Z, Shen X, Ci D. The relationship between methylenetetrahydrofolate reductase C677T polymorphism and diabetic retinopathy: a meta-analysis in multiethnic groups. *Ophthalmic Genet.* 2018;39(2):200–207.
49. Hishida A, Okada R, Guang Y, et al. MTHFR, MTR and MTRR polymorphisms and risk of chronic kidney disease in Japanese: cross-sectional data from the J-MICC Study. *Int Urol Nephrol.* 2013;45(6):1613–1620.

DOI: 10.1093/labmed/lmab004

Cell-Derived Microparticles in Blood Products from Blood Donors Deficient in Glucose-6-Phosphate Dehydrogenase

Egarit Noulsri, PhD,[1,*] *Surada Lerdwana, BSc,*[2] *Duangdao Palasuwan, PhD,*[3] *Attakorn Palasuwan, PhD*[3]

Laboratory Medicine 2021;52:528-535

DOI: 10.1093/labmed/lmab007

ABSTRACT

Objective: To quantitate the microparticles (MPs) in whole blood and blood products obtained from blood donors who are deficient in glucose-6-phosphate dehydrogenase (G6PD).

Methods: The current study analyzed whole blood and blood components prepared from 49 blood donors with G6PD deficiencies and 98 with G6PD-normal results. Packed red blood cells (PRBCs), platelet concentrate (PC), and plasma were prepared according to transfusion laboratory procedures. MP concentrations were determined using a flow cytometer.

Results: Blood components prepared from donors with G6PD deficiency were characterized by higher red blood cell-derived MP (RMP) concentration in PRBCs (25,526 vs 18,738 particles/μL) but lower concentrations of platelet-derived MPs (PMPs; in whole blood and PC), leukocyte-derived MPs (LMP; in whole blood and plasma) and total MP (in PC), compared with those from donors with G6PD-normal test results.

Conclusions: These results suggest that differences in G6PD status may account for variation in RMP levels during processing.

Keywords: transfusion, blood donor, G6PD deficiency, packed red blood cells, microparticle, flow cytometry

Abbreviations:

MPs, microparticles; TF, tissue factor; PS, phosphatidylserine; TRALI, transfusion-related acute lung injury; PMPs, platelet-derived microparticles; PRBC, packed red blood cells; PC, platelet concentrate; FFP, fresh frozen plasma; G6PD, glucose-6-phosphate dehydrogenase; RBCs, red blood cells; RMPs, red blood cell-derived MPs; Annexin V-FITC, fluorescein isothiocyanate-conjugated annexin V; CD235a-PE, phycoerythrin-conjugated CD235a; CD45-PerCP, peridinin chlorophyll-conjugated CD45; CD41a-APC, allophycocyanin-conjugated CD41a; CBCs, complete blood counts; SAGM, saline-adenine-glucose-mannitol solution; PBS, phosphate-buffered saline; FSC, forward scatter; SSC, side scatter; FL, fluorescent parameter; NADPH, nicotinamide adenine dinucleotide phosphate; MCV, mean corpuscular volume; CV, coefficient of variation; Hb, hemoglobin; Hct, hematocrit; MCH, mean corpuscular hemoglobin; MCHC, mean corpuscular hemoglobin concentration; RDW, red blood cell distribution width.

[1]Research Division and [2]Biomedical Research Incubator Unit, Faculty of Medicine Siriraj Hospital, Mahidol University, Bangkok, Thailand
[3]Oxidation in Red Cell Disorders and Health Task Force, Department of Clinical Microscopy, Faculty of Allied Health Sciences, Chulalongkorn University, Bangkok, Thailand

*To whom correspondence should be addressed.
egarit.nou@mahidol.ac.th

Microparticles (MPs) are heterogeneous groups of small extracellular vesicles, ranging from 0.1 μm to 1 μm in size.[1] MPs can be released from various cells on activation, on undergoing apoptosis, or under certain types of stress.[2,3] Certain study results[4,5] have suggested that the cellular mechanism governing MP shedding involves the influx of intracellular calcium and proteolytic cleavage of the cytoskeleton. We note that released MPs show procoagulant activity due to the expression of tissue factor (TF) and phosphatidylserine (PS) on their surface membranes.[6,7] In transfusion medicine, study results[8–11] have suggested that transfusion of blood products containing high concentrations of MPs might increase the risk of thrombosis complications and transfusion-related acute lung injury (TRALI). Given the potential association of MPs with post-transfusion complications, more studies are needed to address the factors contributing to changes in the MP levels of blood products.

Several factors have been suggested as being associated with these changes. Noulsri et al[12] quantitated platelet-derived MPs in platelet components prepared using buffy coat, platelet-rich

plasma, and apheresis. The results showed high variability in the concentration of platelet-derived MPs (PMPs) in platelet products prepared using different approaches, suggesting an effect of blood-component processing on MP release. The examination of MP concentrations in packed red blood cells (PRBCs), platelet concentrate (PC), and fresh frozen plasma (FFP) has also supported the effects of blood-component processing, storage, and donor factors on MP release.[13] Regarding transfusion donors, individuals deficient in glucose-6-phosphate dehydrogenase (G6PD) and without a history of hemolysis may be eligible for blood donation.[14] Study findings[15,16] have shown the ability of G6PD-deficient red blood cells (RBCs) to release red blood cell-derived MPs (RMPs).

Another study[17] examined the MPs in individuals with G6PD deficiency; the findings demonstrated increased numbers of MPs that were mainly from RBCs and platelets. Those results also demonstrated a correlation between G6PD activity and MP concentrations. Given the high prevalence of G6PD in certain areas in Thailand, the variability in G6PD status among transfusion donors might cause variations in MP levels in blood products during laboratory preparation.[18] However, fewer data are available regarding the effect of blood processing on MP release in blood products obtained from eligible donors with G6PD deficiency.

The current study aimed to quantitate the MP concentrations in blood products obtained from donors with G6PD deficiency and to compare these concentrations with those obtained from donors with normal G6PD levels. Understanding the effect of G6PD deficiency on MP release during processing will help to reduce the post-transfusion complications associated with MPs and improve transfusion efficacy.

Materials and Methods

Materials

Fluorescein isothiocyanate-conjugated annexin V (annexin V–FITC), phycoerythrin-conjugated CD235a (CD235a-PE), peridinin chlorophyll-conjugated CD45 (CD45-PerCP), allophycocyanin-conjugated CD41a (CD41a-APC), and 10× annexin V binding buffer were obtained from ImmunoTools. CountBright counting beads were purchased from Thermo Fisher Scientific Inc.

Specimen Collection and Blood-Component Processing

Figure 1 illustrates the overall processes of collecting specimens and manufacturing blood components. After informed consent was obtained, the blood specimens were collected and processed, using a standard procedure, at the Department of Transfusion Medicine, Faculty of Medicine, Siriraj Hospital, Mahidol University, Thailand. The study was approved by the Institutional Review Board of Siriraj Hospital, Mahidol University School of Medicine, Bangkok, Thailand (COA no. 395/2016). The procedures were performed in accordance with international guidelines on the ethical conduct of research involving human subjects.

The whole blood specimens were collected into tubes containing tripotassium ethylenediaminetetraacetic acid and analyzed for complete blood counts (CBCs) using a Coulter AcT five-part differential hematology analyzer (Beckman Coulter, Inc.). These specimens were also analyzed for MP levels and G6PD activity. For blood-component processing, 450 mL of whole blood from donors was collected into triple blood collecting systems (JMS Triple Blood Bag and CPD-SAMG Solution; JMS Singapore Pte. Ltd.).

All whole-blood units were stored at room temperature (mean [SE], 22° [2°]C) for as long as 8 hours before the preparation of blood components. The whole blood units were centrifuged at 3100*g* for 5 minutes at mean (SE) 22° (2°)C in a centrifuge and separated into PRBC and platelet-rich plasma using a manual extractor. Then, the platelet-rich plasma was transferred into a 400 mL bag for platelet storage, centrifuged at 3800*g* for 5 minutes at mean (SE) 22° (2°)C, and separated into platelet-poor plasma and PC. After 100 mL of SAGM (saline-adenine-glucose-mannitol solution) was added, the PRBC units were stored at mean (SE) 4° (2°)C. The plasma units were transferred into a 400 mL bag, rapid-frozen to –30°C using a shock freezer (TPSU 40, Thalheimer; or MBF 12, Dometic) and stored at mean (SE) –30° (10°)C. The plasma specimens were collected before the freezing process.

For specimen gathering, the contents of the bag were thoroughly mixed by hand for 30 seconds, specimens were taken from heat-sealed segments, and the sampling pipette was stripped. The content of each segment was transferred into a 0.5 mL microcentrifuge tube and was carefully mixed; then, the MP concentration was determined. The specimens were processed for MP quantitation within 2 hours after the preparation process was completed.

DOI: 10.1093/labmed/lmab007

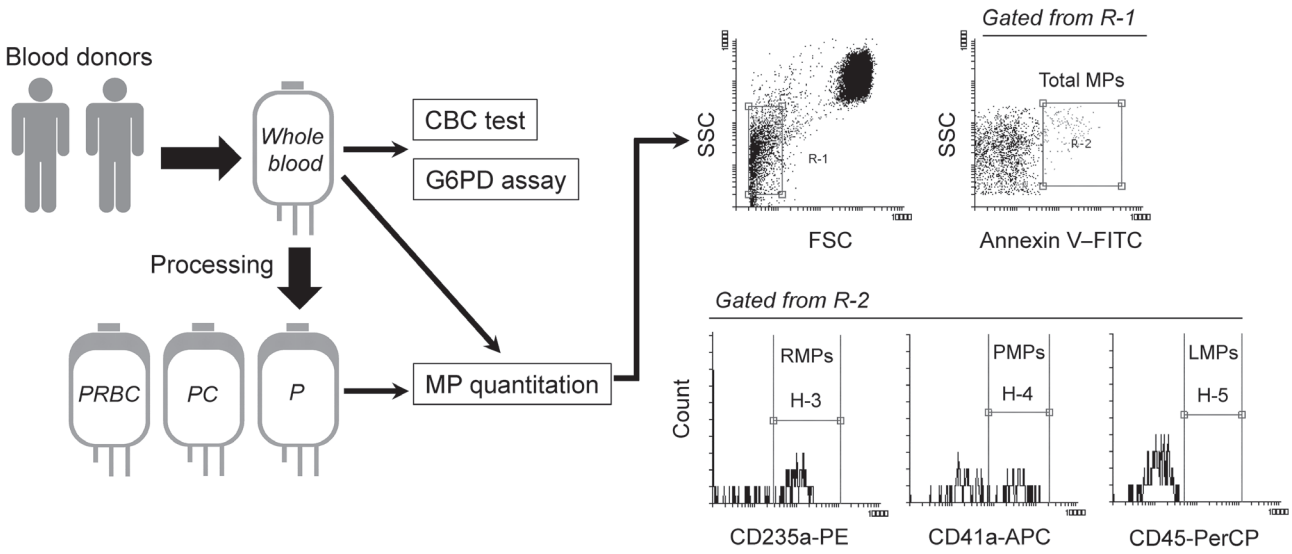

Figure 1

Overall study design and flow cytometry analysis of microparticles (MPs). CBC indicates complete blood count; G6PD, glucose-6-phosphate dehydrogenase; PRBC, packed red blood cell; PC, platelet concentrate; P, plasma; FSC, forward scatter; Annexin V-FITC, fluorescein isothiocyanate-conjugated annexin V; CD235a-PE, phycoerythrin-conjugated CD235a; CD41a-APC, allophycocyanin-conjugated CD41a; CD45-PerCP, peridinin chlorophyll-conjugated CD45.

Flow Cytometry Analysis of MPs

MPs were detected using flow cytometry based on their size and expression of membrane-specific markers. First, the specimen was diluted to 1:100 using phosphate-buffered saline (PBS). Next, 5 μL of the diluted specimens were incubated with 3 μL of annexin V–FITC, 2 μL of CD235a-PE, 3 μL of CD45-PerCP, 3 μL of CD41a-APC, and 20 μL of 1× annexin V binding buffer at room temperature in the dark. After 15 minutes, 300 μL of 1× annexin V binding buffer was added to the tubes. Then, the specimens were analyzed using a FACSCalibur (Becton, Dickinson and Company) flow cytometer. The performance of the flow cytometer was optimized using CaliBRITE beads and FACSComp software, version 5.1 (both by Becton, Dickinson and Company). The flow cytometry data were analyzed using CellQuest software, version 3.3 (Becton, Dickinson and Company).

The forward scatter (FSC), side scatter (SSC), and fluorescent parameter (FL) were set on the logarithmic scale. The threshold was set on the FSC parameter to exclude noise signals and debris. An MP gate (R1) was established using standard beads of 1.09-μm size. The beads were gated in an FSC vs SSC dot plot. The population of R1 was further analyzed on an annexin V vs SSC dot plot to identify annexin V–positive MPs (R2; **Figure 1**). The population of R2 was further plotted on a histogram of CD235a-PE, CD41a-APC, and CD45-PerCP to identify RMPs, PMPs, and LMPs in the H-3, H-4, and H-5 regions, respectively.

The concentrations of MPs were determined using the flow-rate calibration approach, as previously described.[19] Briefly, 50 μL of counting beads with a known concentration were mixed with 300 μL of PBS, mixed gently, and then run at the beginning and end of each batch of specimens. The average of the 2 counting-bead events was calculated. The volume per microliter of specimen material acquired in 120 seconds was obtained by dividing the bead events counted in 120 seconds by the concentration of the counting beads. Given the constant flow rate, the same volume of specimen material was acquired, and then the MP concentrations were calculated by dividing the MP events counted in 120 seconds by the previously calculated volume and multiplying the result by the dilution factor.

Assessment of Accuracy and Precision

To assess the accuracy of the counting approach, the platelets were diluted with PBS to 1:10, 1:00, 1:1000, and 1:10,000. Then, platelet counts were performed using flow cytometry. The precision was addressed by

repeatedly measuring the concentration counting beads to arrive at the within-day and day-to-day counting variations.

To address the specificity of annexin binding, platelet concentrate was first treated with A23187. Then, the treated specimen was incubated with annexin V in the presence of 1× annexin V binding or PBS, and the MPs were determined using flow cytometry.

Diagnosing G6PD Deficiency

The fluorescent spot test and G6PD activity test were used to diagnose G6PD deficiency. In the fluorescent spot test, the diagnosis was performed using a commercial kit (R&D Diagnostics Ltd.). Donors were characterized as having G6PD-normal activity or G6PD-deficient activity according to whether their results showed bright fluorescence or no fluorescence, respectively. The G6PD activity was quantified using a G6PD kit (BIOLABO). To determine the activity of the G6PD enzyme, the change in optical density per minute was calculated. The G6PD activity was expressed as IU per gHb. The production of nicotinamide adenine dinucleotide phosphate (NADPH) was measured kinetically at 340 nm. The donors with G6PD deficiency were diagnosed using previously published reference ranges of G6PD activity in the Thai population.[20]

Statistical Analysis

The statistical analysis was performed using GraphPad Prism software, version 5.0.1 (GraphPad). The results were expressed as mean, SE, and range. Comparison of the MP concentrations between donors with G6PD deficient and those with normal G6PD levels was performed using unpaired *t* testing. The association between the measured and expected platelet counts was analyzed using linear regression. *P* values less than .05 were considered statistically significant.

Results

Donor Characteristics, Hematological Indices, and G6PD Activity

This study evaluated 147 blood donors, of whom 49 had G6PD deficiency and 98 had normal G6PD levels. The mean (SE) age for donors with normal G6PD levels was 36.3 (1.2) years (17.1–59.2 years), and for donors with G6PD deficiency, it was 34.4 (1.5) years (19.1–57.1 years). **Table 1** summarizes the hematological parameters. Among these, only the mean corpuscular volume (MCV) values differed significantly between the donors with normal G6PD levels and those with G6PD deficiency.

Further analysis showed that the RBC G6PD-normal activity was mean (SE) 10.89 (1.88) IU per gHb for male donors and 11.75 (2.04) IU per gHb for female donors. The activity in the G6PD-deficient groups was 4.55 (3.18) IU per gHb for male donors and 5.26 (2.02) IU per gHb for female donors.

MP Levels and Their Origins in Whole Blood, PRBCs, PC, and Plasma in Donors with G6PD Deficiency and Those with Normal G6PD Levels

Next, the MP levels and their origins in whole blood, PRBCs, PC, and plasma were quantitated. A comparison of the MPs in whole blood showed that donors with G6PD deficiency and those with normal G6PD levels had similar levels of total MPs and RMPs (**Table 2**). However, PMP and LMP concentrations were significantly higher in donors with normal G6PD levels than in those with G6PD deficiency. An examination of the MPs in PRBCs demonstrated that RMP concentrations were significantly higher in donors with G6PD deficiency than in those with normal G6PD levels. Other MP concentrations showed no statistically significant differences between the 2 groups.

An examination of the MPs in PC showed that total MP and PMP concentrations were lower in donors with G6PD deficiency than in those with normal G6PD levels. There were no differences in RMP and LMP concentrations between the 2 groups. Regarding plasma, donors with G6PD deficiency and normal G6PD levels had similar concentrations of total MPs, RMPs, and PMPs. LMP concentrations were significantly lower in donors with G6PD deficiency than in those with normal G6PD levels.

Reliability and Accuracy of Flow Cytometry Quantitation of MPs

The current study first addressed whether the established MP gate could determine changes in MP quantity. The whole blood was treated with A23187 to induce MP release. After 15 minutes, the quantity of PS-exposing MPs was determined. The results showed that the percentage and quantity of MPs in platelets treated with A23187 were higher than in the control platelets (25.01% vs 5.58%; 819,527 particles/μL vs 26,651 particles/μL).

DOI: 10.1093/labmed/lmab007

Table 1. Hematology Parameters of Blood Donor with G6PD Deficiency and Normal G6PD Levels

Analyte	Mean (SE) (minimum–maximum)		*P* Value
	G6PD-deficient Group[a]	G6PD-normal Group[b]	
RBC ($\times 10^6/\mu L$)	4.8 (0.05) (3.8–6.2)	4.9 (0.05) (3.9–6.8)	.78
Hb (g/dL)	14.1 (0.2) (11.5–17.4)	13.9 (0.1) (11.7–17.1)	.63
Hct (%)	42.8 (0.6) (36.1–52.6)	42.1 (0.4) (35.3–51.2)	.31
MCV (fL)	88.7 (0.8) (78.4–98.4)	86.8 (0.4) (61.1–95.1)	.01[c]
MCH (pg)	29.2 (0.3) (24.8–33.6)	28.6 (0.2) (25.1–31.3)	.19
MCHC (g/dL)	32.9 (0.1) (30.2–35.2)	33.2 (0.1) (30.8–34.9)	.13
RDW (%)	13.4 (0.1) (11.6–15.8)	13.5 (0.1) (12.2–16.3)	.63
WBC ($\times 10^3/\mu L$)	7.1 (0.2) (4.5–12.3)	7.1 (0.1) (4.4–10.1)	.89

G6PD, glucose-6-phosphate dehydrogenase; RBC, red blood cell; Hb, hemoglobin; Hct, hematocrit; MCV, mean corpuscular volume; MCH, mean corpuscular hemoglobin; MCHC, mean corpuscular hemoglobin concentrate; RDW, red blood cell distribution width; WBC, white blood cell.
[a] *n = 49.*
[b] *n = 98.*
[c] *Indicates a statistically significant difference between the groups.*

Table 2. Concentration of Total MP, RMP, PMP, and LMP in Whole Blood, PRBC, PC, and Plasma from Donors with G6PD Deficiency and Normal G6PD Levels

Analyte	Mean (SE) (minimum–maximum)		*P* Value
	G6PD-deficient Group[a]	G6PD-normal Group[b]	
Whole Blood			
Total MPs	24,584 (935) (13,194–41,067)	28,067 (1307) (12,586–70,825)	.07
RMPs	13,175 (702) (4001–25,387)	11,778 (389) (5322–24,360)	.06
PMPs	8680 (563) (2240–23,329)	10,969 (426) (2842–27,907)	.001[c]
LMPs	158 (32) (0–672)	347 (35) (0–1206)	.001[c]
PRBCs			
Total MPs	40,594 (8266) (18,633–447,253)	31,659 (1032) (14,370–107,169)	.15
RMPs	25,526 (3977) (8526–219,147)	18,738 (563) (7308–36,185)	.02[c]
PMPs	10,777 (3165) (0–157,547)	8084 (619) (1455–59,283)	.26
LMPs	239 (56) (747–2014)	281 (31) (0–1334)	.48
PCs			
Total MPs	26,026 (1589) (16,751–50,598)	40,167 (2660) (17,423–139,253)	.006[c]
RMPs	10,581 (884) (3081–24,904)	9539 (315) (4472–18,779)	.16
PMPs	10,661 (981) (4800–21,953)	15,568 (896) (5619–56,324)	.006[c]
LMPs	163 (52) (0–988)	283 (38) (0–1561)	.11
Plasma			
Total MPs	177,564 (74,176) ($15,960–3.6 \times 10^6$)	145,098 (18,092) ($19,721–1.3 \times 10^6$)	.58
RMPs	10,965 (998) (4032–36,762)	12,042 (511) (4141–31,282)	.28
PMPs	126,524 (63,816) ($6080–3 \times 10^6$)	76,556 (9408) (10,477–617,525)	.29
LMPs	161 (36) (0–1220)	339 (44) (0–2038)	.008[c]

MPs, microparticle; RMPs, red blood cell-derived microparticles; PMPs, platelet-derived microparticles; LMPs, leukocyte-derived microparticles; PRBCs, packed red blood cells; PC, platelet concentrate; G6PD, glucose-6-phosphate dehydrogenase.
[a] *n = 49.*
[b] *n = 98.*
[c] *Indicates a statistically significant difference between the groups.*

For the accuracy, the results showed an r^2 of 0.99 (P <.001) between the measured and expected platelet concentrations (**Figure 2A**). To address the precision of the counting approach, 10 aliquots of referent microbeads with known concentrations were determined in a single run. The results showed a coefficient of variation (CV) of 7.9% (**Figure 2B**). In addition, analysis of the referent microbeads for 10 consecutive days showed a CV of 10%.

The study also addressed whether positive signals for MPs were a result of specific binding between the annexin and the expressed PS. The specimens were

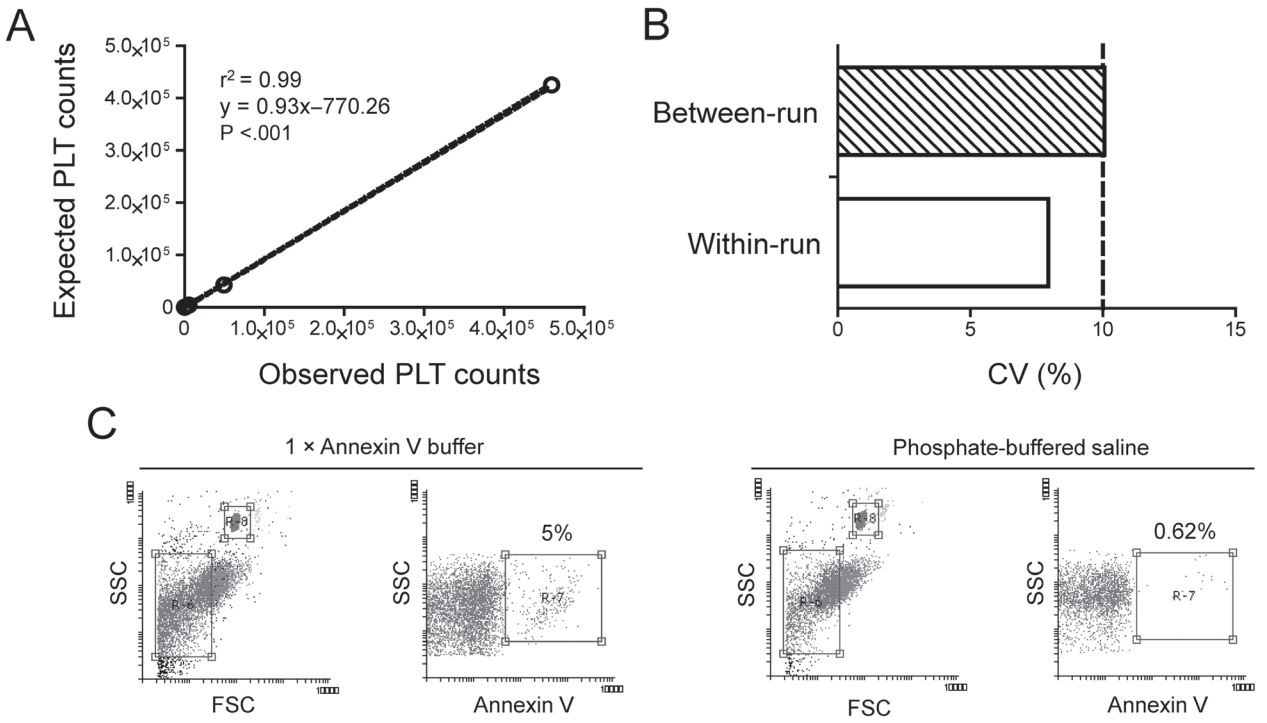

Figure 2

Platelet values. **A**, Linear regression analysis of measured platelets and their expected values in diluted specimens. **B**, Bar plots showing the within-run and between-run coefficients of variation (CVs) of the counting approach. **C**, Dot-plots of the annexin V vs side scatter (SSC) of platelet concentrates in the presence and absence of annexin V binding buffer. The numbers indicate phosphatidylserine (PS)–exposing microparticles (MPs) (%). FSC indicates forward scatter.

examined for the presence of PS-exposing MPs, which were shown to be 5% after incubation with 1× annexin V buffer (**Figure 2C**). In contrast, the percentage of PS-exposing MPs decreased to 0.62% in the absence of 1× annexin V buffer. Similarly, the quantity of PS-exposing MPs was 115,613 particles per μL in the presence of 1× annexin V buffer but decreased to 7,650 particles per μL in the absence of the buffer.

Discussion

The current study aimed to address whether the G6PD statuses of eligible blood donors are associated with MP concentrations in blood products. Comparison of the quantities of RMPs in whole blood and PRBCs suggests a potential influence of G6PD status on MP release.

A study by Francis et al[21] examined the effect of storage on the quality of PRBCs from volunteers with G6PD deficiency, after 42 days. The results showed that the average post-transfusion RBC recovery was lower in donors with G6PD deficiency than in those with normal G6PD levels, and that the former donors demonstrated defects in the oxidative-phosphate pathway, suggesting an effect of storage on the quality of RBCs from such donors.

The results of 1 study[22] also suggested the risks of transfusion using G6PD-deficient RBCs due to changes in the RBC antioxidant system during refrigerated storage. The current study determined the G6PD activity of donors and then examined the quantities of MPs before and after blood-component preparation. In whole blood specimens, the quantities of RMPs were similar in donors with G6PD deficiency and donors with normal G6PD levels.

Our findings were in line with those of Tzounakas et al,[23] which showed similar levels of RMPs positive for annexin

DOI: 10.1093/labmed/lmab007

V in fresh whole blood from donors with G6PD deficiency and those with normal G6PD levels. However, this finding contrasts with those of Nantakomol et al,[17] who found higher quantities of MPs in whole blood obtained from G6PD-deficient individuals. This difference might be due to the variability in severity among populations with G6PD deficiency: the current study results found the average G6PD activity of groups with G6PD deficiency (4.55–5.26 IU/gHb) to be within the ranges of heterozygous G6PD deficiency. However, the current study found a significant difference in the quantities of RMPs in PRBCs from the 2 groups of donors. The quantity of RMPs in the groups with G6PD-deficient groups was 1.4-fold higher than in the G6PD-normal group, suggesting a potential effect of blood processing on RMP release in donors with G6PD deficiency. This suggestion is supported by the results of a study[24] that showed that exposing PRBCs to high shear stress during PRBC preparation induced changes in RBC properties and deformability. High shear stress might cause increased numbers of RMPs in PRBCs during preparation in products from donors with G6PD deficiency. Considering this observation, monitoring the quantities of RMPs in PRBCs might be necessary to minimize post-transfusion complications in countries where the prevalence of G6PD deficiency is relatively high.

Our study results also found that the levels of PMPs and LMPs in whole blood, PC, and plasma prepared from donors with G6PD deficiency were lower than those in products prepared from donors with normal G6PD levels. In the case of PMPs, this is an unexpected finding; however, because G6PD-deficient cells are sensitive to oxidative damage, platelets might shed more PMPs in response to this stress. Also, increased PMP levels have been reported in individuals with G6PD deficiency.[17] Considering the difference in the sizes of the 2 cohorts in the current study, more data from donors with G6PD deficiency are required to confirm the lower PMP concentrations. In the case of LMPs, although the current study found a significant difference between the donor groups, the clinical significance of these differences requires further investigation, given the low concentrations compared to other MP subpopulations.

Regarding the hematological parameters, the current study found similar values for RBC counts, hemoglobin (Hb), hematocrit (Hct), mean corpuscular hemoglobin (MCH), mean corpuscular hemoglobin concentration (MCHC), and RBC distribution width (RDW). However, a slight but significant difference in MCV was found between donors with G6PD deficiency and those with normal G6PD levels, although the average values for both groups were within normal ranges compared to previous study reports.[25,26] Considering this point, further study is required to confirm this difference in donors with G6PD deficiency and to assess the association between MP levels and MCV values.

Results of some studies[27–29] have suggested variability in MP quantitation using flow cytometry. However, the accuracy of the flow cytometry approach for MP quantitation, as investigated in the current study, was supported by the following evidence. First, the results of dilution experiments showed a good correlation between the expected and measured values for platelet concentration. Second, the within-run and between-run values were less than 10%, suggesting the precision of the counting approach used. Finally, A23187-treated PC showed increased MP concentrations, suggesting the success of the strategy for optimizing flow-cytometry gating.

We note that our study used A23187 to induce the release of MPs. Accumulated evidence has shown that A23187 can induce MP release, which involves the influx of intracellular calcium, reorganization of the cytoskeleton, and induction of caspase protein.[30,31] Also, our results showed that the percentage of MPs without 1× annexin V binding buffer was less than 1%, compared with the percentage with annexin V binding buffer, suggesting the specificity of annexin V staining.

One limitation of the current study is that it addressed MP concentrations at only a single time point because the continuing high need for transfusion products resulted in a limited number of available blood products. Hence, there were no data regarding the effect of storage on the MP release in products from donors with G6PD deficiency. Another limitation is that although the study considered blood quality, it did not include post-transfusion data from recipients. Therefore, future studies are needed to address the efficacy of blood products obtained from donors with G6PD deficiency.

Our investigation revealed increased numbers of RMPs in the PRBCs obtained from eligible blood donors with G6PD deficiency. The implementation of routine quantitation of MPs in blood products might be necessary in transfusion laboratories to monitor the changes in MP levels in blood products after processing or storage. This finding could be of clinical relevance in managing the quality of blood components in transfusion laboratories. **LM**

Acknowledgments

This research is funded by Chulalongkorn University, Bangkok, Thailand (CU-GES-60-05-30-01). Also, we thank the Faculty of Medicine Siriraj Hospital, Mahidol University, Bangkok, Thailand, for its support of the project.

Personal and Professional Conflicts of Interest

None reported.

References

1. Herring JM, McMichael MA, Smith SA. Microparticles in health and disease. *J Vet Intern Med.* 2013;27(5):1020–1033.
2. Barteneva NS, Fasler-Kan E, Bernimoulin M, et al. Circulating microparticles: square the circle. *BMC Cell Biol.* 2013;14:23.
3. Schindler SM, Little JP, Klegeris A. Microparticles: a new perspective in central nervous system disorders. *Biomed Res Int.* 2014;2014:756327.
4. György B, Szabó TG, Pásztói M, et al. Membrane vesicles, current state-of-the-art: emerging role of extracellular vesicles. *Cell Mol Life Sci.* 2011;68(16):2667–2688.
5. Benameur T, Osman A, Parray A, Ait Hssain A, Munusamy S, Agouni A. Molecular mechanisms underpinning microparticle-mediated cellular injury in cardiovascular complications associated with diabetes. *Oxid Med Cell Longev.* 2019;2019:6475187.
6. Nomura S, Shimizu M. Clinical significance of procoagulant microparticles. *J Intensive Care.* 2015;3(1):2.
7. Owens AP 3rd, Mackman N. Microparticles in hemostasis and thrombosis. *Circ Res.* 2011;108(10):1284–1297.
8. Kriebardis A, Antonelou M, Stamoulis K, Papassideri I. Cell-derived microparticles in stored blood products: innocent-bystanders or effective mediators of post-transfusion reactions? *Blood Transfus.* 2012;10(Suppl 2):s25–s38.
9. Aung HH, Tung JP, Dean MM, Flower RL, Pecheniuk NM. Procoagulant role of microparticles in routine storage of packed red blood cells: potential risk for prothrombotic post-transfusion complications. *Pathology.* 2017;49(1):62–69.
10. Fischer D, Büssow J, Meybohm P, et al. Microparticles from stored red blood cells enhance procoagulant and proinflammatory activity. *Transfusion.* 2017;57(11):2701–2711.
11. Noulsri E. Quantitation of cell-derived microparticles in blood products and its potential applications in transfusion laboratories. *Lab Med.* 2020;51(5):452–459.
12. Noulsri E, Udomwinijsilp P, Lerdwana S, Chongkolwatana V, Permpikul P. Differences in levels of platelet-derived microparticles in platelet components prepared using the platelet rich plasma, buffy coat, and apheresis procedures. *Transfus Apher Sci.* 2017;56(2):135–140.
13. Noulsri E, Palasuwan A. Effects of donor age, donor sex, blood-component processing, and storage on cell-derived microparticle concentrations in routine blood-component preparation. *Transfus Apher Sci.* 2018;57(4):587–592.
14. WHO Guidelines Approved by the Guidelines Review Committee. *Blood Donor Selection: Guidelines on Assessing Donor Suitability for Blood Donation.* World Health Organization; 2012.
15. Pantaleo A, Ferru E, Carta F, et al. Irreversible AE1 tyrosine phosphorylation leads to membrane vesiculation in G6PD deficient red cells. *PLoS One.* 2011;6(1):e15847.
16. Cappellini MD, Fiorelli G. Glucose-6-phosphate dehydrogenase deficiency. *Lancet.* 2008;371(9606):64–74.
17. Nantakomol D, Palasuwan A, Chaowanathikhom M, Soogarun S, Imwong M. Red cell and platelet-derived microparticles are increased in G6PD-deficient subjects. *Eur J Haematol.* 2012;89(5):423–429.
18. Kittisares K, Palasuwan D, Noulsri E, Palasuwan A. Thalassemia trait and G6PD deficiency in Thai blood donors. *Transfus Apher Sci.* 2019;58(2):201–206.
19. Noulsri E, Lerdwana S, Kittisares K, Palasuwan A, Palasuwan D. Flow rate calibration to determine cell-derived microparticles and homogeneity of blood components. *Transfus Apher Sci.* 2017;56(4):585–590.
20. Nantakomol D, Paul R, Palasuwan A, Day NP, White NJ, Imwong M. Evaluation of the phenotypic test and genetic analysis in the detection of glucose-6-phosphate dehydrogenase deficiency. *Malar J.* 2013;12:289.
21. Francis RO, D'Alessandro A, Eisenberger A, et al. Donor glucose-6-phosphate dehydrogenase deficiency decreases blood quality for transfusion. *J Clin Invest.* 2020;130(5):2270–2285.
22. Francis RO, Jhang JS, Pham HP, Hod EA, Zimring JC, Spitalnik SL. Glucose-6-phosphate dehydrogenase deficiency in transfusion medicine: the unknown risks. *Vox Sang.* 2013;105(4):271–282.
23. Tzounakas VL, Kriebardis AG, Georgatzakou HT, et al. Data on how several physiological parameters of stored red blood cells are similar in glucose 6-phosphate dehydrogenase deficient and sufficient donors. *Data Brief.* 2016;8:618–627.
24. Barshtein G, Gural A, Zelig O, Arbell D, Yedgar S. Preparation of packed red blood cell units in the blood bank: Alteration in red blood cell deformability. *Transfus Apher Sci.* 2020;59(3):102738.
25. Pengon J, Svasti S, Kamchonwongpaisan S, Vattanaviboon P. Hematological parameters and red blood cell morphological abnormality of Glucose-6-Phosphate dehydrogenase deficiency co-inherited with thalassemia. *Hematol Oncol Stem Cell Ther.* 2018;11(1):18–24.
26. Kotepui M, Uthaisar K, PhunPhuech B, Phiwklam N. Prevalence and hematological indicators of G6PD deficiency in malaria-infected patients. *Infect Dis Poverty.* 2016;5:36.
27. Yuana Y, Bertina RM, Osanto S. Pre-analytical and analytical issues in the analysis of blood microparticles. *Thromb Haemost.* 2011;105(3):396–408.
28. Piccin A, Murphy WG, Smith OP. Circulating microparticles: pathophysiology and clinical implications. *Blood Rev.* 2007;21(3):157–171.
29. Lacroix R, Robert S, Poncelet P, Dignat-George F. Overcoming limitations of microparticle measurement by flow cytometry. *Semin Thromb Hemost.* 2010;36(8):807–818.
30. Ponomareva AA, Nevzorova TA, Mordakhanova ER, et al. Intracellular origin and ultrastructure of platelet-derived microparticles. *J Thromb Haemost.* 2017;15(8):1655–1667.
31. Koshiar RL, Somajo S, Norström E, Dahlbäck B. Erythrocyte-derived microparticles supporting activated protein C-mediated regulation of blood coagulation. *PLoS One.* 2014;9(8):e104200.

DOI: 10.1093/labmed/lmab007

Using the BDFX40 Automated Continuous Blood Culture System to Isolate and Recover *Streptobacillus moniliformis* in the Presence of 0.05% SPS: A 55-Year, 56-Strain Retrospective Study

Adam M. Szewc, BS SM(ASCP), MB, QLS,[1,] Melissa E. Bell, MS,[1] Aubree J. Kelly, MS,[1] Ben W. Humrighouse, MS,[1] John R. McQuiston, PhD[1]*

Laboratory Medicine 2021;52:536-549

DOI: 10.1093/labmed/lmab009

ABSTRACT

Rat bite fever and Haverhill fever are often difficult to diagnose in a clinical setting. This difficulty results in part from clinicians and laboratory professionals not being able to reliably recover the causative agent *Streptobacillus moniliformis* using culture-based methods. After utilizing an automated continuous-monitoring blood culture bottle system, we showed that the organism can be reliably cultured when a blood volume inoculum of 10 mL is used. Further, we showed that when the above recommendation is followed, sodium polyanethole sulfonate (up to a concentration of 0.05% w/v) in commercially purchased blood culture bottle formulations seems to be inactivated, allowing for the growth and detection of *S. moniliformis*. Herein, we offer data and methods used to overcome these clinical limitations. This is a comprehensive study of the historical collection of *S. moniliformis* isolates maintained by our facility and believed to be the largest of its kind to date.

Keywords: Haverhill fever, Liquoid, rat-bite fever, sodium polyanethole sulfonate, *Streptobacillus moniliformis*

Streptobacillus moniliformis is the primary etiologic agent of rat bite fever (RBF) and Haverhill fever (HF), zoonotic diseases with similar clinical presentations but acquired through 2 separate routes of infection. Typically, RBF is associated with bites or scratches from rats or other animals that serve as a reservoir for the bacterium, whereas HF is associated with the consumption of foods contaminated with rat urine or feces. Clinical presentation often includes but is not limited to fever, chills, myalgia, headache, and vomiting. Patients may also develop or present with a maculopapular rash covering their extremities approximately 2 to 4 days after onset of fever followed by polyarthritis, which is reported in roughly 50% of all patients. If left untreated, the mortality rate for RBF is reported to be 10% to 13%.[1-3] Considered rare, these diseases are difficult to diagnose because of the nonspecific presentation of symptoms, lack of reporting rodent exposures, and difficulty recovering *S. moniliformis* in the clinical laboratory. As a result, RBF and HF are most likely underreported in the United States.[1]

Abbreviations:

RBF, rat bite fever; HF, Haverhill fever; SPS, sodium polyanethole sulfonate; HIA, heart infusion agar; BHI, brain heart infusion; ZOI, zone of inhibition; MALDI-TOF, matrix-assisted laser desorption/ionization time-of-flight mass spectrometry; PCR, polymerase chain reaction; NG, no growth; TK, time-kill; CFU, colony forming unit; Ct, threshold value; TTD, time to detection; BSI, bloodstream infection.

[1]Bacterial Special Pathogens Branch (BSPB), Division of High-Consequence Pathogens and Pathology, National Center for Emerging and Zoonotic Infectious Diseases, Centers for Disease Control and Prevention, Atlanta, Georgia, USA

*To whom correspondence should be addressed.
aszewc@cdc.gov

The bacterium *S. moniliformis* is a gram negative pleomorphic rod, occurring frequently in chains and tangled filaments with bulbous or *Monilia*-like swellings (**Figure 1**). The organism presents phenotypically as being facultatively anaerobic and nonmotile, weakly ferments glucose and maltose, is catalase- and oxidase-negative, does not reduce nitrate, and exhibits no growth on MacConkey agar.[4] Morphologically, colonies of *S. moniliformis* are 1 to 2 mm

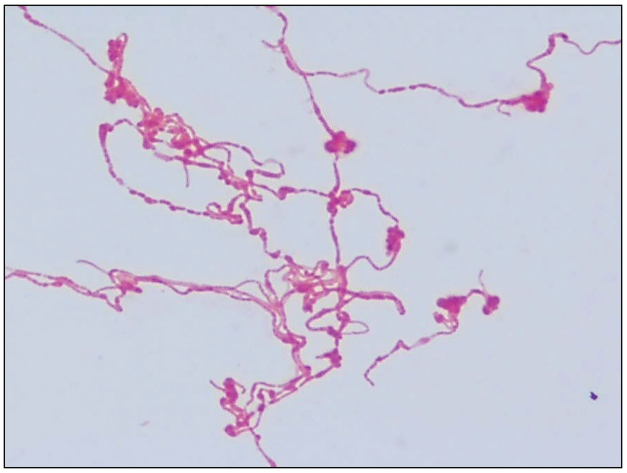

Figure 1

Gram stain image from culture of *S. moniliformis* showing pleomorphic, gram negative rods in chains and tangled filaments with bulbous-like swellings (×1000).

in size, smooth, convex, nonhemolytic (varied presentation with an α-hemolysis is not uncommon), and gray in color. When cultured in broth, a typical "puffball" appearance is seen (**Figure 2**).

The fastidious nature of *S. moniliformis* makes it difficult to culture, with current published recommendations stating that it requires media supplemented with 20% serum, ascitic fluid, or whole blood to grow.[1] Numerous published reports have also stated that the organism is inhibited by the polyanionic detergent sodium polyanethole sulfonate (SPS; trade name, Liquoid; Hoffman-La Roche, Inc., Nutley, NJ), the main anticoagulant in modern commercially available blood culture bottles, used in automated continuous blood culture instruments.[1-3]

In the present study, we research the reported fastidious nature of *S. moniliformis,* its inhibition by the anticoagulant SPS, and culturing guidelines in patients with suspected RBF while also providing methods for reliably culturing *S. moniliformis* using an automated continuous blood culture system. New research is also presented and data are provided showing that when a specific volume of blood was used for inoculum, it resulted in the 100% recovery and successful growth of this organism and seemed to overcome the inhibitions and limitations that historically have been observed when using SPS for blood culturing and recovering *S. moniliformis* in a clinical setting.[1,5-7]

Materials and Methods

Bacterial Strains

The strains examined in this study (n = 56), along with their sources, are presented in **Table 1**. Dating from 1965, all isolates (excluding the type strain) were submitted to our facility's Special Bacteriology Reference Laboratory for identification.

All isolates were recovered from frozen stocks, subcultured on heart infusion agar (HIA) supplemented with 5% rabbit blood, inoculated in brain heart infusion (BHI), and grown aerobically at 35°C. It was unnecessary to cultivate isolates in a CO_2-enriched environment. Frozen stocks, upon the initial culturing, were immediately placed back into a –80°C freezer and were not subcultured again until the main SPS study was to begin. This process minimized specimen processing and optimized data collection for fresh-/low-passage isolates. The working stock/growth from the initial frozen stocks was used to carry out species/isolate confirmation, biplate growth, and the SPS disk zone of inhibition (ZOI)/sensitivity studies.

Confirmation of Bacterial Species

Confirmation of the bacterial species used within this study was performed via 16S rRNA sequencing and/or matrix-assisted laser desorption/ionization time-of-flight mass spectrometry (MALDI-TOF MS; Bruker Daltonics, Bremen, Germany).

MALDI-TOF

All specimens were plated and processed on a MALDI biotyper SMART (Bruker Daltonics, Bremen, Germany) using the extended direct transfer method, with all accepted scores for species identification being >2.00.

16S rRNA Sequence Analysis

Purification of genomic DNA, primers for polymerase chain reaction (PCR), and amplification of near-full-length 16S rRNA gene fragments, purification of amplicons, and DNA cycle sequencing were performed as described previously.[8] Consensus 16S rRNA gene sequences were assembled and edited using Geneious software, version 11.1.5 (https://www.geneious.com), and were submitted to GenBank using BLASTn software (https://www.ncbi.nlm.nih.gov/blast/; Supplemental Figure 1).

DOI: 10.1093/labmed/lmab009

Figure 2

S. moniliformis growth showing colony morphology on HIA with 5% rabbit blood: 1 to 2 mm in size, smooth, convex, nonhemolytic, and grey in color with characteristic "puffball" appearance in BHI broth after 48 hours. BHI, bone heart infusion; HIA, heart infusion agar.

S. moniliformis Growth Observations With and Without Blood Supplementation

All isolates were grown from frozen stock and subcultured for purity on HIA supplemented with 5% rabbit blood and incubated aerobically at 35°C without supplemental CO_2. Colonies were streaked to HIA biplates (5% rabbit blood/no blood) and allowed to incubate for 72 hours. Final growth determination was made at 72 hours and documented qualitatively (+/++/+++/++++/no growth [NG]).

S. moniliformis ZOI with 1 mg SPS Disks

Similar to the growth observations of *S. moniliformis* noted above, all isolates were grown from frozen stock and subcultured for purity on HIA supplemented with 5% rabbit blood and incubated aerobically at 35°C without supplemental CO_2. Colonies were streaked to HIA (with 5% rabbit blood), and a 1 mg impregnated SPS disk (Hardy Diagnostics) was placed in quadrant 1 and allowed to incubate at the above conditions. Measurements of inhibition zones were taken at 24 hours with final measurements being taken at 48 hours for isolates requiring longer incubation times to accurately record a zone measurement.

Edberg and Edberg Time-Kill Procedure and Modification(s)

This experiment idea was conceptualized from a 1983 publication by Edberg and Edberg,[7] which included a "time-kill" (TK) study looking at the relationship of SPS and hemoglobin using strains of *Neisseria meningitidis* and *Neisseria gonorrhoeae.* Per their design, the authors inoculated both *N. meningitidis* and *N. gonorrhoeae* at a concentration of 1×10^5 in 0.05% SPS with and without 3% hemoglobin. The specimens were incubated under appropriate

Table 1. Collection/Submission History for *S. moniliformis* Strains Used

	Strain Identifier	Year of Isolation	Source	Final Identification Method (MALDI-TOF/16S)
1	A3410	1965	Human Blood	MALDI-TOF
2	A3531	1965	Human Blood	MALDI-TOF
3	A7171	1967	Human Blood	MALDI-TOF
4	B8900[a]	1971	Human Blood	16S
5	C7016	1973	Human Blood	MALDI-TOF
6	C7795	1973	Human Blood	MALDI-TOF
7	D7626	1976	Human Blood	MALDI-TOF
8	ATCC 14647[b]	1980	Septicemia	16S
9	F2022	1981	Human Blood	MALDI-TOF
10	F1527	1981	Human Blood	MALDI-TOF
11	F2396	1982	Human Blood	MALDI-TOF
12	F2384	1982	Human Blood	MALDI-TOF
13	F3043	1982	Human Blood	MALDI-TOF
14	F4559	1983	Joint Fluid	MALDI-TOF
15	F4558	1983	Human Blood	MALDI-TOF
16	F5001	1983	Joint Fluid	MALDI-TOF
17	F5599	1984	Human Blood	MALDI-TOF
18	F5431	1984	Joint Fluid	MALDI-TOF
19	F6762	1985	Joint Fluid	MALDI-TOF
20	F8454	1986	Joint Fluid	MALDI-TOF
21	G0716	1987	Heart Tissue	MALDI-TOF
22	G4934	1990	Joint Fluid	MALDI-TOF
23	G6651	1991	Pustule	MALDI-TOF
24	G6134	1991	Joint Fluid	MALDI-TOF
25	G6483	1991	Human Blood	MALDI-TOF
26	G7408	1992	Human Blood	MALDI-TOF
27	G7586	1992	Human Blood	MALDI-TOF
28	G7806	1992	Human Blood	MALDI-TOF
29	G7643A	1992	Shoulder Aspirate	MALDI-TOF
30	G7587	1992	Human Blood	MALDI-TOF /16S
31	G8797	1993	Human Blood	MALDI-TOF
32	G8599	1993	Human Blood	MALDI-TOF
33	G8611	1993	Human Blood	MALDI-TOF
34	G8568	1993	Joint Fluid	MALDI-TOF
35	G8683A	1993	Joint Fluid	MALDI-TOF
36	G8718	1993	Human Blood	MALDI-TOF
37	G9007	1994	CSF	MALDI-TOF
38	G9037	1994	Human Blood	MALDI-TOF
39	G9555	1995	Septicemia	MALDI-TOF
40	G9874	1996	Human Blood	MALDI-TOF
41	H0896	1998	Human Blood	MALDI-TOF
42	H0840	1998	Skin Lesion	MALDI-TOF
43	H1141	1999	Human Blood	MALDI-TOF
44	H1600	2000	Human Blood	MALDI-TOF
45	H1736	2000	Human Blood	MALDI-TOF
46	H1765	2000	Human Blood	MALDI-TOF
47	H1924	2001	Human Blood	MALDI-TOF
48	H2730	2003	Human Blood	MALDI-TOF
49	H3645	2005	Human Blood	16S
50	H4152	2006	Hip Fluid	16S
51	H5065	2009	Human Blood	16S
52	H6118	2012	Human Blood	16S
53	H6036	2012	Hand Wound	MALDI-TOF
54	H6796	2018	Human Blood	16S
55	H6798	2019	Joint Fluid	16S
56	H6799	2019	Human Blood	16S

CSF, cerebrospinal fluid; MALDI-TOF, matrix-assisted laser desorption/ionization time-of-flight mass spectrometry; 16S, 16S RNA gene sequencing.
[a]*Designates isolate used by Lambe et al.*[5]
[b]*Designates type of strain used in this study.*

DOI: 10.1093/labmed/lmab009

conditions for their organisms and sampled every 2 hours for a total of 24 hours. Viable cell counts and colony forming unit (CFU) observations were performed in their study by the Koch method.

We used and modified this method to test our hypothesis regarding blood volume needed for optimal organism growth in a 0.05% SPS formulation. Conditions were modified as follows: the organism inoculum tested was 1×10^3 (1 mL); the blood culture broth used was a commercially available aerobic blood bottle (BD BACTEC Plus Aerobic/F, Becton Dickinson, Franklin Lakes, NJ; 30 mL volume); the blood inoculum tested was 4 mL, 7 mL, and 10 mL; bottles were incubated at 35°C, aerobically, without shaking; 1 mL aseptic sampling was performed at 20, 28, 44, 52, 68, 76, and 92 hours and then frozen (–80°C); DNA was extracted from all specimens; and specimens were run, analyzed, and interpreted using a real-time PCR instrument.

Modified TK Procedure Using Strain B8900 in 0.05% SPS to Determine Optimal Blood Volume for Growth/Detection

Strain B8900 was grown from frozen stock and subcultured on HIA supplemented with 5% rabbit blood and incubated aerobically at 35°C without supplemental CO_2. Once grown, colonies were suspended in BHI to a 1.00 McFarland turbidity value and serially diluted. Final dilutions were plated in triplicate and allowed to incubate for 48 hours in the aforementioned conditions. Plate counts were conducted manually, and a starting CFU/mL was determined. Three 1 mL aliquots of a 500 to 1000 CFU/mL suspension were then inoculated into 3 separate BD BACTEC Plus Aerobic/F blood culture bottles, each containing anticoagulant-free whole human blood at volumes of 4 mL, 7 mL, and 10 mL. Bottles were placed upright inside a 35°C incubator without supplemental CO_2 and were allowed to remain stationary until sampling. One mL sampling was performed at 8- and 16-hour increments (inverting the bottles and mixing the contents 3 to 4 times before sampling) and frozen at –80°C until the end of the experiment, which concluded at 91 hours and included 21 specimens covering 7 timepoints.

In addition to the above specimen setup, 3 additional BD BACTEC Plus Aerobic/F blood culture bottles were inoculated with the same 1 mL aliquot serial dilutions with anticoagulant-free blood volumes of 4 mL, 7 mL, and 10 mL and loaded into the BDFX40 automated continuous blood culture bottle instrument to run a side-by-side comparison of growth and detection utilizing clinical laboratory automated instrumentation. Once an optimal blood volume was determined, this procedure was repeated for 3 additional specimens, which included the strains ATCC 14647 and ATCC 14647 in BHI without blood or SPS and the strain H3645 as a baseline control.

DNA Lysis and Extraction

DNA from the frozen timepoint specimens, collected from the modified Edberg and Edberg TK study[7] (n = 84) consisting of the ATCC 14647, B8900, H3645, and ATCC 14647 strains in BHI without blood or SPS, were extracted using an in-house custom protocol utilizing 180 μL of bacterial lysis buffer (Roche, Basel, Switzerland) with 20 μL of PCR grade proteinase K (Roche) for a total of 200 μL. The blood culture timepoint specimens were then thawed on ice, and 200 μL of blood culture specimens was then added to the lysis mix, vortexed, and incubated at 65°C for 10 minutes (an additional 95°C inactivation step was omitted to avoid whole blood clotting). After incubation, each specimen was vortexed briefly again and extracted using the Roche automated MagNA Pure Compact instrument (MagNA Pure Compact Nucleic Acid Isolation Kit 1; v.17, bacterial protocol) with an initial input volume of 400 μL and stored in a final elution buffer volume of 100 μL.

Topoisomerase Based Cloning Clone and *S. moniliformis* Specific Standard(s) Creation/ PCR and Analysis

Topoisomerase based cloning (TOPO) cloning was utilized to make stable positive controls and standards for the modified TK study. To construct a species-specific standard, a 168 bp amplicon was produced by PCR using primers targeting a conserved region within the GrpE protein in *S. moniliformis* strain ATCC 14647. After purifying the PCR product, the amplicon was directly inserted into a plasmid vector following the manufacturer's instructions (pCR2.1 TOPO, Invitrogen, Carlsbad, CA) and propagated in susceptible *Escherichia coli* hosts. Plasmid DNA was then purified and sequenced using primers M13(-20) forward and reverse, and plasmid insert size was determined. The concentration of plasmid DNA suspended in elution buffer was determined to be 32.6 μg/mL with a 260/230 ratio of 1.98 (obtained via NanoDrop, ThermoFisher, Waltham, MA). The plasmid DNA was then serial diluted in SeraCare Basematrix (Milford, MA; to best replicate human specimen plasma and provide a more long-term stable control) to concentrations ranging from 1×10^8 copies/mL to 1×10^3 copies/mL and extracted via the

Roche MagNA Pure Compact with an initial input volume of 200 μL and stored in a final elution buffer volume of 100 μL using a standard plasma protocol (MagNA Pure Compact Nucleic Acid Isolation Kit 1; v.17).

Using the 6 extracted standards (1×10^8 copies/mL to 1×10^3 copies/mL), a standard curve was constructed using the Bio-Rad CFX96 real-time thermal cycler (Hercules, CA) with an r^2 value of 0.99 and a 92% overall run efficiency (PCR run parameters and conserved sequence primers will be presented in a subsequent publication). Standard-3 (1×10^6 copies per mL) was chosen to be the positive control for the experimental modified TK real-time qualitative PCR assay, with a threshold value (Ct) of 30.98 for the B8900 run and 31.9 for the ATCC/H3645 run. Reproducibility was verified by calculating a 3-day average of standard-3, run in triplicate for a total of 9 specimens. Data showed an average of 31.4 over 3 consecutive days using the 9 data points. Because a qualitative real-time PCR assay was utilized, specimen Ct values obtained during the experiment had to be back-calculated and based on the positive control used for the run to approximately extrapolate sample bacterial load(s). (A perfect PCR standard curve slope or regression line is –3.3, because the standards are made in 10-fold dilutions. This measurement correlated to a ±3.0 to 3.3 Ct change, equating to a difference of approximately 1-log; any change in log resulting in a nonwhole number was rounded based on significant figures in this experimental proof of concept to roughly estimate bacterial load (±) and to help extrapolate an experimental *S. moniliformis* growth curve under the varying conditions being tested.)

Blood Culture Bottles and Instrumentation

All time-to-detection (TTD) studies were performed using the BDFX40 automated continuous blood culture bottle instrument with BD BACTEC Plus Aerobic/F blood culture bottles (Becton Dickinson). Formulations for additional bottle type(s) can be found on the manufacturer's website (http://www.bdbiosciences.com). All organisms, whole blood inoculums, and appropriate blood culture medium bottles utilized in this study were loaded and read continuously every 10 minutes, rocked, and held at a temperature of 34.5°C on the BDFX40 automated continuous blood culture system, which utilizes fluorescence detection technology.

McFarland Turbidity Correlations Between Expected and Observed CFU/mL

McFarland turbidity values were verified using the DensiCHEK plus instrument (Biomérieux, Durham, NC) with plastic vials, and instrument quality control was performed and documented on every day of use. Suspensions of bacterial cells were made in 3 mL BHI to an approximate McFarland standard of 1.0. Serial dilutions were made, and plate counts were performed to obtain estimated CFU/mL for the starting cell suspensions. Various concentrations were also tested to best simulate real-world clinical scenarios and TTDs using automated continuous blood culture instrumentation.

BDFX40 TTD Study in the presence of 0.05% SPS When Using 10^5 CFU/mL with 10 mL Whole Blood Inoculum

Inhibitory effects of SPS on *S. moniliformis* were tested by making suspensions of bacterial cells in 3 mL BHI to McFarland turbidity values ranging from 0.92 to 1.09 with an average of 1.01 (n = 56). Serial dilutions were made to obtain estimated concentrations ranging from 10^8 to 10^5 CFU/mL. One mL of the final concentration (10^5) was then added to 10 mL anticoagulant-free whole human blood and inoculated into BD BACTEC Plus Aerobic/F blood culture bottles (Becton Dickinson). Bottles were incubated for 21 days or until alerted as positive by the instrument. For all positive bottles, TTD was recorded, Gram staining was performed, and blood bottle specimens were recultured to confirm sterility, viability, and cultivability.

Sterility Verification

Initial sterility tests were performed with 10 mL BHI broth used in the study and 10 mL whole human blood and incubated for 7 days in the BD BACTEC Plus Aerobic/F and Anaerobic Plus blood culture bottles. Sterility testing was performed for every new lot of BHI and new shipment/unit of whole human blood. Unless otherwise noted, negative results were obtained after a 7-day incubation time.

Results

Confirmation of Bacterial Species

Confirmation of all *S. moniliformis* strains (n = 56) used within this study and final identification method(s) used are reported in **Table 1**. GenBank accessions, if the final ID was confirmed via 16S, are reported in the supplemental data (Supplemental Figure 1).

Lab Medicine 2021;52;536–549 541
DOI: 10.1093/labmed/lmab009

Modified TK procedure Using Strain B8900 in 0.05% SPS to Determine Optimal Blood Volume for Growth/Detection

Experimenting with varying amounts of blood inoculum, 10 mL blood was determined to provide the best results for detection and growth/viability and propose a theoretical growth curve for the organism (**Figure 3A**). In comparison studies as described, 10 mL also provided a TTD of 33.0 hours whereas 4 mL and 7 mL failed to provide organism growth/recovery and indicated a negative result for BDFX40 detection of the organism. Raw data, interpretations, and quantitative extrapolations are shown in **Table 2**.

Expanded data with the ATCC 14647, H3645, and ATCC 14647 strains in BHI without blood or SPS can be referenced in **Figure 3B** (raw data and quantitative extrapolations not shown). As shown in the B8900 study, 10 mL blood inoculum provided ideal growth conditions, resulting in qPCR data that showed increases in growth and instrument detection at TTDs of 15 hours for ATCC 14647/H3645, whereas ATCC 14647 in BHI without blood and without SPS failed to be detected by the instrument or show viable growth after subculturing at 21 days.

S. moniliformis Growth Observations with and Without Blood Supplementation

S. moniliformis experimental growth requirements and observations with and without blood supplementation on HIA biplates are reported in **Table 3**. Results showed that 33.9% (n = 19) exhibited abundant growth (+4) on blood but showed NG on agar lacking blood supplementation (**Figure 4A**). In addition, 66.1% (n = 37) of the 56 isolates exhibited abundant growth (+4) on blood and limited or diminished growth (1–2+) on agar with no blood supplementation (**Figure 4B**).

S. moniliformis ZOI with 1 mg SPS Disks

S. moniliformis sensitivity when grown around a 1 mg SPS disk (**Figure 5**) are reported in **Table 3**. The largest ZOI recorded was 28 mm (n = 2), with the smallest being 15 mm (n = 6). The average ZOI was 19.1 mm (n = 56), with the mode being 20 mm (n = 13). We found that 76.8% (n = 43) of the specimens had to be read at 48 hours because longer incubation times were needed to accurately record a zone measurement; meanwhile, 23.2% (n = 13) could be read and interpreted after 24 hours of incubation.

McFarland Turbidity Correlations Between Expected and Observed CFU/mL and Final Inoculum Design for BDFX40 TTD Study

According to the manufacturer of the DensiCHEK plus (Biomérieux), the expected CFU/mL at a McFarland turbidity value of 1.0 yields an organism suspension of approximately 10^8. The observed CFU/mL for *S. moniliformis* at a McFarland standard of 1.0 was equivalent to an average of 10^8 ±1 log (data not shown). Because of the filamentous morphology of *S. moniliformis,* estimated CFU/mL are likely to be more variable than those for nonfilamentous bacteria. Using data available to the public via peer reviewed publications[9-12] (n = 15) and based on submitted blood culture bottles to the laboratory in our facility that previously were detected as positive (n = 2), we found that a TTD range of 25 to 35 hours seemed to be common in a majority of clinical RBF published case studies. We were able to use this understanding to test various concentrations that could be detected in a similar time frame and found 10^5 to be the ideal concentration. Over the 56 isolates tested, we obtained an average TTD of 26.5 hours.

BDFX40 TTD in the Presence of 0.05% SPS When Using 10^5 CFU/mL with 10 mL Whole Blood Inoculum

The results of the BDFX40 TTD study in the presence of 0.05% SPS when using 10^5 CFU/mL with a 10 mL whole blood inoculum are shown in **Table 3**. Briefly, for all isolates tested, 100% (n = 56) were detected or alerted as positive by the instrument when 10 mL blood inoculum was used, with the longest time required for detection 102 hours (n = 1) and the fastest TTD recorded at 13.4 hours (n = 1). The average TTD was 26.5 hours (n = 56), with a mode of 18 hours (n = 9).

Discussion

Current reported recommendations for processing specimens from a patient with suspected RBF/HF include using media supplemented with 20% serum, ascitic fluid, or whole blood, and incubation in an atmosphere of 5% to 10% CO_2. Research has reported SPS to be inhibitory at concentrations ranging from 0.0125% to 0.05%,[1-3, 13, 14] so it is

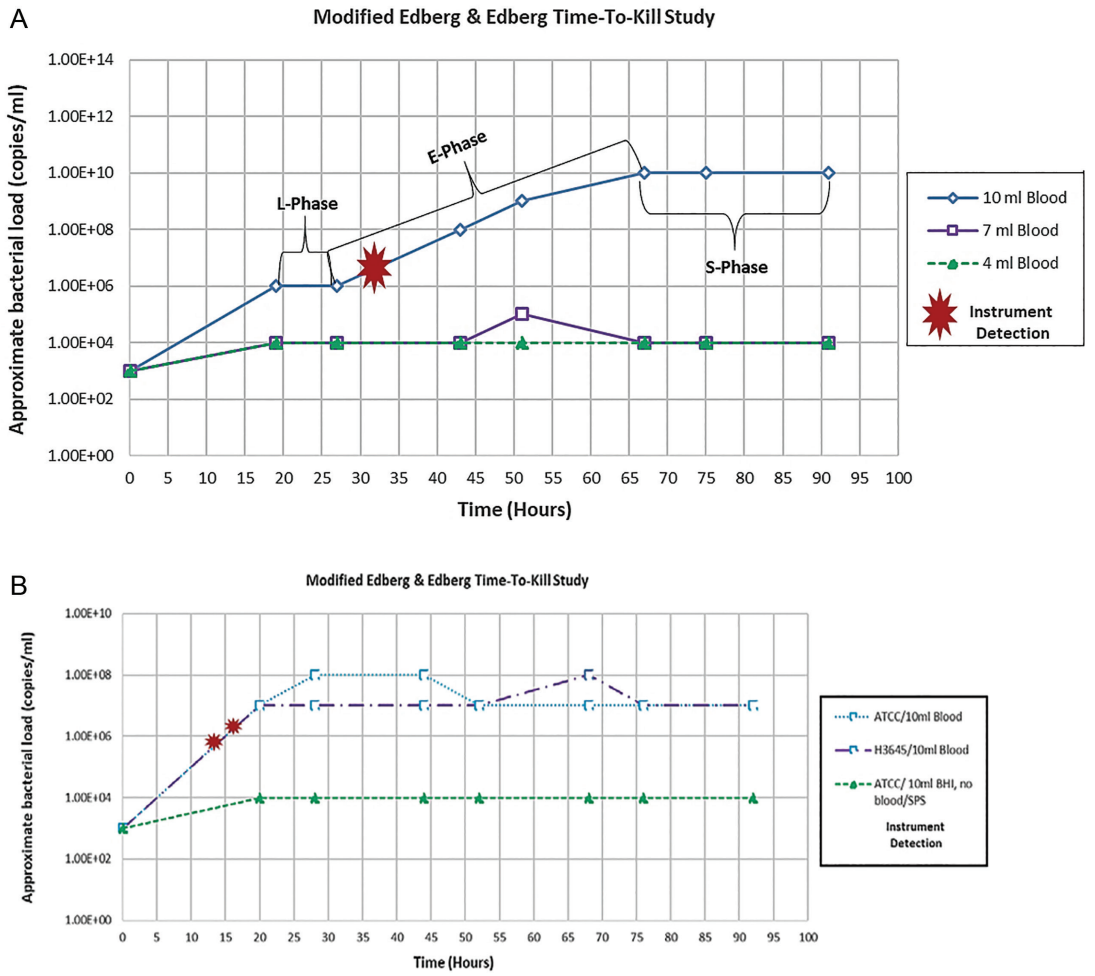

Figure 3

A. Modified Edberg and Edberg[7] TK qPCR experiment data using 4 mL, 7 mL, and 10 mL blood with strain B8900 to determine optimal blood volume and theoretical growth curve. **B.** Modified Edberg and Edberg[7] TK qPCR experiment data using 10 mL whole blood with strains ATCC 14647 (with and without blood/SPS) and H3645. qPCR, quantitative polymerase chain reaction; SPS, sodium polyanethol sulfonate; TK, time-kill.

suggested to avoid using blood culture bottles/media containing SPS as an additive altogether, but if needed, then to not exceed a concentration above 0.025%. *S. moniliformis* is best isolated from specimens such as blood, synovial fluid, and abscess material.[2] In a hospital setting, inoculation of these fluids, abscess material excluded, into a blood culture bottle and incubation in an automated continuous blood culture instrument would be standard practice. However, based on the current recommendations for this organism, blood culture bottles should be avoided because of the use of SPS.

In some resources, there is guidance to use anaerobic blood bottles when RBF is suspected, due to the absence of SPS in the formulation.[1, 2] Biomérieux and Becton Dickinson use SPS in the formulations of all their bottles. ThermoFisher Scientific uses saponin instead of SPS in its anaerobic bottle only. Although the use of anaerobic bottles for the detection of *S. moniliformis* was not tested within the scope of our study, this type of bottle is specified for use with strict anaerobes, which would exclude it from consideration for the isolation and growth of *S. moniliformis* in a clinical setting (**Table 4**). However, there have been published cases of the

Lab Medicine 2021;52;536–549
DOI: 10.1093/labmed/lmab009

Table 2. Modified TK qPCR Time Sampling, Data, and Quantification (CFU/mL) Extrapolation Using 10 mL, 7 mL, and 4 mL Blood with Strain B8900

Strain	Amount of Human Whole Blood (mL)	Amount of SPS, % (w/v)	Sampling Time (h)	Ct/Δ in Ct with PC (±)/Δ in Bacterial Load (log) (±)	Quantitative Interpretation/ Approximation (c/mL)	BDFX40 Instrument Detection (yes/no)
…	10	0.05	19.0	31.1/+0.12/0.04	1×10^6	…
…	10	0.05	27.0	30.9/0.00/0.00	1×10^6	…
…	10	0.05	43.0	24.2/–6.8/+2.3	1×10^8	…
…	10	0.05	51.0	21.6/–9.4/+3.1	1×10^9	Yes[a]
…	10	0.05	67.0	19.4/–11.6/+3.9	1×10^{10}	…
…	10	0.05	75.0	19.8/–11.1/+3.7	1×10^{10}	…
…	10	0.05	91.0	19.9/–11.1/+3.7	1×10^{10}	…
…	7	0.05	19.0	35.7/+4.7/–1.6	1×10^4	…
…	7	0.05	27.0	36.4/+5.4/–1.8	1×10^4	…
…	7	0.05	43.0	37.1/+6.1/–2.0	1×10^4	…
B8900 (MF: 1.00)	7	0.05	51.0	34.6/+3.6/–1.2	1×10^5	No[b]
…	7	0.05	67.0	37.2/+6.2/–2.1	1×10^4	…
…	7	0.05	75.0	36.6/+5.6/–1.9	1×10^4	…
…	7	0.05	91.0	37.1/+6.2/–2.1	1×10^4	…
…	4	0.05	19.0	35.1/+4.2/–1.5	1×10^4	…
…	4	0.05	27.0	35.2/+4.3/–1.5	1×10^4	…
…	4	0.05	43.0	36.8/+5.9/–1.9	1×10^4	…
…	4	0.05	51.0	35.8/+4.9/–1.5	1×10^4	No[b]
…	4	0.05	67.0	36.2/+5.3/–1.8	1×10^4	…
…	4	0.05	75.0	36.3/+5.4/–1.8	1×10^4	…
…	4	0.05	91.0	35.8/+4.9/–1.6	1×10^4	…

CFU, colony forming unit; Ct, threshold value; MF, McFarland turbidity reading; PC, positive control; qPCR, quantitative polymerase chain reaction; SPS, sodium polyanethole sulfonate; TK, time-kill.

[a]*BDFX40 time to detection was 33 hours.*

[b]*Blood culture bottle was not detected on BDFX40 after 21 days of incubation, and subculturing resulted in no growth after 72 hours.*

successful isolation and growth of *S. moniliformis* from anaerobic bottles in a clinical setting, most likely because of a varying SPS formulation, ranging anywhere from 0.025% to 0.05% depending on the manufacturer used.[9] Although this study was designed and completed specifically using the BDFX40 from Becton Dickinson, along with the blood culture bottles with a 0.05% SPS formulation also commercially produced by them, the extrapolation could be made that with other manufacturers' formulations within a similar SPS percentage, organism recovery should be achievable following these guidelines, although side-by-side comparison studies should be completed in the future.

A 1983 study that has been seemingly disregarded may be the key to unlocking many of the culturability issues seen when *S. moniliformis* is suspected. Edberg and Edberg,[7] from the clinical microbiology laboratory at Yale-New Haven Hospital (New Haven, CT), published a study on the inactivation of SPS by hemoglobin. During the course of their study, they documented the interactions between the 2 compounds, concluding that SPS and hemoglobin combined in a first-order kinetic interaction forming an insoluble precipitate, essentially inactivating the SPS. To document the protective effects of hemoglobin on SPS-sensitive organisms, they designed a TK study using strains of *N. meningitidis* and *N. gonorrhoeae.* The experiment documented the strains' growth in 0.05% SPS alone and in their hypothesized optimal ratio of 1:6 (SPS: hemoglobin; wt/wt). Specimens were taken at various timepoints ranging from 2 to 24 hours. Data were collected, and a relationship between log (CFU/mL) and time (hours) was observed. When combined with 3% hemoglobin, *N. meningitidis* and *N. gonorrhoeae* strains in 0.05% SPS showed a 3 to 4 log increase in bacterial growth when compared to the same strains in 0.05% SPS and 0% hemoglobin. The authors concluded that the hemoglobin did in fact exercise a protective effect on isolates that were SPS-sensitive.[7] This conclusion may help address and explain why so many modern laboratories are not able to reliably detect and/or grow the organism in the presence of SPS.

Table 3. *S. moniliformis* Biplate Growth, SPS Disk/ZOI, and TTD BDFX40 Data (with MF turbidity readings) for All Strains Used

	Strain Identifier	Growth on TSA Biplate (5% rabbit blood/no blood)	Observed ZOI (1 mg SPS disk; mm)	McFarland Turbidity Reading	TTD in 0.05% SPS with 10 mL Blood (h)
1	A3410	++++/+	19[a]	0.93	22.0
2	A3531	++++/+	20	0.93	18.4
3	A7171	++++/NG	18	0.93	19.6
4	B8900	++++/+	20	1.06	30.0
5	C7016	++++/NG	19	0.93	21.5
6	C7795	++++/+	28[a]	0.90	19.5
7	D7626	++++/+	15[a]	0.96	18.5
8	ATCC 14647	++++/+	20[a]	1.05	102.0
9	F2022	++++/+	20[a]	1.09	42.5
10	F1527	++++/NG	25[a]	1.03	49.4
11	F2396	++++/+	19[a]	0.96	17.3
12	F2384	++++/+	24[a]	0.96	40.6
13	F3043	++++/+	19	0.92	13.4
14	F4559	++++/+	20[a]	0.92	40.4
15	F4558	++++/+	18[a]	0.95	24.5
16	F5001	++++/+	27[a]	1.02	41.0
17	F5599	++++/+	20[a]	1.07	28.7
18	F5431	++++/+	14[a]	0.96	27.3
19	F6762	++++/NG	18[a]	0.95	22.2
20	F8454	++++/+	17[a]	0.98	23.5
21	G0716	++++/+	20[a]	1.03	19.0
22	G4934	++++/+	22	0.97	18.3
23	G6651	++++/+	20[a]	1.00	18.6
24	G6134	++++/+	23[a]	0.98	26.1
25	G6483	++++/+	18[a]	1.01	19.5
26	G7408	++++/+	15[a]	1.06	16.0
27	G7586	++++/+	18[a]	0.93	24.6
28	G7806	++++/NG	25[a]	1.05	18.1
29	G7643A	++++/+	16[a]	1.03	19.2
30	G7587	++++/+	21[a]	1.04	22.6
31	G8797	++++/NG	20[a]	1.05	17.2
32	G8599	++++/NG	17	1.08	16.2
33	G8611	++++/NG	18[a]	1.04	18.2
34	G8568	++++/+	15[a]	1.07	16.2
35	G8683A	++++/+	25[a]	0.98	16.5
36	G8718	++++/+	20[a]	1.03	23.6
37	G9007	++++/NG	25[a]	0.95	20.5
38	G9037	++++/NG	25[a]	1.06	33.3
39	G9555	++++/NG	20[a]	0.95	51.5
40	G9874	++++/NG	18[a]	1.09	18.4
41	H0896	++++/+	18	1.06	14.4
42	H0840	++++/+	20[a]	0.94	18.4
43	H1141	++++/NG	15	1.01	21.5
44	H1600	++++/NG	23[a]	1.07	20.2
45	H1736	++++/+	18[a]	0.97	26.3
46	H1765	++++/NG	25[a]	1.00	20.0
47	H1924	++++/+	23[a]	1.02	21.5
48	H2730	++++/NG	28[a]	1.01	31.6
49	H3645	++++/+	15[a]	1.15	25.0
50	H4152	++++/NG	19	1.17	30.0
51	H5065	++++/+	23	1.10	52.0
52	H6118	++++/+	17[a]	1.10	42.0
53	H6036	++++/+	17	1.01	23.4
54	H6796	++++/+	16	1.12	42.0
55	H6798	++++/NG	18[a]	0.97	22.4
56	H6799	++++/NG	15[a]	1.09	18.4

NG, no growth observed; SPS, sodium polyanethol sulfonate; TSA, Trypticase soy agar; TTD, time to detection; ZOI, zone of inhibition.
[a]*Designates a ZOI reading made at 48 hours.*

Lab Medicine 2021;52;536–549
DOI: 10.1093/labmed/lmab009

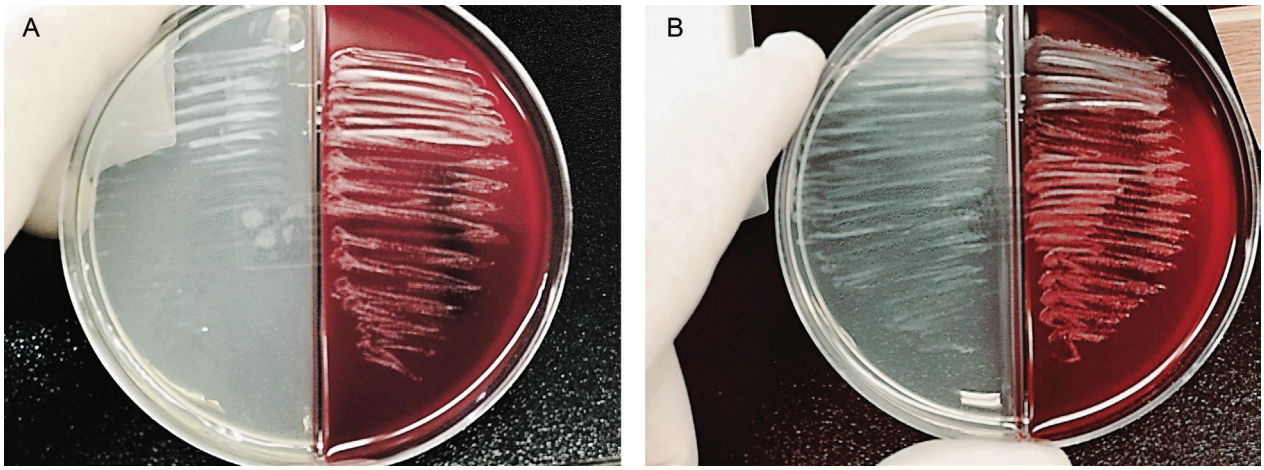

Figure 4

A. *S. moniliformis* growth on biplate with 0% and 5% rabbit blood; image shows NG on side without blood supplementation and abundant growth (4+) on side with blood supplementation after 24 to 48 hours. **B.** *S. moniliformis* growth on biplate with 0% and 5% rabbit blood; image shows diminished growth (1+/2+) on side without blood supplementation and abundant growth (4+) on side with blood supplementation after 24 to 48 hours. NG, no growth.

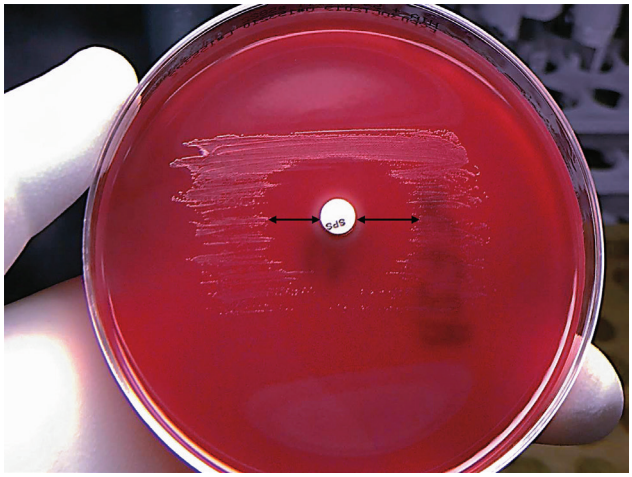

Figure 5

S. moniliformis growth showing observed ZOI ("sensitivity") with a 1 mg SPS disk on HIA with 5% rabbit blood after 24 to 48 hours of incubation. HIA, heart infusion agar; SPS, sodium polyanethol sulfonate; ZOI, zone of inhibition.

We found that in 100% of the isolates tested (and all the variations of testing within), SPS (up to a concentration of 0.05% w/v) in commercially available blood culture bottles seemed to be inactivated, allowing for the growth detection and culturing of *S. moniliformis* using an automated continuous blood culture system when 10 mL blood was inoculated. Even though inhibition and lack of growth in our modified TK experiment was observed when blood volumes of 4 mL and 7 mL were used, inhibition or "sensitivity" was better visualized when 1 mg SPS disk testing was performed. The ZOI testing using SPS disks helped us tangibly visualize SPS inhibition, if any, and document ZOIs that have never been studied in regard to *S. moniliformis.* The disks had the additional benefit of allowing us to presumptively "screen" for *S. moniliformis.* This screening was accomplished by observing either a mixed colony population

growing within the observed ZOI (n = 2; *Paenibacillus spp.)* or no zone with isolates suspected of being RBF (n = 2; *Leptotrichia spp., Streptococcus spp.).* Note that there are no published guidelines for the interpretation of SPS ZOI sizes with *S. moniliformis;* therefore, no interpretations could be made other than documenting a measurable ZOI, and these results should be considered experimental only because more data are needed.

Using the molecular data previously obtained for strain ATCC 14647 in BHI without blood or SPS, we noted that when there was a lack of blood, or no blood given to the organism as supplemental or "nutritional," then there also was no organism recovery or viable growth. This finding was further tested by using biplates with and without blood supplementation. In this experiment, 33.9% of the biplates exhibited abundant growth (4+) with blood and showed NG without blood supplementation. However, 66.1% of all isolates tested showed abundant growth (4+) with blood as well as some growth (1–2+) without blood supplementation (**Figure 4A** and **Figure 4B**). We believe that strain variation aside, this finding helps show how crucial blood supplementation is when growing the organism and offers a plausible explanation for the lack of abundant growth observed in past published studies that did not use blood supplementation with and without SPS additives.[5, 6, 15]

When we used blood culture bottles with a known concentration of 0.05% SPS, a 0.025% increase from current recommendations,[5] there was a 100% detection rate (n = 56) with the BDFX40 instrument for 10^5 CFU/mL concentrations when 10 mL blood inoculum was used, as shown in **Table 3**. To date, there have been no published studies or data discussing an infectious dose or a clinically relevant analysis between CFU growth and clinical patient severity. More studies are needed to provide more accurate data on the organism as a whole along with its growth curve and virulence.

Clinical institutions should be aware that when inoculating blood culture bottles with a high concentration of bacterial suspension (ie, $10^{8\text{-}9}$) using an automated continuous blood culture instrument, there may be a false-negative result, which our laboratory observed. Upon closer examination, it was determined that although the organism grew when subcultured at day 5, the instrument failed to detect the organism because of the high background level(s) from the whole blood (Becton Dickinson research and development department, personal communication, 30 November 2018) and the high concentration of the inoculum used (Supplemental Figure 2A, Supplemental Figure 2B, Supplemental Figure 2C). Such an elevated bacterial load presenting in a clinical patient is not likely to be observed in a real-world scenario.

Table 4. Published Amounts of Liquoid/SPS in Commercially Available Blood Culture Bottles

Manufacturer	Blood Culture Bottle Type	% SPS (w/v)
BD	BD BACTEC Peds Plus/F	0.020
BD	BD BACTEC Plus Aerobic/F	0.050
BD	BD BACTEC Standard/10 Aerobic/F	0.035
BD	BD BACTEC Plus Anaerobic/F	0.050
BD	BD BACTEC Standard Anaerobic/F	0.025
Biomérieux	BacT/ALERT FA Plus	≥0.083[a]
Biomérieux	BacT/ALERT FN Plus	≥0.083[a]
Biomérieux	BacT/ALERT PF Plus	≥0.083[a]
Biomérieux	BacT/ALERT SA Plus	0.035
Biomérieux	BacT/ALERT SN Plus	0.035
ThermoFisher	REDOX 1	0.0125
ThermoFisher	REDOX 2	None

SPS, sodium polyanethol sulfonate.
[a]Biomérieux package insert(s) for FA, FN, and PF bottles list an anticoagulant concentration of ≥0.083% but do not specifically list SPS. SPS is mentioned in the "chemical or physical indications of instability" section and briefly in "specimen collection and preparation" and is implied to be part of the formulation.

In a clinical laboratory, bloodstream infections (BSIs) are routinely identified and carried out using blood cultures submitted to the laboratory. One of the biggest issues in performing blood cultures is the inoculation volume of blood. As reported, "The optimal volume of blood that should be drawn from infants, children to adolescents and adult patients has not been well defined with absolute certainty, but past data indicate[s] that there appears to be a direct relationship between the volume of blood obtained and the ability to detect BSIs."[16]

According to previous literature, using blood culture bottles with a 0.05% SPS formulation should be avoided altogether for the growth and recovery of *S. moniliformis.*[1] We show here that even at this percentage of SPS, the organism grew successfully and was detected by the instrument 100% of the time for all 56 isolates tested in this study when the appropriate blood volume (10 mL) inoculum was used. When dealing with a closed commercial automated blood culture system with an initial broth volume of 30 mL, we found that that *S. moniliformis* was reliably and consistently detected with an inoculum of 10 mL, which is approximately 25% (40 mL total) blood when combined with 30 mL broth in a

DOI: 10.1093/labmed/lmab009

standard aerobic adult blood culture bottle. This study implies that blood volume is critical when utilizing a closed commercial automated blood culture system to detect *S. moniliformis.*

Although not addressed in this article, in patients with pediatric bacteremia, it is likely that by calculating a similar blood-to-broth ratio, the instrument should reliably detect the organism using the BD BACTEC Peds Plus pediatric bottles (Becton Dickinson). Based on the work within this article, we hypothesize that 4 to 5 mL blood in these patients would likely be sufficient volumes and required for optimal growth because commercial pediatric culture bottles contain a lower SPS concentration (0.02% w/v) overall. Evidence from both adult and pediatric studies has shown that the probability of recovering a pathogen from blood culture increases as the volume of blood increases.[15, 16]

In an effort to provide updated recommendations for specimen handling and processing when RBF or HF is suspected, we tested modern blood culture formulations and instrumentation considering past and currently published recommendations. Currently, the literature states that in infection with *S. moniliformis* as the suspected etiological agent, all media containing SPS as an additive should be avoided.[1-3, 12, 13] However, avoiding media with SPS removes a reliable tool for detecting bacteria in the blood, possibly resulting in the failure to isolate an organism and providing the clinician with little or no diagnostic help and, in the most extreme situations, a poor patient outcome.

Although more studies are needed to fully understand the effects of SPS on *S. moniliformis,* we believe that if suspected, S. *moniliformis* growth may be greatly improved if an appropriate blood volume is used for inoculation to counteract the inhibitory effects of SPS in modern blood culture bottles.

Conclusion

Any clinical team should consider RBF when presented with a patient with a history of rodent exposure and with symptoms similar to those documented for RBF or HF, which include maculopapular rash covering the extremities, fever, chills, myalgia, headache, and vomiting.

Having completed a comprehensive study of our facility's historical collection of isolates of *S. moniliformis* regarding SPS, we provide data and propose an updated recommendation that 10 mL blood be drawn at a minimum (following clinical draw guidelines) in adolescent and adult patients with suspected RBF/HF to provide the best chance of isolating the organism while limiting the occurrence of false negatives because of insufficient amounts of blood used for culture.

Optimizing the best chances for organism recovery should include aseptic collection of blood into commercial blood culture bottles (documenting the amount of blood drawn from the patient if applicable) during the acute phase of infection, collected in duplicate if possible based on total body volume. Optimal volumes of inoculation for the isolation and growth of *S. moniliformis* are 10 mL for adolescent to adult patients, extrapolated to 4 to 5 mL in a pediatric population. Bottles should be incubated for 7 days at minimum to ensure the best chance for organism recovery when working with low levels of bacteremia, and if the organism is not yet detected by day 7 then the bottles should blind subcultured to rule out a false-negative blood culture result. Automated continuous blood culturing instrumentation growth and fluorescent detection data should be checked manually during the course of incubation to rule out missed false-negative specimens, as was experienced and documented within this study (Supplemental Figure 2A, Supplemental Figure 2B, Supplemental Figure 2C).

Once a bottle shows signs of organism growth and detection, a Gram stain should be performed followed by the inoculation of blood into rabbit or sheep blood agar and BHI broth and incubated aerobically at 35°C to 37°C within a 5% CO_2-enriched (microaerophilic) environment for a minimum of 3 to 4 days. In this study, visible growth from blood culture bottles was observed for every isolate tested after 24 hours.

Clinicians and clinical scientists should recognize that by ensuring the appropriate amount of blood or specimen(s) collected from patients, they dramatically increase the likelihood of recovering and growing the suspected etiological agents, thereby directly impacting patient care and outcome. **LM**

Acknowledgments

The authors thank Ashley Simon and Margaret Williams of the Centers for Disease Control and Prevention Division of Bacterial Diseases for their help throughout the course of this study. The data obtained, which made this manuscript

possible, were greatly appreciated. The findings and conclusions in this report are those of the authors and do not necessarily represent the official position of the Centers for Disease Control and Prevention.

Supplemental Data

Supplemental figures can be found in the online version of this article at www.labmedicine.com.

References

1. Elliot SP. Rat bite fever and Streptobacillus moniliformis. *Clin Microbiol Rev.* 2007;20:13–22.
2. American Academy of Pediatrics. Rat bite fever. In: Kimberlin DW, Brady MT, Jackson MA, Long SS, eds. *Red Book: Report of the Committee on Infectious Diseases*. 31st ed. Itasca, IL: American Academy of Pediatrics; 2018: 680–682.
3. Zbinden R. Aggregatibacter, Capnocytophaga, Eikenella, Kingella, Pasteurella, and other fastidious or rarely encountered Gram-negative rods. In: Jorgenson, JH, Pfaller MA, Carrol KC, et al, eds. *Manual of Clinical Microbiology*. 2nd ed. Vol. 1. 11th ed. Washington, DC: ASM Press; 2015: 652–665.
4. Weyant RS, Moss CW, Weaver RE, et al. *Identification of Unusual Pathogenic Gram-negative Aerobic and Facultatively Anaerobic Bacteria*. 2nd ed. Baltimore, MD: Williams and Wilkins; 1995: 538–539.
5. Lambe Jr DW, McPhedran MD, Mertz J, Stewart P. *Streptobacillus moniliformis* isolated from a case of Haverhill fever. *Am J Clin Path.* 1973;60:854–860.
6. von Haebler TM, Miles AA. The action of sodium polyanethol sulphonate ("Liquoid") on blood cultures. *J Path Bact.* 1938;46:245–252.
7. Edberg SC, Edberg MK. Inactivation of the polyanionic detergent sodium polyanethol sulfonate by hemoglobin. *J Clin Microbiol.* 1983;18(5):1047–1050.
8. Morey RE, Galloway RL, Bragg SL, Steigerwalt AG, Mayer LW, Levett PN. Species-specific identification of Leptospiraceae by 16S rRNA gene sequencing. *J Clin Microbiol.* 2006;44(10):3510–3516.
9. Rodino KG, Miller NE, Pethan KD, DeSimone DC, Schuetz AN. The brief case: rat bite fever from a kiss. *J Clin Microbiol* 2019;58:e00677-19.
10. Onodera H, Uekita H, Watanabe T, et al. Rat-bite fever due to streptobacillus moniliformis in a patient without bite history: an unexpected cause of consciousness disturbance. *Jpn J Infect Dis* 2020;73(1):85–87.
11. Pena E, Jordão S, Simões MJ, Oleastro M, Neves I. A rare cause of vertebral osteomyelitis: the first case report of rat-bite fever in Portugal. *Rev Soc Bras Med Trop* 2020;53:e20190328.
12. Giorgiutti S, Lefebvre N. Rat bite fever. *N Engl J Med.* 2019;381(18):1762.
13. Eisenberg T, Glaeser SP, Blom J, Rau J, Kampfer P. Streptobacillus. In: Trujillo ME, Dedysh S, DeVos P, et al, eds. *Bergey's Manual of Systematics of Archaea and Bacteria*. https://doi.org/10.1002/9781118960608.gbm00774.pub2. Published 2018. Accessed January 28, 2021.
14. Linscott AJ. Specimen collection, transport, and acceptability. In: Leber AL, ed. *Clinical Microbiology Procedures Handbook*. 4th ed. Washington, DC: ASM Press; 2016.
15. Gonsalves WI, Cornish N, Moore M, Chen A, Varman M. Effects of volume and site of blood draw on blood culture results. *J Clin Microbiol.* 2009;47(11):3482–3485.
16. Dien Bard J, McElvania TeKippe E. Diagnosis of bloodstream infections in children. *J Clin Microbiol.* 2016;54(6):1418–1424.

Pancreatic Cancer Insights: Optimization of the Diagnostic Capacity of Tumor Biomarkers

Jose Antonio Delgado, PhD,[1,] Maria Antonieta Ballesteros, PhD,[1] María Magdalena Parera, PhD,[1] Josep Miquel Bauça, PhD[1,2]*

Laboratory Medicine 2021;52:550-557

DOI: 10.1093/labmed/lmab016

ABSTRACT

Objective: Pancreatic cancer (PC) is one of the deadliest malignancies. The aim of this study was to determine the usefulness of the carbohydrate antigen 19.9 (CA19.9)/ carcinoembryonic antigen (CEA) ratio as a diagnostic tool.

Methods: This was a retrospective observational study (2015–2019), including laboratory requests with increased CA19.9 and CEA but no previous neoplasia. Receiver operating characteristic (ROC) curve analyses were performed for the CA19.9/CEA ratio and for CA19.9 and CEA alone for the detection of PC, and cutoff values for all strategies were selected separately and in combination.

Results: A total of 373 individuals were included. The area under the curve (AUC) for CA19.9/CEA was 0.872, whereas the AUC for CA19.9 was 0.847 and for CEA was 0.554. Cutoff values with the greatest diagnostic power were CA19.9/CEA >40, CA19.9 >1130 U/mL, and CEA > 14.5 U/mL. The combination of CA19.9/CEA > 40 with CA19.9 > 550 U/mL maximized the diagnostic accuracy for PC.

Conclusion: Our results highlight the relevance of the measurement of serum CA19.9 and CEA in the detection of PC.

Keywords: gastrointestinal, clinical pathology, tumor marker, pancreas, clinical chemistry, management/administration

The main functions of pancreatic cells include the synthesis and secretion of digestive enzymes, bicarbonate, and different types of hormones. Pancreatic cancer (PC) is one of the malignancies with the highest mortality rate, despite its low prevalence.[1,2] Most PCs are adenocarcinomas, although low prevalent neoplasia has also been described, such as neuroendocrine tumors (producing insulin or glucagon) or acinar carcinomas (producing digestive enzymes). It is estimated that only 20% of pancreas carcinomas are surgically treatable upon diagnosis and among these, only half are truly resectable.[3] There are large differences in incidence between regions worldwide, highlighting the fact that lifestyle variables (smoking habit, alcohol, diet) and environmental factors could influence such variation.[4] In Europe, PC has an approximate incidence of 78,000 diagnoses/year (8,169 new diagnoses in Spain in 2019), representing the third cause of cancer deaths in Spain in 2018, with a total of 7,132,[5] and it is expected to become the second cause of death from cancer in the next decade, if the incidence does not change.[6] One of the main causes of such a poor prognosis for PC is its detection at advanced stages, especially because of the lack of specific symptoms, the absence of sensitive and specific tumor biomarkers, and the difficulties in performing imaging studies in early stages.[2]

The 2 main risk factors for the development of PC are age, with a maximum number of diagnoses between the seventh and eighth decades of life, and smoking habit, with a clear dose-response relationship.[7] Obesity and physical inactivity have also been associated with the development of PC, alongside with saturated fat–rich diets and a strong alcohol habit. Likewise, diabetes mellitus has been reported both as cause and as consequence in the first stages of PC.[8]

Icterus is one of the characteristic clinical signs of PC, along with blood glucose decompensations and abdominal pain

Abbreviations:

PC, pancreatic cancer; CA19.9, carbohydrate antigen 19.9; CEA, carcinoembryonic antigen; ROC, receiver operating characteristic; AUC, area under the curve; TM, tumor marker; OR, odds ratio; CI, confidence interval.

[1]Department of Laboratory Medicine, Hospital Universitari Son Espases, Palma, Spain, [2]Institut d'Investigació Sanitària de les Illes Balears, Palma, Spain

*To whom correspondence should be addressed.
jose.delgado@ssib.es

originating in the stomach zone and radiating to the back. Patients often refer to weight loss in previous months and a loss of appetite for no apparent reason. Most symptoms are rather unspecific, which hinders the diagnosis of PC.

No population-based screening strategies exist to date, so diagnosis is established by means of imaging studies and, ultimately, by means of a tissue biopsy (gold standard). Unlike other pathologies, simple, economic, and low-invasive methods for the early detection of PC are still lacking.

Tumor markers (TM) are different molecules (eg, carbohydrates, proteins, peptides) produced or induced by the tumor or by tissues in response to the presence of the tumor, and they can be detected and quantified in serum, biological fluids, and tissues.[9] Carbohydrate antigen 19.9 (CA19.9), also known as sialyl Lewis A, is the recommended TM in case of suspicion of malignancy of the gastrointestinal tract, with special relevance for a pancreatic orientation. Nevertheless, different sources of increased CA19.9 values exist in the absence of malignancy, including several benign pathologies (biliopancreatic, pancreatitis, cholangitis, choledocolithiasis, and kidney disease).[10,11] This fact stimulated the publication of multiple studies in which cutoff values for CA19.9 were examined, aiming to increase the capacity of this biomarker to differentiate between benign pathologies and neoplasia.[12,13] In addition, it has long been accepted that patients who are Lewis-negative (approximately 5% of the population) do not express this antigen, leading to false-negative CA19.9 values. However, Luo, Fan, et al[14] recently reported that up to 27.4% of patients who were Lewis-negative with PC had CA19.9 >37 U/mL. Pairing this together with the fact that only 65% of patients with resectable PC have elevated levels of CA19.9 in serum,[15] different authors have advised against the use of CA19.9 in the differential diagnosis of PC, although great discrepancies exist.[16-18]

Another TM used in cancer screening is carcinoembryonic antigen (CEA), a glycoprotein produced during fetal development and found in concentrations <5 ng/mL in the blood of healthy adults. This marker was the first human antigen associated with the presence of colon cancer in 1965[19] and has been widely researched as a diagnostic marker for other types of cancer.[20-24] Nevertheless, as is the situation with other tumor markers, CEA is not free from false-positive results. Some studies have suggested that values between 5 ng/mL and 10 ng/mL have a high probability of representing false-positive results as a consequence of comorbid situations, such as diabetes, smoking habit, or colorectal polyps.[25,26] Along these lines, some authors have reported false-positive values for CEA up to 20 ng/mL in patients with kidney or liver disease.[27]

The usefulness of CEA in the diagnosis of PC is still under controversy, as happens with CA19.9. Extensive research has been done on the diagnostic value of CA19.9 and CEA for PC, with inconsistent conclusions. Xing et al[28] reported that CA19.9 has a higher diagnostic value than CEA, except for specificity, which opens the door to the need for a combination of both biomarkers (CEA and CA19.9) to improve their diagnostic value and to differentiate their levels within PC stages.

The main advantages of serum TMs are the ease and readiness of their quantification (immunoassays are available in almost all clinical laboratories worldwide), their noninvasiveness (they are measured in blood or, at low frequency, in urine), and their low cost. Therefore, their implementation is healthcare is widely extended.

As mentioned above, given the nonspecific clinical symptomatology of PC, a differential diagnosis with other digestive neoplasia is usually necessary. Considering that 85% of PCs are ductal adenocarcinomas,[29] some authors have included additional TM in their diagnostic algorithms, such as CEA) secretory mucin 5AC, or carbohydrate antigen 125.[30,31]

The aim of this study was to determine the usefulness of CA19.9 in combination with CEA (CA19.9/CEA ratio) as a diagnostic tool for the differentiation of PC from benign pathology (cirrhosis, acute or chronic pancreatitis, cholangitis, choledocolithiasis) or other types of cancers in our hospital.

Materials and Methods

A retrospective observational study was performed at Hospital Universitari Son Espases (Palma de Mallorca, Spain), a tertiary-level hospital that provides healthcare for an approximate population of 325,000 individuals. The assessed period was from January 2015 to December 2019. Analytical data were obtained from the laboratory

Lab Medicine 2021;52;550–557 551
DOI: 10.1093/labmed/lmab016

information system GestLab (Indra, Spain), and the clinical information (diagnostic data and smoking habit) was extracted from the hospital information system Millennium (Cerner Corporation). The current reference intervals in our hospital for serum CA19.9 and CEA were provided by the manufacturer (Abbott Diagnostics): CA19.9 (0 U/mL–37 U/mL), CEA (nonsmokers <5 ng/mL; smokers <10 ng/mL).

Inclusion Criteria

All laboratory requests were considered if they included CA19.9 and CEA, with the results for both biomarkers above the upper limit of the reference interval (CA19.9 >37 U/mL; CEA (nonsmokers) >5 ng/mL). In the case of patients who smoked, only those with CEA values >10 ng/mL were included. Only the first request for each individual with both TMs was included in the study. Both CA19.9 and CEA were quantified using a chemiluminescent microparticle immunoassay on the Architect i2000 platform (Abbott Diagnostics).

Exclusion Criteria

Individuals with a diagnosis of neoplasia before the determination of TM were excluded, as were those individuals without a clear diagnosis in the medical records. Likewise, patients diagnosed with neoplasia after the determination of TM but with an unknown primary origin were also removed from the study.

Diagnostic Comparison: CA19.9 and CEA vs CA19.9/CEA Ratio

For each individual, age and sex were registered, and different groups were established according to the diagnoses reported on the medical records: individuals with a benign pathology, individuals with PC, and individuals with a neoplasia other than PC. Serum CA19.9 and CEA concentrations and CA19.9/CEA ratio were compared between PC and nonmalignant pathologies and between PC and other malignancies.

To determine which diagnostic strategy had a better discriminating power for PC, a receiver operating characteristic (ROC) curve analysis was performed and the area under the curve (AUC) was quantified. Based on these results, cutoff values (for CA19.9, CEA, and CA19.9/CEA) were selected for the maximization of the diagnostic performance. Cutoff values with maximal discrimination power were used to calculate the odds ratio (OR) for PC. To further complement this study regarding the diagnostic capacity of biomarkers (CA19.9 and CEA individually and the CA19.9/CEA ratio), cutoff values from a previous report on TM for PC[30] were also applied to our population.

Statistical Analysis

The Kolmogorov-Smirnov test was used to assess the normality of all variables. Differences between groups were assessed using an analysis of variance test and the Student's *t*-test if normally distributed and the Kruskal-Wallis test and Mann-Whitney *U* test if not.

We compared the AUCs using the Bamber methodology. SPSS version 24 (IBM Corp.) and XLSTAT (Addinsoft Inc.) software were used for all calculations. Statistical significance was set at 0.05.

Results

During the period studied, and after applying the above-mentioned inclusion/exclusion criteria, a total of 373 individuals with increased concentrations of CA19.9 and CEA were included in the study (**Figure 1**). Anthropometric,

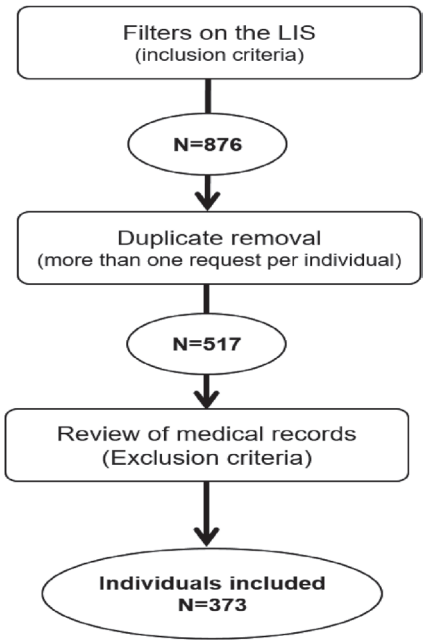

Figure 1

Flow diagram for the inclusion/exclusion of individuals in the study. LIS, laboratory information system.

biochemical, and diagnostic features are described in **Table 1**.

In 305 of the individuals included (82%), the medical records reflected a malignant pathology. Cancers with the highest incidence in our study were colorectal (109, 29%), pancreatic (63, 17%), and lung (57, 15%). Further details on the different stages of PC are presented in **Table 2**.

When assessing the variations between biomarker values for the different diagnoses (PC compared to other neoplasia and benign pathology), we observed statistically significant values. The complete list of marker comparisons among pathologies and their differences is presented in **Table 3**.

The AUC for the CA19.9/CEA ratio was 0.872 (95% confidence interval [CI], 0.824–0.920), whereas the AUC for CA19.9 was 0.847 (95% CI, 0.798–0.896) and for CEA was 0.554 (95% CI, 0.478–0.629; **Figure 2**). No statistical differences were found between the CA19.9/CEA ratio and the CA19.9 AUCs (P = .249). Both CA19.9 individually and the CA19.9/CEA ratio showed statistical differences with the CEA curve (P <.001). A cutoff value of 40 for the CA19.9/CEA ratio had the greatest discriminating power for PC, with a sensitivity of 0.810 (95% CI, 0.694–0.888) and a specificity of 0.790 (95% CI, 0.741–0.832). Regarding CA19.9 alone, the cutoff value with the greatest diagnostic accuracy was 1130 U/mL, with a sensitivity of 0.810 (95% CI, 0.694–0.888) and a specificity of 0.748 (95% CI, 0.697–0.793). For CEA, the optimal cutoff value was 14.5 U/mL, with a sensitivity of 0.576 (95% CI, 0.441–0.702) and a specificity of 0.505 (95% CI, 0.447–0.562).

The combination of the cut-off value CA19.9/CEA >40 with a value of CA19.9 > 550 U/mL had a sensitivity of 0.810 (95% CI, 0.713–0.907) and a specificity of 0.813 (95% CI, 0.764–0.854) for PC. This combination was found to have an OR of 17.7 (95% CI, 8.4–37.0) for PC. Given that the AUC for CEA alone was not better than random chance, it was decided not to include this biomarker in further analyses.

Given the enrollment ratios in our study (PC vs other types of cancer and PC vs benign pathology) and their incidence

Table 1. Descriptive Statistics of the Study Population

	Sex (Male/Female)	Age: Median (y, IQR)	Median CA19.9 (U/mL, IQR)	Median CEA (ng/mL, IQR)	Median CA19.9/CEA (IQR)
Benign disease/no reported disease	36/32	71 (64–81)	240 (61–2265)	30 (9–206)	7 (3–20)
Pancreatic neoplasia	35/28	69 (63–78)	14,716 (1966–95,163)	26 (10–117)	287 (81–2680)
Colorectal neoplasia	59/50	72 (61–80)	225 (65–1929)	36 (11–270)	7 (2–23)
Lung neoplasia	44/13	71 (64–81)	240 (61–2265)	30 (9–206)	7 (3–20)
Other neoplasia	36/40	68 (60–78)	217 (67–3446)	12 (7–53)	16 (7–85)
Total	210/163	71 (61–80)	211 (63–4779)	15 (8–107)	11 (5–84)

CA19.9, carbohydrate antigen 19.9; CEA, carcinoembryonic antigen; IQR, interquartile range.

Table 2. TM Values for PC Depending on Cancer Type and Stage

Type of PC	TM	PC Stage				
		IIA (n = 1)	IB (n = 4)	IIB (n = 2)	III (n = 11)	IV (n = 45)
Adenocarcinoma (n = 62)	Median CA19.9 (U/mL, maximum–minimum)	3639	247 (164–14,716)	6058 (115–12,000)	3366 (98–45,682)	13,515 (98–2,795,204)
	Median CEA (ng/mL, maximum–minimum)	10	8 (7–310)	13 (11–15)	10 (5–278)	18 (5–5593)
Neuroendocrine (n = 1)	Median CA19.9 (U/mL, maximum–minimum)	…	…	…	…	193
	Median CEA (ng/mL, maximum–minimum)	…	…	…	…	6

CA19.9, carbohydrate antigen 19.9; CEA, carcinoembryonic antigen; PC, pancreatic cancer; TM, tumor marker.

DOI: 10.1093/labmed/lmab016

Table 3. TM Value Comparison Between Pathologies: Statistical Significance

	CA19.9 *P* Value	CEA *P* Value	CA19.9/CEA *P* Value
Kruskal-Wallis test	<.001	<.001	<.001
Mann-Whitney *U* test			
Pancreas vs colorectal	<.001	<.001	<.001
Pancreas vs lung	<.001	.085	<.001
Pancreas vs benign	<.001	.439	<.001
Colorectal vs lung	<.001	<.001	<.001
Colorectal vs benign	.699	.372	.194
Lung vs benign	<.001	<.001	.009

CA19.9, carbohydrate antigen 19.9; CEA, carcinoembryonic antigen; PC, pancreatic cancer; TM, tumor marker.

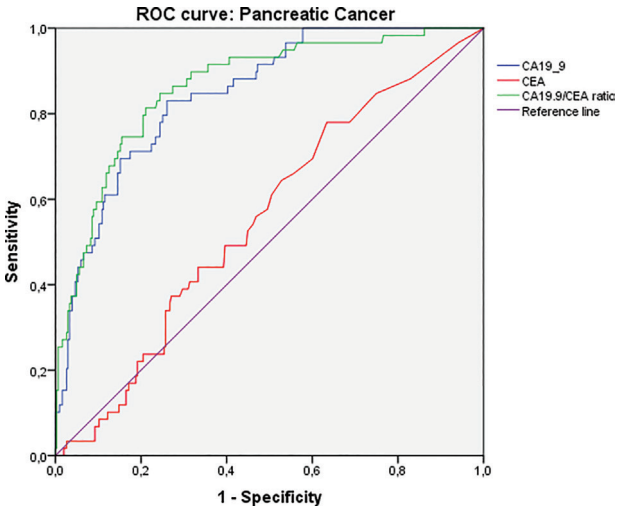

Figure 2

ROC curves: CA19.9/CEA, CA19.9, and CEA for the diagnosis of pancreatic neoplasia. CA19.9, carbohydrate antigen 19.9; CEA, carcinoembryonic antigen; ROC, receiver operating characteristic.

rates in Spain,[5,32] for a statistical power of 80% and a statistical significance of 5%, a sample size of 4725 individuals would have been needed to find significant differences between PC and other types of cancer, and a sample size of 886 individuals would have been needed to find differences between PC and benign pathology.

Discussion

This is one of the few articles assessing the usefulness of the CA19.9/CEA ratio for the diagnosis of PC. Further, this study provides a combined and optimized cutoff value for the commonly used TM for gastrointestinal neoplasia.

The use of classic serum biomarkers for the screening or diagnosis of neoplastic processes has long been under debate. To date, very few molecules are accepted for their use in the clinical setting, given the compelling number of false-positive and false-negative values in different situations.[33] It is widely accepted that most TMs are of great usefulness for the prognosis of neoplasic processes and the monitoring of therapeutic strategies, but not for screening or diagnosis. Fecal occult blood (fecal hemoglobin) for the screening of colon cancer and metanephrines for the diagnosis of pheochromocytoma are examples of the few biomarkers used in this sense. Moreover, the usefulness of prostate specific antigen for screening is under constant debate by different international associations.[34]

Current alternative approaches include the measurement of TM in biological fluids other than blood (eg, pleural fluid or cerebrospinal fluid) or the calculation of ratios between them. In this study, we evaluated the differential capacity of a TM ratio (CA19.9/CEA) for the detection of PC as compared to the absolute concentration of a classic TM (CA19.9).

Up to 82% of individuals with alterations in both CA19.9 and CEA presented a neoplastic process, which points out the relevance of the measurement of these 2 serum biomarkers in the detection of cancer. None of the individuals had a previous blood analysis of these TMs or any diagnosis of cancer before their inclusion in the study.

Our results showed statistically significant differences for both CA19.9 and for the CA19.9/CEA ratio between individuals with a diagnosis of PC as compared with other groups, including those with lung or colorectal cancer, thus verifying the diagnostic usefulness of both strategies. The use of CEA as an individual biomarker for the detection of PC was seen not to be useful in our population.

Multiple reports have evaluated and compared the diagnostic capacity of CA19.9 and CEA for PC, which were integrated in a metanalysis by Xing et al,[28] showing a higher accuracy for CA19.9. The results obtained in our study for CA19.9 and CEA in terms of sensitivity and specificity are similar to the ones reported in that meta-analysis. Nevertheless, the usefulness of their ratio was not fully

explored. Our study brought to light that, if a patient has a CA19.9 value >550 U/mL together with a CA19.9/CEA ratio >40, their risk of being affected with PC is 17.7 times higher.

The consideration of a combined TM ratio enabled the diagnostic capacity for the orientation of PC to be increased. The ROC curve analysis showed a higher AUC for CA19.9/CEA over CA19.9, albeit not statistically significant. The absence of statistical differences in our approach could stem from the low number of results or the high dispersion of CA19.9 values in both groups (PC vs other diagnoses); hence, the statistical power would not be enough to detect differences between AUCs.

A previous report by Molina, Filella, et al[30] had already assessed the capacity of the CA19.9/CEA ratio for the detection of PC and suggested cutoff values of CA19.9/CEA >5 with CA19.9 >1000 U/mL as optimal. When these criteria were applied to our population, a sensitivity of 0.81 and a specificity of 0.77 were found, representing a lower specificity than the values suggested in our study.

The identification of effective biomarkers for the early diagnosis of PC is an ongoing endeavor. Although several diagnostic biomarkers for PC have been investigated using genomic and proteomic approaches, the majority have yielded suboptimal results,[35-37] and to date none have been cleared for clinical use. Verification and validation in large cohorts are still needed for these promising biomarkers.

In addition, some studies have already compared the diagnostic capacity of TMs with imaging studies, such as endoscopic retrograde cholangiopancreatography, in the differentiation of benign pathologies from PC. Although imaging studies have been found to have a higher diagnostic yield, their combination with TMs (CA19.9 and CEA) improved diagnostic sensitivity and accuracy, reduced the rate of missed diagnosis of PC, and elevated the survival rate.[38] However, despite advanced imaging and invasive endoscopic approaches being used to differentiate PC from benign pancreatic disease, early diagnosis of PC remains a significant challenge.[39,40]

Moreover, in our study, CA19.9 levels were seen to correlate with PC stage, with maximum values in patients with stage IV disease. The Kruskal-Wallis test showed statistical differences between stages, which could underline CA19.9 as a useful biomarker for the staging and prognosis of PC.

New strategies based on the study of cell-free tumor DNA in peripheral blood, also known as liquid biopsy, are starting to be implemented for some cancer types with high incidence (eg, breast, colon, lung). In some studies, an excellent correlation has been observed between blood specimens (less invasive, with a lower risk of complications) and tissue biopsies.[41] Along these lines, it is postulated that the development and application of such DNA-based strategies will allow an early diagnosis and a lower risk of complications, which may be of special relevance for PC.[42]

This study has some limitations, mainly related to its retrospective nature and trust in the records from the laboratory and hospital information systems. Nevertheless, larger sample sizes could have enabled us to find statistically significant differences between the use of the TM ratio and the absolute concentration of CA19.9 in the differentiation of PC from other pathologies. Furthermore, the lack of inclusion of individuals with negative TM limits the diagnostic power of the cutoff values suggested in our study, because individuals with Lewis-negative antigen or those with neuroendocrine tumors (pancreatic nonfunctioning) would fall outside the scope of application of the values suggested in our study.

The main strengths of our study include a combined cutoff value for individuals with high values for both CEA and CA19.9. Future studies warrant the validation of our results and the optimization of the combined cutoff value (CA19.9/CEA ratio and CA19.9). In addition, the inclusion of a greater number of individuals will allow the consideration of a higher number of variables for analysis (diet, body mass index, alcoholic habit, presence of diabetes mellitus) and thus defining different cutoff values depending on risk factor or scoring, as already exists for a compelling number of pathologies.

From an economic and practical perspective, classic TMs are relatively inexpensive and easy-to-perform tests (automated immunoassays in peripheral blood specimens), in contrast with imaging studies. Accordingly, despite not being ideal biomarkers for the early detection of neoplasia, classic TMs are convenient tools as a first step in diagnostic strategies, and as such they provide information that complement physical examination and imaging studies.

Conclusion

Screening and diagnosis of PC is still challenging, which implies that most patients with PC are detected at advanced stages. Hence, any strategy that helps classify individuals

DOI: 10.1093/labmed/lmab016

as “potentially affected” is of great interest for this kind of cancer. LM

Acknowledgments

We adhered to the ethical guidelines approved by the ethics boards of our institutions. Consent to submit was received explicitly from all coauthors. Authors whose names appear in this article have contributed sufficiently to the scientific work and therefore share collective responsibility and accountability for the results.

Analytical data were obtained from the laboratory information system GestLab (Indra, Spain), and the clinical information was extracted from the hospital information system Millennium (Cerner Corporation).

All authors contributed to the experimental design and approved the final version of the manuscript. Study conception and design: JAD, JMB, MMP; acquisition of data: JAD, MAB; analysis and interpretation of data: JAD, JMB; drafting of manuscript: JAD, JMB; critical revision: JAD, JMB, MAB, MMP.

References

1. International Agency for Research on Cancer. Population fact sheets. https://gco.iarc.fr/today/fact-sheets-populations. Accessed March 5, 2021.
2. Kleeff J, Korc M, Apte M, et al. Pancreatic cancer. *Nat Rev Dis Primers.* 2016;2:16022.
3. Benson AB 3. Adjuvant therapy for pancreatic cancer: one small step forward. *JAMA.* 2007;297(3):311–313.
4. Raimondi S, Maisonneuve P, Lowenfels AB. Epidemiology of pancreatic cancer: an overview. *Nat Rev Gastroenterol Hepatol.* 2009;6(12):699–708.
5. Las cifras del cáncer en España 2021. Spanish Society of Medical Oncology. https://seom.org/publicaciones/el-cancer-en-espanyacom. Accessed March 5, 2021.
6. Rahib L, Smith BD, Aizenberg R, Rosenzweig AB, Fleshman JM, Matrisian LM. Projecting cancer incidence and deaths to 2030: the unexpected burden of thyroid, liver, and pancreas cancers in the United States. *Cancer Res.* 2014;74(11):2913–2921.
7. Parkin DM. Tobacco-attributable cancer burden in the UK in 2010. *Br J Cancer.* 2011;105(Suppl 2):S6–S13.
8. Bosetti C, Rosato V, Li D, et al. Diabetes, antidiabetic medications, and pancreatic cancer risk: an analysis from the International Pancreatic Cancer Case-Control Consortium. *Ann Oncol.* 2014;25(10):2065–2072.
9. Navarro Expósito F, Prieto Ríos B, Martín Angulo M, Álvarez-Mon Soto M. Indicaciones de solicitud y valor de los marcadores tumorales. *Medicine*. 2009;10(27):1854–1858.
10. Mann DV, Edwards R, Ho S, Lau WY, Glazer G. Elevated tumour marker CA19-9: clinical interpretation and influence of obstructive jaundice. *Eur J Surg Oncol.* 2000;26(5):474–479.
11. Sheen-Chen SM, Sun CK, Liu YW, Eng HL, Ko SF, Kuo CH. Extremely elevated CA19-9 in acute cholangitis. *Dig Dis Sci.* 2007;52(11):3140–3142.
12. Goonnetilleke KS, Siriwardena AK. Systematic review of carbohydrate antigen (CA19.9) as a biochemical marker in the diagnosis of pancreatic cancer. *Eur J Surgery Oncol*. 2007;33(3):266–270.
13. Cao S, Hu Y, Gao X, Liao Q, Zhao Y. Serum carbohydrate antigen 19-9 in differential diagnosis of benign and malignant pancreatic cystic neoplasms: a meta-analysis. *PLoS One.* 2016;11(11):e0166406.
14. Luo G, Fan Z, Cheng H, et al. New observations on the utility of CA19-9 as a biomarker in Lewis negative patients with pancreatic cancer. *Pancreatology.* 2018;18(8):971–976.
15. Goggins M. Molecular markers of early pancreatic cancer. *J Clin Oncol.* 2005;23(20):4524–4531.
16. Ritts RE Jr, Nagorney DM, Jacobsen DJ, Talbot RW, Zurawski VR Jr. Comparison of preoperative serum CA19-9 levels with results of diagnostic imaging modalities in patients undergoing laparotomy for suspected pancreatic or gallbladder disease. *Pancreas.* 1994;9(6):707–716.
17. Duraker N, Hot S, Polat Y, Höbek A, Gençler N, Urhan N. CEA, CA 19-9, and CA 125 in the differential diagnosis of benign and malignant pancreatic diseases with or without jaundice. *J Surg Oncol.* 2007;95(2):142–147.
18. Scarà S, Bottoni P, Scatena R. CA 19-9: biochemical and clinical aspects. *Adv Exp Med Biol.* 2015;867:247–260.
19. Gold P, Freedman SO. Specific carcinoembryonic antigens of the human digestive system. *J Exp Med.* 1965;122(3):467–481.
20. Tang S, Zhou F, Sun Y, et al. CEA in breast ductal secretions as a promising biomarker for the diagnosis of breast cancer: a systematic review and meta-analysis. *Breast Cancer.* 2016;23(6):813–819.
21. Tsai PL, Su WJ, Leung WH, Lai CT, Liu CK. Neutrophil-lymphocyte ratio and CEA level as prognostic and predictive factors in colorectal cancer: a systematic review and meta-analysis. *J Cancer Res Ther.* 2016;12(2):582–589.
22. Zhang ZH, Han YW, Liang H, Wang LM. Prognostic value of serum CYFRA21-1 and CEA for non-small-cell lung cancer. *Cancer Med.* 2015;4(11):1633–1638.
23. Nguyen AH, Miller EJ, Wichman CS, Berim IG, Agrawal DK. Diagnostic value of tumor antigens in malignant pleural effusion: a meta-analysis. *Transl Res.* 2015;166(5):432–439.
24. Deng K, Yang L, Hu B, Wu H, Zhu H, Tang C. The prognostic significance of pretreatment serum CEA levels in gastric cancer: a meta-analysis including 14651 patients. *PLoS One.* 2015;10(4):e0124151.
25. Litvak A, Cercek A, Segal N, et al. False-positive elevations of carcinoembryonic antigen in patients with a history of resected colorectal cancer. *J Natl Compr Canc Netw.* 2014;12(6):907–913.
26. Chung S. False-positive elevations in carcinoembryonic antigen levels at a health screening center. *Lab Med Online.* 2019;9(3):146–152.
27. Molina R, Bosch X, Auge JM, et al. Utility of serum tumor markers as an aid in the differential diagnosis of patients with clinical suspicion of cancer and in patients with cancer of unknown primary site. *Tumour Biol.* 2012;33(2):463–474.
28. Xing H, Wang J, Wang Y, et al. Diagnostic value of CA 19-9 and carcinoembryonic antigen for pancreatic cancer: a meta-analysis. *Gastroenterol Res Pract.* 2018;2018:8704751.
29. Ryan DP, Hong TS, Bardeesy N. Pancreatic adenocarcinoma. *N Engl J Med.* 2014;371(11):1039–1049.
30. Molina R, Filella X, Augé JM, Escudero JM. *Utilidad Clínica de los marcadores tumorales [Estado actual y perspectivas de futuro III].* Barcelona, Spain: Roche Diagnostics S.L.; 2011.
31. Kaur S, Smith LM, Patel A, et al. A combination of MUC5AC and CA19-9 improves the diagnosis of pancreatic cancer: a multicenter study. *Am J Gastroenterol.* 2017;112(1):172–183.

32. Porta M, Costafreda S, Malats N, et al. Validity of the hospital discharge diagnosis in epidemiologic studies of biliopancreatic pathology. *Eur J Epidemiol.* 2000;16(6):533–541.
33. Pavlou MP, Diamandis EP, Blasutig IM. The long journey of cancer biomarkers from the bench to the clinic. *Clin Chem.* 2013;59(1):147–157.
34. Holdenrieder S, Pagliaro L, Morgenstern D, Dayyani F. Clinically meaningful use of blood tumor markers in oncology. *Biomed Res Int.* 2016;2016:9795269.
35. Koopmann J, Rosenzweig CN, Zhang Z, et al. Serum markers in patients with resectable pancreatic adenocarcinoma: macrophage inhibitory cytokine 1 versus CA19-9. *Clin Cancer Res.* 2006;12(2):442–446.
36. Brand RE, Nolen BM, Zeh HJ, et al. Serum biomarker panels for the detection of pancreatic cancer. *Clin Cancer Res.* 2011;17(4):805–816.
37. Hasan S, Jacob R, Manne U, Paluri R. Advances in pancreatic cancer biomarkers. *Oncol Rev.* 2019;13(1):410.
38. Luo B, Peng F, Hong M, et al. ERCP combined with tumor markers in differential diagnosis of pancreatic cancer and pseudotumor-like pancreatitis. *J BUON.* 2019;24(4):1568–1573.
39. Strobel O, Büchler MW. Pancreatic cancer: FDG-PET is not useful in early pancreatic cancer diagnosis. *Nat Rev Gastroenterol Hepatol.* 2013;10(4):203–205.
40. Jenkinson C, Earl J, Ghaneh P, et al. Biomarkers for early diagnosis of pancreatic cancer. *Expert Rev Gastroenterol Hepatol.* 2015;9(3):305–315.
41. Serrano MJ, Garrido-Navas MC, Diaz Mochon JJ, et al.; International Society of Liquid Biopsy. Precision prevention and cancer interception: the new challenges of liquid biopsy. *Cancer Discov.* 2020;10(11):1635–1644.
42. Grunwald MW, Jacobson RA, Kuzel TM, Pappas SG, Masood A. Current status of circulating tumor DNA liquid biopsy in pancreatic cancer. *Int J Mol Sci*. 2020;21(20):E7651.

DOI: 10.1093/labmed/lmab016

MALDI-TOF-MS Analysis in the Discovery and Identification of the Serum Peptide Pattern of Pancreatic Ductal Adenocarcinoma

Yuan Huang, MM,[1] Feng Chen, MD,[2] Linglin Zhang, MB,[1] Qian Lv, MB,[3] Jun Yan, MD,[3] Wei Cui, MD[2,]*

Laboratory Medicine 2021;52:558-566

DOI: 10.1093/labmed/lmab024

ABSTRACT

Objective: To explore the application of serum peptidomics in the early diagnosis of pancreatic ductal adenocarcinoma (PDAC).

Methods: The serum specimens from 176 patients with PDAC and 158 healthy control patients were subjected to matrix-assisted laser desorption ionization time-of-flight mass spectrometry to obtain serum peptide profiles. Next, a classification model by differentiated peptides was established and verified to distinguish the 2 groups. Finally, the peptides were identified by tandem mass spectrometry.

Results: A classification model was established by 13 peptides. For patients with PDAC in the early stage, the sensitivity and specificity of the model reached 100% and 96.7%, respectively. The amino acid sequences of the 13 peptides were then determined and the types of proteins were identified, including platelet basic protein, fibrinogen alpha, complement C3, and secreted frizzled-related protein 4. Some of the 13 peptides could be potential PDAC biomarkers.

Conclusion: Serum peptidomics may have potential application in the early diagnosis of PDAC.

Keywords: pancreatic ductal adenocarcinoma, serum peptidomics, MALDI-TOF, mass spectrometry, gastrointestinal, clinical chemistry

Pancreatic cancer is a highly malignant tumor with a poor prognosis.[1] Pancreatic ductal adenocarcinoma (PDAC) is the most common pathological type of pancreatic cancer. On the one hand, because of the hidden anatomy of the pancreas and the atypical clinical symptoms of pancreatic cancer, early diagnosis is extremely difficult. Most patients are diagnosed at an advanced stage and have lost the best opportunity for treatment. On the other hand, there is also a lack of effective treatments for pancreatic cancer, especially for patients with pancreatic cancer lacking the opportunity for surgical resection. Therefore, to obtain the opportunity for radical surgery, early screening for pancreatic cancer is particularly important.

Compared to tissue specimens, blood specimens are easier to obtain and will change as the disease progresses. The most widely used blood marker for pancreatic cancer is CA19-9 in serum. However, a meta-analysis showed that the sensitivity and specificity of CA19-9 in the diagnosis of pancreatic cancer are approximately 80% and 80%, respectively, which fails to meet clinical needs.[2] In addition, multiple studies have shown that serum CA19-9 detection is not suitable for early screening for pancreatic cancer but can be used for therapeutic efficacy evaluation and illness monitoring

Abbreviations:

PDAC, pancreatic ductal adenocarcinoma; MALDI-TOF MS, matrix-assisted laser desorption ionization time-of-flight mass spectrometry; nano-LC/ESI-MS/MS, nanoliquid chromatography/electrospray ionization-tandem mass spectrometry; ROC, receiver operating characteristic; AUC, area under the curve; CI, confidence interval; PBP, platelet basic protein; SFRP4, secreted frizzled-related protein 4; CTAP-III, connective tissue–activating peptide III; NAP-2, neutrophil-activating peptide 2.

[1]Department of Clinical Laboratory, Peking Union Medical College Hospital, Dongcheng District, Beijing, China, [2]Department of Clinical Laboratory, Cancer Hospital, Chinese Academy of Medical Sciences, Chaoyang District, Beijing, China, [3]Bioyong Technologies Inc., Changping District, Beijing, China

*To whom correspondence should be addressed.
wendycuiwei@sina.cn; cuiwei_2020@163.com

of patients who have been diagnosed with pancreatic cancer.[3,4] Therefore, the search for reliable early diagnostic methods for pancreatic cancer and the search for new serum markers for pancreatic cancer screening have always been major foci of clinical research.

In recent years, matrix-assisted laser desorption ionization time-of-flight mass spectrometry (MALDI-TOF MS)–based serum peptidomics has been increasingly used in clinical research. Serum peptidomics is the study of serum protein fragments and endogenous peptides. Researchers have noted that the serum peptide profiles can reflect the occurrence of tumors and their biological characteristics and may contain a wealth of undeveloped disease-related information.[5] In particular, MALDI-TOF MS–based serum peptidomics expresses the serum peptide profiles in the form of mass spectrum. The mass-to-charge ratio and peak intensity of the mass spectrum reflect the molecular weight and relative abundance of serum peptides. In this study, MALDI-TOF MS–based serum peptidomics was used to distinguish between patients with PDAC and healthy control patients and to identify potential PDAC markers.

Methods

Research Objective

A training set containing 121 patients with PDAC and 110 healthy control patients was used to find differentiated characteristic peptides and to build a classification model. A validation set containing 54 patients with PDAC and 48 healthy control patients was used to validate the model. Serum from patients with PDAC treated at Peking Union Medical College Hospital of the Chinese Academy of Medical Sciences and the Cancer Hospital of the Chinese Academy of Medical Sciences (both in Beijing, China) and serum from healthy control patients were collected from November 2017 to September 2018. All patients underwent surgery or puncture biopsy to confirm the histopathologic diagnosis. None of the patients had received surgery, chemoradiotherapy, or other antitumor treatments at the time of serum collection. The enrollment criteria for the healthy control patients were routine blood tests, routine urine tests, routine stool tests, liver function tests, kidney function tests, physical examinations, chest radiographs, electrocardiograms, and abdominal ultrasound examinations with no obvious abnormalities. The patients enrolled in this study were approved by the hospital ethics committee.

Instruments and Reagents

Instruments

The instruments used in this study included the Magnetic Bead Separator (Bioyong Tech, Beijing, China), the Vortex Mixer (Scientific Industries, USA), the LX-200 Mini Centrifuge (Haimen Qilin Bell Instrument Manufacturing Co., Ltd., China), the ClinTOF MALDI-TOF MS (Bioyong Tech, Beijing, China), the Abbott ARCHITECT i2000 analyzer, the Easy-nanoliquid chromatography 1000 (Thermo Fisher), and the Q Exactive quadrupole orbit-trap mass spectrometer (Thermo Fisher).

Reagents

We used the peptide extraction kit from Bioyong Tech (Beijing, China). This kit mainly consists of magnetic beads, binding buffer, washing buffer, and elution buffer. The MALDI-TOF MS matrix solution included 5 mg/mL α-cyano-4-hydroxycinnamic acid dissolved in 50% acetone and 0.1% trifluoroacetic acid. Other reagents were guanidine (Sigma), urea (Bio-Rad), tris-hydrochloride (Bio-Rad), dithiothreitol (Bio-Rad), indole-3-acetic acid (Sigma), Zeba Spin column (Pierce), trypsin (Promega), chymotrypsin (Sigma), Glu-C (Wako), and LysC (Wako). Serum CA19-9 test kits, calibration solutions, and quality control materials of the Abbott ARCHITECT i2000 analyzer.

Research Methods

Collection of Peripheral Blood, Isolation, and Cryopreservation of Serum

All participants had 3 to 5 mL venous blood collected in the early morning on an empty stomach. It was centrifuged at 2000 g for 10 minutes, and then the upper serum was placed in a cryopreservation tube and stored at –80°C. Serum was collected at room temperature on the day of testing, and the following steps were performed after complete thawing of the serum. Repeated freeze-thaw cycles were avoided before testing.

Lab Medicine 2021;52;558–566
DOI: 10.1093/labmed/lmab024

Extraction of Serum Peptides

The peptides in the serum were extracted using a peptide extraction kit, and the operation steps were strictly performed according to the product's instructions. The basic principle of the kit was the weak positive ion exchange method combined with magnetic bead adsorption, and the extraction solutions could be directly used for the MALDI-TOF MS analysis.

MALDI-TOF MS Detection of Serum Peptide Profiles

Before specimen analysis, 3 standard peptides with different mass-to-charge ratios were used for instrument calibration. Then the peptide extraction solutions were directly used for the MALDI-TOF MS analysis. The best mass-to-charge ratio range for the MALDI-TOF MS scans was 1000 to 10,000. To reduce operating errors, 3 biological replicates were performed on each specimen to obtain the original serum peptide profiles.

Determination of Peptide Amino Acid Sequence by nanoliquid chromatography-electrospray ionization-tandem MS

First, 90 specimens were randomly selected from the disease group and mixed. Another 90 specimens were randomly selected from the control group and mixed. Finally, 2 serum peptide mixtures were formed. Trypsin endoproteinase was used to digest the serum peptide mixtures. Next, nanoliquid chromatography/electrospray ionization-tandem mass spectrometry (nano-LC/ESI-MS/MS) was used to determine the amino acid sequences of the digested samples. The nano-LC/ESI-MS/MS consisted of ultraperformance liquid chromatography and an ion-trap electrostatic field orbit-trap mass spectrometer equipped with a nano-electrospray source. Finally, Mascot software was used to identify the protein species.

Detection of Serum CA19-9

The Abbott ARCHITECT i2000 analyzer was used to detect the CA19-9 level in the serum of the disease group. Because of the low serum volume of some specimens, only 162 patients with PDAC were detected. The operation steps were carried out strictly in accordance with the product's instructions, and calibration and indoor quality control were performed before detection.

Statistical Analysis

The MALDIquant package of the R language was used to preprocess the original spectrum of the MALDI-TOF MS. Next, the linear discriminant analysis algorithm in the sda package of R was used to rank the differentially expressed peptides between the disease group and the control group. The top peptides with a high ranking (score >5) were selected as the differentiated characteristic peptides. The *t*-test and χ^2 test using SPSS 17.0 software compared age and sex between the 2 groups, respectively. Logistic binary classification regression analysis using SPSS 17.0 software established a serum peptide classification model. Receiver operating characteristic (ROC) analysis was performed with MedCalc software.

Results

Patient Characteristics

The basic clinical information on the training set and validation set participants is shown in **Table 1**. There was no significant difference in age between the disease group and the control group ($P > .05$) according to the *t*-test and no significant difference in sex between the 2 groups according to the χ^2 test ($P > .05$). There was no significant difference in age between the training set and the validation set participants ($P > .05$) according to the *t*-test and no significant difference in sex between the two sets according to the χ^2 test ($P > .05$).

Establishment and Verification of Serum Peptide Classification Model

In the analysis phase for the training set participants, serum specimens from 175 patients with PDAC and 158 healthy control patients were subjected to weak cation exchange magnetic beads combined with MALDI-TOF MS to obtain serum peptide profiles. The results showed that the peptide abundance of the disease group was significantly different from that of the control group. Through R language analysis, we found that there were 64 peptides with scores >5 in the range of m/z 1000 to 10,000, which meant that there was a total of 64 differentially expressed peptides. From these 64 differentially expressed peptides, 13 differentiated characteristic peptides were selected to establish a serum peptide classification model through logistic binary classification regression analysis using SPSS statistical analysis software. The m/z values of these 13 differentiated characteristic

Table 1. Basic Clinical Information of Training Set and Validation Set Participants

	Training Set Participants		Validation Set Participants	
	Patients with PDAC	Healthy Control Patients	Patients with PDAC	Healthy Control Patients
Number of patients	121	110	54	48
Age (y)				
Median	61	56	61	57
Range	23–82	34–70	44–83	38–68
Sex				
Male	71	62	31	28
Female	50	48	23	20
TNM classification				
Stage I/II	6/37	—	3/23	—
Stage III/IV	12/30	—	8/11	—
Unknown	36	—	9	—

PDAC, pancreatic ductal adenocarcinoma.

peptides were 1202, 1337, 1720, 1758, 2648, 2846, 2926, 3138, 3176, 3189, 3260, 4364, and 5901, respectively.

The formula of the serum peptide classification model was as follows: P=1/(1+e^(-X)), X=8.926 + 0.690×x1- 0.408×x2 + 0.668×x3 + 0.591×x4 + 0.039×x5 + 0.201×x6- 0.092×x7- 0.133×x8- 0.055×x9- 0.338×x10- 0.009×x11- 0.308×x12- 0.043×x13. In this formula, x1 to x13 represent the abundance value of the corresponding differentiated characteristic peptides: x1 = 1202, x2 = 1337, x3 = 1720, x4 = 1758, x5 = 2648, x6 = 2846, x7 = 2926, x8 = 3138, x9 = 3176, x10 = 3189, x11 = 3260, x12 = 4364, and x13 = 5901. By entering the abundance value of each differentiated characteristic peptide of a patient specimen, the probability of the value of P being classified as PDAC could be the output. The higher the P value, the higher the probability that the patient had PDAC.

Through MedCalc software, the ROC curve was drawn using the probability value P, with the area under the curve (AUC) = 0.999 (95% confidence interval [CI], 0.982–1.000; P <.0001; **Figure 1**). We set P = .5 was set as the cutoff value. When P >.5, the patient was classified by the model as a patient with PDAC. When P <.5, the patient was classified by the model as a healthy person. At this time, the sensitivity of the model to diagnose PDAC was equal to the true positive rate (118/121 = 97.52%), and the specificity was equal to the true negative rate (106/110 = 96.36%).

Subsequently, we validated the serum peptide classification model using the serum peptide results from 54 patients with PDAC and 48 healthy control patients in the validation set. The abundances of the 13 differentiated characteristic peptides from the 102 patients were input into the formula of the classification model, and the probability value P of each patient classified as having PDAC was obtained. The ROC curve was plotted using the probability value P, and the AUC was 1.000 (95% CI, 0.964–1.000; P <.0001; **Figure 1**). We set P = .5 as the cutoff value. The results showed that all 54 patients with PDAC were successfully classified as such, and the sensitivity was 54/54 (100%). Among the 48 healthy individuals, 47 were successfully classified as healthy, and 1 was misclassified (**Table 2**). The specificity was 47/48 (97.91%).

Diagnostic Effect of Serum Peptide Classification Model on PDAC in TNM Stages

We further applied the model to analyze patients with PDAC in different TNM stages. Of the 175 patients with PDAC, 130 had explicit TNM stages: 9 patients were in stage I disease, 60 were in stage II disease, 20 were in stage III disease, 41 were in stage IV disease, and 45 were in an unknown stage. The diagnostic sensitivity of the patients with PDAC with stage I disease was 100% (9/9), that of patients with stage II disease was 96.7% (58/60), that of patients with stage III disease was 95% (19/20), and that of patients with stage IV disease was 100% (19/20).

Comparison of Serum Peptide Classification Model and Serum CA19-9 in PDAC Diagnosis

A total of 162 patients with PDAC achieved CA19-9 results. Taking the upper limit of 37.0 U/mL of the 99% normal reference interval (0.0–37.0 U/mL) of CA19-9 as the cutoff value, the sensitivity of serum CA19-9 to diagnose PDAC

DOI: 10.1093/labmed/lmab024

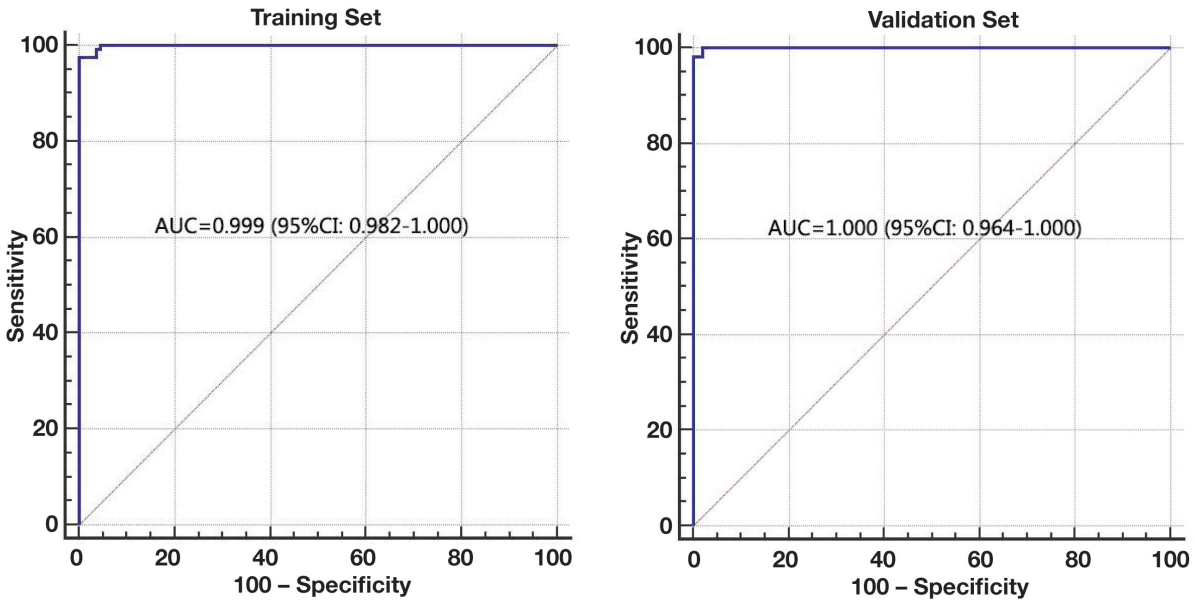

Figure 1

The ROC curves of the serum peptide classification model in the training set and the validation set. AUC, area under the curve; CI, confidence interval; ROC, receiver operating characteristic.

Table 2. Validation Results of Serum Peptide Classification Model

	Patients with PDAC	Healthy Control Patients	Total
Patients classified as PDAC by the model	54	1	55
Patients classified as healthy person by the model	0	47	47
Total	54	48	102

PDAC, pancreatic ductal adenocarcinoma.

was 124/162 (76.54%). Among these patients, 38 were CA19-9-negative. For these 38 patients, the serum peptide classification model was successfully classified as PDAC. However, the sensitivity of the serum peptide classification model to diagnose PDAC was 172/175 (98.29%).

Determination of Amino Acid Sequences of Serum Differentiated Characteristic Peptides and Identification of Protein Species

The 13 modeling differentiated characteristic peptides were successfully identified by tandem MS, including the peptide fragments of platelet basic protein (PBP), fibrinogen alpha, complement C3, and secreted frizzled-related protein 4 (SFRP4; **Table 3**). The expression heatmaps of the 13 modeling peptides are shown in **Figure 2**. The detailed expression data on the 13 peptides in the disease group and control group are shown in **Table 3**. After a *t*-test of 2 independent samples, we found that the expression of these 13 peptides in patients with PDAC was significantly different from that in healthy control patients and that the *P* values were all <.001. Of the 13 peptides, 5 peptides were significantly increased in the disease group and 8 peptides were significantly decreased in the disease group. In single-factor ROC analysis, the characteristic peptides m/z 3176, m/z 3189, m/z 3260, and m/z 5901 had relatively high AUCs for PDAC diagnosis, reaching >0.75. These 4 peptides were all peptide fragments of fibrinogen and were significantly reduced in PDAC. The AUCs of the other characteristic peptides were all <0.75, which meant that the diagnostic value for PDAC was limited.

It is worth noting that m/z 1202 (peptide fragment of PBP), m/z 1720 (peptide fragment of fibrinogen), and m/z 1758 (peptide fragment of SFRP4) were expressed only in the disease group and were not expressed in the control group. However, m/z 1337 (peptide fragment of complement C3),

Table 3. Expression and Identification of 13 Modeling Peptides in Patients with PDAC and Healthy Control Patients

Order Number	m/z	AUC	Patients with PDAC (Mean)	Healthy Control Patients (Mean)	*P* Value	Sequence	Protein Name
x1	1202	0.640	10.926 ↑	0.000	<.001	NLAKGKEESLD	Platelet basic protein (44–54)
x2	1337	0.573	0.000 ↓	8.041	<.001	THRIHWESASL	Complement C3 (1308–1318)
x3	1720	0.677	23.425 ↑	0.000	<.001	NRGDSTFESKSYKMA	Fibrinogen alpha chain (590–604)
x4	1758	0.583	10.878 ↑	0.000	<.001	GKPPAPKPASPKKNIKT	Secreted frizzled-related protein 4 (318–334)
x5	2648	0.655	34.614 ↑	20.102	<.001	KQFTSSTSYNRGDSTFESKSYKMA	Fibrinogen alpha chain (581–604)
x6	2846	0.737	32.080 ↑	3.085	<.001	SSYSKQFTSSTSYN(+.98)RGDSTFESKSY	Fibrinogen alpha chain (577–601)
x7	2926	0.606	1.998 ↓	10.382	<.001	YSKQFTSSTSYNRGDSTFESKSYKM	Fibrinogen alpha chain (579–603)
x8	3138	0.680	15.753 ↓	40.997	<.001	SYKMADEAGSEADHEGTHSTKRGHAKSRP	Fibrinogen alpha chain (600–628)
x9	3176	0.808	35.939 ↓	86.965	<.001	SSYSKQFTSSTSYN(+.98) RGDSTFESKSYKMA	Fibrinogen alpha chain (577–604)
x10	3189	0.769	0.000 ↓	23.194	<.001	SSYSKQFTSSTSYN(+.98) RGDSTFESKSYKM(+15.99)A	Fibrinogen alpha chain (577–604)
x11	3260	0.786	25.823 ↓	58.922	<.001	SSSYSKQFTSSTSYNRGDSTFESKSYKMA	Fibrinogen alpha chain (576–603)
x12	4364	0.589	0.000 ↓	7.924	<.001	NRGDSTFESKSYKMADEAGSEADHEGTHS TKRGHAKSRPV	Fibrinogen alpha chain (590–629)
x13	5901	0.775	181.527 ↓	247.626	<.001	SSSYSKQFTSSTSYN(+.98)RGDSTFESK SYKMADEAGSEADHEGTHSTKRGHAK SRPV	Fibrinogen alpha chain (576–629)

AUC, area under the curve; PDAC, pancreatic ductal adenocarcinoma.

m/z 3189 (peptide fragment of fibrinogen), and m/z 4364 (peptide fragment of fibrinogen) were expressed only in the control group and not in the disease group.

Discussion

Pancreatic cancer is the sixth leading cause of cancer death in China and the third leading cause of cancer death in the United States. Its 5-year survival rate is only 9%.[1,6] Because of the lack of highly sensitive and highly specific biomarkers related to pancreatic cancer, researchers have invested much energy into the discovery of new biomarkers. In 2009, more than 2500 biomarkers were reported for pancreatic cancer diagnosis.[7] However, none of these biomarkers have been proven to be useful in clinical practice. Although serum CA19-9 has insufficient sensitivity and specificity for the diagnosis of pancreatic cancer, it is still a commonly used biomarker for the diagnosis and treatment of pancreatic cancer.[2] Although there has been no major breakthrough in screening for new single biomarkers, the use of an MS platform for serum peptidomics analysis is a new direction for pancreatic cancer diagnosis.

During the tissue microenvironment or disease process, the body will produce peptides of various small molecular weights, which may come from the normal physiological process of the tissue microenvironment or from pathological processes. For example, during the occurrence and development of cancer, tumor cells may release certain specific proteins that are then hydrolyzed by proteolytic enzymes into small molecule fragments. On the other hand, tumor cells may also increase or decrease the activity of certain proteolytic enzymes, causing some proteins to be hydrolyzed more or less than under normal physiological conditions, thereby increasing or decreasing

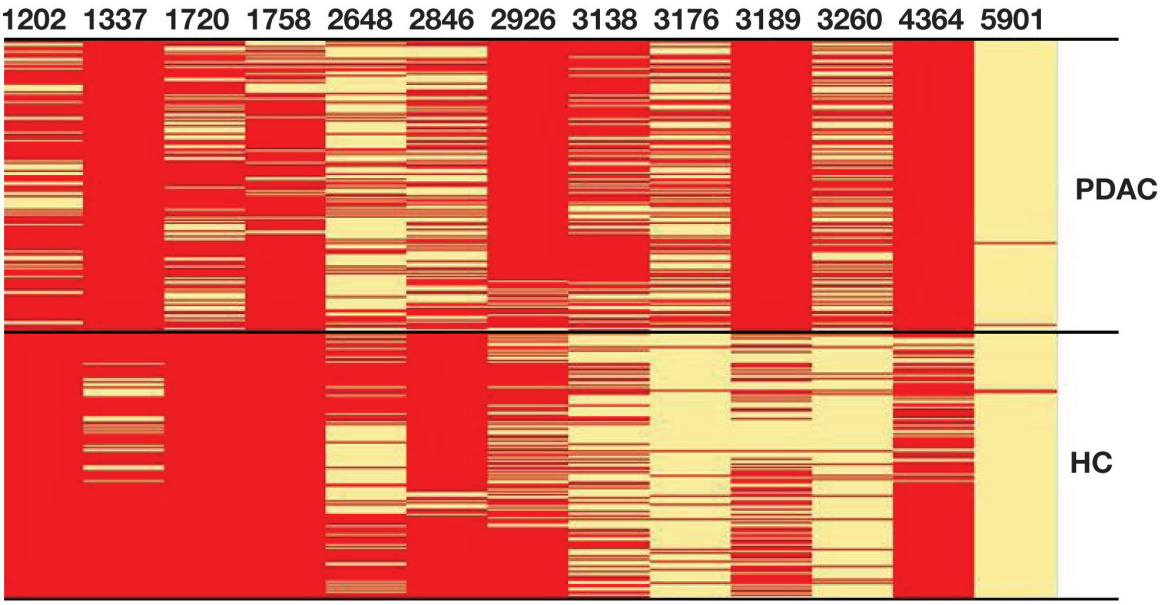

Figure 2

Heatmap of 13 modeling peptides in patients with PDAC and healthy control patients. The yellow horizontal line represents the presence of a peptide with the corresponding mass-to-charge ratio in a patient. The red horizontal line represents the absence of a peptide with the corresponding mass-to-charge ratio in a patient. HC, healthy control patients; PDAC, pancreatic ductal adenocarcinoma.

the corresponding small molecule peptide fragments. Therefore, there may be protein degradation patterns related to cancer hidden in serum peptidomics that may have potential clinical application value.[8,9]

In early screening for pancreatic cancer, some researchers, such as Andrea et al[10] and Velstra et al,[11] have used MALDI-TOF MS to make relevant explorations, but these 2 studies included relatively few patients. In this study, the serum peptide profiles of 175 patients with PDAC and 158 healthy control patients were detected by the weak cationic magnetic bead method combined with MALDI-TOF MS. The patients were randomly divided into a training set and a validation set according to a ratio of 7 to 3. In the training set, a logistic regression analysis algorithm model was established by using the abundance of 13 differentiated characteristic peptides to distinguish patients with PDAC from healthy control patients. The sensitivity and specificity of the model reached 97.52% and 96.36%, respectively, in the training set. In the validation set, the sensitivity and specificity of the model were 100% and 97.91%, respectively. For patients with stage I and II PDAC who had radical surgery opportunities, the sensitivity of this model was 100% and 96.7%, respectively. In addition, the sensitivity of CA19-9 to diagnose PDAC was only 76.54%, which was much lower than that of the serum peptide classification model. However, note that this study was a single-center study, and only internal verification was completed. The most crucial stage of clinical validation research is the blinded testing stage using independent, large clinical study sets that are drawn from separate locations.[12] Thus, there is still much work to be done to truly apply the classification model to clinical practice.

Finally, the amino acid sequences of the 13 modeling differentiated characteristic peptides were successfully determined by tandem MS, and the types of proteins were identified. The peptides m/z 1202, m/z 1720, and m/z 1758 were identified as peptide fragments of PBP, fibrinogen alpha chain, and SFRP4, respectively, and the AUCs to diagnose PDAC were 0.640, 0.677, and 0.583, respectively. Although the diagnostic efficacy of the 3 peptides was not high, they were only expressed in the disease group, not in the control group. Multiple studies have shown that SFRP4 is closely related to pancreatic cancer. Yang et al[13] found that the expression of SFRP4 in tumor lesions was higher than in adjacent nontumor tissues. Later survival analysis revealed that high expression

of SFRP4 in serum and tumor lesions predicted a poor prognosis in patients with pancreatic cancer. Our results showed that the peptide fragment of SFRP4 was only elevated in the serum of some patients with PDAC and was not expressed in healthy people. Whether its expression level in peripheral blood is related to prognosis needs further study.

M/z 1202 was the peptide fragment of PBP for amino acid sequence 44–54. PBP can be cleaved into 10 functional proteins, including connective tissue–activating peptide III (CTAP-III) and neutrophil-activating peptide 2 (NAP-2). When CTAP-III is cleaved by leukocyte lyase to produce NAP-2, it will release the peptide fragment at amino acid sequence 44–54, which happens to be the peptide fragment m/z 1202. Increased m/z 1202 levels in the serum of patients with PDAC may indicate an increase in this lysis process during the development of PDAC.

M/z 1337 is the peptide fragment of complement C3. Multiple studies have suggested that complement C3 is involved in the development of cancer.[14,15] In our study, the peptide fragment of complement C3 was significantly lower in patients with PDAC than in healthy people, meaning that complement C3 may be consumed in the development of cancer.

Among the 13 modeling peptides, there were 10 peptides belonging to the fibrinogen alpha chain. The AUCs of fibrinogen alpha chain m/z 3176, m/z 3189, m/z 3260, and m/z 5901 to diagnose PDAC were 0.808, 0.769, 0.786, and 0.775, respectively. These relatively high AUCs meant that these peptide fragments had potential value for PDAC diagnosis. Several studies have found that not only fibrinogen alpha itself but also its peptide fragments are associated with tumors. Peptide fragments of fibrinogen alpha are also thought to be tumor markers for ovarian cancer,[16] gastric cancer,[17] and bile duct cancer.[18] These results imply that the increased or decreased concentrations of peptides in tumors may originate not only from the increase or decrease in the protein itself but also from the increase or decrease in the activity of cancer-related exocrine proteases. The activity of these exocrine proteases partly coincides with the coagulation cascade, resulting in tumor-associated elevated or decreased peptide fragments in the serum.

Conclusion

We established a serum peptide classification model with 13 peptides by the weak cation magnetic bead method combined with MALDI-TOF MS technology. The classification model achieved high sensitivity and specificity to discriminate patients with pancreatic cancer from healthy control patients and provided new ideas for the further development of simple and noninvasive diagnosis methods for pancreatic cancer. In addition, the changes in the fragments of serum PBP, fibrinogen alpha, C3, and SFRP4 deepened our understanding of the mechanism of pancreatic cancer and have potential application value in the diagnosis and prognosis of pancreatic cancer. **LM**

Acknowledgments

This research was supported by two funds. The first one is Chinese Academy of Medical Sciences (CAMS) Innovation Fund for Medical Sciences (CIFMS) (Grant No. 2017-I2M-3-005 and No. 2019-I2M-2-002). The second one is Beijing Key Clinical Specialty for Laboratory Medicine - Excellent Project (No. ZK201000).

References

1. Siegel RL, Miller KD, Jemal A. Cancer statistics, 2019. *CA Cancer J Clin.* 2019;69(1):7–34.
2. Huang Z, Liu F. Diagnostic value of serum carbohydrate antigen 19-9 in pancreatic cancer: a meta-analysis. *Tumor Biol.* 2014;35(8):7459–7465.
3. Kim JE, Lee KT, Lee JK, et al. Clinical usefulness of carbohydrate antigen 19-9 as a screening test for pancreatic cancer in an asymptomatic population. *J Gastroenterol Hepatol.* 2010;19(2):182–186.
4. Steinberg W. The clinical utility of the CA19-9 tumor-associated antigen. *Am J Gastroenterol.* 1990;85(4):350.
5. Liotta LA, Ferrari M, Petricoin E. Clinical proteomics: written in blood. *Nature.* 2003;425(6961):905.
6. Chen WQ, Li H, Sun KX, et al. Report of cancer incidence and mortality in China, 2014. *Zhonghua Zhong Liu Za Zhi.* 2018;40(1):5–13.
7. Harsha HC, Kandasamy K, Ranganathan P, et al. A compendium of potential biomarkers of pancreatic cancer. *PLoS Med.* 2009;6(4):e1000046.
8. Richter R, Schulz-Knappe P, Schrader M, et al. Composition of the peptide fraction in human blood plasma: database of circulating human peptides. *J Chromatogr B.* 1999;726(1–2):25–35.
9. Zlotta AR. Differential exoprotease activities confer tumor-specific serum peptidome patterns. *J Clin Invest.* 2006;49(4):756–757.
10. Andrea P, Roberta S, Daniela B, et al. Usefulness of MALDI-TOF/MS identification of low-MW fragments in sera for the differential diagnosis of pancreatic cancer. *Pancreas.* 2013;42(4):622.

11. Velstra B, Vonk MA, Bonsing BA, et al. Serum peptide signatures for pancreatic cancer based on mass spectrometry: a comparison to CA19-9 levels and routine imaging techniques. *J Cancer Res Clin Oncol.* 2015;141(3):531–541.

12. Petricoin EF, Belluco C, Araujo RP, et al. The blood peptidome: a higher dimension of information content for cancer biomarker discovery. *Nat Rev Cancer.* 2007;6(12):961–967.

13. Yang MW, Tao LY, Yang JY, et al. SFRP4 is a prognostic marker and correlated with Treg cell infiltration in pancreatic ductal adenocarcinoma. *Am J Cancer Res.* 2019;9(2):363–377.

14. Ye J, Ren Y, Chen J, et al. Prognostic significance of preoperative and postoperative complement C3 depletion in gastric cancer: a three-year survival investigation. *Biomed Res Int*. 2017;2017:2161840.

15. Chen J, Wu W, Chen L, et al. Profiling the potential tumor markers of pancreatic ductal adenocarcinoma using 2D-DIGE and MALDI-TOF-MS: up-regulation of Complement C3 and alpha-2-HS-glycoprotein. *Pancreatology.* 2013;13(3):290–297.

16. Bergen HR, Vasmatzis G, Cliby WA, et al. Discovery of ovarian cancer biomarkers in serum using NanoLC electrospray ionization TOF and FT-ICR mass spectrometry. *Dis. Markers* 2004;19:239–249.

17. Wu C, Luo Z, Tang D, et al. Identification of carboxyl terminal peptide of fibrinogen as a potential serum biomarker for gastric cancer. *Tumor Biol.* 2016;37(5):6963–6970.

18. Sandanayake NS, Camuzeaux S, Sinclair J, et al. Identification of potential serum peptide biomarkers of biliary tract cancer using MALDI MS profiling. *BMC Clin Pathol.* 2014;14(1):7.

Is Serum-Ascites Vitamin D Gradient a Valid Marker for Diagnosing Spontaneous Bacterial Peritonitis in Patients with Cirrhotic Ascites?

Hanan Abdel Hafez, MD,[1] *Hanan Madani, MD,*[2] *Shereen Abdel Alem, MD,*[1,*] *Ahmed Farrag, MSc,*[1] *Wael Fathy, MD,*[3] *Mahmoud Abdo, MD*[1]

Laboratory Medicine 2021;52:567-573

DOI: 10.1093/labmed/lmab019

ABSTRACT

Objective: Spontaneous bacterial peritonitis (SBP) is considered the paradigmatic model of infection in patients with liver cirrhosis. Therefore, there is a need for an accurate and rapid method for SBP diagnosis. The aim of this study was to evaluate the validity of serum-ascites 25-hydroxyvitamin D (25-OH vitamin D) gradient (SADG) as a marker for diagnosing SBP in patients with cirrhotic ascites.

Methods: We conducted a cross-sectional analytic study of 88 patients with portal hypertensive ascites resulting from liver cirrhosis of any etiology. The demographic, clinical, and laboratory characteristics of the patients were recorded. The level of 25-OH vitamin D in serum and ascitic fluid was measured using high-performance liquid chromatography autoanalyzer. The SADG was calculated with the formula: 25-OH vitamin D in serum − 25-OH vitamin D in ascites.

Results: Vitamin D deficiency was detected in 89.8% of the studied patients. The SADG values ranged between 0 and 69.2 ng/mL, with a median value of 5.58 ng/mL. It was significantly lower in patients with SBP than in those without SBP ($P = .004$). The area under the curve for SADG in exclusion of SBP was 0.67 at a cutoff value of ≥5.57 ng/mL.

Conclusion: We found that SADG may be a valid marker of SBP in patients with cirrhotic ascites.

Keywords: vitamin D deficiency, spontaneous bacterial peritonitis, diagnosis, marker, serum-ascites 25-OH vitamin D gradient, cirrhotic ascites

Spontaneous bacterial peritonitis (SBP) is a bacterial infection of ascitic fluid without any intra-abdominal surgically treatable source of infection. It is also the most common infective complication of ascites because of liver cirrhosis and mostly results from gram negative bacteria.[1] When first described, its mortality exceeded 90% but has been reduced to approximately 20% with early diagnosis and treatment. The cornerstone of the diagnosis of SBP is based on a neutrophil count in ascitic fluid of >250/mm^3.[2] However, it has been suggested that the dosage of specific molecules in ascitic fluid, ie, C-reactive protein, lactoferrin, and calprotectin, may be an additional prognostic or diagnostic tool in patients with SBP.[3] With the role of vitamin D increasingly recognized in various body processes, serum-ascites 25-OH vitamin D gradient (SADG) is among these tools that have been recently investigated as a possible diagnostic marker for SBP.[4]

Vitamin D is a steroid hormone involved in several processes in addition to bone and calcium homeostasis.[5] However, vitamin D can increase innate defense and modulate the activation of lymphocytes implicated in the immune response; therefore, it has numerous additional roles such as combating bacteria and preventing both autoimmune diseases and chronic inflammatory states.[6]

Abbreviations:

SBP, spontaneous bacterial peritonitis; 25-OH D3, 25-hydroxyvitamin D3; 25-OH vitamin D, 25-hydroxyvitamin D; SADG, serum-ascites 25-OH vitamin D gradient; PMN, polymorph nuclear leukocyte; ALT, alanine aminotransferase; AST, aspartate aminotransferase; INR, international normalized ratio; HPLC, high-performance liquid chromatography; CTP, Child-Turcotte-Pugh; MELD, Model for End-Stage Liver Disease; SD, standard deviation; IQR, interquartile ratio; ROC, receiver operating characteristic; WBC, white blood cell.

[1]Endemic Medicine and Hepatology Department, Faculty of Medicine, Cairo University, Cairo, Egypt, [2]Chemical Pathology Department, Faculty of Medicine, Cairo University, Cairo, Egypt, [3]Tropical Medicine Department, Faculty of Medicine, Beni Suef University, Beni Suef, Egypt

*To whom correspondence should be addressed.
shery_2424@yahoo.com

The liver is a vital organ for vitamin D biotransformation, where vitamin D is metabolized, a process carried out by a cytochrome P450 enzyme, into 25-hydroxyvitamin D2 and 25-hydroxyvitamin D3 (25-OH D3).[7] 25-OH vitamin D (25-OH D) undergoes a second hydroxylation mainly in the kidney to form 1,25 (OH) D, known as calcitriol, the active form.[8]Research has shown that 25-OH D, the major circulating form of vitamin D, is used to determine a patient's vitamin D status.[8] Recently, 25-OH D levels have been found to be low in patients with liver cirrhosis vs in control patients, and the severity of 25-OH D deficiency in these patients correlated with the severity of liver dysfunction.[1,9,10] The causes of vitamin D deficiency in cirrhosis are the decreased number of hepatocytes, reduced exposure to sunlight, malabsorption of vitamin D, and altered hydroxylation of vitamin D because of liver impairment.[11]

Studies have found that low levels of circulating 25-OH D are associated with infections in patients with cirrhosis.[12,13] Moreover, several recent studies found that vitamin D deficiency was an independent risk factor for infection and even mortality in patients with liver cirrhosis.[14,15]

The diagnosis of SBP is based on neutrophil count in the ascitic fluid > 250/mm^3 as determined by microscopy.[2] The serum-ascites 25-OH vitamin D gradient (SADG) is a novel index in the diagnosis of SBP. The SADG, calculated as the difference between serum and ascites vitamin D, was recently explored by Buonomo et al,[4] aiming to investigate the role of vitamin D levels in ascitic fluid in patients with SBP, and concluded that the SADG was significantly lower in patients with SBP than in those without SBP. However, data in the literature on the SADG as a potential diagnostic biomarker in the diagnosis of SBP in patients with cirrhotic ascites are scarce.

Therefore, this study was conducted to assess the validity of the SADG as a marker for diagnosing SBP in patients with cirrhotic ascites and to identify a cutoff level that can be used for SBP diagnosis.

Patients and Methods

Patient Populations

Between October 2019 and March 2020, patients with portal hypertensive ascites because of liver cirrhosis of any etiology presenting to the Endemic Medicine and Hepatology Department, Faculty of Medicine, Cairo University were consecutively recruited into the cross-sectional analytic study. Patients with cirrhotic ascites aged ≥18 years were recruited. Furthermore, patients who presented with SBP that was diagnosed according to current guidelines by an elevation of ascitic fluid absolute polymorph nuclear leukocyte (PMN) count (≥250 cells/mm^3) were also included in the study.[2] Patients with ascites from causes other than portal hypertension (eg, ascites from peritoneal diseases, malignant ascites, nephrogenic ascites, and pancreatic ascites), infection other than SBP, or patients who received oral vitamin D supplementation in the previous 12 months were excluded. The patients were further subdivided into 2 groups according to the presence or absence of SBP. Group I comprised 44 patients with SBP, and group II comprised 44 patients without SBP; these patients served as a control group.

Patients were subjected to detailed history including demographic data, date of diagnosis of liver cirrhosis, manifestations of hepatic decompensation, etiology of cirrhosis, and date of developing ascites and underwent clinical examination with special emphasis on stigmata of chronic liver disease such as ascites, splenomegaly, spider naevi, palmar erythema, lower limb edema, and gynecomastia in addition to general and local signs of peritonitis and its sequelae (signs of hepatic encephalopathy, reduced urine output or bleeding).

Laboratory evaluation included complete blood count, liver biochemical profile (total serum bilirubin, liver enzymes [alanine aminotransferase (ALT), aspartate aminotransferase (AST)], serum albumin, and the international normalized ratio [INR]), renal function tests (serum urea and creatinine), and electrolytes (serum sodium and potassium); all chemistry analysis was performed on a Beckman Coulter AU680 autoanalyzer according to the manufacturer's methods. In addition, serum 25-OH D was measured on the same day that the patient underwent diagnostic paracentesis.

Regarding ascitic fluid analysis, specimens were examined for PMN cell count using manual microscopy, ascitic fluid chemistry including total proteins and albumin on a Beckman Coulter AU680 autoanalyzer, and 25-OH D level in the ascitic fluid using the high-performance liquid chromatography (HPLC) autoanalyzer Agilent 1260.[16] The severity of liver diseases was assessed using the Child-Turcotte-Pugh (CTP) score[17] and the Model for End-Stage Liver Disease (MELD).[18] All patients underwent abdominal ultrasonography to examine liver size and texture, portal vein diameter, spleen size, and splenic vein diameter, to grade the amount of ascites, and to exclude focal hepatic lesions.

Ultrasonographic criteria for the diagnosis of cirrhosis included volume redistribution of the right and left liver lobes, the presence of surface nodularity, the coarseness of texture, the attenuation of hepatic veins, and signs of portal hypertension such as a dilated portal vein (≥14 mm), splenomegaly, ascites, and collaterals.[19]

Measurement of 25-OH D

25-OH D3, after deproteinization with a specific reagent and after purification with Clean-up Columns (extraction with a solid phase extraction column), was injected directly into the isocratic HPLC system (HPLC Agilent 1260). It had sensitivity up to 1.5 ng/mL with a linearity of 2 to 500 ng/mL for detection. Serum 25-OH D3 concentrations <20 ng/mL were defined as severe vitamin D deficiency, levels from 21 to 29 ng/mL were considered as insufficient, and serum levels from 30 to 100 ng/mL were considered normal.[20] The SADG was calculated with the following formula: 25-OH D in serum — 25-OH D in ascites.[4]

The study was designed to respect all ethical guidelines issued by the 1975 Declaration of Helsinki and was approved by the institutional review board of the Faculty of Medicine, Cairo University. Informed consent was obtained before specimen collection.

Statistical Analysis

Descriptive statistics were calculated, categorical variables were presented as frequency and percentages, and numerical variables were presented as mean (standard deviation [SD]) or median (IQR). A comparison between the 2 independent groups was done using the independent-samples *t*-test or the Mann-Whitney *U* test according to the normality of data. For categorical variables, the comparison was done with the χ^2 test. The receiver operating characteristic (ROC) curve was constructed to assess the diagnostic ability of the SADG in detecting SBP. We used STATA 15 for the analysis and deemed *P* values <.05 as significant.

Results

Eighty-eight patients with portal hypertensive ascites resulting from liver cirrhosis of any etiology were included in the present study. The main characteristics of the patients are summarized in **Table 1**. The mean age of patients with SBP was 55.9 years (range, 37–80 years) with male predominance (77.3%), and the mean age of patients without SBP was 58.3 years (range, 42–77 years) with male predominance (59.1%) as well. Regarding the severity of liver diseases, all the patients in both groups were CTP class C or B, and none of them were classified as CTP class A. Specifically, among the 88 patients, 38 (43.2%) belonged to CTP class B and 50 (56.8%) belonged to CTP class C. In addition, there was no statistically significant difference in the CTP or the MELD scores between the 2 groups (*P* = .7 and *P* = .9, respectively).

In comparing the laboratory characteristics in patients with SBP and patients without SBP as shown in **Table 2**, it was observed that the patients with SBP had a significant lower median hemoglobin level (7.45 g/dL [IQR, 4.9–9.3] vs 8.9 g/dL [IQR, 7.15–10.7]; *P* = .03) and a significant higher median blood urea nitrogen level (66 mg/dL [IQR, 42–125.5] vs 49.5 mg/dL [IQR, 29.5–84.5]; *P* = .02). Notably, no difference was observed in relation to analyses on the following laboratory variables: white blood cell (WBC) count, platelets, AST, ALT, total serum bilirubin, serum albumin, INR, and serum creatinine.

Vitamin D deficiency was observed in the majority of the studied patients (n = 79/88, 89.8%). Moreover, it was observed that patients with SBP had nonsignificantly lower

Table 1. Demographic Features of Both Studied Groups

Variables	Patients with SBP (n = 44)	Patients without SBP (n = 44)	*P* Value
Age (y)	55.9 (11.43)	58.3 (7.95)	.3
Sex			
Male	34 (77.3%)	26 (59.1%)	.07
Female	10 (22.7%)	18 (40.9%)	
Severity of liver disease			
A-CTP			
1-score	10.3 (1.7)	10.11 (2.002)	.7
2-class			
B, n (%)	18 (40.9%)	20 (45.5%)	.7
C, n (%)	26 (59.1%)	24 (54.5%)	
B-MELD score	21.6 (6.22)	21.5 (8.1)	.9

CTP, Child-Turcotte-Pugh; MELD, Model for End-Stage Liver Disease; SBP, spontaneous bacterial peritonitis.
Data are expressed as the mean (SD), or number (%).

DOI: 10.1093/labmed/lmab019

median serum 25-OH D in relation to patients without SBP (7.3 [IQR, 4.7–14.7] vs 9.4 [5.8–15.3]; *P* = .2), but the median level of 25-OH D in ascitic fluid did not differ between patients with or without SBP (*P* = .08) as shown in **Table 2**.

We used CTP class to evaluate the severity of the liver disease and found no significant difference between the CTP class and the status of the serum 25-OH D level in the studied patients (*P* = .4). We also noted that the mean value of serum 25-OH D was lower in CTP class B than in CTP class C with no significant difference between them (11.5 [SD, 8.002] ng/mL vs 12.2 [SD, 12.8] ng/mL; *P* = 7), but the median value of 25-OH D in the ascitic fluid was significantly higher in CTP class B than in CTP class C (2.7 ng/mL [IQR, 1–4.1] vs 1 ng/mL [IQR, 1–1]; *P* = .0007), as shown in **Table 3**.

In the entire sample of patients, the SADG values ranged between 0 and 69.2 ng/mL, with a median value of 5.58 ng/mL (IQR, 3.02–12.2). They were significantly lower in patients with SBP than in those without SBP (3.45 ng/mL [IQR, 2.45–11.95] vs 8.75 ng/mL [IQR, 5–13.3]; *P* = .004), as shown in **Table 2**. However, the median SADG did not differ significantly between patients in CTP class B and in CTP class C (5.2 ng/mL [IQR, 3–10] vs 7 ng/mL [IQR, 3.1–13]; *P* = .5), as shown in **Table 3**.

An ROC curve was designed to evaluate the ability of the SADG in exclusion of SBP; results showed a SADG with a cutoff value of ≥5.57 ng/mL had a sensitivity of 70.5%, a specificity of 68.2%, an overall accuracy of 69.32%, and an area under the curve of 0.67, as shown in **Figure 1**.

Table 2. Analysis of Laboratory Characteristics of Both Studied Groups

Variables	Patients with SBP (n = 44)	Patients without SBP (n = 44)	*P* Value
Laboratory parameters			
White blood cell ($\times 10^3/mm^3$)	8.5 (7.8–10.3)	8.4 (5.85–9.85)	.08
Hemoglobin (g/dL)	7.45 (4.9–9.3)	8.9 (7.15–10.7)	.03[a]
Platelets ($\times 10^3/mm^3$)	77 (56–128)	82.5 (70.5–129.5)	.4
AST (U/L)	51 (37–79.5)	54 (36–76)	.9
ALT (U/L)	24 (13–37.5)	26 (21.5–41)	.5
Total bilirubin (mg/dL)	3.15 (1.2–5.7)	2.2 (1.1–3.4)	.1
Albumin (g/dL)	2.4 (2.1–2.9)	2.15 (1.9–2.8)	.3
INR	1.6 (1.4–1.8)	1.67 (1.39–2)	.4
Blood urea nitrogen level (mg/dL)	66 (42- 125.5)	49.5 (29.5–84.5)	.02[a]
Creatinine (mg/dL)	1.2 (0.98–1.5)	1.1 (0.7- 1.65)	.3
Ascitic fluid analysis			
TLC (mm^3)	410 (360–1360)	110 (60–290)	.09
SAAG (g/dL), mean (SD)	1.87 (0.37)	1.74 (0.33)	.08
Serum 25-OH vitamin D (ng/mL)	7.3 (4.7–14.7)	9.4 (5.8- 15.3)	.2
Ascitic fluid 25-OH vitamin D (ng/mL)	1 (1–4.1)	1 (1–2.2)	.08
SADG (ng/mL)	3.45 (2.45–11.95)	8.75 (5–13.3)	.004[a]

ALT, alanine aminotransferase; AST, aspartate aminotransferase; INR, international normalized ratio; SAAG, serum-ascites albumin gradient; SADG, serum-ascites 25-OH vitamin D gradient; SBP, spontaneous bacterial peritonitis; SD, standard deviation; TLC, total leukocyte count.
Data are expressed either as mean (SD) or median (IQR).
[a]Values were statistically significant.

Discussion

SBP is considered the paradigmatic model of infection in patients with liver cirrhosis and is peculiar to those with the decompensated disease, being associated with significant morbidity and mortality. In addition to the diagnostic tools available, multiple efforts have been developed for the rapid diagnosis of SBP. The SADG is among these tools that have been recently investigated

Table 3. Vitamin D Assessment in Relation to Liver Disease Severity

Variables	CTP Class B (n = 38)	CTP Class C (n = 50)	*P* Value
Vitamin D status n (%)			
Sufficient	3 (7.9%)	1 (2%)	.4
Insufficient	2 (5.3%)	3 (6%)	
Deficient	33 (86.8%)	46 (92%)	
Serum 25-OH D (ng/mL), mean (SD)	11.5 (8.002)	12.2 (12.8)	.7
Ascitic fluid 25-OH D (ng/mL)	2.7 (1–4.1)	1 (1–1)	.0007[a]
SADG (ng/mL)	5.2 (3–10)	7 (3.1–13)	.5

CTP, Child-Turcotte-Pugh; IQR, interquartile ratio; SADG, serum-ascites 25-OH vitamin D gradient; SD, standard deviation.
Unless otherwise stated, numerical data are expressed as mean (SD) or median (IQR).
[a]Statistically significant value.

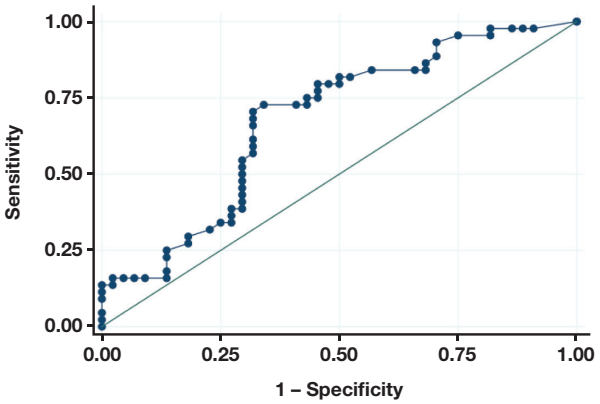

Variable	Cutoff Point	AUC	Sensitivity	Specificity	Overall Accuracy
SADG (ng/mL)	≥5.57	0.67	70.5%	68.2%	69.32%

Figure 1

ROC curve analysis of validity of SADG in exclusion of SBP. AUC, area under the curve; ROC, receiver operating characteristic; SADG, serum-ascites 25-OH vitamin D gradient; SBP, spontaneous bacterial peritonitis.

as a possible diagnostic marker for SBP.[4] This study was conducted to assess the validity of the SADG as a marker for diagnosing SBP in patients with cirrhotic ascites.

In reviewing the laboratory characteristics, we noted that there were no significant differences concerning WBC count, serum albumin, total serum bilirubin, or INR between patients with and without SBP. Similar findings were noted by the Evans et al. study,[21] which assessed 427 patients with ascites and observed that 3.5% had SBP. At the same time, we noticed that there was an increase in WBC count in the SBP group when compared to the non-SBP group; this finding could help predict the appearance of SBP in patients with ascites with no clinical signs or symptoms of infection, owing to the immunocompromised state observed in liver cirrhosis.[22]

In addition, we observed that patients in the SBP group showed a nonsignificant increase in serum creatinine compared with those in the non-SBP group (P = .3), whereas the blood urea nitrogen level was significantly higher in those in the SBP group compared with the level in those in the non-SBP group (P = .02). Patients with cirrhosis are susceptible to renal dysfunction as a result of a variety of etiologies, and measures of renal dysfunction (serum creatinine, blood urea nitrogen/azotemia) are strong predictors of mortality in decompensated cirrhosis.[23] Infection, particularly SBP, is a common precipitating factor of renal dysfunction in cirrhosis and may be associated with septic shock in up to 10% of patients.[2,24] Traditionally, the diagnosis of renal dysfunction in liver disease is still based on serum creatinine, but it is not a reliable marker of renal function in cirrhosis because it still has several well-known limitations.[25]

The classic function of vitamin D is to regulate calcium homeostasis and bone formation and resorption. However, vitamin D could increase innate defense and modulate the activation of lymphocytes implicated in the immune response,[26] so vitamin D insufficiency may predispose to or increase the risk of bacterial infections and SBP in patients with cirrhosis.[7] We observed a high prevalence of vitamin D deficiency in our patients (n = 79/88, 89.8%), and patients with SBP had lower serum 25-OH D concentrations than patients without SBP. These findings were consistent with the observations of Zhang, Zhao, and Ma,[11] who showed a high prevalence of vitamin D insufficiency in patients with cirrhosis and ascites. Moreover, the authors found that serum vitamin D deficiency was observed in patients with SBP. A low level of vitamin D in patients with chronic liver disease (CLD) may be attributed to several mechanisms such as insufficient exposure to sunlight or an inadequate dietary intake of vitamin D.[11] In addition, patients affected by chronic liver disease may have impeded intestinal luminal absorption of the dietary sources of vitamin D because of intestinal edema, which complicates portal hypertension, or to cholestasis-induced bile salt disruption.[27]

Furthermore, we used CTP class to evaluate the severity of liver disease in relation to the status of vitamin D. We found that 92% of patients with CTP class C had vitamin D

DOI: 10.1093/labmed/lmab019

deficiency, indicating that vitamin D status may be determined in part by chronic liver disease severity. Our finding was in agreement with the results of Arteh et al[9] and Fisher and Fisher,[26] who showed that patients with cirrhosis have much lower vitamin D concentrations than patients without cirrhosis.

In the current study, however, the SADG was found to be significantly lower in patients with SBP than in those without SBP. This finding agrees with the results of Buonomo et al,[4] who investigated 54 patients with liver cirrhosis and ascites for the possible role of vitamin D in ascites in patients with SBP. The available evidence indicates that there seems to be a compartmentalization of vitamin D from serum to ascites in patients with SBP that exists to increase local, peritoneal levels of vitamin D, which acts as a chemotactic and antibacterial agent that exerts its effects locally in ascitic fluid. This compartmentalization could explain our finding of a low SADG in patients with SBP. Our results are also potentially in accordance with those obtained by Trépo et al,[27] who reported a tendency to an increased incidence of SBP (15.7% vs 6.9%) in patients with cirrhosis with vitamin D deficiency.

Another important finding of this study based on the ROC curve was that the SADG with a cutoff value of ≥5.57 ng/mL had a sensitivity of 70.5%, a specificity of 68.2%, and an area under the curve of 0.67 in exclusion of SBP.

Vitamin D deficiency is associated with an increased incidence of bacterial infections and increased all-cause mortality risk in patients with liver cirrhosis.[13,14] Indeed, it can modulate the host's innate and adaptive immune defense mechanisms through diverse immunomodulatory functions mediated by the vitamin D receptor.[28] On the level of ascites, this immunological role seems to be carried out through vitamin D–mediated enhancement of peritoneal leukocytic, phagocytic, chemotactic, and antimicrobial effects, including in particular the antimicrobial peptide cathelicidin.[29,30]

Conclusion

We found that a lower SADG was associated with SBP in patients with cirrhotic ascites and that it may be a valid marker for diagnosing SBP in such patients. Vitamin D deficiency is universal in patients with cirrhotic ascites regardless of SBP diagnosis. Adequate vitamin D is vital for the body to improve antimicrobial immune response.

This study has some limitations. We assessed the diagnostic significance of the SADG in SBP diagnosis in patients with cirrhotic ascites and excluded those who received vitamin D supplementation from our study. Therefore, more powered studies are needed to determine whether SADG has any prognostic significance in patients with SBP and to establish a reliable cutoff value for diagnosing SBP. The response of the SADG and the recurrence of SBP after vitamin D supplementation need further evaluation. **LM**

References

1. Gentile I, Buonomo AR, Scotto R, Zappulo E, Borgia G. Infections worsen prognosis of patients with cirrhosis irrespective of the liver disease stage. *Eur J Intern Med.* 2017;46:e45–e47.
2. European Association for the Study of the Liver. EASL Clinical Practice Guidelines for the management of patients with decompensated cirrhosis. *J Hepatol*. 2018;69(2):406–460.
3. Kadam N, Acharya S, Shukla S, Gupta K. Ascitic fluid high sensitive C-reactive protein (hs-CRP). a prognostic marker in cirrhosis with spontaneous bacterial peritonitis. *J Clin Diagn Res.* 2016;10(4):OC20–OC24.
4. Buonomo AR, Arcopinto M, Scotto R, et al. The serum-ascites vitamin D gradient (SADG): a novel index in spontaneous bacterial peritonitis. *Clin Res Hepatol Gastroenterol.* 2019;43(4):e57–e60.
5. Pludowski P, Holick MF, Grant WB, et al. Vitamin D supplementation guidelines. *J Steroid Biochem Mol Biol.* 2018;175:125–135.
6. Baeke F, Takiishi T, Korf H, Gysemans C, Mathieu C. Vitamin D: modulator of the immune system. *Curr Opin Pharmacol.* 2010;10(4):482–496.
7. Cheng JB, Motola DL, Mangelsdorf DJ, Russell DW. De-orphanization of cytochrome P450 2R1: a microsomal vitamin D 25-hydroxilase. *J Biol Chem.* 2003;278(39):38084–38093.
8. Rosen JC. Vitamin D insufficiency. *NEJM* 2011;364:248–254.
9. Arteh J, Narra S, Nair S. Prevalence of vitamin D deficiency in chronic liver disease. *Dig Dis Sci.* 2010;55(9):2624–2628.
10. Stokes CS, Volmer DA, Grünhage F, Lammert F. Vitamin D in chronic liver disease. *Liver Int.* 2013;33(3):338–352.
11. Zhang C, Zhao L, Ma L, et al. Vitamin D status and expression of vitamin D receptor and LL-37 in patients with spontaneous bacterial peritonitis. *Dig Dis Sci.* 2012;57(1):182–188.
12. Anty R, Tonohouan M, Ferrari-Panaia P, et al. Low levels of 25-hydroxy vitamin D are independently associated with the risk of bacterial infection in cirrhotic patients. *Clin Transl Gastroenterol.* 2014;5:e56.
13. Finkelmeier F, Kronenberger B, Zeuzem S, Piiper A, Waidmann O. Low 25-hydroxyvitamin D levels are associated with infections and mortality in patients with cirrhosis. *PLoS One.* 2015;10(6):e0132119.
14. Yang F, Ren H, Gao Y, Zhu Y, Huang W. The value of severe vitamin D deficiency in predicting the mortality risk of patients with liver cirrhosis: a meta-analysis. *Clin Res Hepatol Gastroenterol.* 2019;43(6):722–729.

15. Stokes CS, Krawczyk M, Reichel C, Lammert F, Grünhage F. Vitamin D deficiency is associated with mortality in patients with advanced liver cirrhosis. *Eur J Clin Invest.* 2014;44(2):176–183.
16. Keyfi F, Nahid S, Mokhtariye A, et al. Evaluation of 25-OH vitamin D by high performance liquid chromatography: validation and comparison with electrochemiluminescence. *J Anal Sci Technol* 2018;9:25.
17. Child CG, Turcotte JG. Surgery and portal hypertension. *Major Probl Clin Surg.* 1964;1:1–85.
18. Kamath PS, Kim WR; Advanced Liver Disease Study Group. The model for end-stage liver disease (MELD). *Hepatology.* 2007;45(3):797–805.
19. Berzigotti A, Piscaglia F. Ultrasound in portal hypertension—part 1. *Ultraschall Med.* 2011;32(6):548–568.
20. Holick MF, Binkley NC, Bischoff-Ferrari HA, et al.; Endocrine Society. Evaluation, treatment, and prevention of vitamin D deficiency: an Endocrine Society clinical practice guideline. *J Clin Endocrinol Metab.* 2011;96(7):1911–1930.
21. Evans LT, Kim WR, Poterucha JJ, Kamath PS. Spontaneous bacterial peritonitis in asymptomatic outpatients with cirrhotic ascites. *Hepatology.* 2003;37(4):897–901.
22. Kasztelan-Szczerbinska B, Słomka M, Celinski K, Serwacki M, Szczerbinski M, Cichoz-Lach H. Prevalence of spontaneous bacterial peritonitis in asymptomatic inpatients with decompensated liver cirrhosis—a pilot study. *Adv Med Sci.* 2011;56(1):13–17.
23. D'Amico G, Garcia-Tsao G, Pagliaro L. Natural history and prognostic indicators of survival in cirrhosis: a systematic review of 118 studies. *J Hepatol.* 2006;44(1):217–231.
24. Moreau R, Lebrec D. Review article: hepatorenal syndrome—definitions and diagnosis. *Aliment Pharmacol Ther.* 2004;20(Suppl 3):24–28.
25. Piano S, Romano A, Di Pascoli M, Angeli P. Why and how to measure renal function in patients with liver disease. *Liver Int.* 2017;37(Suppl 1):116–122.
26. Fisher L, Fisher A. Vitamin D and parathyroid hormone in outpatients with noncholestatic chronic liver disease. *Clin Gastroenterol Hepatol.* 2007;5(4):513–520.
27. Trépo E, Ouziel R, Pradat P, et al. Marked 25-hydroxyvitamin D deficiency is associated with poor prognosis in patients with alcoholic liver disease. *J Hepatol.* 2013;59(2):344–350.
28. Ragab D, Soliman D, Samaha D, Yassin A. Vitamin D status and its modulatory effect on interferon gamma and interleukin-10 production by peripheral blood mononuclear cells in culture. *Cytokine.* 2016;85:5–10.
29. Lin R. Crosstalk between Vitamin D metabolism, VDR signalling, and innate immunity. *Biomed Res Int.* 2016;2016:1375858.
30. Zhang C, Zhao L, Ding Y, et al. Enhanced LL-37 expression following vitamin D supplementation in patients with cirrhosis and spontaneous bacterial peritonitis. *Liver Int.* 2016;36(1):68–75.

DOI: 10.1093/labmed/lmab019

Evaluation of Polarized Light and Fluorescence Microscopy of Congo Red Stain in the Diagnosis of Renal Amyloidosis

Adrian Y. S. Lee, MBBS,[1,2,*] *Angela Bayly, BMBS,*[1] *Ming-Wei Lin, MBBS*[1,2]

Laboratory Medicine 2021;52:574-577

DOI: 10.1093/labmed/lmab022

ABSTRACT

Background: Amyloidosis is a devastating multisystemic disease resulting from organ deposition of misfolded proteins and subsequent organ dysfunction. An accurate diagnosis relies frequently on biopsies and microscopy techniques to detect amyloid deposition. We evaluated the diagnostic performance of Congo red staining using polarized light (PM) and fluorescence microscopy (FM) techniques in renal amyloidosis.

Methods: We performed a retrospective and prospective analysis of all renal biopsies submitted at a large quarternary hospital in Sydney, Australia, that had undergone PM and FM evaluation using Congo red staining. Identification of amyloid fibrils on electron microscopy was considered the reference method.

Results: PM and FM displayed very high sensitivity and specificity in correctly identifying amyloid deposits in renal biopsies that tested positive via Congo red staining. Comparison of the diagnostic statistics revealed that they are diagnostically equivalent.

Conclusion: In the diagnosis of renal amyloidosis on biopsy, evaluation of Congo red staining may be reliably performed via PM or FM.

Keywords: amyloidosis, biopsies, Congo red staining, fluorescence microscopy, polarized microscopy.

Amyloidosis is a devastating multisystemic disease caused by the deposition of abnormal, misfolded proteins in various organs. The kidneys are one of the most commonly affected organs (*renal amyloidosis*); this disease often presents with subnephrotic to nephrotic-range proteinuria. Biopsy remains the criterion standard for diagnosis.[1]

Congo red (CR) staining is a qualitative method for identifying amyloid deposits on biopsies and can be detected via a classic apple-green birefringence under polarized light microscopy (PM; **Figure 1A**), or fluorescence microscopy (FM).[2] Under FM, using the tetramethylrhodamine (TRITC) filter, CR produces a characteristic bright red appearance with its emission wavelength of 614 nm (**Figure 1B**). Because there are more than 60 subtypes of amyloid protein, CR only serves to identify the presence of amyloid and does not distinguish one subtype from another, which would require additional analytical techniques.[3] The comparative diagnostic performance of CR using PM or FM microscopy is not known for renal amyloidosis. We therefore undertook a retrospective and prospective review of all renal biopsies at our quarternary hospital to ascertain their relative diagnostic merits.

Abbreviations:

CR, Congo red; PM, polarized light microscopy; TRITC, tetramethylrhodamine; PPV, positive predictive value; NPV, negative predictive value; FM, fluorescence microscopy

[1]ICPMR and NSW Health Pathology, Westmead Hospital, and [2]Sydney Medical School, The University of Sydney, Westmead, NSW, Australia

*To whom correspondence should be addressed.
adrian.lee1@health.nsw.gov.au

Methods

Renal biopsies examined at Institute of Clinical Pathology and Medical Research (ICPMR), Westmead Hospital (Sydney, Australia) were collated and retrospectively and prospectively analyzed during a 4-year period between 2017 and 2020. This is a major institute that is one of the largest health networks, geographically and infrastructurally, in the state of New South Wales. As an adult hospital network, only patients aged 16 years or older were included in this study. Paraffin-embedded sections or frozen sections of renal core tissue

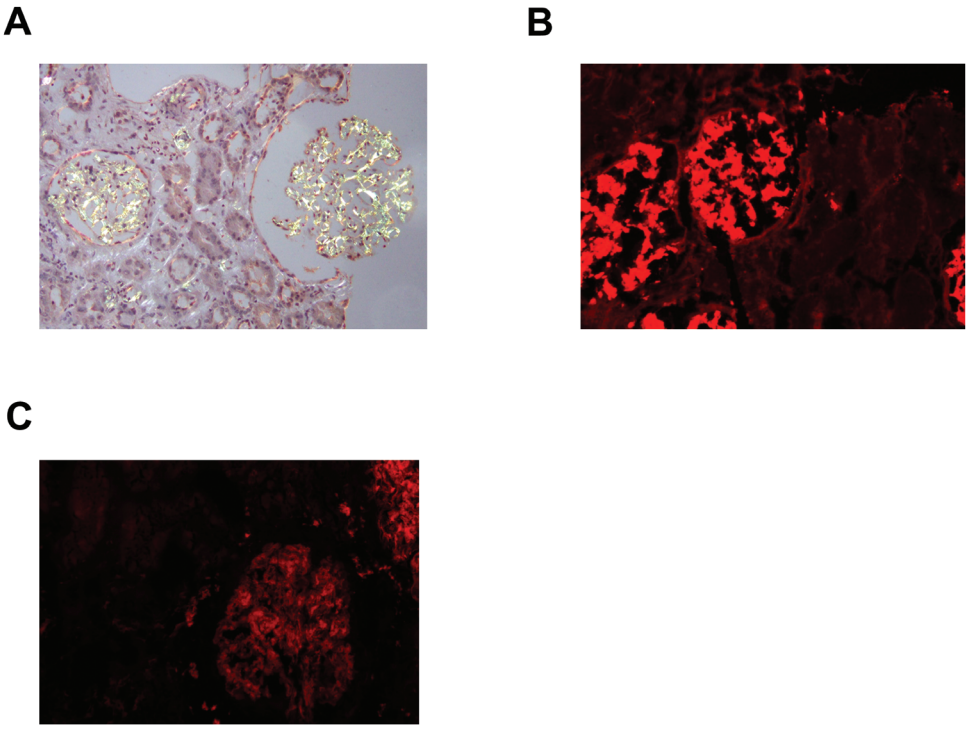

Figure 1

Positive Congo red staining in renal tissue as observed by polarized light (**A**) and fluorescence microscopy (**B**). **C**, Weaker Congo red staining observed under fluorescence microscopy in a case of Congophilic fibrillary glomerulonephritis.

were prepared int 4-μm sections. CR dissolved in 1% sodium hydroxide was applied to deparaffinized tissue or frozen tissue for 20 minutes before washing and then dehydration.

CR staining was requested when there was clinical suspicion for amyloidosis, microscopic appearance was suspicious for amyloidosis, there was unexplained proteinuria, or the clinicopathological diagnosis remained unexplained. For PM, apple-green birefringence was observed using polarized light. For FM, CR was read using the green laser (Nikon Eclipse 80i microscope; Nikon Corporation) independently by at least 2 laboratory physicians (A.Y.S.L., M-W.L. and others). Evaluators were masked to the final diagnosis. The practical reference standard for this study was the electron microscopy detection of amyloid fibrils in the renal tissue. The final diagnosis was always correlated clinically in weekly clinicopathological meetings.

Statistical analysis was performed using the SPSS statistical software, package, version 19.0 (IBM Corporation). $P < .05$ was deemed to be statistically significant. As a quality-assurance project, this study was exempt from formal ethics approval as per the Western Sydney Local Health District Research Office policy.

Results

During a 4-year period, there were 379 renal biopsies that involved CR staining evaluated using PM and FM. There were 24 cases (6.3%) of renal amyloidosis and a large range of other nonamyloidosis cases (Table 1). The prevalence of amyloidosis was comparable to that reported in an earlier study report.[4]

CR staining on FM correctly identified all 24 cases of amyloidosis (sensitivity, 100.0% [range, 85.8%–100.0%]). There were 3 cases of false-positive FM CR results from patients with congophilic fibrillary glomerulonephritis. The staining

Lab Medicine 2021;52;574–577
DOI: 10.1093/labmed/lmab022

Table 1. Tabulation of Final Diagnoses for Renal Biopsies in Audit Period

Diagnosis	Frequency, No. (%)
Amyloidosis	24 (6.3%)
Diabetic nephropathy	83 (21.9%)
Focal and segmental glomerulosclerosis (no specific cause)	40 (10.6%)
Membranous nephropathy	33 (8.7%)
IgA nephropathy	23 (6.1%)
Hypertensive nephropathy	20 (5.3%)
Podocytopathy	18 (4.7%)
Tubulointerstitial pathology	18 (4.7%)
Membranoproliferative glomerulonephritis	17 (4.5%)
Lupus nephritis	17 (4.5%)
Ischemic/vascular nephropathy	9 (2.4%)
Minimal change disease	8 (2.1%)
Cast nephropathy	7 (1.8%)
Monoclonal Ig-deposition disease	7 (1.8%)
Thin basement-membrane disease	4 (1.1%)
Fibrillary glomerulonephritis	4 (1.1%)
Crescentic glomerulonephritis	2 (0.5%)
C3 glomerulonephritis	2 (0.5%)
Thrombotic microangiopathy	1 (0.3%)
IgG4-related disease	1 (0.3%)
Immunotactoid glomerulopathy	1 (0.3%)
Antiglomerular basement-membrane disease	1 (0.3%)
Nondiagnostic	39 (10.3%)

Ig, immunoglobulin.

in these 3 cases was weaker than that found in classical amyloid cases and sometimes formed coalescing, mesangial glomerular staining (**Figure 1C**) rather than discrete deposits (**Figure 1B**). This yielded a specificity of 99.2% (97.6%–99.8%) for renal amyloidosis. A positive predictive value (PPV) of 88.9% (72.2%–96.1%) and a negative predictive value (NPV) of 100.0% for renal amyloidosis were obtained.

PM correctly identified 23 out of 24 renal amyloidosis cases (sensitivity, 95.8% [78.9%–99.9%]). In 2 cases, the CR PM result was reported as being positive in a case of cast nephropathy and congophilic fibrillary glomerulonephritis. This combination yields specificity of 99.4% (98.0%–99.9%) for amyloidosis. PM assessment of CR has a PPV of 92.0% (74.2%–97.9%) and a NPV of 99.7% (98.1%–100.0%) for renal amyloidosis.

There was excellent agreement between the 2 methods (kappa = 0.937 [0.87–1.00]). The McNemar test with Yates correction was performed, comparing the sensitivities and specificities of each method. There were neither differences in sensitivity (P = .62) nor specificity (P = .72), indicating that the 2 methods of evaluation are equivalent.

Discussion

When comparing the 2 methods, the literature is somewhat divided about the value of each methodology over the other;[5,6] however, this finding may relate to which tissue has been submitted for biopsy. For example, in bone marrow, FM appears to be more sensitive than PM for the detection of amyloid P deposits; yet, it had equivalent high specificity.[7] In cutaneous biopsies of cutaneous amyloid deposition, PM was superior to FM in sensitivity.[6] However, it is possible that differing techniques and examined tissues contribute to varying performance of CR in the literature. The findings of 1 study[8] found that the type of clinical microscopy and cover slip may adversely impact the ability to sensitively detect positive CR staining; hence, the investigators argue that the examination technique plays an important role in the sensitivity of CR for amyloid deposits.

Several expert, international consensus committees[9–11] have advocated for CR staining being evaluated by PM; however, they do not discuss the diagnostic merit of evaluation with FM nor the method of evaluation. As such, it is prudent that future studies continue to evaluate the methodology for CR determination. Congophilic fibrillary glomerulonephritis is an important differential diagnosis that yields positive CR staining results through binding the dye.[12] Therefore, pathologists and laboratorians need to be aware of this diagnosis and investigate further accordingly; electron microscopy would be helpful in these cases. Nevertheless, in this dedicated comparative study of renal amyloidosis, we show that evaluations via PM and FM are diagnostically similar, and both methods demonstrate high sensitivities and specificities for renal amyloidosis, in agreement with the findings of a previous study.[4]

A limitation of our study is that CR was performed selectively on renal biopsies, possibly leading to results biasing; yet, the great variety of diagnoses (**Table 1**) and the congruent prevalence of amyloidosis, compared to reports in the literature, gives us confidence that a fair spectrum of renal pathology was tested. Further, amyloid fibrils that are scant or focal in renal tissue may be missed on electron microscopy, depending on the specimen submitted for this technique.[1] Therefore, it is possible that a few cases of early amyloidosis may have been unaccounted for with our routine diagnostic techniques.

In conclusion, our findings emphasize the high diagnostic utility of CR staining for renal amyloidosis diagnoses and, in addition,

prove that CR stainings serve as good rule-out tests. PM and FM are diagnostically similar, and these additional methods for detecting amyloid deposits add to the sensitivity and confidence in initial detection, prompting future specialized testing for diagnostic confirmation and typing. Because both methods of evaluation are not perfect, combined assessments with both methods are still advisable, considering current consensus guidelines advocates for the use of PM. Further studies are required to assess the utility and performance of the 2 methods in a range of other tissues. **LM**

Acknowledgments

We thank Ms Lyn Thai, BMedSc, the Anatomical and Immunopathology Laboratories for their technical expertise.

Personal and Professional Conflicts of Interest

None reported.

References

1. Dember LM. Amyloidosis-associated kidney disease. *J Am Soc Nephrol.* 2006;17(12):3458–3471.
2. Yakupova EI, Bobyleva LG, Vikhlyantsev IM, Bobylev AG. Congo Red and amyloids: history and relationship. *Biosci Rep.* 2019;39(1):BSR20181415.
3. Baker KR, Rice L. The amyloidoses: clinical features, diagnosis and treatment. *Methodist Debakey Cardiovasc J.* 2012;8(3):3–7.
4. Sen S, Başdemir G. Diagnosis of renal amyloidosis using Congo red fluorescence. *Pathol Int.* 2003;53(8):534–538.
5. Clement CG, Truong LD. An evaluation of Congo red fluorescence for the diagnosis of amyloidosis. *Hum Pathol.* 2014;45(8):1766–1772.
6. Fernandez-Flores A. Comparative study of Congo red fluorescence and immunohistochemistry in cutaneous amyloidosis. *Rom J Morphol Embryol.* 2010;51(4):683–686.
7. Marcus A, Sadimin E, Richardson M, Goodell L, Fyfe B. Fluorescence microscopy is superior to polarized microscopy for detecting amyloid deposits in Congo red-stained trephine bone marrow biopsy specimens. *Am J Clin Pathol.* 2012;138(4):590–593.
8. El-Meanawy A, Mueller C, Iczkowski KA. Improving sensitivity of amyloid detection by Congo red stain by using polarizing microscope and avoiding pitfalls. *Diagn Pathol.* 2019;14(1):57.
9. Adams D, Ando Y, Beirão JM, et al. Expert consensus recommendations to improve diagnosis of ATTR amyloidosis with polyneuropathy. *J Neurol.* 2020. https://doi.org/10.1007/s00415-019-09688-0
10. Benson MD, Buxbaum JN, Eisenberg DS, et al. Amyloid nomenclature 2020: update and recommendations by the International Society of Amyloidosis (ISA) nomenclature committee. *Amyloid.* 2020;27(4):217–222.
11. Gillmore JD, Wechalekar A, Bird J, et al; BCSH Committee. Guidelines on the diagnosis and investigation of AL amyloidosis. *Br J Haematol.* 2015;168(2):207–218.
12. Alexander MP, Dasari S, Vrana JA, et al. Congophilic fibrillary glomerulonephritis: a case series. *Am J Kidney Dis.* 2018;72(3):325–336.

DOI: 10.1093/labmed/lmab022

Comparative Evaluation of the Modified Carbapenem Inactivation Method for Phenotypic Detection of Guiana Extended-Spectrum β-Lactamase-Type Carbapenemases in *Enterobacterales*

A-Jin Lee, MD, PhD[1,*] *and Hun Suk Suh, MD, PhD*[1]

Laboratory Medicine 2021;52:578-583

DOI: 10.1093/labmed/lmab026

ABSTRACT

Objective: We comparatively evaluated the performance of 3 phenotypic tests for the detection of carbapenemase production.

Materials and Methods: Carbapenemase production was evaluated using the modified Hodge test (MHT), the modified carbapenemase inhibition method (mCIM), and the Rapidec Carba NP test (RCNP).

Results: Among the 170 isolates, 79 were CP-CRE and 91 were non-CP-CRE. The CP-CRE isolates produced GES-5 (n = 66), KPC (n = 4), NDM (n = 7), NDM and OXA-48 (n = 1), and VIM (n = 1). For KPC producers, all 3 methods showed a sensitivity of 75%. The sensitivities of MHT, mCIM, and RCNP were 14.3%, 100%, and 71.4%, respectively, for NDM producers, and 1.5%, 12.1%, and 18.2% for GES-5 producers, respectively.

Conclusion: The performance of the phenotypic tests varied depending on the type of carbapenemase. For intensive infection control, phenotypic and molecular tests are required for the detection of common and rare types of carbapenemases.

Keywords: carbapenemase, carbapenemase-producing carbapenem-resistant *Enterobacterales*, phenotypic methods, GES-5, evaluation, infection control

The prevalence of carbapenem-resistant *Enterobacterales* (CRE) has increased globally, and CRE has become a major cause of health care-associated and community-associated infections.[1,2] Carbapenem resistance poses a concern because effective therapeutic options for CRE are very limited and alternative therapies are lacking.[3] Carbapenem resistance occurs through various mechanisms, including carbapenemase production in carbapenemase-producing CRE (CP-CRE).[4] Based on the presence or absence of carbapenemase production, CRE is classified as CP-CRE or non-CP-CRE. Carbapenemase genes are mostly plasmid-encoded and can spread easily and rapidly; as a result, the spread of CP-CRE poses a severe public health threat.[1] Carbapenemase production confers resistance without the need for additional chromosomal mutations.[5] Plasmids in CP-CRE occasionally carry additional resistance elements.[6] Therefore, CP-CRE tends to be resistant not only to most β-lactams, but also to other antibiotic classes, and shows strong multidrug resistance.[7,8] For effective infection control and public security, rapid and accurate detection of carbapenemase production is essential.

There are several types of carbapenemases according to the Ambler classification system: class A, including the *Klebsiella pneumoniae* carbapenemase (KPC) and Guiana extended-spectrum β-lactamase (GES) types;

Abbreviations:

MHT, modified Hodge test; mCIM, modified carbapenemase inhibition method; RCNP, Rapidec Carba NP test; CP-CRE, carbapenemase-producing carbapenem-resistant Enterobacterales; GES, Guiana extended-spectrum β-lactamase; KPC, Klebsiella pneumoniae; NDM, New Delhi metallo-β-lactamase; OXA, oxacillinase; VIM, verona integron-encoded metallo-β-lactamase; CRE, carbapenem-resistant Enterobacterales; IMP, imipenemase; MIC, minimal inhibitory concentration; CLSI, Clinical and Laboratory Standards Institute; MHA, Mueller Hinton agar; TSB, tryptic soy broth; PCR, polymerase chain reaction.

[1]Department of Laboratory Medicine, Daegu Catholic University School of Medicine, Daegu, South Korea

*To whom correspondence should be addressed.
ajinlee@cu.ac.kr

class B, including the New Delhi metallo-β-lactamase (NDM), imipenemase (IMP), and verona integron-encoded metallo-β-lactamase (VIM) types; and class D, including the oxacillinase (OXA) type. The KPC, NDM, and OXA-48 types are the most commonly encountered[8]; however, the distribution of CP-CRE varies among regions and nations, and several newly emerging carbapenemases have been reported. Early identification of newly emerging pathogens and careful monitoring are important to avoid exponential spreading of these types of carbapenemases.

There are various screening tests for the detection of carbapenemase production, including phenotypic and molecular tests. Most assays target the common carbapenemase types, including KPC, NDM, OXA-48-like, VIM, and IMP. The performance of these tests differs considerably depending on the type of carbapenemase; therefore, accurate detection of CP-CRE can be challenging. The modified Hodge test (MHT), also known as the cloverleaf technique, was initially used as a phenotypic test to detect carbapenemase activity.[9,10] However, result interpretation is often difficult and is subjective, and the turnaround time is long.[10] Several tests have been developed to overcome these limitations. However, the detection of rare or novel carbapenemases in routine clinical laboratory settings remains challenging.

In this study, we evaluated the performance of several phenotypic tests for the detection of carbapenemase production, especially for GES-type carbapenemases, and investigated the antimicrobial susceptibility testing results.

Materials and Methods

Bacterial Strains and Antimicrobial Susceptibility Testing

In total, 170 CRE isolates were obtained at a tertiary-care hospital between 2016 and 2019. Species were identified and antimicrobial susceptibility was evaluated using the VITEK II system (bioMérieux, Marcy l'Etoile, France). Minimal inhibitory concentrations (MICs) of the antimicrobial agents (amikacin, ampicillin, azithromycin, cefazolin, cefepime, cefotaxime, cefoxitin, ceftazidime, ciprofloxacin, gentamicin, ertapenem, imipenem, piperacillin-tazobactam, tigecycline, and trimethoprim-sulfamethoxazole) were determined using the VITEK II system (bioMérieux) and interpreted according to the Clinical and Laboratory Standards Institute (CLSI) guidelines (document M100-S27).[11] *Escherichia coli* ATCC 25922 was used as a quality control strain. The study was approved by the Institutional Review Board (IRB number CR-18–152).

Phenotypic Tests for Carbapenemase Production

Carbapenemase production was detected using the MHT, the modified carbapenemase inhibition method (mCIM), and the Rapidec Carba NP test (RCNP; bioMérieux). The MHT was conducted as described in CLSI document M100-S27.[11] A suspension of an MHT indicator organism (*E. coli* ATCC 25922, which is a carbapenem-susceptible stain) at 0.5 McFarland turbidity was prepared and inoculated on the surface of a Mueller-Hinton agar (MHA; Becton, Dickinson and Company, Sparks, MD). A 10 μg meropenem disk (BD BBL Sensi-Disc susceptibility test disc, Becton, Dickinson and Company) was placed on the inoculated agar, and the isolates (3–5 colonies) were thickly inoculated in a straight line from the edge to the periphery of the agar using a sterile loop. Next, the plates were incubated in ambient air at 35°C ± 2°C for 16 to 20 hours. Widening of the inoculation line on the edge of an inhibition zone was considered to indicate carbapenemase production.

The mCIM assay was performed as follows. Using an aseptic inoculation loop, 1 μL of an isolate solution was added into a tube containing 2 mL of tryptic soy broth (TSB; BD BBL Tryptic Soy Broth; Becton, Dickinson and Company). The bacterial suspension was vortexed for 10 to 15 seconds. A 10 μg meropenem disk (BD BBL Sensi-Disc Susceptibility Test Disc) was added to the bacterial suspension using a sterile technique. The tube was then incubated in ambient air at 35°C ± 2°C for 4 hours. Before the completion of the 4-hour carbapenem inactivation step, a suspension of the mCIM indicator organism (*E. coli* ATCC 25922) at 0.5 McFarland turbidity was spread on the surface of an MHA plate (Becton, Dickinson and Company). The meropenem disk was then removed from the TSB bacterial suspension using a 10 μL inoculation loop and placed on the inoculated MHA plate, which was incubated in an inverted position in ambient air at 35°C ± 2°C for 18 to 24 hours. After the incubation, the diameter of the inhibition zone around each meropenem disk was measured. A zone diameter of ≥19 mm was

DOI: 10.1093/labmed/lmab026

considered a negative result, a diameter of 16 to 18 mm was considered an indeterminate result, and a diameter of 6 to 15 mm was considered a positive result—ie, carbapenemase activity.

The RCNP was carried out according to the manufacturer's instructions. Using a sterile inoculation loop, a 10 μL inoculum of colonies taken from a culture plate was added to the cell. After a 30-minute incubation at 37°C, the plate was read with the naked eye. A red-to-yellow or red-to-orange color change was considered a positive result.

Detection of *bla* genes

Carbapenemase genes in CP-CRE isolates were detected using polymerase chain reaction (PCR) and amplicon sequencing. The presence of carbapenemase genes, including bla_{KPC}, bla_{NDM}, bla_{VIM}, bla_{OXA-48}, bla_{IMP}, and bla_{GES}, was determined using gene-specific primers. The primers used are listed in **Table 1**. The PCR products were sequenced using a 373XL sequencer (Applied Biosystems, Weiterstadt, Germany). The sequences were aligned using BLAST (http://blast.ncbi.nlm.nih.gov/Blast.cgi).

Results

In total, 170 CRE isolates, including 79 CP-CRE isolates and 91 non-CP-CRE isolates, were evaluated (**Table 2**). The CP-CRE isolates included 45 *K. pneumoniae,* 20 *Enterobacter cloacae,* 8 *E. coli*, 4 *Enterobacter amnigenus,* and 2 *Klebsiella aerogenes.* The CP-CRE clinical isolates produced GES-5 (n = 66), KPC (n = 4), NDM (n = 7), NDM and OXA-48 (n = 1), and VIM (n = 1) carbapenemases. The non-CP-CRE isolates included 65 *K. pneumoniae,* 13 *E. cloacae,* 12 *E. coli,* and 1 *K. aerogenes.*

Antimicrobial susceptibility patterns are shown in **Table 2**. Of the 79 CP-CRE isolates, 78 isolates (98.7%) showed resistance to ertapenem and 5 (6.3%) were susceptible to imipenem. Among the 91 non-CP-CRE isolates, 88 isolates (96.7%) were not susceptible to ertapenem, whereas 22 isolates (24.2%) were susceptible to imipenem.

The results of the phenotypic tests for the different carbapenemase types are shown in **Table 3**. Of the 4 KPC-producing isolates, 3 isolates (75%) yielded positive results in the MHT, mCIM, and RCNP. Of the 66 GES-5-producing isolates, only 1 isolate (1.5%) yielded a positive result in the MHT. Eight isolates (12.1%) and 12 isolates (18.2%) yielded positive results in the mCIM and RCNP, respectively. Of the 7 NDM-producing isolates, only 1 isolate (14.3%) yielded a positive result in the MHT, whereas 5 isolates (71.4%) produced positive results in the RCNP and all 7 isolates (100%) yielded positive results in the mCIM. The VIM-producing isolate (n = 1) and the NDM and OXA-48-coproducing isolate (n = 1) produced negative results in all 3 phenotypic tests. Regardless of carbapenemase type, the overall sensitivities of the mCIM and RCNP were 22.8% and 25.3%, respectively, which were higher than that of the MHT (6.3%). All of the non-CP-CRE isolates yielded negative results in the MHT and mCIM, regardless of carbapenem susceptibility.

Table 1. Primers Used for PCR Detection of Carbapenemase-Encoding Genes

Target	PCR Primers	Sequence (5'-3')	Amplicon Size (bp)	Temperature
bla_{KPC} type	KPC-F	CGTCTAGTTCTGCTGTCTTG	798	52°C
	KPC-R	CTTGTCATCCTTGTTAGGCG		
bla_{NDM} type	NDM-F	GGTTTGGCGATCTGGTTTTC	621	59°C
	NDM-R	CGGAATGGCTCATCACGATC		
bla_{OXA-48} type	OXA-48-F	GCGTGGTTAAGGATGAACAC	438	52°C
	OXA-48-R	CATCAAGTTCAACCCAACCG		
bla_{IMP} type	IMP-F	GGAATAGAGTGGCTTAAYTCTC	232	52°C
	IMP-R	GGTTTAAYAAAACAACCACC		
bla_{VIM} type	VIM-F	GATGGTGTTTGGTCGCATA	390	52°C
	VIM-R	CGAATGCGCAGCACCAG		
bla_{GES} type	GES-F	CTATTACTGGCAGGGATCG	594	59°C
	GES-R	CCTCTCAATGGTGTGGGT		

F, sense primer; GES, Guiana extended-spectrum β-lactamase; IMP, imipenemase; KPC, Klebsiella pneumoniae; *NDM, New Delhi metallo-β-lactamase; OXA, oxacillinase; PCR, polymerase chain reaction; R, antisense primer; VIM, verona integron-encoded metallo-β-lactamase.*

Table 2. *Enterobacterales* Isolates Tested, Ertapenem and Imipenem Susceptibility

	CP-CRE (n = 79)	Non-CP-CRE (n = 91)
	Number (%) of Isolates	
Species		
Klebsiella pneumoniae	45 (57.0)	65 (71.4)
Enterobacter cloacae	20 (25.3)	13 (14.3)
Escherichia coli	8 (10.1)	12 (13.2)
Enterobacter amnigenus	4 (5.1)	0 (0.0)
Klebsiella aerogenes	2 (2.5)	1 (1.1)
Ertapenem		
Resistant	78 (98.7)	83 (91.2)
Intermediate	0 (0.0)	5 (5.5)
Susceptible	1 (1.3)	3 (3.3)
Imipenem		
Resistant	62 (78.5)	62 (68.1)
Intermediate	12 (15.2)	7 (7.7)
Susceptible	5 (6.3)	22 (24.2)

CP-CRE, carbapenemase-producing carbapenem-resistant Enterobacterales; *non-CP-CRE, non-carbapenemase-producing carbapenem-resistant* Enterobacterales.

and accurate identification of CP-CRE is essential. Screening of carbapenemase production can be useful for guiding appropriate antimicrobial therapy, effective infection control implementation, and epidemiological investigation. Phenotypic tests are widely and easily used to detect CP-CRE in clinical laboratories. In this study, 170 CRE isolates, including 79 CP-CRE isolates and 91 non-CP-CRE isolates, were used to evaluate the performance of the MHT, mCIM, and RCNP for the detection of carbapenemase production.

The MHT is a phenotypic method that was routinely used to detect carbapenemases with high sensitivity, especially in detecting the KPC and OXA-48 types, and it was initially recommended by the CLSI for *Enterobacterales* with elevated carbapenem MICs or reduced disk diffusion inhibition zones.[11,12] However, the MHT shows limited sensitivity for the NDM-type carbapenemase and is no longer recommended as a reliable carbapenemase detection method.[12,13] The performance of the MHT for the detection of other types of carbapenemases has also been evalu-

Table 3. Phenotypic and Susceptibility Test Results with 79 Carbapenemase-Producing Isolates

Group (n)	Species (n)	Number (%) of Isolates Nonsusceptible		Number (%) of Isolates with Positive Results		
		Ertapenem	Imipenem	MHT	mCIM	RCNP
Class A						
GES (66)	*Klebsiella pneumoniae* (40)	40 (100)	37 (92.5)	0 (0)	7 (17.5)	11 (27.5)
	Enterobacter cloacae (19)	19 (100)	19 (100)	0 (0)	0 (0)	0 (0)
	Klebsiella aerogenes (2)	2 (100)	2 (100)	0 (0)	0 (0)	0 (0)
	Enterobacter amnigenus (4)	4 (100)	4 (100)	0 (0)	0 (0)	0 (0)
	Escherichia coli (1)	1 (100)	1 (100)	1 (100)	1 (100)	1 (100)
	All	66 (100)	63 (95.5)	1 (1.5)	8 (12.1)	12 (18.2)
KPC (4)	*K. pneumoniae* (3)	2 (66.7)	3 (100)	2 (66.7)	3 (100)	2 (66.7)
	E. coli (1)	1 (100)	1 (100)	1 (100)	0 (0)	1 (100)
	All	3 (75)	100 (100)	3 (75)	3 (75)	3 (75)
Class B						
NDM (7)	*E. coli* (6)	6 (100)	6 (100)	1 (16.7)	6 (100)	4 (66.7)
	E. cloacae (1)	1 (100)	1 (100)	0 (0)	1 (100)	1 (100)
	All	7 (100)	7 (100)	1 (14.3)	7 (100)	5 (71.4)
VIM (1)	*K. pneumoniae* (1)	1 (100)	0 (0)	0 (0)	0 (0)	0 (0)
NDM + OXA-48 (1)	*K. pneumoniae* (1)	1 (100)	0 (0)	0 (0)	0 (0)	0 (0)

GES, Guiana extended-spectrum β-lactamases; KPC, Klebsiella pneumoniae *carbapenemases; mCIM, modified carbapenem inactivation method; MHT, modified Hodge test; NDM, New Delhi metallo-β-lactamases; OXA, oxacillinases; RCNP, Rapidec Carba NP test; VIM, Verona integron-encoded metallo-β-lactamases.*

Discussion

The dissemination of CRE, especially CP-CRE, contributes to serious and devastating clinical outcomes; therefore, rapid

ated, but only in small numbers of isolates.[14-16] In this study, the sensitivity of the MHT for KPC-producing isolates was 75.0% (3/4). However, it showed poor sensitivity for GES, NDM, OXA-48, and VIM producers, which is in accordance

DOI: 10.1093/labmed/lmab026

with previous observations for these producers.[12,14-16] In particular, the MHT showed poor sensitivity for GES-type carbapenemases, which can therefore be underestimated.

The interpretation of MHT results is subjective and requires experienced staff. To overcome these limitations, several phenotypic tests have been developed. These new phenotypic methods are generally cheaper and simpler, with a shorter incubation time and increased sensitivity. The mCIM was designed to improve the limited sensitivity of the CIM for certain carbapenemases and for simplicity. It is considered as an alternative method to the MHT, CIM, and RCNP for carbapenemase detection.[11] The RCNP, a ready-to-use kit using colorimetry, is convenient in clinical laboratories. However, it requires specific, costly reagents.[17]

The sensitivity of the mCIM was 75% for KPC, 100% for NDM, and 12.1% for GES-5, with an overall sensitivity of 22.8%. The relatively lower sensitivity when compared with the results of a previous study may have resulted from the inclusion of a high number of GES-5 carbapenemase-producing isolates (n = 66). The sensitivity of the RCNP was comparable to that of the mCIM, with 75% for KPC, 100% for NDM, 18.2% for GES-5, and an overall sensitivity of 25.3%. Several studies have reported sensitivities of 975 to 98% for the mCIM and 90% to 99% for the RCNP.[17-21] In the present study, the sensitivities were lower, possibly because of differences in the numbers of carbapenemase-producing isolates.

When the first CRE was isolated in our hospital, we sent the isolate to the reference laboratory of the Korean Center for Disease Prevention and Control, which identified the isolate as a GES-5-producer. Since then, PCR targeting the GES genes was performed. Conventional phenotypic tests have limited sensitivity for GES producers, and the prevalence of GES-type carbapenemases can be underestimated with nonmolecular tests. Although the prevalence of GES is lower than that of other common types, GES-producing CRE is increasingly reported worldwide.[4] Strains with rare carbapenemases can also cause nosocomial outbreaks and can show strong multidrug resistance. Therefore, laboratory tests to detect the common and rare types of carbapenemases can be useful for effective infection and epidemiological control.

This study has a limitation stemming from its small sample size, and the phenotypic tests were performed based on CLSI document M100-S27. We only have performed 3 phenotypic tests and have not included various other tests such as eCIM and Triton Hodge tests for carbapenemase detection.

These various tests each have their advantages and disadvantages. Phenotypic tests can be routinely performed and are inexpensive, but they cannot discriminate among the various carbapenemase types. Targeted PCR can accurately detect and identify known carbapenemase genes; however, new and rare genes cannot be detected. Although whole-genome sequencing and next-generation sequencing can be used to detect carbapenemase-encoding genes, these molecular methods cannot be routinely performed in the clinical laboratory setting and require experienced staff and specific equipment. It is important to establish a systematic algorithm to detect common and rare carbapenemase types, and screening for carbapenemases, including rare types, should be considered. The molecular characteristics of CP-CRE are useful for preventing the spread of these isolates.

Conclusion

The performance of the phenotypic tests varied depending on the carbapenemase type. For the detection of GES-type carbapenemase, the sensitivity of the mCIM was comparable to that of the RCNP and superior to that of the MHT. When a positive result is obtained in a test covering a broad range of carbapenemases, it is necessary to detect the specific type of carbapenemase using phenotypic and molecular tests for intensive infection control. It may be helpful to establish an algorithm for the systematic detection of common and rare types of carbapenemases in clinical laboratories. **LM**

References

1. van Duin D, Paterson DL. Multidrug-resistant bacteria in the community: trends and lessons learned. *Infect Dis Clin North Am.* 2016;30(2):377–390.
2. Nordmann P, Naas T, Poirel L. Global spread of carbapenemase-producing Enterobacteriaceae. *Emerg Infect Dis.* 2011;17(10):1791–1798.
3. Elshamy AA, Aboshanab KM. A review on bacterial resistance to carbapenems: epidemiology, detection and treatment options. *Future Sci OA.* 2020;6(3):FSO438.
4. Naas T, Dortet L, Iorga BI. Structural and functional aspects of class A carbapenemases. *Curr Drug Targets.* 2016;17(9):1006–1028.

5. Lutgring JD, Limbago BM. The problem of carbapenemase-producing-carbapenem-resistant-Enterobacteriaceae detection. *J Clin Microbiol.* 2016;54(3):529–534.
6. Srinivasan A, Patel JB. Klebsiella pneumoniae carbapenemase-producing organisms: an ounce of prevention really is worth a pound of cure. *Infect Control Hosp Epidemiol.* 2008;29(12):1107–1109.
7. Mathers AJ, Peirano G, Pitout JD. The role of epidemic resistance plasmids and international high-risk clones in the spread of multidrug-resistant Enterobacteriaceae. *Clin Microbiol Rev.* 2015;28(3):565–591.
8. van Duin D, Doi Y. The global epidemiology of carbapenemase-producing Enterobacteriaceae. *Virulence.* 2017;8(4):460–469.
9. Miriagou V, Cornaglia G, Edelstein M, et al. Acquired carbapenemases in Gram-negative bacterial pathogens: detection and surveillance issues. *Clin Microbiol Infect.* 2010;16(2):112–122.
10. Carvalhaes CG, Picão RC, Nicoletti AG, Xavier DE, Gales AC. Cloverleaf test (modified Hodge test) for detecting carbapenemase production in Klebsiella pneumoniae: be aware of false positive results. *J Antimicrob Chemother.* 2010;65(2):249–251.
11. Clinical and Laboratory Standards Institute. *Performance Standards for Antimicrobial Susceptibility Testing: Approved Guideline—27th edition*. M100-S27. Wayne, PA: Clinical and Laboratory Standards Institute; 2017.
12. Girlich D, Poirel L, Nordmann P. Value of the modified Hodge test for detection of emerging carbapenemases in Enterobacteriaceae. *J Clin Microbiol.* 2012;50(2):477–479.
13. Saito R, Koyano S, Dorin M, et al. Evaluation of a simple phenotypic method for the detection of carbapenemase-producing Enterobacteriaceae. *J Microbiol Methods.* 2015;108:45–48.
14. van der Zwaluw K, de Haan A, Pluister GN, Bootsma HJ, de Neeling AJ, Schouls LM. The carbapenem inactivation method (CIM), a simple and low-cost alternative for the Carba NP test to assess phenotypic carbapenemase activity in Gram-negative rods. *PLoS One.* 2015;10(3):e0123690.
15. Song W, Kim H-S, Kim J-S, et al. Carbapenem inactivation method: accurate detection and easy interpretation of carbapenemase production in *Enterobacteriaceae* and *Pseudomonas* spp. *Ann Clin Microbiol.* 2016;19:83–87.
16. Baeza LL, Pfennigwerth N, Greissl C, et al. Comparison of five methods for detection of carbapenemases in Enterobacterales with proposal of a new algorithm. *Clin Microbiol Infect.* 2019;25(10):1286.e9–1286.e15.
17. Tamma PD, Opene BN, Gluck A, Chambers KK, Carroll KC, Simner PJ. Comparison of 11 phenotypic assays for accurate detection of carbapenemase-producing Enterobacteriaceae. *J Clin Microbiol.* 2017;55(4):1046–1055.
18. Pierce VM, Simner PJ, Lonsway DR, et al. Modified carbapenem inactivation method for phenotypic detection of carbapenemase production among Enterobacteriaceae. *J Clin Microbiol.* 2017;55(8):2321–2333.
19. Poirel L, Nordmann P. Rapidec Carba NP test for rapid detection of carbapenemase producers. *J Clin Microbiol.* 2015;53(9):3003–3008.
20. Song W, Yoo G, Hwang GY, et al. Evaluation of diagnostic performance of RAPIDEC CARBA NP test for carbapenemase-producing *Enterobacteriaceae*. *Ann Clin Microbiol.* 2016;19:59–64.
21. Sun K, Xu X, Yan J, Zhang L. Evaluation of six phenotypic methods for the detection of carbapenemases in Gram-negative bacteria with characterized resistance mechanisms. *Ann Lab Med.* 2017;37(4):305–312.

DOI: 10.1093/labmed/lmab026

Association of *SLC22A1,SLCO1B3* Drug Transporter Polymorphisms and Smoking with Disease Risk and Cytogenetic Response to Imatinib in Patients with Chronic Myeloid Leukemia

Fatemeh Mohammadi, PhD,[1] Golale Rostami, PhD,[2] Dlnya Assad, PhD,[3] Mohammad Shafiei, PhD,[1,4] Mohammad Hamid, PhD,[2,] Hasan Jalaeikhoo, MD[5]*

Laboratory Medicine 2021;52:584-596

DOI: 10.1093/labmed/lmab023

ABSTRACT

Objective: To determine whether polymorphisms of *SLC22A1* and *SLCO1B3* genes could predict imatinib (IM) response and chronic myeloid leukemia (CML) risk.

Methods: We genotyped *SLC22A1 (c.480G > C, c.1222A > G)* and *SLCO1B3 (c.334T > G, c.699G > A)* polymorphisms in 132 patients with CML and 109 sex- and age-matched healthy subjects. The patients were evaluated for cytogenetic response by standard chromosome banding analysis (CBA).

Results: Polymorphism analysis showed significant increased risk of IM resistance for *SLC22A1c.1222AG* ($P = .03$; OR = 2.2), *SLCO1B3c.334TT/TG* genotypes ($P = .007$; OR = 4.37) and 334T allele ($P = .03$; OR = 2.86). The double combinations of *SLC22A1c.480CC* and *c.1222AG* polymorphisms with *SLCO1B3c.334TT/TG* were significantly associated with complete cytogenetic response (CCyR) ($P < .05$; OR> 7). The interaction between all polymorphisms and smoking were associated with CML development and IM resistance ($P \leq .04$; OR> 3).

Conclusions: Our study results suggest the influence of *SLC22A1* and *SLCO1B3* polymorphisms and the interaction of smoking on CML development and IM response.

Keywords: chronic myeloid leukemia, complete cytogenetic response, imatinib mesylate, *SLC22A1*, *SLCO1B3*, *smoke*

Abbreviations:

CML, chronic myeloid leukemia; IM, imatinib mesylate; CP, chronic phase; AP, accelerated phase; BP, blastic phase; MCyR, major cytogenetic response; CCyR, complete cytogenetic response; MMR, major molecular response; ELN, european leukemia net; OR, odds ratio; CI, confidence interval; EFS, event- free survival; OS, overall survival; SLC22A1, solute carrier 22A1; SLCO1B3, solute carrier organic anion transporter family member 1B3; PCR–RFLP, Polymerase Chain Reaction–Restriction Fragment Length Polymorphism; LD, linkage disequilibrium; SNP, single nucleotide polymorphism; LOR, loss of response.

[1]Department of Biology, School of Science, Shahid Chamran University of Ahvaz, Ahvaz, Iran, [2]Department of Molecular Medicine, Biotechnology Research Center, Pasteur Institute of Iran, Tehran, Iran, [3]Department of Biology, College of Science, Sulaimani University, Sulaymanyah, Iraq, [4]Biotechnology and Biological Science Research Center, Shahid Chamran University of Ahvaz, Ahvaz, Iran, [5]AJA Cancer Epidemiology Research and Treatment Center (AJA-CERTC), AJA University of Medical Sciences, Tehran, Iran

*To whom correspondence should be addressed.
hamid143@yahoo.com

Fatemeh Mohammadi and Golale Rostami contributed equally to this manuscript.

Chronic myeloid leukemia (CML) is a myeloproliferative disorder marked by the attendance of the Philadelphia (Ph) chromosome resulting from a balanced translocation between chromosomes 9 and 22, t (9; 22) (q34; q11), which creates a fusion oncogene, *BCR-ABL1*. This gene encodes a *Bcr-Abl1* chimeric protein with constitutively tyrosine kinase activity that leads to uncontrolled cell division.[1] Imatinib mesylate (IM; trade name, Glivec or Gleevec), a tyrosine kinase inhibitor (TKI), is a powerful Bcr-Abl1–targeting drug that is currently used as the first-line treatment for patients with newly diagnosed CML in the chronic phase (CML-CP).[2]

Despite significant improvements in clinical response rates and survival outcomes in patients with CML who undergo imatinib therapy, approximately 30% to 40% of patients develop failure in the cytogenetic and molecular response.[3,4] Several resistance mechanisms have been proposed; the most important include gene amplification, clonal

chromosome abnormalities in ph + cells, and mutations in the tyrosine kinase domain of *BCR-ABL1*. Further, the decrease bioavailability of IM in leukemic cells has been proposed as a major pharmacokinetic factor that participates in the development of resistance to IM.[5]

Seven of 55 *SLC* gene families encode drug-carrier transporters that participate in the influx of drugs into the cell.[6] The findings of 2 studies[7,8] showed that the levels of plasma concentration of IM are important for clinical outcomes in patients with CML; besides, active-transport processes could mediate the concentration of IM into mononuclear cells. IM is a substrate for influx transporters such as *SLC22A1* (solute carrier 22A1, organic cation transporter1, OCT1) (GenBank accession number; NC_000006.12) and *SLCO1B3* (solute carrier organic anion transporter family member 1B3, organic anion transporting polypeptide 1B3 [*OATP1B3*]) (NC_000012.12).[9]

White et al[10] found that the activity rate of *SLC22A1* is associated with the achievement of major molecular response (MMR), so MMR was observed with an increase of transporter activity. These investigators also showed that despite the decrease of *SLC22A1* activity, the MMR was achieved with an elevated IM dose. Further, in patients achieving complete cytogenetic response (CCyR), the *SLC22A1* mRNA expression was significantly higher than in patients with partial cytogenetic response (PCyR) and patients with resistance to IM.[11] It has been reported[12] that *SLC22A1* *c.480C > G* (p. L160F, db SNP ID number; rs683369) single nucleotide polymorphism (SNP) affects IM pharmacokinetics, event-free survival (EFS) duration, and rates of exposure to the drug. Another *SLC22A1* polymorphism, *c.1222A > G* (p.M408V, dbSNP ID number;rs628031), influences the prevalence of poor response, duration of EFS, and overall survival (OS).[13]

Another transporter, known as *SLCO1B3*, has a key role in the uptake of IM into hepatocytes and intracellular IM accumulation in leukocytes.[14] *SLCO1B3* has 2 major SNPs, including c.334T > G (p.Ser112Ala,dbSNP ID number; rs4149117) in exon 3 and c.699 G > A (p. Met233Ile,dbSNP ID number; rs7311358) in exon 6.[15] Some studies, such as de Lima et al,[16] have found that the aforementioned polymorphisms are associated with nonresponse to IM. Other study reports, such as Sayyed et al,[17] established that cigarette smoke inhibits the activity of drug transporters and alters their expression. Cigarette smoke directly inhibits activity of transporters, reduces the uptake function of the drug into the cell, and causes drug resistance.

The biological response to carcinogens activates several metabolic pathways that are involved in exclusion, such as transporters; detoxification agents, such as drug-metabolizing enzymes; and DNA repair. The polymorphisms of genes belonging to these pathways can modulate gene activity; however, carcinogens, including smoke, can modify the association of these polymorphisms with cancer risk and chemotherapy resistance.[18] Several studies, such as Björk et al,[19] have reported that benzene in cigarette smoke is associated with leukemia risk, and a relationship exists between cytogenetic abnormalities and AML risk in subjects who smoke. Some study reports, such as Kim HN et al,[20] have revealed that the association of GSTT1 polymorphisms with AML risk is dependent on smoking status.

To our knowledge, no study in the literature has investigated the joint effect of the smoking (as a synergistic factor) and genetic polymorphisms in *SLC22A1* and *SLCO1B3* genes on treatment response and CML risk. Moreover, we have also analyzed the impact of SNP combinations on response to IM and CML susceptibility.

Materials and Methods

Study Population

In this study, peripheral blood specimens were collected from 132 Ph + CML patients undergoing IM therapy (300–800 mg/day) at Arad Hospital and Saba Oncology Clinic in Tehran, Iran. This study was approved by the Research Ethics Committee of the Pasteur Institute of Iran, and specimens were used according to ethical standards (ethical approval no. IR.PII.REC.1397.56). Written informed consent was obtained from all patients and control individuals.

The median duration of IM treatment was 46 months (range, 10–175 months). Based on the response to IM therapy, the patients were classified into 2 groups: the responder group consisted of 58 patients who acquired a CCyR within 12 months from IM therapy, and the nonresponder group included 74 patients who had no CCyR. Moreover, venous blood specimens were obtained from 109 sex- and age-matched healthy individuals with the same ethnicity

DOI: 10.1093/labmed/lmab023

and without medical history or hematological evidence of leukemia or other chronic diseases. Smoking criteria were described as follows: *active smokers* were people have smoked at least pack of cigarettes daily; *passive smokers*, those exposed to cigarette smoke or have smoked 1 to 2 cigarettes daily; and *never smokers*, those who have never smoked. The characteristics of the participants are shown in **Table 1**.

Assessment of Response

Disease-phase definitions include chronic phase (CP), accelerated phase (AP), and blastic phase (BP); also, CCyR were determined according to World Health Organization (WHO) criteria[21] and European Leukemia Net (ELN) criteria.[22,23] The patients were evaluated at regular intervals for cytogenetic response using standard chromosome banding analysis (CBA) of bone-marrow-cell metaphases, as previously described.[24,25] CCyR was described as 0% Ph + chromosome in at least 20 metaphases.

SNPs Genotyping

Genomic DNA was extracted from blood using the salting-out extraction technique.[26] Genotype analysis was conducted by the PCR-restriction fragment length polymorphism (PCR-RFLP) and sequencing methods. Suitable enzymes were used to digest PCR products according to manufacturer instructions (Thermo Fisher Scientific Inc.). To confirm the quality of genotyping, 10% of the specimens were randomly sequenced; the results of both methods were consistent. Primer sequences, restriction enzymes, and PCR conditions are shown in Supplementary Table S1.

Statistical Analysis

Hardy-Weinberg equilibrium was calculated by comparing the observed and expected genotype frequencies for all SNPs using χ^2 testing. The distribution of baseline features between groups was compared for qualitative variables using χ^2 testing and for a quantitative variable (age) using *t* testing. In this study we used different genetic models for determining the association between all genotypes and alleles, with disease risk and response to IM determined using logistic regression test. The odds ratios (ORs), along with 95% confidence intervals (CIs), were also estimated.

Linkage disequilibrium (LD) analysis and calculation of haplotype frequencies were performed using the software HaploView ver. 4.2 AVAILABILITY: (https://www.broadinstitute.org/haploview/haploview). The association between combined polymorphisms, and also polymorphisms–smoking interaction with CML and IM resistance risk, was determined using logistic regression analysis. Because several comparisons can lead to false-positive results, Bonferroni correction of *P* values was carried out. *P* values of less than .05 were considered statistically significant. Statistical analysis was performed using SPSS software, version 22 (IBM Corporation).

Results

Baseline Characteristics of the Studied Subjects

The study-subjects cohort consisted of 132 patients with CML and 109 controls, of whom 56.1% of patients were in the IM nonresponder group and 43.9% in the IM responder group (**Table 1**). There was no significant difference in mean age in male or female participants between cases and controls ($P > .05$). However, the mean age difference was significant for male responders compared with nonresponders (39.55 vs 47.06; $P = .02$), as well as for male nonresponders compared with female nonresponders (39.55 vs 48.12; $P = .20$; data not shown). Smoking status was significantly different between cases and controls and also among drug response groups ($P < .001$). Moreover, there was a significant difference regarding smoking in females and male participants, between patients and controls ($P < .001$), as well as between response groups ($P = .001$; $P = .005$), respectively.

Allelic and Genotypic Frequencies of SNPs

All of the SNPs were in agreement with Hardy-Weinberg equilibrium (HWE) in the CML patients and controls. The only exception was *SLC22A1c.480G > C* polymorphism, which was inconsistent with HWE only in patients.

The distribution of the genotypes in cases and controls, as well as in IM response groups, is shown in **Table 2**. We used different genetic models to evaluate the relationship between SNPs with CML risk and response to IM. The frequencies of genotypes and alleles of *SLCO1B3* (*c.334T > G*, *c.699G > A*) and *SLC22A1* (*c.480G > C*, *c.1222A > G*) polymorphisms were similar among patients with CML and

Table 1. Baseline Features of the Studied Subject Individuals

Features		Control Individuals	Patients	*P* Value[a]	IM Responders[b]	IM Nonresponders	*P* Value[a]
Individuals, no.		109	132		58	74	
Age (y)							
Sex, mean (SD)		43.27 (15.23)	44.6 (15.08)	.65	46.02 (14.44)	43.49 (15.57)	.34
Male		42.44 (14.6)	43.05 (14.2)	.81	47.06 (13.6)	39.55 (13.94)	**.02**
Female		45.12 (15.9)	46.63 (16.05)	.66	44.43 (15.8)	48.12 (16.29)	.40
Sex, no. (%)							
Male		57 (52.3%)	75 (56.8%)	.48	35 (60.3%)	40 (54.1%)	.47
Female		52 (47.7%)	57 (43.2%)		23 (39.7%)	34 (45.9%)	
Smoking status, no (%)							
Total	Active	10 (9.2%)	35 (26.5%)	**<.001**	9 (15.5%)	26 (35.1%)	**<.001**
	Passive	9 (8.3%)	35 (26.5%)		9 (15.5%)	26 (35.1%)	
	Never	90 (82.6%)	62 (47%)		40 (69.0%)	22 (29.7%)	
Males	Active	9 (15.8%)	33 (44.0%)	**<.001**	9 (25.7%)	24 (60.0%)	**.005**
	Passive	5 (8.8%)	11 (14.7%)		5 (14.3%)	6 (15.0%)	
	Never	43 (75.4%)	31 (41.3%)		21 (60.0%)	10 (25.0%)	
Females	Active	1 (1.9%)	2 (3.5%)	**<.001**	0	2 (5.9%)	**.001**
	Passive	4 (7.7%)	24 (42.1%)		4 (17.4%)	20 (58.8%)	
	Never	47 (90.4%)	31 (54.4%)		19 (82.6%)	12 (35.3%)	
Follow- up duration (mo)							
Mean (SD)					62.67 (36.986)	57.70 (30.518)	
IM treatment duration (mo)							
Mean (SD)					58.88 (35.635)	50.65 (23.105)	

IM; imatinib mesylate.
[a]P *<.05 (bolded) was considered statistically significant.*

healthy individuals (*P*> .05), indicating no relationship between these SNPs and CML risk (**Table 2**).

The frequency of the major allele C and the minor allele G for *SLC22A1c.480G > C* was 0.88 and 0.12. respectively; for *SLC22A1 c.1222A > G*, the frequency of the major allele G and the minor allele A were 0.70 and 0.30, respectively. In the case of *SLCO1B3c.699A > G*, the frequency of major allele A and minor allele G was 0.93 and 0.07, respectively; also, for *SLCO1B3c.334T > G*, the frequency of major and minor alleles was 0.87 and 0.13, respectively. There was no significant difference in the genotype and allele frequency of *SLCO1B3c.699G > A* and *SLC22A1c.480G > C* polymorphisms between IM responders and IM nonresponders (*P*> .05).

The *SLCO1B3c.334TG* (codominant model) and *SLCO1B3c.334 TG/TT* genotypes (dominant model) were associated with IM resistance: patients with 334TG and 334 TG/TT genotypes had a higher risk of resistance (*P* = .01, OR = 6.02; *P* = .007, OR = 4.37). There was also an increased risk of IM resistance in patients with the 334T allele (*P* = .03; OR = 2.86). *SLC22A1c.1222 AA* (recessive model) and *SLC22A1c. 1222* AG genotypes (codominant model) were associated with IM response—those with the *SLC22A1c.1222 AA* genotype had decreased IM resistance risk (*P* = .04; OR = 0.25) and those with the *SLC22A1c.1222 AG* genotype had increased resistance risk to IM (*P* = .03; OR = 2.20; **Table 2**).

In female and male groups, there was no relationship between *SLCO1B3* (*c.334T > G*, *c.699G > A*) and *SLC22A1* (*c.480G > C*, *1222A > G*) SNPs with CML risk and IM response. The only exception was the AG genotype from *SLC22A1 c.1222A > G* SNP, which was associated with increase of IM resistance risk in female participants, following the codominant model (*P* = .03; OR = 8.68; Supplementary Tables S2, S3, S4, S5).

Haplotyping

Haplotype analysis revealed a strong linkage disequilibrium between *SLCO1B3 c.334T > G*, *c.699G > A* polymorphisms (D′ = 1; r^2=0.53; LOD = 25.5), and also between *SLC22A1 c.480G > C*, *c.1222A > G* polymorphisms (D′ = 0.88; r^2 = 0.2;, LOD = 16.4; **Figure 1**, **Table 2**). The *SLCO1B3 c.334G- c.699A* haplotype was associated with decreased risk of IM response failure—its frequency was significantly lower in IM nonresponders than in responders (85.1% vs 93.1%; *P* = .04, OR = 0.43). None of the haplotypes were

DOI: 10.1093/labmed/lmab023

Table 2. Association Analyses Between SLC22A1, SLCO1B3 SNP Genotypes and Haplotypes with Imatinib Response and CML Risk

SNP Model	Genotype Allele	CCyR, no. (%)[a]	Non-CCyR[b]	OR (95% CI)[c]		Control Individuals[d]	Patients[e]	*P* Value	OR (95% CI)
SLC22A1c.480G > C									
Codominant	CC	46 (79.3)	62 (83.8)		1 [reference]	82 (75.9)	108 (81.8)		1 [reference]
	GC	11 (19.0)	9 (12.2)	.51	0.58 (0.20–1.69)	23 (21.3)	20 (15.2)	.38	0.61 (0.29–1.25)
	GG	1 (1.7)	3 (4.0)		1.89 (0.16–21.83)	3 (2.8)	4 (3.0)		1.17 (0.23–6.02)
Missing data						1			
Dominant	CC	46 (79.3)	62 (83.8)		1 [reference]	82 (75.9)	108 (81.8)		1 [reference]
	GC/GG	12 (20.7)	12 (16.2)	.48	0.70 (0.26–1.87)	26 (24.1)	24 (18.2)	.24	0.67 (0.34–1.32)
Recessive	CC/GC	57 (98.3)	71 (96.0)		1 [reference]	105 (97.2)	128 (97.0)		1 [reference]
	GG	1 (1.7)	3 (4.0)	.58	2.00 (0.17–22.99)	3 (2.8)	4 (3.0)	.76	1.28 (0.25–6.54)
Allele	C	103 (89.0)	133 (90.0)	[reference]	1	187 (86.6)	236 (89.4)	[reference]	1
	G	13 (11.0)	15 (10.0)	.69	0.84 (0.35–1.99)	29 (13.4)	28 (10.6)	.36	0.75(0.41–1.37)
SLC22A1c.1222A > G									
Codominant	GG	30 (51.7)	36 (48.6)		1 [reference]	52 (47.7)	66 (50.0)		1 [reference]
	AG	21 (36.2)	32 (43.2)	.03[c]	2.20 (0.92–5.27)	46 (42.2)	53 (40.2)	.46	1.01 (0.57–1.81)
	AA	7 (12.1)	6 (8.1)		0.33 (0.08–1.26)	11 (10.1)	13 (9.8)		0.54 (0.20–1.47)
Dominant	GG	30 (51.7)	36 (48.6)		1 [reference]	52 (47.7)	66 (50.0)		1 [reference]
	AG/AA	28 (48.3)	38 (51.4)	.36	1.43 (0.66–3.08)	57 (52.3)	66 (50.0)	.73	0.91 (0.52–1.57)
Recessive	GG/AG	51 (87.9)	68 (91.9)		1 [reference]	98 (89.9)	119 (90.2)		1 [reference]
	AA	7 (12.1)	6 (8.1)	.04[c]	0.25 (0.07–0.94)	11 (10.1)	13 (9.8)	.21	0.54 (0.21–1.41)
Allele	G	81 (69.8)	104 (70.3)		1 [reference]	150 (68.8)	185 (70.1)		1 [reference]
	A	35 (30.2)	44 (29.7)	.83	0.94 (0.52–1.69)	68 (31.2)	79 (29.9)	.41	0.838 (0.55–1.28)
SLCO1B3c.699G > A									
	AA	54 (93.1)	64 (86.5)		1 [reference]	88 (80.7)	118 (89.4)		1 [reference]
	GA	4 (6.9)	10 (13.5)	.13	2.85 (0.74–11.08)	21 (19.3)	14 (10.6)	.08	0.50 (0.23–1.10)
Allele	A	112 (96.6)	138 (93.2)		1 [reference]	197 (90.4)	250 (94.7)		1 [reference]
	G	4 (3.4)	10 (6.8)	.14	2.67 (0.72–9.83)	21 (9.6)	14 (5.3)	.10	0.53 (0.25–1.13)
SLCO1B3c.334T > G									
Codominant	GG	51 (87.9)	52 (70.3)		1 [reference]	79 (72.5)	103 (78)		1 [reference]
	TG	6 (10.3)	22 (29.7)	.01[c]	6.02 (1.88–19.26)	28 (25.7)	28 (21.2)	.41	0.70 (0.36–1.34)
	TT	1 (1.7)	0		NA	2 (1.8)	1 (0.8)		0.34 (0.02–4.68)
Dominant	GG	51 (87.9)	52 (70.3)		1 [reference]	79 (72.5)	103 (78.0)		1 [reference]
	TG/TT	7 (12.1)	22 (29.7)	.007[c]	4.37 (1.49–12.84)	30 (27.5)	29 (22.0)	.22	0.67 (0.35–1.28)
Recessive	GG/TG	57 (98.3)	74 (100)		1 [reference]	107 (98.2)	131 (99.2)		1 [reference]
	TT	1 (1.7)	0	1	NA	2 (1.8)	1 (0.8)	.44	0.37 (0.03–5.09)
Allele	G	108 (0.93)	126 (85.1)		1 [reference]	186 (85.3)	234 (88.6)		1 [reference]
	T	8 (6.9)	22 (14.9)	.03[c]	2.86 (1.11–7.36)	32 (14.7)	30 (11.4)	.20	0.68 (0.38–1.22)

Table 2. Continued

Gene	Haplotype	CCyR N (%)	Non-CCyR N (%)	*P* Value	OR (95% CI)	Controls, no. (%)	Patients, no. (%)	*P* Value	OR (95% CI)
SLC22A1	C-G	81 (69.8)	103 (69.5)	.97	0.99 (.58–1.68)	184 (69.6)	147 (67.3)	.59	1.11 (0.75–1.63)
	C-A	22 (19.0)	30.1 (20.3)	.79	1.09 (0.59–2.01)	52 (19.8)	42 (19.4)	.91	1.03 (0.65–1.61)
	G-A	13 (11.1)	13.9 (9.4)	.64	0.83 (0.37–1.84)	27 (10.1)	26 (11.8)	.55	0.84 (0.47–1.50)
SLCO1B3	G-A	108 (93.1)	126 (85.1)	**.04**[c]	0.43 (0.18–0.992)	234 (86.6)	186 (85.3)	.27	1.34 (0.79–2.29)
	T-A	4 (3.4)	12 (8.1)	.12	2.47 (0.77–7.87)	14 (5.3)	21 (9.6)	.07	0.53 (0.26–1.06)
	T-G	4 (3.4)	10 (6.8)	.23	2.03 (0.62–6.64)	16 (6.1)	11 (20.7)	.63	1.21 (0.55–2.67)

SNP, single nucleotide polymorphism; CCyR, complete cytogenetic response;OR, odds ratio; CI, confidence interval; SLC22A1, solute carrier 22A1 (GenBank accession number; NC_000006.12); SLCO1B3, solute carrier organic anion transporter family member 1B3(NC_000012.12); NA, nonapplicable.
[a] *n = 58.*
[b] *n = 74.*
[c] *P <.05 was considered statistically significant. Logistic regression model adjusted for age, sex, and smoking status.*
[d] *n = 109.*
[e] *n = 132.*
[f] *D′=0.88; LOD = 16.4; r^2=0.23.*
[g] *D′=1; LOD = 25.5; r^2 =0.53.*

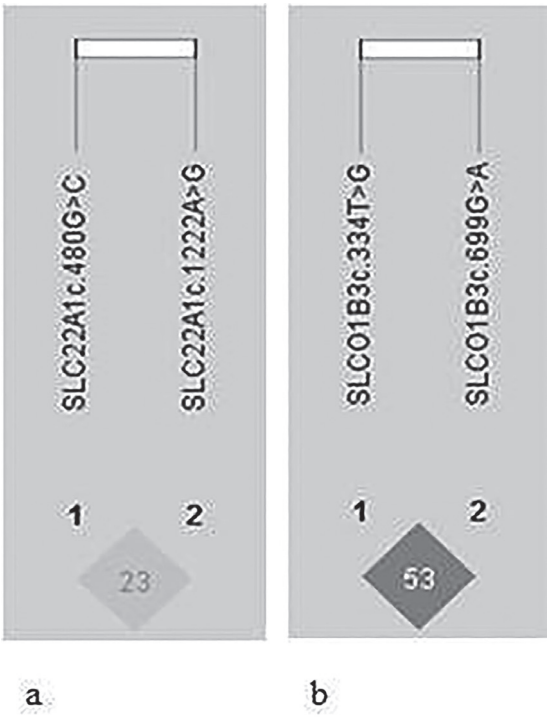

Figure 1

Haploview linkage disequilibrium (LD) map of studied-genes polymorphisms: The plots show the r^2 values. A, LD Plot of SLC22A1 (c.480G > C, c.1222A > G) Polymorphisms (GenBank accession number; NC_000006.12). B, LD Plot of SLCO1B3 (c.334T > G, c.699G > A) Polymorphisms (SLCO1B3; NC_000012.12).

associated with CML risk. The haplotype frequency of *SLCO1B3* and *SLC22A1* polymorphisms are shown in **Table 2**.

Assessment of Combined Genotypes

We considered AA genotype to be a reference genotype for *SLCO1B3c.699A > G*, an overdominant model for *SLC22A11222A > G* and dominant model for *SLC22A1c.480G > C, SLCO1B3c.334T > G* polymorphisms, to evaluate the joint effect of double SNP combination on CML susceptibility and CCyR to IM. An increased risk of non-CCyR to IM was observed in patients carrying the double combination of *SLCO1B3 c.334TG/TT* genotypes with any of *SLC22A1 c.480CC* and *SLC22A1c.1222AG* genotypes (*P* = .006, OR = 8.84; *P* = .05, OR = 7.73, respectively; **Table 3**). In female and male groups, there were no significant association between the double combined genotypes of the SNPs with increased risk of IM resistance and CML development (Supplementary Tables S6–S8).

Gene-Smoking Interaction

The effect of the interaction between *SLC22A1, SLCO1B3* SNPs with smoking on the risk of IM resistance and CML risk are shown in **Tables 4** and **5**, respectively. The reference group was nonsmoker subjects with any of the *SLC22A1c.480 CC*, *SLC22A1c.1222GG/AA,*

DOI: 10.1093/labmed/lmab023

Table 3. Combined SLC22A1 and SLCO1B3 SNP Genotypes and Imatinib Response

SNP–SNP Combination		CCyR, no. (%)[a]	Non-CCyR, no. (%)[b]	Adjusted OR (95% CI)	*P* Value[b]	*P* Value, Bonferroni-Corrected
SLC22A1c.1222A > G	SLC22A1c.480G > C					
GG/AA	CC	32 (55.2%)	39 (52.7%)	1 [reference]		>.99
	GG/GC	5 (8.6%)	3 (4.1%)	0.33 (0.06–1.72)	.33	>.99
AG	CC	14 (24.1%)	23 (31.1%)	2.61 (1.00–6.85)	.05	.31
	GG/GC	7 (12.1%)	9 (12.2%)	1.69 (0.48–5.98)	.48	>.99
SLCO1B3c.699G > A	SLC22A1c.480G > C					
AA	CC	42 (72.4%)	53 (71.6%)	1 [reference]		
	GG/GC	12 (20.7%)	11 (14.9%)	0.64 (0.23–1.78)	.39	>.99
GA	CC	4 (6.9%)	9 (12.2%)	2.06 (0.50–8.49)	.32	>.99
	GG/GC	0	1 (1.4%)	NA	>.99	>.99
SLCO1B3c. 334T > G	SLC22A1c.480G > C					
GG	CC	42 (72.4%)	41 (55.4%)	1 [reference]		
	GG/ GC	9 (15.5%)	11 (14.9%)	1.29 (0.43–3.85)	.65	>.99
TG/TT	CC	4 (6.9%)	21 (28.4%)	8.84 (2.33–33.49)	.001	.006[d]
	GG/ GC	3 (5.2%)	1 (1.4%)	0.29 (0.02–3.83)	.35	>.99
SLCO1B3c. 699G > A	SLC22A1c.1222A > G					
AA	GG/AA	35 (60.3%)	35 (47.3%)	1 [reference]		
	AG	19 (32.8%)	29 (39.2%)	3.20 (1.28–8.05)	.01	.78
GA	GG/AA	2 (3.4%)	7 (9.5%)	6.85 (1.02–45.93)	.048	.29
	AG	2 (3.4%)	3 (4.1%)	3.52 (0.41–30.37)	.25	>.99
SLCO1B3c. 334T > G	SLC22A1c.1222A > G					
GG	GG/AA	34 (58.6%)	29 (39.2%)	1 [reference]		
	AG	17 (29.3%)	23 (31.1%)	2.86 (1.09–7.47)	.03	.19
TG/TT	GG/AA	3 (5.2%)	13 (17.6%)	6.54 (1.34–31.83)	.02	.12
	AG	4 (6.9%)	9 (12.2%)	7.73 (1.69–35.36)	.008	.048[d]
SLCO1B3c. 334T > G	SLCO1B3c. 699G > A					
GG	AA	51 (87.9%)	52 (70.3%)	1 [reference]		
	GA	0	0	NA	NA	
TG/TT	AA	3 (5.2%)	12 (16.2%)	5.48 (1.23–24.35)	.02	.15
	GA	4 (6.9%)	10 (13.5%)	3.55 (0.89–14.20)	.07	.44

SNP, single nucleotide polymorphism; CCyR, complete cytogenetic response; OR, odds ratio; CI, confidence interval; SLC22A1, solute carrier 22A1 (GenBank accession number; NC_000006.12); SLCO1B3, solute carrier organic anion transporter family member 1B3(NC_000012.12);

[a] *n = 58.*

[b] *n = 74.*

[c] *Logistic regression model adjusted for age, sex, and smoking status.*

[d] *P <.05 was considered statistically significant.*

SLCO1B3c.699AA, and *SLCO1B3c.334GG* genotypes. We considered the sum of active and passive groups as smokers. The risk of IM resistance increased in the smoker subjects with the *SLC22A1c.480CC*; *SLC22A1c.1222AA/GG,AG*; *SLCO1B3c.699AA*; and *SLCO1B3c.334GG,TG/TT* genotypes (*P* <.001; OR = 7.03, 12.67, 16.74, 5.58, 8.13, and 22.09, respectively). Moreover, nonsmoker patients with the SLCO1B3c.334TG/TT genotype had an increased risk of IM resistance (*P* = .04; OR = 5.86). We also observed that the *SLC22A1c.480CC*; *SLC22A1c.1222AA/GG,AG*; and *SLCO1B3c.334GG,TG* genotypes in male smoker participants were associated with increased resistance to IM (*P* = .01, OR = 6.09; *P* = .03, OR = 8.33; *P* = .03, OR = 9.36; *P* = .02, OR = 5.98; and *P* = .04, OR = 24.10, respectively). The female smoker participants with genotypes including *SLC22A1c.480CC*, *SLC22A1c.1222AA/GG*, *SLCO1B3c.699AA*, and *SLCO1B3c.334GG* genotypes had an increased risk of resistance to IM (*P* = .004, OR = 11.74; *P* <.001, OR = 27.54; *P* = .004, OR = 9.42; and *P* = .004, OR = 11.22, respectively; **Table 4**).

Regarding CML risk, the smoker subjects carrying *SLC22A1c.480CC*; *SLC22A1c.1222AA/GG, AG*; *SLCO1B3c.699AA*; and *SLCO1B3c.334GG* genotypes had an increased risk for CML development (*P* <.001, OR = 5.48; *P* < .001, OR = 8.67; *P* = .01, OR = 4.09; *P* <.001, OR = 5.59; and *P* <.001, OR = 6.18, respectively). The smoker females with *SLC22A1c.480CC*, *SLC22A1c.1222AA/GG*,

Table 4. Gene-Smoking Interaction and Imatinib Response in Patient Groups

SNP	Current or Ever Smoking	CCyR, no. (%)	Non-CCyR, no. (%)	Adjusted OR (95% CI)	*P* Value[a,b]	*P* Value,' Bonferroni corrected[b]
Patients[c]						
SLC22A1c.480G > C						
CC	N	33 (56.9%)	18 (24.3%)	1 [reference]		
	Y	13 (22.4%)	44 (59.5%)	7.03 (2.93–16.87)	<.001	<.001[b]
GC/GG	N	7 (12.1)	4 (5.4%)	1.06 (0.26–4.28)	.93	>.99
	Y	5 (8.6%)	8 (10.8%)	3.49 (0.96–12.70)	.06	.23
SLC22A1c.1222A > G						
GG/AA	N	24 (41.4%)	6 (8.1%)	1 [reference]		
	Y	13 (22.4%)	36 (48.6%)	12.67 (4.07–39.43)	<.001	<.001[b]
AG	N	16 (27.6%)	16 (21.6%)	4.22 (1.32–13.45)	.01	.06
	Y	5 (8.6%)	16 (21.6%)	16.74 (4.10–68.43)	<.001	<.001[b]
SLCO1B3c.699G > A						
AA	N	36 (62.1%)	19 (25.7%)	1 [reference]		
	Y	18 (31.0%)	45 (60.8%)	5.58 (2.45–12.74)	<.001	<.001[b]
GA	N	4 (6.9%)	3 (4.1%)	1.69 (0.33–8.63)	.53	>.99
	Y	0	7 (9.5%)	NA	>.99	>.99
SLCO1B3c.334T > G						
GG	N	35 (60.3%)	14 (18.9%)	1 [reference]		
	Y	16 (27.6%)	38 (51.4%)	8.13 (3.14–21.02)	<.001	<.001[b]
TG/TT	N	5 (8.6%)	8 (10.8%)	5.86 (1.50–22.89)	.01	.04[b]
	Y	2 (3.4%)	14 (18.9%)	22.09 (4.22–115.73)	<.001	<.001[b]
Female[d]						
SLC22A1c.480G > C						
CC	N	16 (69.6%)	9 (26.5%)	1 [reference]		
	Y	3 (13.0%)	19 (55.9%)	11.74 (2.66–51.77)	.001	.004[b]
GC/GG	N	3 (13.0%)	3 (8.8%)	2.03 (0.32–12.88)	.45	>.99
	Y	1 (4.3%)	3 (8.8%)	5.03 (0.45–56.58)	.19	.76
SLC22A1c.1222A > G						
GG/AA	N	12 (52.2%)	2 (5.9%)	1 [reference]		
	Y	4 (17.4%)	18 (52.9%)	27.54 (4.28–177.29)	<.001	<.001[b]
AG	N	7 (30.4%)	10 (29.4%)	8.75 (1.45–52.69)	.02	.07
	Y	0	4 (11.8%)	NA	>.99	>.99
SLCO1B3c.699G > A						
AA	N	19 (82.6%)	10 (29.4%)	1 [reference]		
	Y	4 (17.4%)	20 (58.8%)	9.42 (2.52–35.27)	.001	.004[b]
GA	N	0	2 (5.9%)	NA	>.99	>.99
	Y	0	2 (5.9%)	NA	>.99	>.99
SLCO1B3c.334T > G						
GG	N	19 (82.6%)	9 (26.5%)	1 [reference]		
	Y	3 (13.0%)	16 (47.1%)	11.22 (2.59–48.66)	.001	.004[b]
TG/TT	N	0	3 (8.8%)	NA	>.99	>.99
	Y	1 (4.4%)	6 (17.6%)	12.47 (1.28–121.70)	.03	.12
Male[e]						
SLC22A1c.480G > C						
CC	N	17 (48.6%)	9 (22.5%)	1 [reference]	[reference]	
	Y	10 (28.6%)	25 (62.5%)	6.09 (1.86–19.88)	.003	.01[b]
GC/GG	N	4 (11.4%)	1 (2.5%)	1.04 (0.09–12.25)	.97	>.99
	Y	4 (11.4%)	5 (12.5%)	2.89 (0.55–15.03)	.21	.83
SLC22A1c.1222A > G						
GG/AA	N	12 (34.3%)	4 (10.0%)	1 [reference]		
	Y	9 (25.7%)	18 (45.0%)	8.33 (1.82–38.13)	.008	.03[b]
AG	N	9 (25.7%)	6 (15.0%)	2.66 (0.52–13.70)	.24	.97
	Y	5 (14.3%)	12 (30.0%)	9.36 (1.78–49.24)	.008	.03[b]
SLCO1B3c.699G > A						

DOI: 10.1093/labmed/lmab023

Table 4. Continued

SNP	Current or Ever Smoking	CCyR, no. (%)	Non-CCyR, no. (%)	Adjusted OR (95% CI)	*P* Value[a,b]	*P* Value,' Bonferroni corrected[b]
AA	N	17 (48.6%)	9 (22.5%)	1 [reference]		
	Y	14 (40.0%)	25 (62.5%)	3.80 (1.27–11.38)	.02	.07
GA	N	4 (11.4%)	1 (2.5%)	0.33 (0.03–3.82)	.38	>.99
	Y	0	5 (12.5%)	NA	>.99	>.99
SLCO1B3c.334T > G						
GG	N	16 (45.7%)	5 (12.5%)	1 [reference]		
	Y	13 (37.1%)	22 (55.0%)	5.98 (1.68–21.33)	.006	.02[b]
TG	N	5 (14.3%)	5 (12.5%)	2.74 (0.52–14.42)	.23	.94
	Y	1 (2.9%)	8 (20.0%)	24.10 (2.25–258.24)	.009	.04[b]

SNP, single nucleotide polymorphism; CCyR, complete cytogenetic response; OR, odds ratio; CI, confidence interval; SLC22A1, solute carrier 22A1 (GenBank accession number; NC_000006.12); SLCO1B3, solute carrier organic anion transporter family member 1B3(NC_000012.12).
[a]P-value logistic regression model adjusted for age status.
[b]P <.05 was considered statistically significant.
[c]n = 132.
[d]n = 57.
[e]n = 75.

SLCO1B3c.699AA, and *SLCO1B3c.334GG* genotypes had an increased risk of CML development (*P* = .004, OR = 14.49; *P* < .001, OR = 13.19; *P* = .004, OR = 7.71; and *P* = .02, OR = 5.8, respectively). Also, the carriers of *SLC22A1c.480CC*; *SLC22A1c.1222AA/GG,AG*; *SLCO1B3c.699AA*, and *SLCO1B3c.334GG* genotypes in male smokers had an increased risk of CML (*P* = .004, OR = 3.92; *P* <.001, OR = 6.75; *P* = .036, OR = 4.23; *P* <.001, OR = 4.77; and *P* <.001, OR = 6.66, respectively; **Table 5**).

Discussion

Many studies have been carried out to identify pharmacogenetic factors that predict IM treatment outcomes in patients with CML. To our knowledge, this is the first study that evaluates the association of 4 polymorphisms in *SLC22A1* and *SLCO1B3*, along with SNP combinations and SNP-smoking interaction, with the risk of CML development and IM resistance in the Iranian population. In this study, minor allele frequency (MAF) of the *SLC22A1c.480G > C*, *c.1222A > G*, *SLCO1B3c.699G > A*, and *c.334T > G* polymorphisms, compared with other populations (1000 Genomes Project Phase 3) was closer to American, African, South Asian, and European populations, respectively (Ensembl.org).

An important finding of our study was the lower mean age of male nonresponders than male responders. Some studies, such as Singh et al,[27] have shown that younger patients have a better response to the drug, compared with older patients. However, the results of a more recent study[28] showed no difference in achieving the optimal response among elderly patients than younger ones. Based on our findings, a significant association was observed between *SLC22A1c.1222AA* with higher CCyR achievement. A significant association between *SLC22A1c.1222A > G* with IM response was revealed by another study report[29] as well.

In contrast to our results, there are conflicting findings in the literature. For instance, Makhtar et al[30] found that the *SLC22A1c.1222AA* genotype, together with 8-bp insertion and 3-bp deletion, and M420del alleles increased the risk of resistance to IM. Also, Vaidya et al[31] and Takahashi et al[32] reported the association of the GG genotype of *SLC22A1c.1222* SNP with better response to IM.

Some study reports found no relationship between this polymorphism and IM response.[33,34] These findings may be due to the different ethnicities of the studied populations.[35] Our findings showed no association between *SLC22A1c.408G > C* polymorphism and IM treatment response, which is consistent with the findings of 2 studies[36,37] and contradicts other findings.[30,38]

We analyzed 2 known polymorphisms in the *SLCO1B3* gene, namely, c.699G > A and C.334T > G, that are related

Table 5. Gene-Smoking Interaction and CML Risk in All Subjects, the Female Group, and the Male Group

SNP	Current or Ever Smoking	Controls	Patients	Adjusted OR (95% CI)	*P* Value[a,b]	*P* Value, Bonferroni Corrected[b]
Subjects[c]						
SLC22A1c.480G > C						
CC	N	68 (63.1%)	51 (38.5%)	1 [reference]		
	Y	14 (13.1%)	57 (43.2%)	5.48 (2.73–10.97)	<.001	>.99
GC/GG	N	21 (19.41%)	11 (8.3%)	0.69 (0.30–1.56)	.37	>.99
	Y	5 (4.6%)	13 (9.8%)	3.44 (1.15–10.32)	.03	.11
SLC22A1c.1222A > G						
GG/AA	N	53 (48.6%)	30 (22.7%)	1 [reference]		
	Y	10 (9.2%)	49 (37.1%)	8.67 (3.84–19.59)	<.001	<.001
AG	N	37 (33.9%)	32 (24.2%)	1.55 (0.80–2.98)	.19	.77
	Y	9 (8.3%)	21 (15.9%)	4.09 (1.64–10.20)	.003	<.01
SLCO1B3c.699G > A						
AA	N	73 (67.0%)	55 (41.7%)	1 [reference]		
	Y	15 (13.8%)	63 (47.7%)	5.59 (2.86–10.93)	<.001	<.001
GA	N	17 (15.6%)	7 (5.3%)	0.55 (0.21–1.41)	.21	.85
	Y	4 (3.7%)	7 (5.3%)	2.34 (0.65–8.46)	.19	.78
SLCO1B3c.334T > G						
GG	N	67 (61.5%)	49 (37.1%)	1 [reference]		
	Y	12 (11.0%)	54 (40.9%)	6.18 (2.96–12.89)	<.001	<.001
TG/TT	N	23 (21.1%)	13 (9.8%)	0.77 (0.36–1.68)	.52	>.99
	Y	7 (6.4%)	16 (12.1%)	3.15 (1.20–8.30)	.02	<.08
Female[d]						
SLC22A1c.480G > C						
CC	N	33 (63.5%)	25 (43.9%)	1 [reference]		
	Y	2 (3.8%)	22 (38.6%)	14.49 (3.11–67.45)	.001	.004
GC/GG	N	14 (26.9%)	6 (10.5%)	0.57 (0.19–1.69)	.31	>.99
	Y	3 (5.8%)	4 (7.0%)	1.72 (0.35–8.46)	.51	>.99
SLC22A1c.1222A > G						
GG/AA	N	25 (48.1%)	14 (24.6%)	1 [reference]		
	Y	3 (5.8%)	22 (38.6%)	13.19 (3.34–52.13)	<.001	<.001
AG	N	22 (42.3%)	17 (29.8%)	1.42 (0.56–3.60)	.46	>.99
	Y	2 (3.8%)	4 (7.0%)	3.54 (0.57–21.85)	.17	.69
SLCO1B3c.699G > A						
AA	N	38 (73.1%)	29 (50.9%)	1 [reference]		
	Y	4 (7.7%)	24 (42.1%)	7.71 (2.40–24.75)	.001	.004
GA	N	9 (17.5%)	2 (3.5%)	0.28 (0.05–1.41)	.12	.49
	Y	1 (1.9%)	2 (3.5%)	2.56 (0.22–29.78)	.45	>.99
SLCO1B3c.334T > G						
GG	N	35 (67.3%)	28 (49.1%)	1 [reference]		
	Y	4 (7.7%)	19 (33.3%)	5.80 (1.76–19.07)	.004	.02
TG/TT	N	12 (23.1%)	3 (5.3%)	0.29 (0.07–1.17)	.08	.33
	Y	1 (1.9%)	7 (12.3%)	8.46 (0.98–73.18)	.05	.21
Male[e]						
SLC22A1c.480G > C						
CC	N	35 (62.5%)	26 (37.4%)	1 [reference]		
	Y	12 (21.4%)	35 (46.7%)	3.92 (1.71–8.98)	.001	.004
GC/GG	N	7 (12.5%)	5 (6.7%)	0.95 (0.26–3.39)	.99	>.99
	Y	2 (3.6%)	9 (12%)	6.01 (1.19–30.31)	.03	.12
SLC22A1c.1222A > G						
GG/AA	N	28 (49.1%)	16 (21.3%)	1 [reference]		
	Y	7 (12.3%)	27 (36.0%)	6.75 (2.40–18.96)	<.001	<.001
AG	N	15 (26.3%)	15 (20.0%)	1.75 (0.68–4.49)	.25	.99
	Y	7 (12.3%)	17 (22.7%)	4.23 (1.45–12.40)	.009	.04
SLCO1B3c.699G > A						

DOI: 10.1093/labmed/lmab023

Table 5. Continued

SNP	Current or Ever Smoking	Controls	Patients	Adjusted OR (95% CI)	*P* Value[a,b]	*P* Value, Bonferroni Corrected[b]
AA	N	35 (61.4%)	26 (34.7%)	1 [reference]		
	Y	11 (19.3%)	39 (52.0%)	4.77 (2.06–11.06)	<.001	<.001
GA	N	8 (14.0%)	5 (6.7%)	0.85 (0.25–2.91)	.79	>.99
	Y	3 (5.3%)	5 (6.7%)	2.25 (0.49–10.26)	.30	>.99
SLCO1B3c.334T > G						
GG	N	32 (56.1%)	21 (28.0%)	1 [reference]		
	Y	8 (14.0%)	35 (46.7%)	6.66 (2.59–17.14)	<.001	<.001
TG/TT	N	11 (19.3%)	10 (13.0%)	1.39 (0.50–3.85)	.53	
	Y	6 (10.5%)	9 (12.0%)	2.29 (0.71–7.41)	.17	.66

SNP, single nucleotide polymorphism; CCyR, complete cytogenetic response; OR, odds ratio; CI, confidence interval; SLC22A1: solute carrier 22A1 (GenBank accession number; NC_000006.12); SLC22A1: solute carrier 22A1 (GenBank accession number; NC_000006.12).
[a]*Logistic regression model adjusted for age status.*
[b]*P <.05 was considered statistically significant.*
[c]*N = 241.*
[d]*n = 57.*
[e]*n = 75.*

to IM response. Although no association was found between the c.699G > A SNP and CCyR, a strong association was observed between the c.334T > G SNP and CCyR because the patients with the c.334TT/TG genotype (dominant genetic model) showed statistically significant lack of response ($P = .007$). Nair et al[39] showed the relationship between *SLCO1B3c.334TT* genotype and failure of CCyR, and de Lima et al[16] reported an increased risk of IM resistance in patients with *SLCO1B3c.334TT* and *c.699GG* genotypes.

We were intrigued to discover that, in our patients and the Nair et al study,[39] the frequency of the TT genotype was very low (0.7% and 1.96%, respectively), whereas in the de Lima et al[16] study, was approximately 56%, which is similar to genotypic variation in other populations.[15] Inconsistent with our findings, some study reports showed no association between *SLCO1B3c. 334T > G* with clinical response to IM.[14] Other study results found a relationship between this polymorphism with IM clearance[40] and its intracellular concentration,[9] whereas in a recent study report, no impact of pharmacogenetic items, such as *SLCO1B3c.699G > A, c.334T > G*, was found in IM pharmacokinetics in Chinese patients with CML.[41] In our study findings, haplotype analysis showed no association between haplotypes with response to IM, except the 334G-699A haplotype in *SLCO1B3*, as frequency of 334G-699A haplotype in nonresponder patients was lower than in responders, which suggests a protective role on IM resistance risk.

In accordance with our results, Kim DHD et al[38] found no association between *SLC22A1c.480G > C*, *1222A > G*, and *156T > C* haplotypes and major cytogenetic response (MCyR), CCyR, loss of response (LOR), or treatment failure. Moreover, in our study results, we showed a strong complete linkage disequilibrium ($D' = 1$, $r^2=0.53$, LOD = 25.5) between *SLCO1B3* SNPs, similar to the findings of other studies.[9,15,16] In the present study, we found no statistically significant association between these SNPs and their combinations with CML risk. These findings are in concordance with those of de Lima et al,[16] regarding the association of *SLCO1B3* polymorphisms and CML risk.

We observed considerable differences between the male and female groups. First, the mean age of nonresponder females was significantly higher than that in nonresponder males (48.1 years vs 39.5 years). Secondly, the female group with the *SLC22A1c.1222AG* genotype has significantly increased risk of IM resistance, unlike the group of males with that genotype. Although these results have not been reported so far, these differences between females and males appear to be due to the effect of female hormones, such as progesterone, on drug transporters.

Some study reports, such as Vasconselos et al,[42] indicate that an efflux transporter, P-glycoprotein (Pgp), has low activity in young females and that synthetic progestins inhibit Pgp, in vitro and ex vivo. However, there is no report of such effect on influx transporters.

Our study is the first in the literature to show the joint effect of influx-transporter genes and smoking on CML risk and IM resistance. In general, few studies have been conducted on

this issue. In our study findings, neither the polymorphisms by themselves nor their combinations had any role in CML risk; however, the association of transporter polymorphism with CML risk was dependent on smoking status. This result is compatible with those of Kim HN et al,[20] namely, that the relationship of the GSTT1 polymorphism with AML risk is dependent on smoking status. In 1 study report,[43] it was revealed that there was a higher probability of survival and lower rate of disease progression in nonsmokers than smokers among patients with CML, as well as a similar molecular response rate in the 2 groups.

Another study report[3] has discussed the association of the smoking–metabolizing genes interaction with CML risk. Taken together, previous data[17] have suggested that cigarette smoke can inhibit expression and/or activity of *SLC22A1* and *SLCO1B3*. Such changes may be attributed to cigarette smoke–induced alteration of pharmacokinetics. It seems that cigarette smoke changes the expression and activity of the transporter and reduces the uptake function of the IM into the cells by influx transporters and causes drug resistance.

In conclusion, our findings have revealed the impact of *SLC22A1*, *SLCO1B3* polymorphisms on cytogenetic response to IM, and also the influence of SNP combinations and the joint effect of SNPs and smoking as a synergistic factor affecting treatment response and CML risk. Also, we demonstrated the usefulness of the pharmacogenetic-environmental approach for predicting the clinical outcome of IM therapy, which may help in personalized treatment in patients with CML. **LM**

Acknowledgments

We are grateful for the help and collaboration of the patients, as part of their participation in the study.

Personal and Professional Conflicts of Interest

None reported.

Funding

This work was supported by the Pasteur Institute of Iran (grant no. 1033).

References

1. Rostami G, Hamid M, Yaran M, Khani M, Karimipoor M. Incidence and clinical importance of BCR-ABL1 mutations in Iranian patients with chronic myeloid leukemia on imatinib. *J Hum Genet*. 2015;60:253–258.
2. Jabbour E, Kantarjian H. Chronic myeloid leukemia: 2018 update on diagnosis, therapy and monitoring. *Am J Hematol*. 2018;93(3):442–459.
3. Rostami G, Assad D, Ghadyani F, et al. Influence of glutathione S-transferases (GSTM1, GSTT1, and GSTP1) genetic polymorphisms and smoking on susceptibility risk of chronic myeloid leukemia and treatment response. *Mol Genet Genomic Med*. 2019;7(7):e00717.
4. Cargnin S, Ravegnini G, Soverini S, Angelini S, Terrazzino S. Impact of SLC22A1 and CYP3A5 genotypes on imatinib response in chronic myeloid leukemia: a systematic review and meta-analysis. *Pharmacol Res*. 2018;131:244–254.
5. Jaruskova M, Curik N, Hercog R, et al. Genotypes of SLC22A4 and SLC22A5 regulatory loci are predictive of the response of chronic myeloid leukemia patients to imatinib treatment. *J Exp Clin Cancer Res*. 2017;36:55.
6. He L, Vasiliou K, Nebert DW. Analysis and update of the human solute carrier (SLC) gene superfamily. *Hum Genomics*. 2009;3:195.
7. Picard S, Titier K, Etienne G, et al. Trough imatinib plasma levels are associated with both cytogenetic and molecular responses to standard-dose imatinib in chronic myeloid leukemia. *Blood*. 2006;109(8):3496–3499.
8. Widmer N, Decosterd LA, Csajka C, et al. Population pharmacokinetics of imatinib and the role of α1-acid glycoprotein. *Br J Clin Pharmacol*. 2006;62(1):97–112.
9. Nambu T, Hamada A, Nakashima R, et al. Association of *SLCO1B3* polymorphism with intracellular accumulation of imatinib in leukocytes in patients with chronic myeloid leukemia. *Biol Pharm Bull*. 2011;34(1):114–119.
10. White DL, Saunders VA, Dang P, et al. Most CML patients who have a suboptimal response to imatinib have low OCT-1 activity: higher doses of imatinib may overcome the negative impact of low OCT-1 activity. *Blood*. 2007;110(12):4064–4072.
11. Zhong J-S, Meng F-Y, Xu D, Zhou H-S, Dai M. Correlation between imatinib trough concentration and efficacy in Chinese chronic myelocytic leukemia patients. *Acta Haematol*. 2012;127(4):221–227.
12. Di Paolo A, Polillo M, Capecchi M, et al. The c. 480C>G polymorphism of hOCT1 influences imatinib clearance in patients affected by chronic myeloid leukemia. *Pharmacogenomics J*. 2014;14:328–335.
13. Koren-Michowitz M, Buzaglo Z, Ribakovsky E, et al. OCT 1 genetic variants are associated with long term outcomes in imatinib treated chronic myeloid leukemia patients. *Eur J Haematol*. 2014;92(4):283–288.
14. Bedewy AML, El-Maghraby SM. Do SLCO1B3 (T334G) and CYP3A5*3 polymorphisms affect response in Egyptian chronic myeloid leukemia patients receiving imatinib therapy? *Hematol*. 2013;18(4):211–216.
15. Smith NF, Marsh S, Scott-Horton TJ, et al. Variants in the *SLCO1B3* gene: interethnic distribution and association with paclitaxel pharmacokinetics. *Clin Pharmacol Ther*. 2007;81(1):76–82.
16. de Lima LT, Bueno CT, Vivona D, et al. Relationship between SLCO1B3 and ABCA3 polymorphisms and imatinib response in chronic myeloid leukemia patients. *Hematol*. 2015;20(3):137–142.
17. Sayyed K, Le Vee M, Abdel-Razzak Z, et al. Alteration of human hepatic drug transporter activity and expression by cigarette smoke condensate. *Toxicology*. 2016;363:58–71.
18. Marsh S, McLeod H. Cancer pharmacogenetics. *Br J Cancer*. 2004;90(1):8–11.
19. Björk J, Albin M, Mauritzson N, Strömberg U, Johansson B, Hagmar L. Smoking and acute myeloid leukemia: associations with morphology and karyotypic patterns and evaluation of dose–response relations. *Leuk Res*. 2001;25(10):865–872.
20. Kim HN, Kim NY, Yu L, et al. Association of *GSTT1* polymorphism with acute myeloid leukemia risk is dependent on smoking status. *Leuk Lymphoma*. 2012;53(4):681–687.
21. Haznedaroğlu İC, Kuzu I, İlhan O. WHO 2016 definition of chronic myeloid leukemia and tyrosine kinase inhibitors. *Turk J Haematol*. 2020;37(1):42–47.

22. Baccarani M, Cortes J, Pane F, et al. Chronic myeloid leukemia: an update of concepts and management recommendations of European LeukemiaNet. *J Clin Oncol*. 2009;27(35):6041–6051.
23. Baccarani M, Deininger MW, Rosti G, et al. European LeukemiaNet recommendations for the management of chronic myeloid leukemia: 2013. *Blood*. 2013;122(6):872–884.
24. Schoch C, Schnittger S, Bursch S, et al. Comparison of chromosome banding analysis, interphase-and hypermetaphase-FISH, qualitative and quantitative PCR for diagnosis and for follow-up in chronic myeloid leukemia: a study on 350 cases. *Leukemia*. 2002;16:53–59.
25. Sumner AT, Evans HJ, Buckland RA. New technique for distinguishing between human chromosomes. *Nature New Biology*. 1971;232:31–32.
26. Miller SA, Dykes DD, Polesky HF. A simple salting out procedure for extracting DNA from human nucleated cells. *Nucleic Acids Res*. 1988;16(3):1215.
27. Singh M, Gupta AK, Singh JK, et al. Effect of age and sex under imatinib mesylate therapy on chronic myeloid leukaemia patients: a pilot study from India. *Int J Pharm Sci Res*. 2017;8(4):1727–1733.
28. Belohlavkova P, Steinerova K, Karas M, et al. First-line imatinib in elderly patients with chronic myeloid leukaemia from the CAMELIA registry: age and dose still matter. *Leuk Res*. 2019;81:67–74.
29. Watkins DB, Hughes TP, White DL. OCT1 and imatinib transport in CML: is it clinically relevant? *Leukemia.* 2015;29:1960–1969.
30. Makhtar SM, Husin A, Baba AA. Genetic variations in influx transporter gene *SLC22A1* are associated with clinical responses to imatinib mesylate among Malaysian chronic myeloid leukaemia patients. *J Genet*. 2018;97(4):835–842.
31. Vaidya S, Ghosh K, Shanmukhaiah C, Vundinti BR. Genetic variations of hOCT1 gene and CYP3A4/A5 genes and their association with imatinib response in Chronic Myeloid Leukemia. *Eur J Pharmacol*. 2015;765:124–130.
32. Takahashi N, Miura M, Scott SA, et al. Influence of CYP3A5 and drug transporter polymorphisms on imatinib trough concentration and clinical response among patients with chronic phase chronic myeloid leukemia. *J Hum Genet*. 2010;55(11):731–737.
33. Maffioli M, Camós M, Gaya A, et al. Correlation between genetic polymorphisms of the *h*OCT1 and *MDR1* genes and the response to imatinib in patients newly diagnosed with chronic-phase chronic myeloid leukemia. *Leuk Res*. 2011;35(8):1014–1019.
34. White DL, Saunders VA, Dang P, Engler J, Hughes TP. OCT-1 activity measurement provides a superior imatinib response predictor than screening for single-nucleotide polymorphisms of OCT-1. *Leukemia*. 2010;24:1962–1965.
35. Umamaheswaran G, Praveen RG, Arunkumar AS, Das AK, Shewade DG, Adithan C. Genetic analysis of *OCT1* gene polymorphisms in an Indian population. *Indian J Hum Genet*. 2011;17(3):164–168.
36. Gromicho M, Magalhães M, Torres F, et al. Instability of mRNA expression signatures of drug transporters in chronic myeloid leukemia patients resistant to imatinib. *Oncol Rep*. 2013;29(2):741–750.
37. Belohlavkova P, Vrbacky F, Voglova J, et al. The significance of enzyme and transporter polymorphisms for imatinib plasma levels and achieving an optimal response in chronic myeloid leukemia patients. *Arch Med Sci*. 2018;14(6):1416–1423.
38. Kim DHD, Sriharsha L, Xu W, et al. Clinical relevance of a pharmacogenetic approach using multiple candidate genes to predict response and resistance to imatinib therapy in chronic myeloid leukemia. *Clin Cancer Res*. 2009;15(14):4750–4758.
39. Nair D, Dhangar S, Shanmukhaiah C, Vundinti BR. Association of genetic polymorphisms of the ABCG2, ABCB1, SLCO1B3 genes and the response to imatinib in chronic myeloid leukemia patients with chronic phase. *Meta Gene*. 2017;11:14–19.
40. Yamakawa Y, Hamada A, Nakashima R, et al. Association of genetic polymorphisms in the influx transporter SLCO1B3 and the efflux transporter ABCB1 with imatinib pharmacokinetics in patients with chronic myeloid leukemia. *Ther Drug Monit*. 2011;33(2):244–250.
41. Wang Q, Jiang Z-P, Yu E-Q, et al. Population pharmacokinetic and pharmacogenetics of imatinib in Chinese patients with chronic myeloid leukemia. *Pharmacogenomics*. 2019;20(4):251–260.
42. Vasconcelos FC, Bonecker ST, de Souza PS, et al. Age, gender and efflux transporter activity influence imatinib efficacy in chronic myeloid leukemia patients. *Leuk Res*. 2019;82:33–35.
43. Lauseker M, Hasford J, Saussele S, et al. Smokers with chronic myeloid leukemia are at a higher risk of disease progression and premature death. *Cancer*. 2017;123(13):2467–2471.

Liver Blood Tests in the Management of Suspected Choledocholithiasis

Francesco Mongelli, MD,[1,] Matteo Di Giuseppe, MD,[2] Iride Porcellini, MD,[2] Francesco Proietti, MD,[1] Alessandra Cristaudi, MD,[1] Ramon Pini, MD,[2] Davide La Regina, MD[2]*

Laboratory Medicine 2021;52:597-602

DOI: 10.1093/labmed/lmab042

ABSTRACT

Objective: The likelihood of common bile duct (CBD) stones considers liver blood tests (LBTs) if they are markedly altered only. The aim of our study was to find a reliable tool based on LBTs to predict the presence of CBD stones.

Methods: We retrospectively considered all patients who underwent magnetic resonance cholangiopancreatography (MRCP) because of suspected CBD stones from January 2014 to June 2019. Demographic, clinical data, and LBT values were collected and analyzed.

Results: We selected 191 patients, 64 (33.5%) with positive MRCP and 127 (66.5%) with negative MRCP. The analysis showed that our compound LBT-based score had 83.6%, 90.7%, and 90.6% sensitivity, specificity, and negative predictive values, respectively, in determining MRCP results.

Conclusion: We designed a weighted score with high diagnostic power in determining MRCP results that could help in differentiating between candidates for primary cholecystectomy and patients who benefit from preoperative MRCP.

Keywords: cholestasis, common bile duct gallstones, magnetic resonance cholangiopancreatography, gallbladder, predictive value of tests, cholecystectomy

Gallstones are a common disease worldwide, affecting up to 21% of the general population.[1] Approximately 35% of patients with gallstones develop symptoms or complications.[2] Medical conditions such as biliary colic, jaundice, pancreatitis, cholecystitis, and cholangitis are common indications for hospital admission.[3] Up to 15% of patients with symptomatic gallstone disease have common bile duct (CBD) stones, which may be asymptomatic in 5% to 12% of patients or lead to more severe conditions.[4]

Abbreviations:

CBD, common bile duct; LBT, liver blood test; MRCP, magnetic resonance cholangiopancreatography; ERCP, endoscopic retrograde cholangiopancreatography; EUS, endoscopic ultrasonography; TotBil, total bilirubin; DirBil, direct bilirubin; AST, aspartate aminotransferase; ALT, alanine aminotransferase; GGT, gamma-glutamyltransferase; AP, alkaline phosphatase; ROC, receiver operating characteristic; AUC, area under the ROC curve.

[1]Department of Surgery, Ospedale Regionale di Lugano, Lugano, Switzerland, [2]Department of Surgery, Ospedale Regionale di Bellinzona e Valli, Bellinzona, Switzerland

*To whom correspondence should be addressed.
francesco.mongelli@mail.com

Patients admitted to the hospital with biliary colic are usually evaluated with clinical history, physical examination, blood tests, and abdominal ultrasound,[5] not only to confirm the diagnosis of gallstones but also to evaluate the risk of CBD stones, because missing their occurrence can result in complications such as cholangitis, acute biliary pancreatitis, and symptomatic choledocholithiasis.[5] The guidelines of the European Association for the Study of the Liver support the routine use of serum liver biochemical tests and abdominal ultrasound as the initial evaluation to stratify the risk of CBD stones. American, European, British, and German societies' guidelines suggest predictors for CBD stones and propose management algorithms.[6-9] Most societies advocate preoperative endoscopic retrograde cholangiopancreatography (ERCP) in patients with a high likelihood of CBD stones, whereas magnetic resonance cholangiopancreatography (MRCP), endoscopic ultrasonography (EUS), or intraoperative cholangiography are indicated in case of intermediate probability. Finally, patients with a low probability of CBD stones should undergo a cholecystectomy with or without an intraoperative cholangiography.

Therefore, clinical suspicion, abdominal ultrasound, and liver blood tests (LBTs) play the main role in predicting the

presence of CBD stones. However, none of them has an adequate sensitivity or specificity when used alone, and the recent literature is still controversial.[5,10,11] The aim of our study was to develop a mathematical equation based on LBT values and to use it as a score to predict the presence of CBD stones.

Materials and Methods

Data Collection

Written consents were administered to all patients, and the local ethics committee approved the study (Comitato Etico Cantonale Ticino number 2019–02060 CE 3535) in accordance with the principles set forth in the Helsinki Declaration.

At our institution, we retrospectively evaluated all surgical patients affected from biliary colic who underwent MRCP from January 2014 to June 2019. Patients with a past history of ERCP and/or biliary stent and/or known hepatobiliary pancreatic neoplastic lesions or known primary sclerosing cholangitis were excluded. The dataset included age, sex, symptoms, and LBTs. Specifically, we collected total (TotBil, mg/dL), direct bilirubin (DirBil, mg/dL), aspartate aminotransferase (AST, U/L), alanine aminotransferase (ALT, U/L), gamma-glutamyltransferase (GGT, U/L), and alkaline phosphatase (AP, U/L). The LBT values were recorded on admission day (@time0) and 2 days later (@time1). Afterward, we recorded the variation in the values of such parameters over time as delta scores (Δ): ΔTotBil, ΔDirBil, ΔAST, ΔALT, ΔGGT, and ΔAP.

Statistical Analysis

For statistical software, we used MedCalc Statistical Software version 19.7 (MedCalc Software Ltd, Ostend, Belgium; https://www.medcalc.org; 2021). An analysis of variance test was used to evaluate demographic, clinical outcome, and LBTs differences between groups. For all LBTs at different time points, a receiver operating characteristic (ROC) curve,[12] sensitivity, specificity, positive predictive value, and negative predictive value were calculated. The Youden's index was used to establish the best threshold on the ROC curve.[13] A logistic regression analysis was used to find the best area under the ROC curve (AUC) value, single coefficients were therefore collected, and an LBT-weighted score was calculated (LBT_{score}). The K-folds cross-validation method (K = 5) was used to create multiple validation subsets of our data sample and to assess our prediction model reliability.[14] The sample size calculation set an amount of 149 patients to achieve 80% power with a type I error of 0.05. The threshold of statistical significance was $P < .05$.

Data Availability

The data associated with this article are not publicly available but are available from the corresponding author on reasonable request.

Results

Over the study period, out of 224 identified patients, 33 were excluded (26 patients had known hepatobiliary pancreatic neoplastic lesions and 7 patients suffered from primary sclerosing cholangitis; **Figure 1**). The demographic and clinical features of the 191 patients who matched the inclusion and exclusion criteria are shown in **Table 1**.

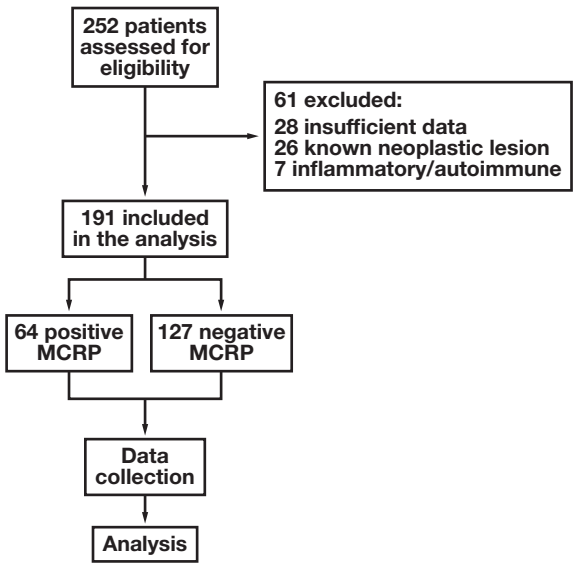

Figure 1

Flow chart of patients' selection and study methodology. MRCP, magnetic resonance cholangiopancreatography.

Table 1. Demographic and Clinical Characteristics of Patients Included in the Study

	Positive MRCP n = 64	Negative MRCP n = 127	*P*
Age (y, SD)	67.2 (16.9)	60.1 (18.1)	.009
Male (n, %)	34 (53)	53 (42)	.368
Abdominal pain (n, %)	47 (73)	105 (83)	.611
Acute cholecystitis (n, %)	5 (8)	16 (13)	.369
Acute pancreatitis (n, %)	10 (16)	30 (24)	.295
Jaundice without symptoms (n, %)	15 (23)	1 (1)	<.001
Altered LBTs without symptoms (n, %)	6 (9)	20 (16)	.287
Increased LBTs (%)			
TotBil (n, %)	48 (75)	74 (50)	.294
DirBil (n, %)	49 (76)	67 (53)	.125
AST (n, %)	48 (75)	82 (65)	.592
ALT (n, %)	48 (75)	92 (72)	.883
GGT (n, %)	56 (87)	99 (78)	.611
AP (n, %)	57 (89)	102 (80)	.647

ALT, alanine aminotransferase; AP, alkaline phosphatase; AST, aspartate aminotransferase; DirBil, direct bilirubin; GGT, gamma-glutamyltransferase; LBTs, liver blood tests; MRCP, magnetic resonance cholangiopancreatography; SD, standard deviation; TotBil, total bilirubin.
Values are expressed as number of patients and percentage of the total.

The MRCP was negative in 127 patients (66.5%). Among the 64 patients (33.5%) with a positive MRCP finding, 50 of them (26.2%) had 1 or more stones, whereas 14 patients (7.3%) had no stones but lesions of another nature that required further investigations.

Results on ROC analyses are reported in **Table 2**. Among all LBTs, DirBil at MRCP was found to have the best diagnostic power in predicting MRCP result (73.7%, 88.8%, 76.4%, and 86.3% sensitivity, specificity, positive predictive value, and negative predictive values, respectively). Coefficients of the logistic regression analysis were used as follows:

$$\begin{aligned} LBT_{score} : &-2.21347 - 0.00947 * TotBil_{time0} - 0.01218 \\ &* DirBil_{time0} - 0.00048 * AST_{time0} - 0.00041 \\ &* ALT_{time0} - 0.00160 * GGT_{time0} + 0.00199 \\ &* ALP_{time0} - 0.01971 * TotBil_{time1} + 0.11127 \\ &* DirBil_{time1} + 0.00258 * AST_{time} + 0.00009 \\ &* ALT_{time1} + 0.00184 * GGT_{time1} + 0.00023 * ALP_{time1} \end{aligned}$$

The AUC of the LBT_{score} was 0.890 ($P < .001$) and was the best value as compared to the single LBT (**Figure 2**). The score predicted 92.4% of patients correctly, all 14 patients with positive MRCP because of unclear lesions were classified as high risk, and further investigation was correctly suggested.

The K-folds cross-validation method confirmed the high diagnostic power of our LBT_{score} prediction model. The sensitivity, specificity, positive predictive value, and negative predictive value were 83.6%, 90.7%, 82.7%, and 90.6%, respectively.

Discussion

This is the first report that combines LBT values and their trend over time (specifically over 48 hours) in a mathematical model. The LBT_{score} showed high diagnostic value in patients with suspected CBD stones, and 92.4% of MRCP findings could be correctly predicted.

When misdiagnosed, CBD stones can lead to severe complications.[5] Therefore, several studies have tried to stratify patients with suspected CBD stones in different risk categories. American, European, British, and German societies' guidelines, among others, suggest predictors for CBD stones along with management algorithms.[6-9] According to the guidelines of Williams et al,[9] the likelihood of CBD stones should be established on history-taking, LBTs, and abdominal ultrasound findings. The American guidelines identify a high probability of CBD stones in patients with gallstones and visible CBD stones on ultrasound, symptoms and signs of cholangitis, or a combination of CBD dilatation and jaundice.[8] Altered LBTs are helpful in stratifying the risk, although a quantitative threshold is not commonly used in clinical practice.[11-22] Patients admitted with biliary colic often present with abnormal LBTs, so that with inconclusive ultrasound findings, a preoperative diagnostic of the biliary tree is often performed to rule out CBD stones.

An MRCP is an excellent imaging tool to study the biliary tree; however, it is not the only available method. According to a recent Cochrane systematic review,[24] MRCP is highly sensitive (93%) and specific (96%) in diagnosing CBD stones. In addition, MRCP is widely available in developed countries, not invasive, and, unlike EUS, suitable in case of altered gastroduodenal anatomy. However, it cannot be used in patients with mechanical heart valves and pacemakers. Claustrophobia and obesity represent further

DOI: 10.1093/labmed/lmab042

Table 2. ROC Analyses Showing the Diagnostic Power of Each LBT

LBT	Associated Threshold (Youden's index)	Sensitivity (%)	Specificity (%)	PPV (%)	NPV (%)	AUC	*P*
On hospital admission							
TotBil (mg/dL)	>1.55	75.0	50.8	43.6	80.0	0.651	<.001
DirBil (mg/dL)	>0.91	68.7	62.7	41.4	79.8	0.675	<.001
AST (U/L)	>78	71.9	39.7	37.7	73.5	0.524	.592
ALT (U/L)	>40	85.9	23.8	36.4	76.9	0.507	.876
GGT (U/L)	>316	62.5	57.1	42.6	75.0	0.595	.030
ALP (U/L)	>183	59.4	69.1	49.4	77.0	0.647	.001
Day of MRCP							
TotBil (mg/dL)	>2.34	71.9	84.5	69.5	86.0	0.813	<.001
DirBil (mg/dL)	>1.20	73.7	88.8	76.4	86.3	0.848	<.001
AST (U/L)	>80	70.2	66.4	50.6	81.9	0.702	<.001
ALT (U/L)	>361	31.6	88.8	58.1	72.5	0.613	.014
GGT (U/L)	>276	78.9	57.8	47.9	84.8	0.685	<.001
ALP (U/L)	>166	79.0	63.8	51.7	86.0	0.741	<.001
Δ values							
TotBil (mg/dL)	<–0.15	52.6	84.5	62.5	78.4	0.695	<.001
DirBil (mg/dL)	<–0.01	59.6	83.6	64.2	80.8	0.720	<.001
AST (U/L)	<72	73.7	46.6	40.4	78.3	0.622	.007
ALT (U/L)	<125	86.0	36.2	39.8	84.0	0.614	.011
GGT (U/L)	<–1	42.1	75.9	46.2	72.7	0.579	.094
ALP (U/L)	<–50	33.3	90.5	63.3	73.4	0.581	.103
LBT weighted formula	>–0.98	83.6	90.7	82.7	90.6	0.890	<.001

ALT, alanine aminotransferase; AP, alkaline phosphatase; AST, aspartate aminotransferase; AUC, area under the ROC curve; DirBil, direct bilirubin; GGT, gamma-glutamyltransferase; LBT, liver blood test; MRCP, magnetic resonance cholangiopancreatography; NPV, negative predictive value; PPV, positive predictive value; ROC, receiver operating characteristic; TotBil, total bilirubin.

Δ indicates the difference of all variables over the time period.

limitations. An EUS shows high sensitivity (95%) and specificity (97%) in detecting CBD stones as well. Because of the high diagnostic value of such techniques, both can be considered in the preoperative diagnosis of CBD stones. We considered MRCPs as a reference, and the LBT_{score} should be used to select patients for such an investigation because preoperative EUS is not directly applicable.

Most societies recommend preoperative ERCP in patients with a high likelihood of CBD stones, whereas MRCP, EUS, or intraoperative cholangiography are indicated in intermediate probability.[6-9] Patients with a low probability of CBD stones should undergo a cholecystectomy with or without intraoperative cholangiography without further investigations.[24] In acute patients, carrying out unnecessary MRCP, ERCP, and EUS can delay cholecystectomy and increase the length of stay and the hospital costs.[25] In our series, we observed a large number of negative MRCPs, so we tried to find a more reliable parameter that could justify MRCP before cholecystectomy using, retrospectively, the LBT values of 191 patients and a mathematical model based on regression analysis. Thereby, in measuring the LBT values at time 0 (day of admission) and at time 1 (48 hours later) and combining these values according to the above-detailed formula, we found an interesting diagnostic tool that we named the LBT_{score}. Our score reliability was also confirmed by the K-folds cross-validation method.[14] According to our results, in a patient admitted with biliary colic and observed for 48 hours, $LBT_{score} > -0.98$ would indicate a high probability of negative MRCP results. Once validated in a prospective study design, the LBT_{score} could be helpful in indicating whether preoperative MRCP, eventually followed by ERCP, or primary cholecystectomy is necessary.

This study has several limitations. A retrospective data collection was used to construct the predictive score. The relatively small number of patients does not allow strong conclusions but is nevertheless statistically significant because the sample size calculation set an amount of 149 patients to achieve 80% power with a type I error of 0.05.

In addition, our study does not predict the presence of choledocholithiasis but rather the result of MRCP. However, MRCP is an excellent imaging tool to study the biliary tree

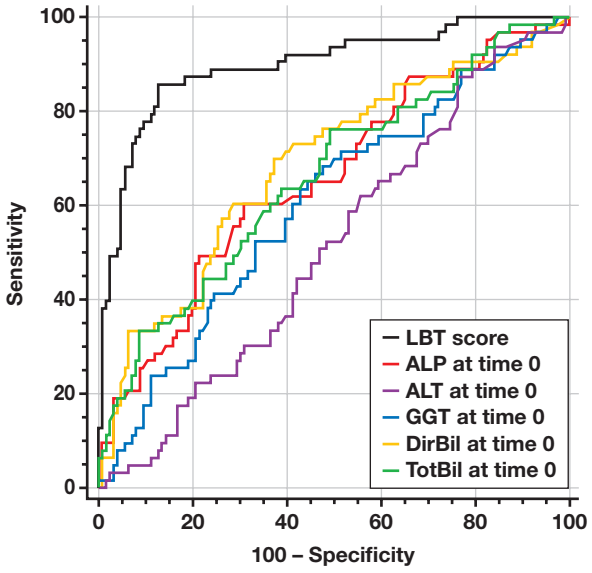

Figure 2

ROC curve analyses. ALT, alanine aminotransferase; AP, alkaline phosphatase; DirBil, direct bilirubin; GGT, gamma-glutamyltransferase; LBT, liver blood test; ROC, receiver operating characteristic; TotBil, total bilirubin.

and an equivalence might be argued. In 2003, Topal et al[26] showed that MRCP has a positive predictive value of 100% and a negative predictive value of 98% in diagnosing CBD stones. According to a recent Cochrane systematic review,[24] MRCP is highly sensitive (93%) and specific (96%) in diagnosing CBD stones. In addition, MRCP is widely available in developed countries, is not invasive, and, unlike EUS, is suitable in case of altered gastroduodenal anatomy. In this context, our work can be considered as a pilot study to be integrated into a more comprehensive algorithm to predict the presence of CBD stones.

Conclusion

Patients with suspected CBD stones are usually managed according to stratification into low-, intermediate-, and high-risk groups. In such patients, planning and carrying out unnecessary MRCP and EUS can lead to a delay of surgical treatment, increasing the length of hospital stay and costs. We designed a score based on LBT values over a 48-hour time frame. Based on our retrospective data, the LBT_{score} showed a high diagnostic power in predicting MRCP results. Once the score is validated in a prospective study design, it may be helpful in selecting patients with suspected CBD stones who would definitely benefit from a preoperative MRCP. LM

Acknowledgments

The authors thank Professor Pietro Majno-Hurst for comments and suggestions. Written nonopposition consents were administered to patients, and the local ethics committee approved the study (Comitato Etico Cantonale Ticino number 2019–02060 CE 3535). Consent for publication was obtained from all patients.

References

1. Aerts R, Penninckx F. The burden of gallstone disease in Europe. *Aliment Pharmacol Ther.* 2003;18(Suppl 3):49–53.
2. Schirmer BD, Winters KL, Edlich RF. Cholelithiasis and cholecystitis. *J Long Term Eff Med Implants.* 2005;15(3):329–338.
3. Farthing M, Roberts SE, Samuel DG, et al. Survey of digestive health across Europe: final report. Part 1: the burden of gastrointestinal diseases and the organisation and delivery of gastroenterology services across Europe. *United European Gastroenterol J.* 2014;2(6):539–543.
4. Rosseland AR, Glomsaker TB. Asymptomatic common bile duct stones. *Eur J Gastroenterol Hepatol.* 2000;12(11):1171–1173.
5. Kamath SU, Dharap SB, Kumar V. Scoring system to preoperatively predict choledocholithiasis. *Indian J Gastroenterol.* 2016;35(3):173–178.
6. European Association for the Study of the Liver (EASL). EASL Clinical Practice Guidelines on the prevention, diagnosis and treatment of gallstones. *J Hepatol.* 2016;65(1):146–181.
7. Gutt C, Jenssen C, Barreiros AP, et al. Updated S3-Guideline for Prophylaxis, Diagnosis and Treatment of Gallstones. German Society for Digestive and Metabolic Diseases (DGVS) and German Society for Surgery of the Alimentary Tract (DGAV)—AWMF Registry 021/008. Article in German. *Z Gastroenterol.* 2018;56(8):912–966.
8. ASGE Standards of Practice Committee, Maple JT, Ben-Menachem T, Anderson MA, et al. The role of endoscopy in the evaluation of suspected choledocholithiasis. *Gastrointest Endosc.* 2010;71(1):1–9.
9. Williams E, Beckingham I, El Sayed G, et al. Updated guideline on the management of common bile duct stones (CBDS). *Gut.* 2017;66(5):765–782.
10. Peng WK, Sheikh Z, Paterson-Brown S, Nixon SJ. Role of liver function tests in predicting common bile duct stones in acute calculous cholecystitis. *Br J Surg.* 2005;92(10):1241–1247.
11. Menezes N, Marson LP, debeaux AC, Muir IM, Auld CD. Prospective analysis of a scoring system to predict choledocholithiasis. *Br J Surg.* 2000;87(9):1176–1181.
12. Zweig MH, Campbell G. Receiver-operating characteristic (ROC) plots: a fundamental evaluation tool in clinical medicine. *Clin Chem.* 1993;39(4):561–577.
13. Youden WJ. Index for rating diagnostic tests. *Cancer.* 1950;3(1):32–35.
14. Zhang P. Model selection via multifold cross validation. *Ann Stat.* 1993;21(1):299–313.

15. Taylor AC, Little AF, Hennessy OF, Banting SW, Smith PJ, Desmond PV. Prospective assessment of magnetic resonance cholangiopancreatography for noninvasive imaging of the biliary tree. *Gastrointest Endosc.* 2002;55(1):17–22.
16. Kiechle FL, Weisenfeld MS, Karcher RE, Epstein E. Alkaline phosphatase in the assessment of choledocholithiasis before surgery. *Am J Emerg Med.* 1985;3(6):556–560.
17. Pereira-Limâ JC, Jakobs R, Busnello JV, Benz C, Blaya C, Riemann JF. The role of serum liver enzymes in the diagnosis of choledocholithiasis. *Hepatogastroenterology.* 2000;47(36):1522–1525.
18. Abboud PA, Malet PF, Berlin JA, et al. Predictors of common bile duct stones prior to cholecystectomy: a meta-analysis. *Gastrointest Endosc.* 1996;44(4):450–455.
19. Saltzstein EC, Peacock JB, Thomas MD. Preoperative bilirubin, alkaline phosphatase and amylase levels as predictors of common duct stones. *Surg Gynecol Obstet.* 1982;154(3):381–384.
20. Notash AY, Salimi J, Golfam F, Habibi G, Alizadeh K. Preoperative clinical and paraclinical predictors of choledocholithiasis. *Hepatobiliary Pancreat Dis Int.* 2008;7(3):304–307.
21. Videhult P, Sandblom G, Rudberg C, Rasmussen IC. Are liver function tests, pancreatitis and cholecystitis predictors of common bile duct stones? Results of a prospective, population-based, cohort study of 1171 patients undergoing cholecystectomy. *HPB (Oxford).* 2011;13(8):519–527.
22. Yang MH, Chen TH, Wang SE, et al. Biochemical predictors for absence of common bile duct stones in patients undergoing laparoscopic cholecystectomy. *Surg Endosc.* 2008;22(7):1620–1624.
23. Iranmanesh P, Frossard JL, Mugnier-Konrad B, et al. Initial cholecystectomy vs sequential common duct endoscopic assessment and subsequent cholecystectomy for suspected gallstone migration: a randomized clinical trial. *JAMA*. 2014;312(2):137–144.
24. Giljaca V, Gurusamy KS, Takwoingi Y, et al. Endoscopic ultrasound versus magnetic resonance cholangiopancreatography for common bile duct stones. *Cochrane Database Syst Rev.* 2015;2015(2):CD011549.
25. Onken JE, Brazer SR, Eisen GM, et al. Predicting the presence of choledocholithiasis in patients with symptomatic cholelithiasis. *Am J Gastroenterol.* 1996;91(4):762–767.
26. Topal B, Van de Moortel M, Fieuws S, et al. The value of magnetic resonance cholangiopancreatography in predicting common bile duct stones in patients with gallstone disease. *Br J Surg.* 2003;90(1):42–47.

D-Dimer Combined With CRP Can Improve the Differential Value of Bacterial Meningitis and Tuberculous Meningitis

*Liuyi Lu, BSc, Yunwei Qi, BSc, Huaping Chen, BSc, Zuojian Hu, BSc, Sitao Yang, BSc, Simeng Qin, BSc, Linyan Zhang, BSc, Mingxing Chen, BSc, Xue Qin, PhD**

Laboratory Medicine 2021;52:603-608

DOI: 10.1093/labmed/lmab005

ABSTRACT

Objective: To explore the diagnostic value of the coagulation marker D-dimer and its combination with the traditional marker C-reactive protein (CRP) in distinguishing bacterial meningitis (BM) from tuberculous meningitis (TM).

Methods: We performed a retrospective study on specimens from 173 patients with meningitis who were hospitalized at the First Affiliated Hospital of Guangxi Medical University, Guangxi, China, from 2012 through 2020. The patient records were divided into the BM group and the TM group, and hematological parameters D-dimer and CRP were evaluated for the 2 groups.

Results: The levels of D-dimer and CRP in the BM group were significantly higher than those levels in the TM group ($P < .001$ for each), and the sensitivity and specificity of the combined detection of the 2 markers was 86.3% to 100%; the area under the receiver operating characteristic (ROC) curve reached 0.983 (95% confidence interval [CI], 0.966–0.999).

Conclusion: D-dimer testing has high specificity in distinguishing between BM and TM; CRP testing also has high sensitivity. The combined diagnosis of the 2 biomarkers helps to distinguish TM from BM.

Keywords: D-dimer, CRP, bacterial meningitis, tuberculous meningitis, biomarkers, joint diagnosis

Bacterial meningitis (BM) is an infectious disease with relatively high morbidity and mortality worldwide. A few patients with BM have typical meningitis symptoms; in these patients, positive results of cerebrospinal fluid (CSF) bacterial culture are low. The clinical symptoms and laboratory test parameters of BM and tuberculous meningitis (TM) may overlap, making BM difficult to distinguish.[1] Tuberculosis has always been a global health problem; the most deadly and disabling form of tuberculosis is TM. It is estimated[2] that the diagnosis of more than 100,000 new cases of BM each year is often delayed, due to the insensitivity of the testing and the lengthy testing techniques required for disease confirmation.

Clinicians often use antibiotics empirically to control the development of BM. To prevent the abuse of antibiotics from causing refractory BM, it is important to quickly and correctly classify patients with suspected meningitis. Results reported in reviews published in recent years on the pathogenesis of meningitis brain injury, including Weisfelt et al,[3] increasingly point to the role of coagulation and thrombosis. D-dimer is one of the degradation products of cross-linked fibrin and is a diagnostic marker of diffuse intravascular coagulation. Early results reported by Mertens et al[4] showed that D-dimer can help evaluate the coagulation disorders of meningococcal disease and prevent the fatal consequences of meningococcal sepsis. The determination of C-reaction protein (CRP) is helpful in the diagnosis of bacterial meningitis.[5]

Abbreviations:

BM, bacterial meningitis; CSF, cerebrospinal fluid; TM, tuberculous meningitis; CRP, C-reactive protein; WBCs, white blood cells; MPV, mean platelet volume; RDW, red blood cell distribution width; ADA, adenosine deaminase; IQR, interquartile range; ROC, receiver operating characteristic; AUC, area under the curve; CI, confidence interval; Ig, immunoglobulin; ADA, adenosine deaminase

Clinical Laboratory Department, First Affiliated Hospital of Guangxi Medical University, Nanning, Guangxi, China

*To whom correspondence should be addressed.
qinxue919@126.com

In recent years, D-dimer and CRP often have been used as joint diagnostic indicators for various infectious diseases. However, to our knowledge, no study reports have shown the value of D-dimer combined with CRP in the differential diagnosis of BM and TM.

In this study, our purpose is to evaluate the value of D-dimer and CRP levels in the blood in BM and TM. We also examined traditional markers such as white blood cells (WBCs); neonatal inflammation markers such as mean platelet volume (PDW), mean red blood cell distribution width (RDW), cerebrospinal fluid (CSF) parameters such as CSF protein, glucose, adenosine deaminase (ADA) value, etc; and imaging changes in the 2 sets of data, such as from brain CT or MRI.

Materials and Methods

Patients

This retrospective study included a total of 173 patients, divided into the BM group (n = 75) and the TM group (n = 98; **Figure 1**), all of whose records were selected from the medical database of the First Affiliated Hospital of Guangxi Medical University from 2013 through 2020. The diagnosis of BM is based on the diagnosis of CNS infection through blood and imaging examinations, with clinical features of BM or positive bacterial culture in the CSF.[6] TM is diagnosed based on clinical manifestations, CSF parameters, brain imaging, and other tuberculosis evidence. Responses to empirical antituberculosis treatment were also classified as TM. The exclusion criteria were as follows: having infections other than meningitis, such as severe liver and kidney infections; lack of complete medical records; or having viral meningitis, cryptococcal meningitis, or brucella meningitis.

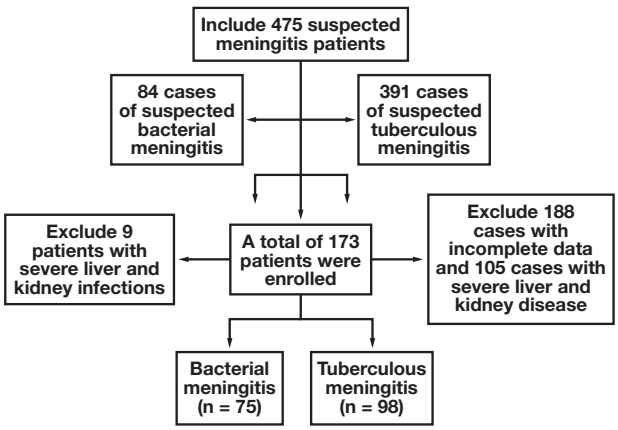

Figure 1

Flowchart of the population with meningitis.

Clinical data, laboratory parameters, and treatment plans were collected prospectively. This study complies with the ethical requirements of the Declaration of Helsinki and was approved by the Ethics Committee of the First Affiliated Hospital of Guangxi Medical University. The written informed consent of all participants was obtained.

Statistical Analysis

The normality of continuous variables is determined by the Kolmogorov-Smirnov test. The tested variables are normally distributed with mean (SD), variables that are not normally distributed are represented by median (interquartile [IQR]) range to describe continuous numerical variables; qualitative variables are represented by percentages. The analysis of statistical differences between the 2 groups used the χ^2 test, Fisher exact test (minimum expected count <5), and independent-samples Mann-Whitney U testing.

The probability model is derived from multiple logistic regression, and the receiver operating characteristic (ROC) curve and the area under the curve (AUC) were used to evaluate the diagnostic efficiency of the D-dimer and CRP multiple regression models. At the same time, we selected the appropriate cutoff point and calculated the biological sensitivity and specificity of each marker. We used SPSS, version 25.0 (IBM Corporation) and GraphPad Prism 8 (GraphPad Software) to perform statistical analysis and graph processing on all data. A P value of less than .05 was considered statistically significant.

Result

In this study, we observed 475 patients with suspected meningitis; that number was narrowed down to 173 patients

included in the study (75 in the BM group and 98 in the TM group), after the exclusions (**Figure 1**). Among the patients in the BM group, the median age in the BM group was 45 years; 51 patients (68.0%) were men and 24 patients (32.0%) were women. In the TM group, the median age was 42 years; 57 patients (58.1%) were men and 41 patients were women (41.8%). There was no significant difference in sex and age between the 2 groups ($P > .05$), which proved that the 2 groups were comparable (**Table 1**).

In the BM group, 12 patients (16.0%) tested positive for CSF culture. Among them, 8 cases of gram positive bacteria and 4 cases of gram negative bacteria were found. The reason for the low positivity rate of CSF culture may be that the patients had received antibiotic treatment. A total of 51 patients (68.0%) with BM underwent head CT scan or MRI; the scan results suggested hydrocephalus or meningitis. Among 98 patients with TM, only 11 patients (11.2%) tested positive for *Mycobacterium tuberculosis* by CSF culture, smear, or PCR, and only 16 patients had extrapulmonary tuberculosis.

In total, 73 patients of the 98 with TM (74.5%) underwent a head CT scan, MRI test, or chest CT test; the results suggested inflammatory changes. The common initial symptoms when all patients were first admitted to the hospital were fever and headache. Compared with the TM group, patients diagnosed with BM had more symptoms of vomiting, convulsions, disturbance of consciousness, and meningitis irritation when they were admitted to the hospital. The course of BM was longer than that of TM ($P < .05$). There was no significant differences in the number of patients with fever, headache, hydrocephalus, and other clinical symptoms between the 2 groups.

The typical WBC count of the BM group was higher than that of the TM group, whereas the ADA was lower than that of the tuberculous meningitis group ($P < .05$). Other hematological parameters such as mean platelet volume (MPV), RDW levels, CSF protein, and CSF glucose had no significant differences (**Table 1**). We note that the results of independent-sample Mann-Whitney U testing showed that CRP and D-dimer levels in patients with BM at admission were significantly higher than those of patients with TM (**Table 2**).

By constructing a multiple logistic regression probability models and drawing the ROC curve, the AUC of CRP was 0.965 (95% confidence interval [CI], .941-.989), and the

Table 1. Demographic and Laboratory Characteristics of Patients with BM and Those with TM

Parameter	BM Group	TM Group	*P* Value
Age (y), mean (SD)	45 (38)	41.9 (16.7)[a]	.52
Sex (female/male)	24/51	41/57	.19
Clinical characterization (%)			
Length of hospital stay (d), mean (SD)	16 (13)	13 (9)	.02[b]
Headache	97.3	93.8	.73
Fever	97.3	95.9	.70
Vomiting	42.6	27.5	.04[b]
Loss of consciousness	30.6	12.2	.003[b]
Hydrocephalus	13.3	10.2	.52
Twitching	20	8	.02[b]
Meningitis irritation	46.6	20.4	<.001[b]
CT/MRI changes	68	74.4	.35
Blood Profile, Mean (SD)			
WBC ($\times 10^9$/L)	10.3 (4.49)	7.1 (2.88)	<.001[b]
MPV (fl/L)	7.74 (1.81)	7.88 (1.42)	.97
RDW	0.15 (0.03)	0.14 (0.03)	.36
CSF Profile			
CSF protein (mmol/L)	1033 (1091)	1095 (1016)	.17
CSF glucose (mmol/L)	2.59 (1.18)[a]	2.1 (0.91)[a]	.09
ADA (U/L)	3.1 (4.3)	4.6 (5.1)	.02[b]

BM, bacterial meningitis; TM, tuberculous meningitis; WBC, white blood cell; MPV, mean platelet volume; RDW, red blood cell distribution width; CSF, cerebrospinal fluid; ADA, adenosine deaminase.
[a]*(X±S), denoted by "a", and other data in the table are denoted by (M±IR).*
[b]*Statistically significant.*

Table 2. Comparison of Peripheral Blood D-Dimer and CRP in the BM Group and TM Group

Group	No.	IQR	
		CRP (mg/L)[a,b]	D-dimer (ng/mL)[b,c]
BM	75	45.8 (82.2)	610 (1514)
TM	98	3.1 (4.9)	248 (253)

CRP, C-reactive protein; BM, bacterial meningitis; TM, tuberculous meningitis.
[a]*Z = −9.476.*
[b]*P <.001.*
[c]*Z = −6.994.*

D-dimer was 0.874 (.812-.937); the combined diagnosis of CRP + D-dimer was 0.983 (0.966-0.999; **Figure 2**). The specificity of the D-dimer (cutoff value of 472.5 ng/mL) is higher (97.1%) than CRP (86.4%), whereas the sensitivity of D-dimer is lower, at only 66.7%. CRP (cutoff value, 7.85 mg/L) has the highest sensitivity, reaching 93.4%. The comprehensive diagnosis of the two can increase the sensitivity to 86.3% and the specificity to 100% (**Table 3** and **Figure 3**).

DOI: 10.1093/labmed/lmab005

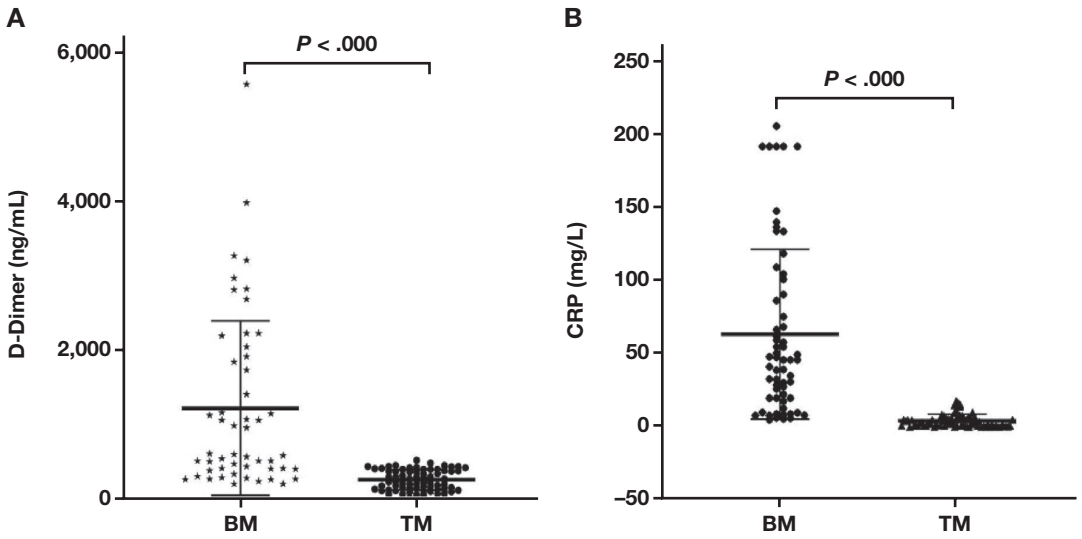

Figure 2

The levels of D-dimer and C-reactive protein (CRP) in peripheral blood of the bacterial meningitis (BM) and tuberculous meningitis (TM) groups. **A**, Peripheral blood levels of D-dimer. **B,** Peripheral blood levels of CRP.

Table 3. D-Dimer and CRP in Distinguishing BM and TM

Index	AUC	95% CI	SE	Cutoff Value	Sensitivity (%)	Specificity (%)
CRP (mg/L)	0.965	0.941–0.989	0.012	7.85	93.4	86.4
D-dimer (ng/mL)	0.874	0.812–0.937	0.032	472.5	66.7	97.1
CRP + D-dimer	0.983	0.966–0.999	0.009	0.29	86.3	100

CRP, C-reactive protein; BM, bacterial meningitis; TM, tuberculous meningitis; AUC, area under the curve; CI, confidence internal.

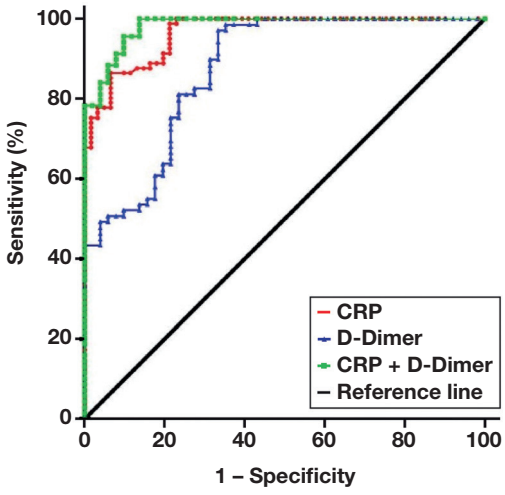

Figure 3

Receiver operating characteristic (ROC) curves of peripheral blood D-dimer, C-reactive protein (CRP), and the combination of those analytes in differentiating between bacterial meningitis (BM) and tuberculous meningitis (TM).

Discussion

Meningitis remains a serious infectious disease worldwide, causing serious neurological sequelae and high mortality.[7] The gold standard test for the diagnosis of BM is CSF analysis, whereas the detection of CNS bacteria is time-consuming and has poor sensitivity. The empirical use of antibiotics makes the diagnosis less sensitive.[1,8] The initial hematological abnormalities in TM show neutrophilia.[9]

It is difficult to discriminate between tuberculous and bacterial causes of meningitis. Many patients receive unnecessary antituberculosis treatment or antibiotic treatment. Ziehl-Neelsen staining of CSF is a rapid and reliable technique; however, the sensitivity is low (approximately 10%–20%). Also, the cultivation of *M. tuberculosis* takes 4 to 6 weeks to show growth.[9]

In recent years, new rapid molecular detection methods have emerged; however, the new method lacks the

sensitivity and negative predictive value to confidently rule out BM and TM.[10] Therefore, distinguishing between BM and TM by identifying abnormal inflammatory substances in the disease process is an important clue when choosing an appropriate treatment.[7]

CRP was discovered by William Tillett and Thomas Francis in 1930. It was first identified as a substance in the serum of patients with acute inflammation, which reacted with the "c" carbohydrate antibody of pneumococcal capsules.[11] Traditionally, CRP, as an acute protein, is considered a marker of infection and cardiovascular disease. When inflammation occurs in bacterial infection, the level of CRP in serum can increase as much as 1000-fold.[12] Also, the increase in CRP is associated with a higher incidence of neurological complications.[13] CRP can activate the cell-mediated immune pathway by activating complement and binding to the Fc receptor for immunoglobulin (Ig)G. CRP binds to the Fc receptor and interacts to cause the release of proinflammatory cytokines.[14]

Proinflammatory cytokines and chemokines can activate the coagulation system and downregulate important physiological anticoagulation mechanisms. A large amount of evidence, including Levi and van der Poll,[15] indicates that there is extensive crosstalk between inflammation and coagulation. In addition to inflammation-induced coagulation activation, coagulation also significantly affects inflammatory activities.

Blood coagulation is an important pathological mechanism of bacterial meningitis brain injury. When the coagulation pathway is activated, the diagnostic value of D-dimer becomes important. D-dimer abnormalities have been reported in many types of meningitis. Kowalik et al[16,17] found that most patients with bacterial meningitis had activated coagulation function, and the detection rate of D-dimer (>500 ng/mL) was 88% at the time of admission. Also, coagulation abnormalities are considered a risk factor for poor prognosis in patients with BM. D-dimer can be produced when cross-linked fibrin is formed and degraded. Therefore, D-dimer provides a global marker for the activation of the coagulation and fibrinolytic system and serves as an indirect marker of thrombosis activity. Serum D-dimer levels have been reported to be a sensitive test to assess coagulation and fibrinolysis.[18]

When acute bacterial meningitis occurs, the inflammation of the meninges and subarachnoid space caused by bacteria triggers the cascade reaction of CSF proinflammatory cytokines and chemokines, which triggers the invasion of neutrophils, in turn causing the steep rise of WBCs in BM.[19] A meta-analysis published by Pormohammad et al[10] showed that detection of ADA in CSF is a valuable test for the diagnosis of BM and TM.

In the results of our experiments, we have verified the predictive effect of CSF ADA on TMs. To our knowledge, this study is the first to explore the role of the combination of the coagulation marker D-dimer and CRP in the differentiation of BM and TM. We found that the levels of D-dimer and CRP in BM are significantly higher than those in TM, which can be used as a supplementary diagnosis of traditional markers such as WBC and ADA, and can improve the sensitivity and specificity of distinguishing BM from TM.

Because medical care has made great progress over the years, the morbidity and mortality of meningitis have been significantly reduced. However, 30% to 50% of surviving patients will have a series of neurological sequelae. With appropriate indications, anticoagulation therapy in the acute phase may help the clinical process and outcome of BM.[16] Discovering diagnostic markers in the cascade of inflammation, coagulation, or fibrinolysis will help the development of drugs for specific mediators.[20]

Conclusion

In this study, we found that the combined screening of D-dimer and CRP can help distinguish BM from TM. The detection methods for both diseases are simple and quick, and the results can be obtained in the central laboratory. These tests can be used as supplementary diagnostic methods for bacteriological diagnosis, to effectively reduce unnecessary treatment for patients. However, CRP and D-dimer tests lack diagnostic specificity, so the diagnosis should be based on the clinical characteristics of and other test results from each patient. Also, the sample size of this study is small. In the future, the sample size should be expanded to evaluate the diagnostic role of CRP and D-dimer in BM and TM testing. **LM**

Personal and Professional Conflicts of Interest

None reported.

Lab Medicine 2021;52;603–608 607
DOI: 10.1093/labmed/lmab005

References

1. Sanaei Dashti A, Alizadeh S, Karimi A, Khalifeh M, Shoja SA. Diagnostic value of lactate, procalcitonin, ferritin, serum-C-reactive protein, and other biomarkers in bacterial and viral meningitis: a cross-sectional study. *Medicine (Baltimore).* 2017;96(35):e7637.
2. Wilkinson RJ, Rohlwink U, Misra UK, et al; Tuberculous Meningitis International Research Consortium. Tuberculous meningitis. *Nat Rev Neurol.* 2017;13(10):581–598.
3. Weisfelt M, Determann RM, de Gans J, et al. Procoagulant and fibrinolytic activity in cerebrospinal fluid from adults with bacterial meningitis. *J Infect.* 2007;54(6):545–550.
4. Mertens R, Peschgens T, Granzen B, Heimann G. Diagnosis and stage-related treatment of disseminated intravascular coagulation in meningococcal infections. *Klin Padiatr.* 1999;211(2):65–69.
5. Mortensen RF, Osmand AP, Lint TF, Gewurz H. Interaction of C-reactive protein with lymphocytes and monocytes: complement-dependent adherence and phagocytosis. *J Immunol.* 1976;117(3):774–781.
6. van de Beek D, Cabellos C, Dzupova O, et al. ESCMID guideline: diagnosis and treatment of acute bacterial meningitis. *Clin Microbiol Infect.* 2016;22(Suppl 3):S37–S62.
7. Shokrollahi MR, Shabanzadeh K, Noorbakhsh S, Tabatabaei A, Movahedi Z, Shamshiri AR. Diagnostic value of CRP, procalcitonin, and ferritin levels in cerebrospinal fluid of children with meningitis. *Cent Nerv Syst Agents Med Chem.* 2018;18(1):58–62.
8. Carbonnelle E. Laboratory diagnosis of bacterial meningitis: usefulness of various tests for the determination of the etiological agent [article in French]. *Med Mal Infect.* 2009;39(7–8):581–605.
9. Belagavi AC, Shalini M. Cerebrospinal fluid C reactive protein and adenosine deaminase in meningitis in adults. *J Assoc Physicians India.* 2011;59:557–560.
10. Pormohammad A, Riahi S-M, Nasiri MJ, et al. Diagnostic test accuracy of adenosine deaminase for tuberculous meningitis: A systematic review and meta-analysis. *J Infect.* 2017;74(6):545–554.
11. Nehring SM, Goyal A, Bansal P, et al. *C Reactive Protein (CRP).* StatPearls Publishing LLC; 2020.
12. Thompson D, Pepys MB, Wood SP. The physiological structure of human C-reactive protein and its complex with phosphocholine. *Structure.* 1999;7(2):169–177.
13. Fuentes-Antrás J, Ramírez-Torres M, Osorio-Martínez E, et al. Acute community-acquired bacterial meningitis: update on clinical presentation and prognostic factors. *New Microbiol.* 2019;41(4):81–87.
14. Sproston NR, Ashworth JJ. Role of C-reactive protein at sites of inflammation and infection. *Front Immunol.* 2018;9:754.
15. Levi M, van der Poll T. Coagulation and sepsis. *Thromb Res.* 2017;149:38–44.
16. Kowalik MM, Smiatacz T, Hlebowicz M, Pajuro R, Trocha H. Coagulation, coma, and outcome in bacterial meningitis–an observational study of 38 adult cases. *J Infect.* 2007;55(2):141–148.
17. Kowalik MM, Smiatacz T, Hlebowicz M. Role of coagulation in predicting the outcome of bacterial meningitis. *Ann Neurol.* 2008;64(4):473–474; author reply 474.
18. Weitz JI, Fredenburgh JC, Eikelboom JW. A test in context: D-dimer. *J Am Coll Cardiol.* 2017;70(19):2411–2420.
19. Davis LE. Acute bacterial meningitis. *Continuum (Minneap Minn).* 2018;24(5):1264–1283.
20. Mook-Kanamori BB, Geldhoff M, van der Poll T, van de Beek D. Pathogenesis and pathophysiology of pneumococcal meningitis. *Clin Microbiol Rev.* 2011;24(3):557–591.

Case Study

Anti-S Antibody: A Rare Cause of Fetal Hydrops in a Previously Sensitized Mother

Azad Bakht, MD,[1,2] Bettina Turner, MT(ASCP)SBB,[2] Christina S. Warren, MT(ASCP)SBB,[2] Julie H. Simmons, MPH, MT(ASCP)SBB,[2] Emmanuel A. Fadeyi, MD[1,2,]*

Laboratory Medicine 2021;52:609-613

DOI: 10.1093/labmed/lmab014

ABSTRACT

Anti-S is an IgG antibody and a rare cause of hemolytic disease of the fetus and newborn. A 38 year old woman with blood group O Rh-positive presented to the hospital at 30 weeks gestation. Her past medical history was significant for sickle cell disease and alloantibodies against the Fya, Jkb, and S antigens. Obstetric ultrasound showed the fetus to have developed scalp edema, cardiomegaly, small pericardial effusion, and large ascites. Periumbilical blood sampling results showed the fetus blood type as blood group O Rh-positive with anti-S and hemoglobin of 2 gm/dL. After multiple intrauterine transfusions of red blood cells, the fetal hemoglobin increased to 12.9 g/dL. Anti-S can cause fetal hydrops, although it is rare. All pregnant women with anti-S should be closely monitored and treated during pregnancy for the possibility of developing a severe hemolytic disease of the fetus and newborn.

Keywords: anti-S, CMV, PUBS, RBC, MoM, HDFN

Background

Severe fetal hemolysis can give rise to a condition called erythroblastosis fetalis, requiring intrauterine transfusion. The MNS blood group system, which includes the U antigen, is located on glycophorin A (GPA) and glycophorin B (GPB), respectively. The M and N glycoproteins are located on GPA, and the S, s, and U antigens are on GPB. Individuals who lack GPB are S– and s– and also lack U. The U– phenotype occurs almost exclusively in the African population and has a very low frequency (0.25%).

Abbreviations:

GPA, glycophorin A; GPB, glycophorin B; HDFN, hemolytic disease of the fetus and newborn; IUT, intrauterine transfusion; Rh, Rhesus; MoM, multiples of the mean; PUBS, percutaneous umbilical blood sampling; DAT, direct antiglobulin test; RBC, red blood cell; MCA-PSV, middle cerebral artery peak systolic velocity.

[1]Wake Forest University School of Medicine, Department of Pathology and Laboratory Medicine, Winston-Salem, North Carolina, USA, [2]Wake Forest Baptist Health, Department of Pathology and Laboratory Medicine, Winston-Salem, North Carolina, USA

*To whom correspondence should be addressed.
efadeyi@wakehealth.edu

The M, N, S, s, and U antigens are the most important antigens for transfusion purposes. The antibodies anti-M, anti-S, and anti U of the IgG class have been implicated in severe hemolytic disease of the fetus and newborn (HDFN).[1-3]

Among the antibodies of the MNS blood group system, anti-S is generally IgG antibody reacting at 37 °C. Anti-S is rarely implicated in hemolytic transfusion reactions; however, it can lead to potentially severe transfusion reactions. Anti-S is also capable of causing mild to severe hemolytic disease of the newborn.[4]

Research has shown that HDFN resulting from maternal IgG antibody alloimmunization crossing the placenta into fetal circulation during pregnancy causes hemolytic disease of the fetus in utero and hemolytic disease of the newborn after delivery. However, not all antibodies are associated with severe HDFN. Severe hemolytic disease requiring intrauterine transfusion (IUT) was caused by anti-Rhesus (Rh) D (85%), anti-Kell (10%), and anti-Rhc (3.5%) in a 2005 Dutch study.[5] Overall results from a 2008 Dutch study showed severe HDFN requiring IUT or exchange transfusion in 3.7% of at-risk fetuses; 11.6%

of the 3.7% of at risk fetuses had HDFN due to anti-K, 8.5% of the 3.7% due to anti-C, 1.1% of the 3.7% due to anti-E, 3.8% of the 3.7% due to Rh antibodies other than anti-C, anti-D, or anti-E; and none in antibodies other than Rh and Kell.[6] We present a patient with fetal hydrops because of an undetectable anti-S in maternal plasma.

Clinical History

Our patient was a 38 year old woman, G3P0 at 30 weeks and 1 day gestation, presented to the clinic for routine antenatal examination. The previous obstetric history included 2 spontaneous abortions at 9 and 6 weeks, respectively. This pregnancy was conceived via in vitro fertilization. Her medical history was significant for sickle cell disease and alloimmunization because of multiple transfusions. At this visit, obstetric ultrasound was advised, which showed a single living intrauterine pregnancy with scalp edema, cardiomegaly, small pericardial effusion, and large ascites. Middle cerebral artery Doppler flow result showed >2.0 multiples of the mean (MoM; normal is <1.2 MoM). These findings were all suggestive of fetal hydrops.

The patient was admitted to the hospital for further management. Maternal blood studies and percutaneous umbilical blood sampling (PUBS) were advised to determine the cause of fetal hydrops. The mother was blood group O Rh-positive, and her past medical records showed an antibody screen that was positive for anti-Fya, anti-Jkb, and anti-S. The current antibody screen was negative for anti-S and anti-Jkb and only positive for anti-Fya. The fetal antibody screen was only positive for anti-S and negative for anti-Jkb and anti-Fya. The fetal direct antiglobulin test (DAT) was negative, and the eluate performed was also negative, possibly because they were below the detectability of the normal anti-IgG Coombs reagent. Anti-Jkb and anti-Fya were not present in fetal circulation. Even though we were not able to titer anti-S in the mother, anti-S was present in the fetal antibody screen. The PUBS result of fetal blood is shown in **Table 1**. The PUBS antibody screen was positive for only anti-S, and the fetal DAT was negative.

Table 1. First PUBS Result

Fetal Blood Group	Group O Rh-Positive
Fetal hemoglobin	2 g/dL
Antigens positive on fetal RBCs	c, Jkb, S, Jsa
Antigens negative on fetal RBCs	C, E, K, Fya, Jka
Antibodies identified	Anti-S
Fetal DAT	Negative
Fetal eluate	Negative

DAT, direct antiglobulin test; PUBS, percutaneous umbilical blood sampling; RBCs, red blood cells.

Discussion

Studies have shown that HDFN occurs when there is transplacental passage of maternal IgG antibodies that is directed against certain fetal red blood cell (RBC) antigens and causes their destruction through splenic macrophages. Before birth this process gives rise to hemolytic disease of the fetus, and in its severe form the fetus can present with anemia along with after-birth anemia and hyperbilirubinemia.[7]

Foudoulaki-Paparizos et al[8] investigated 4368 pregnant women, 75.37% of whom were Greek and 24.63% were immigrants. The incidence of alloimmunization was 0.66% in the Greek women and 1.76% in the women who were immigrants. Anti-D was the most frequent alloantibody (0.18%) overall, relatively more frequent in the women who were immigrants: 5.76% compared with 0.56% in the Greek women who were RhD-negative. Other antibodies that the authors found, in descending order, were anti-K, anti-E, anti-Lea, anti-M, anti-c, anti-C e, anti-Jka, anti-Jkb, and anti-C. They further found that a past history of blood transfusion and of multiparity was significantly associated with alloimmunization during pregnancy.[8]

There are more than 50 antibodies associated with HDFN, and among these, anti-D, anti-c, and anti-K are considered to be associated with severe HDFN.[9] There has been a decrease in HDFN resulting from anti-D since the implementation of Rh immunoglobulin administration.[10] An increasing prevalence in non-anti-D alloimmunization has been observed.[11] Therefore, screening all pregnant women for the presence of clinically significant antibodies is important to provide them with appropriate management.[12]

Laboratory Role in the Diagnosis

The S antigen belongs to the MNS blood group system, which is second only to the Rh blood group system, having the largest number of antigens. The Rh blood group has more than 62 antigens, whereas the MNS system has 49 antigens.[4] The antibodies against S antigen are IgG antibodies reacting at 37°C and are associated with hemolytic transfusion reactions as well HDFN.[4,13,14]

With our patient, we were not able to detect anti-S in the maternal plasma during the second half of gestation, but the patient had a history of previous anti-S. This circumstance may have resulted from the adsorption of anti-S by the fetal RBCs after crossing the placenta, causing fetal hydrops. It is our speculation that the fetal DAT on the first PUBS specimen was negative because the number of IgG molecules in the RBCs may have been less than the number needed to cause a positive DAT but may still have been enough to cause in vivo RBC destruction. Another possible reason could be that the fetal cells had all been destroyed either through intravascular hemolysis or clearance of shortened fetal RBC survival in the presence of the antibody. The combined findings of an absence of anti-S in the mother's plasma and a negative fetal DAT and negative fetal eluate (for anti-S) are distinctly and totally noncharacteristic findings of the expected normal physiology of HDFN. Normally the fetal cells are coated with anti-S, producing a positive DAT and anti-S eluted from the fetal cells. Similar observations were also reported by Chown et al[15] in one of their case reports of hemolytic disease of the fetus resulting from anti-S.

Anti-S-mediated hemolytic disease of the newborn was described in the literature for the first time in 1952 by Levine et al.[16] They described a case of a newborn who presented with jaundice after birth. Forty hours after birth, the infant's hemoglobin dropped from 15 g/dL to 11 g/dL. Physicians started transfusion, but the infant did not survive. It was later confirmed that the hemolysis resulted from the presence of anti-S.

Mayne et al[17] reported a case of severe hemolytic disease of a newborn who developed severe jaundice and a significant drop in his hemoglobin level soon after birth. The mother had anti-S detected. The infant required 3 exchange transfusions in addition to phototherapy.

Anti-S usually causes a mild type of HDFN,[18] but in rare patients it can cause severe hemolysis and can be fatal. Although anti-S/s represent 2% of the alloantibodies detected in pregnant women, minimizing the exposure of childbearing-age women to incompatible RBC antigens through unnecessary transfusions can help reduce the incidence of RBC alloimmunization and the risk of HDFN.[12] In some patients, middle cerebral artery peak systolic velocity (MCA-PSV) may not predict the severity of anemia.[19] Therefore, close monitoring of the fetus using MCA-PSV and antibody titers in the mother is very important when the mother's plasma shows clinically significant RBC antibodies.

Patient Follow-Up

Because fetal hemoglobin was very low, giving rise to fetal hydrops, an intrauterine packed RBC transfusion was planned. For the transfusion, group O Rh-negative hemoglobin S-negative packed RBCs that were also negative for antigens C, E, K, Cw, Jkb, Fya, and S were selected and cross-matched with maternal plasma. As per IUT protocol, the packed RBC unit collected in citrate phosphate dextrose adenine-1 was spiked and drained into a processing set on the COBE 2991 cell processor. We added 0.9% normal saline, and the product was centrifuged with the supernatant being expressed. This process was repeated multiple times, and the RBCs were resuspended in saline until the desired hematocrit level of 80% was reached. The RBCs used were cytomegalovirus (CMV)-seronegative and were irradiated and washed. Results of the IUT are shown in **Table 2**.

During the patient's hospitalization, she began experiencing an increasing need for acute treatment of high blood pressure; she was diagnosed with pre-eclampsia with severe features. This diagnosis was based on systolic blood pressures >160 mm Hg longer than 4 hours apart and persistent, requiring treatment. There was possible pulmonary congestion or edema; however, the clinical team suspected an exacerbation of sickle cell anemia precipitated by evolving preeclampsia and borderline

Lab Medicine 2021;52;609–613 611
DOI: 10.1093/labmed/lmab014

Table 2. Improvement in Hemoglobin Level After Subsequent IUT of Packed RBCs

Date of Transfusion	Amount of Transfused Packed RBCs	Hematocrit of Transfused Packed RBCs	Pretransfusion Hemoglobin	Posttransfusion Hemoglobin
08/18/2020	30 mL	84%	2 g/dL	5.6 g/dL
08/20/2020	45 mL	85%	4.9 g/dL	9.8 g/dL
08/24/2020	35 mL	79.4%	8.6 g/dL	11.8 g/dL
09/01/2020	35 mL	79.7%	10.1 g/dL	12.9 g/dL

DAT, direct antiglobulin; IUT, intrauterine transfusion; RBCs, red blood cells.

liver function test with slightly elevated aspartate aminotransferase (AST).

The decision was made to proceed with induction of labor because of the increased frequency of systolic blood pressure elevation requiring treatment and increasing Procardia (nifedipine) dosing. The patient subsequently underwent induction of labor using cervidil (dinoprostone), Cook's catheter, and pitocin (oxytocin injection). However, the induction of labor was unsuccessful and the patient underwent primary low transverse cesarean delivery of a live-born female infant at 34 weeks gestation weighing 1834 g (4 lb, 0.7 oz) with Apgar scores of 6 and 8 at 1 and 5 minutes, respectively.

The baby was admitted to the neonatal intensive care unit for prematurity and hemolytic disease of the newborn. She received 1 dose of intravenous immunoglobulin (IVIG) at approximately 9 hours of life. Phototherapy was discontinued at 5 days of life; the baby received a total of 3 transfusions of packed RBC during her hospital stay and was discharged 23 days after birth. A 1-day postpartum maternal antibody screen was completed and showed only anti-Fya in the maternal plasma. We did not detect anti-S. The patient did not have any blood bank workup since she was discharged on postpartum day 4.

The history of anti-S in the mother, the presence of anti-S in the PUBS, and the progressive improvement in the fetal hemoglobin after transfusion of S antigen–negative packed RBCs were strongly suggestive of hemolytic disease of the fetus mediated by anti-S in an S antigen–positive fetus. The baby was delivered 6 days after the last IUT, with hemoglobin of 11.7 g/dL (reference value, 13.5-19.5 g/dL), total bilirubin of 7.6 mg/dL (reference value, 1.5-3.2 mg/dL), and direct bilirubin of 0.7 mg/dL (reference value, 0.1-0.2 mg/dL).

This case report shows the importance of anti-S, which can cross the placenta and can cause severe hemolytic disease of the fetus. Anti-S may not be detected in maternal plasma because of adsorptions of all maternal antibodies onto fetal RBCs. All pregnant women with anti-S should be monitored during pregnancy. In rare cases they may need an IUT to treat fetal anemia. In the setting of HDFN, the obstetrician should monitor mothers with a history of anti-S with MCA-PSV regardless of the titer because there is no correlation between titer and pregnancy outcomes and, moreover, the measured value is not invariable throughout pregnancy. The laboratory should communicate to the clinician the importance of anti-S in a previously sensitized mother if the antepartum antibody screen does not show a detectable anti-S. Appropriate management requires a multidisciplinary approach. **LM**

References

1. Pitan C, Syed A, Murphy W, et al. Anti-S antibodies: an unusual cause of haemolytic disease of the fetus and newborn (HDFN). *BMJ Case Rep*. 2013;2013:bcr2012006547.
2. Yu M, Graham K, Pasalic L, Alahakoon TI. Recurrent fetal hydrops with maternal M alloimmunisation: not a benign condition. *BMJ Case Rep.* 2019;12(7):e230552.
3. Dhandsa N, Williams M, Joss V, Patten J, James D, Sinclair L. Haemolytic disease of the newborn caused by anti-U. *Lancet.* 1981;2(8257):1232.
4. Cohn CS, Delaney M, Johnson ST, Katz LM, eds. *Technical Manual*. 20th ed. Bethesda, MD: AABB; 2020: 330–332, 361–362.
5. Van Kamp IL, Klumper FJ, Oepkes D, et al. Complications of intrauterine intravascular transfusion for fetal anemia due to maternal red-cell alloimmunization. *Am J Obstet Gynecol.* 2005;192(1):171–177.
6. Koelewijn JM, Vrijkotte TG, van der Schoot CE, Bonsel GJ, de Haas M. Effect of screening for red cell antibodies, other than anti-D, to detect hemolytic disease of the fetus and newborn: a population study in the Netherlands. *Transfusion.* 2008;48(5):941–952.
7. Eder AF. Update on HDFN: new information on long-standing controversies. *Immunohematology.* 2006;22(4):188–195.
8. Foudoulaki-Paparizos L, Valsami S, Bournas N, et al. Alloimmunisation during pregnancy in Greece: need for nationwide HDFN prevention programme. *Transfus Med*. 2013;23(4):254–259.
9. Dajak S, Stefanović V, Capkun V. Severe hemolytic disease of fetus and newborn caused by red blood cell antibodies undetected at first-trimester screening (CME). *Transfusion.* 2011;51(7):1380–1388.
10. Liumbruno GM, D'Alessandro A, Rea F, et al. The role of antenatal immunoprophylaxis in the prevention of maternal-foetal anti-Rh(D) alloimmunisation. *Blood Transfus.* 2010;8(1):8–16.

11. Pal M, Williams B. Prevalence of maternal red cell alloimmunisation: a population study from Queensland, Australia. *Pathology.* 2015;47(2):151–155.
12. Moinuddin I, Fletcher C, Millward P. Prevalence and specificity of clinically significant red cell alloantibodies in pregnant women—a study from a tertiary care hospital in Southeast Michigan. *J Blood Med.* 2019;10:283–289.
13. Guastafierro S, Sessa F, Cuomo C, Tirelli A. Delayed hemolytic transfusion reaction due to anti-S antibody in patient with anti-Jk(a) autoantibody and multiple alloantibodies. *Ann Hematol.* 2004;83(5):307–308.
14. Yousuf R, Abdul Aziz S, Yusof N, Leong CF. Hemolytic disease of the fetus and newborn caused by anti-D and anti-S alloantibodies: a case report. *J Med Case Rep.* 2012;6:71.
15. Chown B, Lewis M, Best B. Severe haemolytic disease of the newborn due probably to the combined action of anti-A and anti-S. *Can Med Assoc J.* 1957;77(1):31–34.
16. Levine P, Ferraro LR, Koch E. Hemolytic disease of the newborn due to Anti-S: a case report with a review of 12 anti-S sera cited in the literature. *Blood*. 1952;7(10):1030–1037.
17. Mayne KM, Bowell PJ, Green SJ, et al. The significance of anti-S sensitization in pregnancy. *Clin Lab Haematol*. 1990;12(1):105–107.
18. Griffith TK. The irregular antibodies—a continuing problem. *Am J Obstet Gynecol*. 1980;137(2):174–177.
19. Reddy VS, Kohan R. Severe hemolytic disease of fetus and newborn due to anti-s antibodies. *J Clin Neonatol.* 2014;3(2):128–129.

DOI: 10.1093/labmed/lmab014

Whole-Exome Sequencing Reveals a Novel Mutation of *FLNA* Gene in an Iranian Family with Nonsyndromic Tetralogy of Fallot

Samira Kalayinia, PhD,[1] *Majid Maleki, MD,*[1] *Mohammad Mahdavi, MD,*[1] *Nejat Mahdieh, PhD*[1,2,*]

Laboratory Medicine 2021;52:614-618

DOI: 10.1093/labmed/lmab018

ABSTRACT

Objective: Tetralogy of Fallot (TOF) is one of the most common congenital abnormalities that need early intervention. Here, for the first time, we report a nonsyndromic form of TOF caused by a novel variant in the *FLNA* gene in 2 siblings of an Iranian family.

Methods: The family underwent a complete workup, including karyotyping, sequencing of 6 common genes in congenital heart diseases (*GATA4, NKX2-5, ZIC3, FOXH1, NODAL,* and *GJA1*), array comparative genomic hybridization, multiplex ligation-dependent probe amplification, and whole-exome sequencing. Segregation and in silico analysis were also conducted for the identified variant.

Results: A variant, c.3415C>T, in the *FLNA* gene was found in both affected brothers in this family; this variant was heterozygous in their mother. Bioinformatics tools predicted the variant as a pathogenic one.

Conclusion: Many allelic disorders have been reported for *FLNA* mutations. Mutations in this gene may cause a nonsyndromic congenital form of TOF.

Keywords: congenital heart disease, *FLNA,* whole-exome sequencing, mutation, tetralogy of Fallot, nonsyndromic

Congenital heart diseases (CHDs) comprise the most common birth defects in that they affect 10 to 12 per 1000 live births.[1,2] Research has shown that CHDs encompass a large spectrum of cardiac malformations that range from severe forms such as transposition of the great arteries and tetralogy of Fallot (TOF) to mild forms such as bicuspid aortic valve (BAV).[3] The TOF is the most prevalent form of cyanotic CHDs (~3.5%–4%),[4] with an approximate 0.04% rate of incidence.[5] It consists of 4 major cardiac defects that occur together: ventricular septal defect, right ventricular hypertrophy, pulmonary stenosis, and aortic override. The genetic causes of TOF are heterogeneous[6-8] and indicate autosomal dominant inheritance.[9] In approximately 80% of patients with nonsyndromic TOF, the etiology is obscure.[10] There are limited reports regarding the mortality and morbidity of TOF.[11,12]

Despite these limitations, recent studies have provided evidence of mutations in multiple genes implicated in TOF (syndromic/nonsyndromic) such as *GATA*-binding protein 4 (*GATA4*),[13] *NK2* homeobox 5 (*NKX2.5*),[14] Jagged 1 (*JAG1*),[15] forkhead box C2 (*FOXC2*),[16] T-box 5 (*TBX5*),[17,18] T-box 1 (*TBX1*),[19] notch receptor 1 (*NOTCH1*), and Fms-related tyrosine kinase 4 (*FLT4*).[20] The filamin A protein is a member of the filamin family; it is encoded by the *FLNA* gene and widely expressed during heart development.[21] Genetic documents in recent decades have suggested that mutations in *FLNA* are associated with cardiovascular system abnormalities. It has also been indicated that hemizygous males with mutations of *FLNA* are born with cardiac abnormalities or die prenatally; in addition, loss-of-function mutations in the *FLNA* gene result in CHDs such as patent ductus arteriosus and Ebstein anomaly.[22-25] At present, based on Online Mendelian

Abbreviations:

TOF, tetralogy of Fallot; CHD, congenital heart disease; OMIM, Online Mendelian Inheritance in Man; WES, whole-exome sequencing; PCR, polymerase chain reaction; array CGH, array comparative genomic hybridization; MLPA, multiplex ligation-dependent probe amplification; gnomAD, Genome Aggregation Database; esp6500, Exome Sequencing Project 6500; GME, Greater Middle East; ACMG, American College of Medical Genetics and Genomics.

[1]Cardiogenetic Research Center, Rajaie Cardiovascular Medical and Research Center, Iran University of Medical Sciences, Tehran, Iran and [2]Growth and Development Research Center, Tehran University of Medical Sciences, Tehran, Iran

*To whom correspondence should be addressed.
nmahdieh@gmail.com

Inheritance in Man (OMIM) (https://www.omim.org/), 10 *FLNA* gene-phenotype relationships have been introduced: cardiac valvular dysplasia, congenital short-bowel syndrome, frontometaphyseal dysplasia, heterotopia, intestinal pseudo-obstruction, Melnick-Needles syndrome, otopalatodigital syndrome (type I and type II), terminal osseous dysplasia, and FG syndrome (Opitz–Kaveggia syndrome).

There are no TOF clinical reports of *FLNA* mutations worldwide, nor have there ever been reports of *FLNA* mutations in Iranian patients. In this study, we report a novel mutation in the *FLNA* gene that was identified by whole-exome sequencing (WES), associated with TOF in an Iranian family.

Methods

Patients

An Iranian family with 2 affected children was recruited in this study (**Figure 1A**). The proband (the younger boy) was a 2-year-old boy with TOF. His brother, a 10-year-old boy, was also affected with TOF. Their parents were unrelated, and there were 2 abortions in this family. The diagnosed CHDs of the patients were confirmed by echocardiography (**Figure 1B**), and no syndromic features, neurological phenotypes, or periventricular heterotopia, which might be associated with *FLNA* mutations, were observed in their clinical investigations and medical history. A consent form was signed by the parents, and blood specimens were collected from all the family members. The inheritance pattern of CHDs in this family was X-linked recessive because the 2 affected children were born to healthy parents. The affected individuals were checked by our team via karyotyping, polymerase chain reaction (PCR), sequencing of the 6 common genes in CHDs (*GATA4, NKX2-5, ZIC3, FOXH1, NODAL,* and *GJA1*), array comparative genomic hybridization (array CGH), and multiplex ligation-dependent probe amplification (MLPA), and no CHD causative mutations were revealed. This research was carried out in accordance with the Declaration of Helsinki.

Whole-exome sequencing

We extracted DNA from peripheral blood using the salting-out method.[26] The WES was performed on the proband's DNA on an Illumina HiSeq 4000 platform at a mean read depth of 150× (Macrogen, Inc., South Korea). Alignment and variant calling were carried out against the University of California, Santa Cruz (UCSC) human reference genome, the GRCh37/hg19 version. For prioritization, variants with a minimum allele frequency (MAF) of more than 0.01 in the 1000 Genomes Project (https://www.internationalgenome.org), the Genome Aggregation Database (gnomAD; https://gnomad.broadinstitute.org/), the Exome Sequencing Project 6500 (esp6500; https://evs.gs.washington.edu/EVS/), the Greater Middle East (GME) Variome Project (igm.ucsd.edu/gme/), and the Iranome Database (http://iranome.com/) were removed.

In Silico Analysis

The pathogenicity of the variants was predicted using bioinformatic tools encompassing HOPE (https://www3.cmbi.umcn.nl/hope/input/), MutationTaster (www.mutationtaster.org/), PROVEAN (http://provean.jcvi.org/index.php), SIFT (https://sift.bii.a-star.edu.sg), CADD (https://cadd.gs.washington.edu/home), FATHMM (fathmm.biocompute.org.uk), and GERP (http://mendel.stanford.edu/SidowLab/downloads/gerp/). The variants identified by most of the prediction tools as being damaging were selected for future confirmation and segregation analyses. We also used CLUSTALW (https://www.genome.jp/tools-bin/clustalw) for filamin A alignment between humans and some species (**Figure 1E**).

Evaluation of the Candidate Variant

A suspected disease-causing variant, c.3415C>T, in the *FLNA* gene was amplified from the proband's DNA applying the forward primer 5'- GGAAAGTCAAGCAGGAGGTCT-3' and the reverse primer 5'-TGATGGTGACGGTGTAGGC-3' by PCR on a SimpliAmp Thermal Cycler (Thermo Fisher Scientific). The sequencing of the PCR products was performed on an ABI Sequencer 3500XL PE (Applied Biosystems) using the Sanger method, and the products were analyzed using the FinchTV 1.4.0 software. After the variant confirmation in the proband, the other affected brother and the healthy parents were sequenced for the segregation analysis of the variant.

Results

We detected a novel hemizygous variant, NM_001456: c.3415C>T; p.Leu1139Phe, in the *FLNA* gene. The variant

DOI: 10.1093/labmed/lmab018

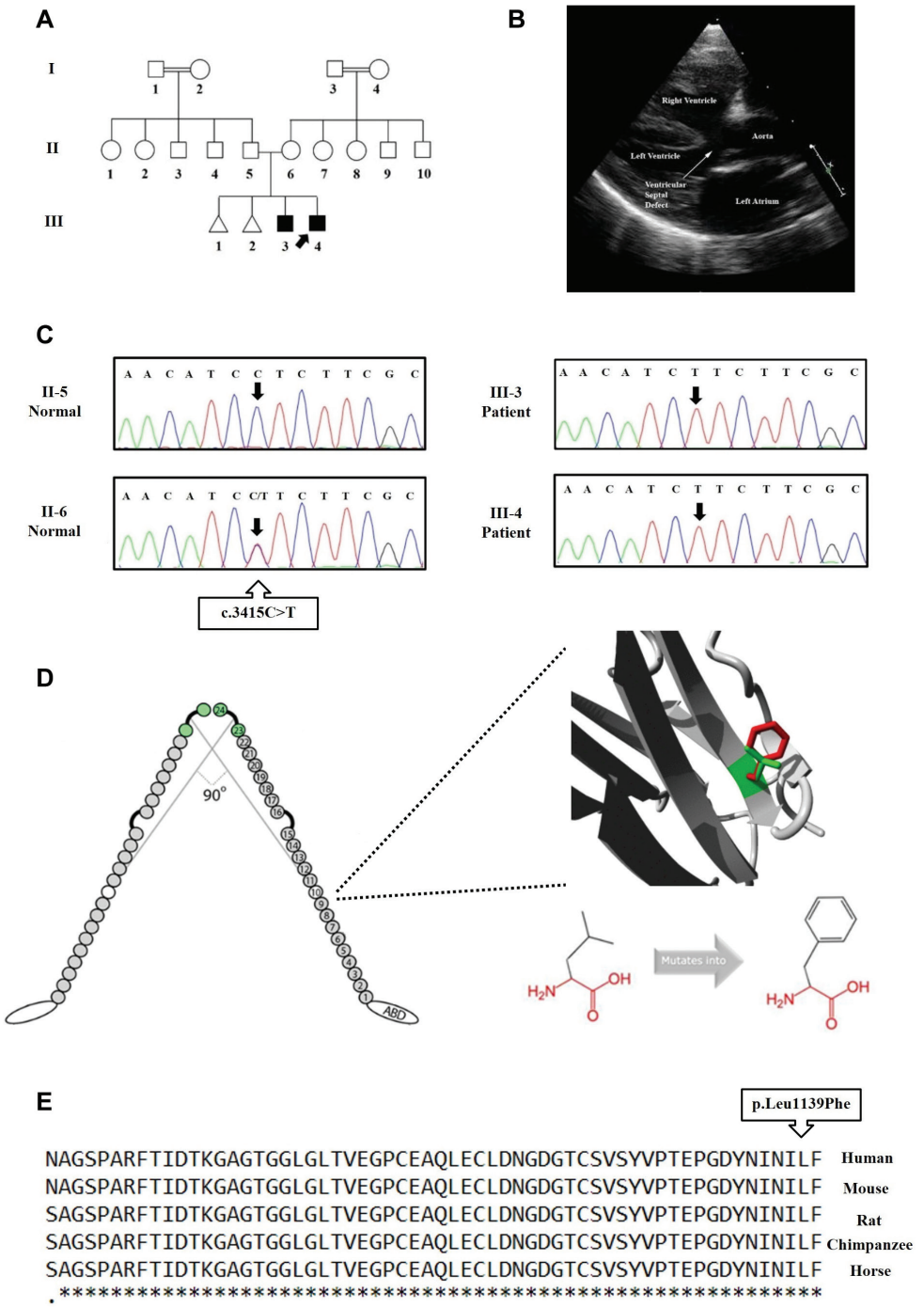

Figure 1

(A) Iranian CHD pedigree was recruited in our study. **(B)** Proband's (III:4) 2-dimensional echocardiogram shows TOF. **(C)** Chromatograms indicates the c.3415C>T variant in the *FLNA* gene. **(D)** Schematic view of the filamin A protein in humans is presented herein. **(E)** Conservation of p.Leu1139Phe amino acid in the filamin A protein across species is depicted herein.

is located within repeat-residues stretch number 9, where the phenylalanine-mutated residue may disturb this repeat and, consequently, any function that this repeat may serve. According to the HOPE server, the mutated residue is not only located in a domain that is important for the binding of other molecules that functionally or structurally interact with this protein but is also in contact with residues in a domain that is also of significance for binding. The mutation may disturb the interaction between these 2 domains and as such affect the function of the protein (**Figure 1D**).

Sanger sequencing indicated the hemizygous pathogenic allele in the proband; the mother and father, respectively, had a heterozygous and normal homozygous status (**Figure 1C**). The c.3415C>T variant has not been reported in any population databases such as the 1000 Genome project, gnomAD, esp6500, the GME Variome Project, the Iranome Database, the Human Gene Mutation Database, and the ClinVar Database. This variant was predicted as a disease-causing variant by MutationTaster, PROVEAN, SIFT, CADD, and FATHMM. The CLUSTALW alignment and GERP also predicted that the nucleotide position was widely conserved (**Figure 1E**). The diagnostic interpretation of the variant was done in keeping with the American College of Medical Genetics and Genomics (ACMG) guidelines.[2]

Discussion

Research has reported *FLNA* mutations to cause a wide spectrum of allelic disorders, including skeletal dysplasias, intellectual disability, and cardiovascular malformations. We checked our 2 patients for any other genetic variations via karyotyping, sequencing of the 6 genes involved in CHDs (*GATA4, NKX2-5, ZIC3, FOXH1, NODAL,* and *GJA1*), array-CGH, and MLPA for known and common variants. The only significant variant was found by WES. Eight syndromes resulting from the *FLNA* mutation have been described in OMIM (MIM# 300017). We present herein the first report of the *FLNA* mutation in TOF. We found the c.3415C>T variant in the *FLNA* gene of 2 children with TOF in an Iranian family; their mother was heterozygous and their father had a normal homozygous status. According to the ACMG guidelines, this variant is categorized as a likely pathogenic one. The *FLNA*-related TOF is a sex-linked phenotype.

The c.3415C>T variant leads to a missense substitution, p.Leu1139Phe. Homo/heterodimeric filamin A has a Y-shaped structure. There is an actin-binding domain at the amino terminus of each chain of the protein. Upon activation, this protein makes signaling scaffolds by self-assembling or cross-links with actin filaments to provide a 3-dimensional structure.[27] The substitution of Leu1139 by phenylalanine could affect this structure (**Figure 1D**). As reported, some missense variants could lead to a disruption in the signaling network mediated by filamin A.[28] Based on the HOPE prediction, p.Leu1139Phe may functionally or structurally affect the interaction of this protein with other proteins; in other words, it is located in an important region. Although it is difficult to prove the pathogenicity of this variant because of its mode of inheritance and the complexity of the disease, the mother is likely to show a mild phenotype and thus the disease remains underdiagnosed.

We can conclude that p.Leu1139Phe could be the causal variant in the family assessed in our study. Further, Leu1139 is a conserved residue among other species; this variant is segregated with the phenotype within the family with an X-linked recessive disease. (The proband was hemizygous and his mother was heterozygous.) We found no other genetic variations in the 2 siblings.

Filamin A is expressed in the heart, and its mutations have been reported to cause cardiovascular disease. Interestingly, our patients had a nonsyndromic disease (TOF), whereas it is known that filamin A is expressed in other organs such as the brain.[29] Other probable proteins may compensate for the role of deficient filamin A in other organs. Indeed, studies have shown gain-of-function mutations leading to syndromic diseases and loss-of-function mutations resulting in nonsyndromic diseases.[30] Further studies are required to find these modifying proteins.

Conclusion

This is the first report of the *FLNA* mutation causing a nonsyndromic CHD. It is possible that *FLNA* has a role in CHDs, especially TOF, in our country and should therefore be

DOI: 10.1093/labmed/lmab018

considered in screening and diagnostic programs. However, further studies are required to elucidate the exact role of this gene and the frequency of its mutation in our subpopulations. LM

Acknowledgments

Informed consent was obtained from the patients' parents by the authors. We special acknowledgments to the family that let us document their story to improve our understanding of the condition. This research was provided by Rajaie Cardiovascular, Medical and Research Center, Tehran, Iran and approved by the Rajaie Heart Center (RHC) Ethics Committee (RHC.AC.IR.REC.1395.46; December 24, 2016). For this article, SK collected data, SK and NM wrote the manuscript, MM and MM evaluated the patients, and SK, and NM performed project management and final approval.

References

1. Moller JH, Taubert KA, Allen HD, Clark EB, Lauer RM. Cardiovascular health and disease in children: current status. A Special Writing Group from the Task Force on Children and Youth, American Heart Association. *Circulation.* 1994;89(2):923–930.
2. Richards S, Aziz N, Bale S, et al.; ACMG Laboratory Quality Assurance Committee. Standards and guidelines for the interpretation of sequence variants: a joint consensus recommendation of the American College of Medical Genetics and Genomics and the Association for Molecular Pathology. *Genet Med.* 2015;17(5):405–424.
3. Pediatric Cardiac Genomics Consortium, et al. The Congenital Heart Disease Genetic Network Study: rationale, design, and early results. *Circ Res.* 2013;112(4):698–706.
4. Apitz C, Webb GD, Redington AN. Tetralogy of Fallot. *Lancet*. 2009;374(9699):1462–1471.
5. Hoffman JI, Kaplan S. The incidence of congenital heart disease. *J Am Coll Cardiol.* 2002;39(12):1890–1900.
6. Wessels MW, Willems PJ. Genetic factors in non-syndromic congenital heart malformations. *Clin Genet.* 2010;78(2):103–123.
7. Mercer-Rosa L, Paridon SM, Fogel MA, et al. 22q11. 2 deletion status and disease burden in children and adolescents with tetralogy of Fallot. *Circ Cardiovasc Genet*. 2015;8(1):74–81.
8. Han S, Zhang YY, Meng MY, et al. Generation of human iPSC line from a patient with Tetralogy of Fallot, YAHKMUi001-A, carrying a mutation in TBX1 gene. *Stem Cell Res.* 2020;42:101687.
9. Rakhmanov Y, Maltese PE, Marinelli C, Beccari T, Dundar M, Bertelli M. Genetic testing for tetralogy of Fallot. *EuroBiotech J.* 2018;2(s1):71–73.
10. Page DJ, Miossec MJ, Williams SG, et al. Whole exome sequencing reveals the major genetic contributors to nonsyndromic tetralogy of Fallot. *Circ Res.* 2019;124(4):553–563.
11. Starr JP. Tetralogy of Fallot: yesterday and today. *World J Surg.* 2010;34(4):658–668.
12. Bertranou EG, Blackstone EH, Hazelrig JB, Turner ME, Kirklin JW. Life expectancy without surgery in tetralogy of Fallot. *Am J Cardiol.* 1978;42(3):458–466.
13. Yang YQ, Gharibeh L, Li RG, et al. GATA4 loss-of-function mutations underlie familial tetralogy of Fallot. *Hum Mutat.* 2013;34(12):1662–1671.
14. Benson DW, Silberbach GM, Kavanaugh-McHugh A, et al. Mutations in the cardiac transcription factor NKX2.5 affect diverse cardiac developmental pathways. *J Clin Invest.* 1999;104(11):1567–1573.
15. Bauer RC, Laney AO, Smith R, et al. Jagged1 (JAG1) mutations in patients with tetralogy of Fallot or pulmonic stenosis. *Hum Mutat.* 2010;31(5):594–601.
16. Töpf A, Griffin HR, Glen E, et al. Functionally significant, rare transcription factor variants in tetralogy of Fallot. *PLoS One.* 2014;9(8):e95453.
17. Baban A, Postma AV, Marini M, et al. Identification of TBX5 mutations in a series of 94 patients with tetralogy of Fallot. *Am J Med Genet A.* 2014;164A(12):3100–3107.
18. Zhang Y, Sun Y-M, Xu Y-J, et al. A new TBX5 loss-of-function mutation contributes to congenital heart defect and atrioventricular block. *Int Heart J*. 2020;61(4):761–768.
19. Griffin HR, Töpf A, Glen E, et al. Systematic survey of variants in TBX1 in non-syndromic tetralogy of Fallot identifies a novel 57 base pair deletion that reduces transcriptional activity but finds no evidence for association with common variants. *Heart.* 2010;96(20):1651–1655.
20. Matos-Nieves A, Yasuhara J, Garg V. Another notch in the genetic puzzle of tetralogy of Fallot. *Am Heart Assoc.* 2019;124(4):462–464.
21. Feng Y, Walsh CA. The many faces of filamin: a versatile molecular scaffold for cell motility and signalling. *Nat Cell Biol.* 2004;6(11):1034–1038.
22. Feng Y, Chen MH, Moskowitz IP, et al. Filamin A (FLNA) is required for cell–cell contact in vascular development and cardiac morphogenesis. *Proc Nat Acad Sci U S A*. 2006;103(52):19836–19841.
23. Fernández L, Tenorio J, Polo-Vaquero C, et al. In-frame variants in FLNA proximal rod 1 domain associate with a predominant cardiac valvular phenotype. *Rev Esp Cardiol (Engl Ed).* 2018;71(7):545–552.
24. Prakash SK, LeMaire SA, Guo DC, et al. Rare copy number variants disrupt genes regulating vascular smooth muscle cell adhesion and contractility in sporadic thoracic aortic aneurysms and dissections. *Am J Hum Genet.* 2010;87(6):743–756.
25. Mercer CL, Andreoletti G, Carroll A, Salmon AP, Temple IK, Ennis S. Familial Ebstein anomaly: whole exome sequencing identifies novel phenotype associated with FLNA. *Circ Cardiovasc Genet*. 2017;10(6):e001683.
26. Miller SA, Dykes DD, Polesky HF. A simple salting out procedure for extracting DNA from human nucleated cells. *Nucleic Acids Res.* 1988;16(3):1215.
27. Camenisch TD, Spicer AP, Brehm-Gibson T, et al. Disruption of hyaluronan synthase-2 abrogates normal cardiac morphogenesis and hyaluronan-mediated transformation of epithelium to mesenchyme. *J Clin Invest.* 2000;106(3):349–360.
28. Duval D, Lardeux A, Le Tourneau T, et al. Valvular dystrophy associated filamin A mutations reveal a new role of its first repeats in small-GTPase regulation. *Biochim Biophys Acta.* 2014;1843(2):234–244.
29. Sauls K, de Vlaming A, Harris BS, et al. Developmental basis for filamin-A-associated myxomatous mitral valve disease. *Cardiovasc Res.* 2012;96(1):109–119.
30. de Wit MC, de Coo IF, Lequin MH, Halley DJ, Roos-Hesselink JW, Mancini GM. Combined cardiological and neurological abnormalities due to filamin A gene mutation. *Clin Res Cardiol.* 2011;100(1):45–50.

The Impact of COVID-19 Containment Actions on Extra-Analytical Phases of the Clinical Laboratory: A Case Report

Mala Mahto, MD,[1,*] *Mukunda Kumar, MD,*[2] *Ayan Banerjee, MD,*[1] *Sushil Kumar, MD*[1]

Laboratory Medicine 2021;52:619-625

DOI: 10.1093/labmed/lmab036

ABSTRACT

Laboratory information systems need to adapt to new demands created by the COVID-19 pandemic, which has set up new normals like containment measures and social distancing. Some of these have negatively impacted the pre- and postanalytical phases of laboratory testing. Here, we present an intriguing finding related to the generation of the accession number/specimen number on the investigation module of a hospital management information system and its impact on the dissemination of reports resulting in the wrong release of reports on a female patient amidst the background of COVID-19 containment measures. We analyze the situation that led to this false reporting and the importance of the proper customization of information software in laboratories along with a robust postanalytical framework of laboratory work culture to avert such untoward incidents. This introspection has made us realize that COVID-19 has been a scientific, medical, and social challenge. We need to redefine our priorities in the days to come because SARS-CoV-2 is here to stay.

Keywords: laboratory errors, extra-analytical phase, hospital information management system, laboratory information system

Laboratory information system (LIS) and hospital management information system (HMIS) play key roles in laboratories regarding meeting quality standards, decreasing transcription errors, reducing the turnaround time from specimen receipt to the reporting of results, and improving patient outcomes.[1] With the advent of evidence-based medicine, the LIS has become a necessity of every laboratory.[2] This increased use of the LIS has allowed end users to more clearly articulate detailed system requirements, in turn leading vendors to develop more attractive, viable, and customized LIS options. However, COVID-19 has brought about an unseen fear that has affected the functioning of the entire medical community, including laboratory services. All attempts have been directed toward the containment of infection, which has led to the implementation of new policies including the significant prohibition on the use of barcoded autogenerated tubes for specimen collection and testing. How the reintroduction of paper-based requisitions and handwritten labeled vacutainers intended to restrict the number of staff involved and the multiperson handling of automated phlebotomy tube labelers (APTL) and to minimize contact with contaminated surfaces, affected the functioning of an in-house hospital laboratory is discussed in this case report.

Abbreviations:

LIS, laboratory information system; HMIS, hospital management information system; APTL, automated phlebotomy tube labeler; IPD, inpatient department; TAT, turnaround time; LFT, liver function test; KFT, kidney function test; CR number, central registration number.

[1]Biochemistry Department, AIIMS Patna, Patna, Bihar, India, [2]Biochemistry Department, All India Institute of Medical Sciences Patna, Patna, Bihar, India

*To whom correspondence should be addressed.
dr.malamahto@gmail.com

Case Report

The biochemistry wing of a central laboratory received specimens for an admitted 20 year old woman who had tested positive for COVID-19 on 3 consecutive days as a part of routine monitoring. The values for the specimen processed on the third day differed remarkably from the values released on the second day, which was revealed after a manual delta check conducted on the third day (**Table 1** shows her reports over the 3-day period). The delta check

Table 1. Investigation Tracking (delta check) on Day 1, Day 2, and Day 3

Name of Parameters/Date	Day 1	Day 2	Day 3	Reference Range	Units
Serum calcium	2.03	1.95	2.1	2.15–2.5	mmol/L
Serum phosphorus	2.65	0.62	2.35	0.87–1.45	mmol/L
Serum uric acid	0.66	0.17	0.54	0.20–0.42	mmol/L
Serum sodium	131.23	138.42	134.12	135–145	meq/L
Serum potassium	5.09	4.16	4.47	3.5–5	meq/L
Serum chloride	92.40	107.27	94.05	98–107	meq/L
Serum urea	22.99	2.96	20.67	2.16–7.15	mmol/L
Serum creatinine	480	36.24	561.34	61.88–114.9	µmol/L

showed high values for urea and creatinine on the first day, normal values on the second day, and high values again on the third day. The fault was believed to be with the values released on the second day, with the following probabilities in mind:

i. Specimen misidentification with mismatched labeling sent from the intensive care unit (ICU) ward, with the specimen from the wrong person (preanalytical error).
ii. Specimen placed in the wrong position in the autoanalyzer instead of the one intended and programmed for (analytical error).
iii. Incorrect data transfer because the bar-code labeled tubes were no longer in use and incorrect manual programming of specimen numbers resulting in mismatched data transfer (postanalytical error).

A recheck of the third day specimen revealed values that were identical to those obtained earlier in the run. This finding led to the analysis of the second day reports on the computer screen of the clinical chemistry autoanalyzer because it was difficult to analyse the first two options ie, whether the right sample was sent from the wards and whether is was run in the right slot in the autoanalyser. This was because of the fact that considerable time had lapsed between the day 2 sample was received and present day of reporting. Moreover the second day sample was discarded and hence a recheck could not be performed. The results seen on the monitor of the autoanalyzer differed from the results on the interfacing computer, showing values from the second day as being very much in sync with the values released on day 1 and day 3. This situation thus involved incorrect data transfer (postanalytical error), so further analysis was conducted to find the root cause of this incorrect data transfer.

Before analyzing the root cause, we first depict the modifications implemented in the functioning of the clinical laboratory to contain the spread of COVID-19 infection. Significant changes were made regarding the day-to-day functioning of the hospital since April 2020, when it was declared a dedicated COVID-19 hospital in an effort toward containing the spread of infection; at that time, there was much speculation about the mode of infection transmission with scant scientific evidence. One of the major decisions made was to send handwritten vacutainers from wards to laboratories instead of the usual practice of sending bar-coded tubes to minimize the number of people handling the APTL machines located on alternate floors of the inpatient department (IPD). The APTL is a fully automated, prelabeled, barcoded vacutainer dispenser that operates according to the availability of necessary information in the LIS. Because there are multiple wards on each floor of the IPD block and the APTL is a costly machine, it was not practically feasible to install in all the wards. Before the pandemic, when requisition raising was done in the HMIS for a particular patient from a particular ward, a requisition would be transferred via health level 7 and was reflected in the LIS, and blood collection tubes would be generated from the APTL located nearest to the ward (**Figure 1** workflow related to specimen collection and report generation in the LIS before COVID-19). During the pandemic, because the collection of tubes requires hospital attendants to move from one floor to another wearing personal protective equipment and handle the APTL to generate the tubes, it was decided in the best interests of the hospital to stop the use of the APTL until the pandemic wanes. Moreover, using 1 system (HMIS alone) rather than 2 systems (LIS and HMIS integrated) with 2 different service providers is a better option during the pandemic. The handwritten vacutainers cannot be read by the barcode readers of the autoanalyzers in the laboratories (**Figure 1**, workflow related to specimen collection and report generation in the HMIS during the pandemic). The tests required for a particular patient must be manually programmed, and the data are transferred from the autoanalyzers directly to the HMIS because the LIS is not being used for the time being. Manual programming is associated with many errors, such as the wrong specimen being run, incorrect or partial selection of tests, and prolonged turnaround time (TAT) because of manual selection of tests.

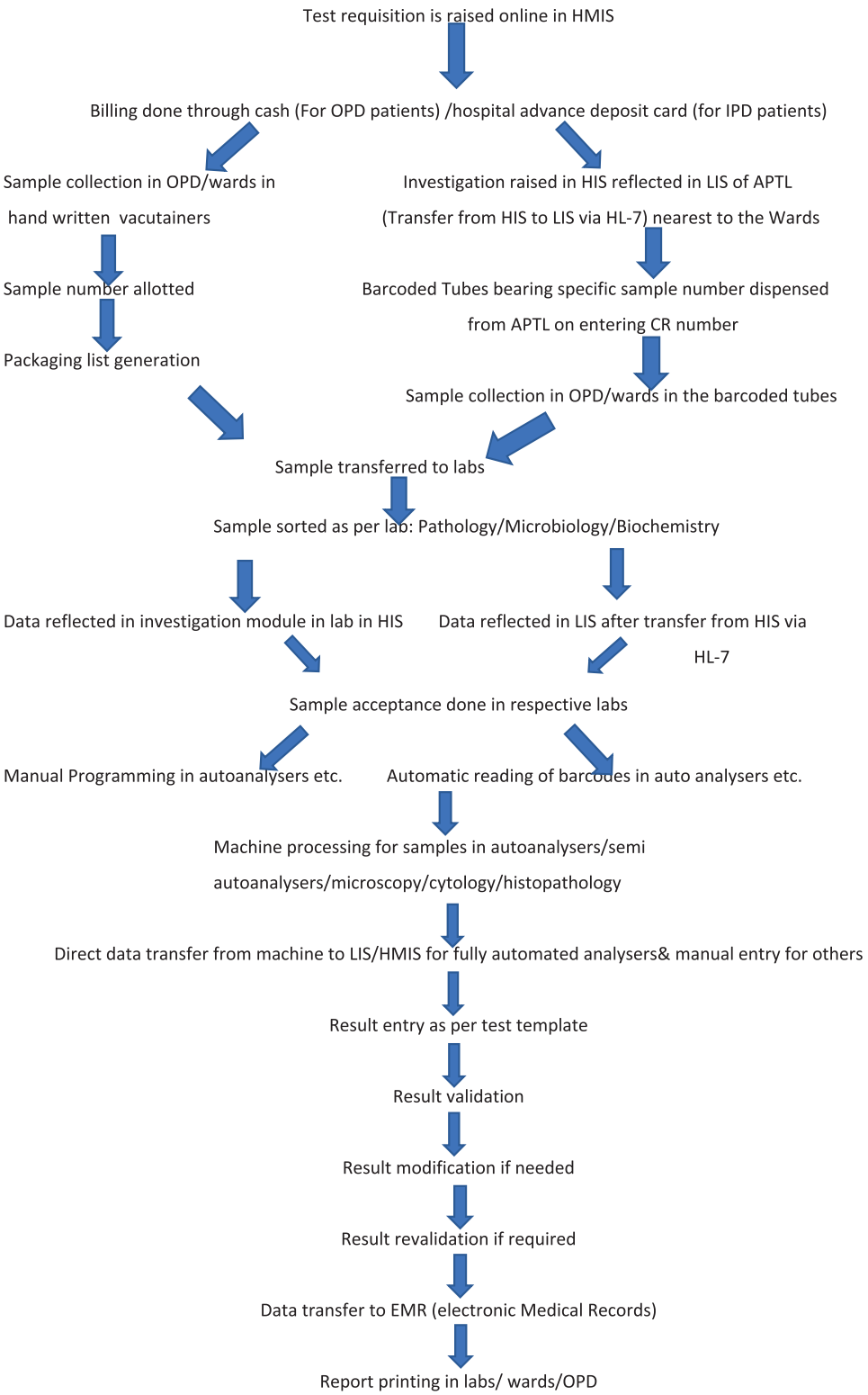

Figure 1

Workflow in HMIS during COVID-19 and workflow in LIS pre-pandemic. APTL, automated phlebotomy tube labeler; HMIS, hospital management information system; IPD, inpatient department; LIS, laboratory information system; OPD, outpatient department.

Lab Medicine 2021;52;619–625
DOI: 10.1093/labmed/lmab036

What Happened?

When the specimen for day 2 was received in the laboratory, it bore the central registration (CR) number 109112000xxxxxx (actual number not revealed to protect patient identity) and the specimen number 0056 for a liver function test (LFT) and kidney function test (KFT) as generated upon requisition-raising in the HMIS. The specimen number in the HMIS for biochemistry is a 4-digit autogenerated number customized in the HMIS; it is generated daily and is not repeated for any 2 different specimen types on the same day. The number is generated starting from 0001, when the time changes at 0000 hours (midnight) in the HMIS marking the start of a new day. It varies for the same CR number depending on the number of vacutainers for different specimen types, eg, LFT/KFT, blood sugar, and complete blood count, withdrawn at the same time. Moreover, for a patient in the IPD, multiple specimens may be sent on the same day for the same analyte. The configuration of the specimen number is very important because it determines the transfer of data for the particular specimen. Problems can crop up if 2 specimens bearing the same specimen number are sent to the laboratory on the same day, as may happen when a requisition is raised on one day but the specimen is sent on the next day.

In our patient, the specimen was not tagged with the date or the patient's CR number in the HMIS. Moreover, specimen number 0066 generated on the HMIS on the same day arrived in the biochemistry laboratory before specimen number 0056. This is a common occurrence because wards are located on different floors and the requisition raising and specimen number generation in the HMIS always does not mean that the specimen with the specimen number generated first in the HMIS will reach the laboratory first. Specimens may not be drawn at the same time as requisition raising for many reasons such as inaccessibility of veins, inadequate staff for phlebotomy or transport of the specimen, or inadequate money in the patient's account. The sequence of events resulting in the release of the wrong reports for specimen number 0056 from the laboratory is described in **Figure 2**.

What Went Wrong?

Mistakes were made at multiple junctures, which were identified too late the next day when a repeat third day specimen came to the laboratory, as follows:

i. Stopping the use of autogenerated barcode tubes and hence the need for manual programming.
ii. Incorrect programming by the technical staff on duty and failure of the doctor to supervise and rectify what the technical staff had missed.
iii. Failure of technical staff and doctor on duty to realize that the specimen number 0056 was run as 0056 but the data for the same were never transferred.
iv. Failure of the doctor on duty to perform a manual delta check.
v. Faulty specimen number customization in the HMIS bearing no link or association to the CR number of the patient or the date.

What Could Have Been Done to Avoid It?

The above patient was in renal failure with altered urea and creatinine values according to the first day specimen received in the laboratory. The specimen in question revealed normal urea and creatinine values on the second day as opposed to the high values released the previous day. Had a delta check been performed manually, this release of the wrong reports could have been averted. Customization of the specimen number in the HMIS, which is generated on a daily basis without bearing any relation to the CR number or date, played a significant role in the incorrect data transfer. The specimen number should either be generated on monthly basis or be tagged with the date or CR number to ensure correct data transfer. We identified this problem with the usage of the specimen number in the HMIS and hence shifted to using the LIS with the customization of the specimen number per our requirements, synchronizing it to the current date on a daily basis.

Discussion

The complex web of events in this case report involved a preanalytical error causing specimen misidentification and data thus being incorrectly transferred, resulting in a transcriptional error despite this error being partially identified and corrected before the release of the laboratory results. The correction done in data entry

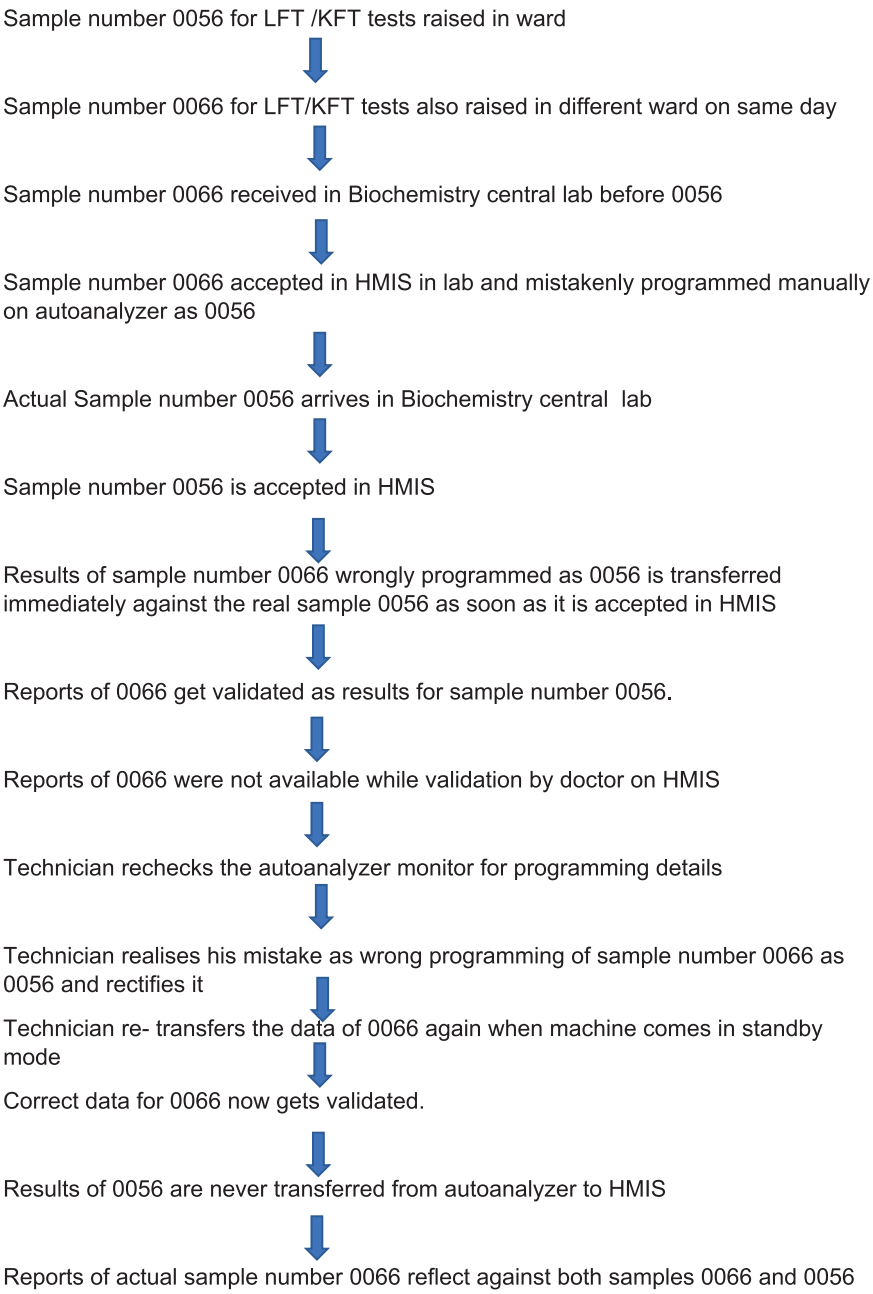

Figure 2

Diagrammatic representation of sequence of events leading to incorrect reporting. HMIS, hospital management information system; KFT, kidney function test; LFT, liver function test.

while programming specimen number 0066 as specimen number 0056 during a recheck being done and subsequent resending of data sorted the reports for specimen number 0066. However, specimen number 0056 was run as the correct number 0056 in the first place but the data could not be transferred because the reporting slot was already occupied by the data for specimen 0066 sent earlier and went unnoticed. This resulted in the monitor of

DOI: 10.1093/labmed/lmab036

the autoanalyzer showing the values of specimen number 0056 as being quite different from the values shown in the HMIS on the second day. With our patient, the incorrect data transfer was the end result of errors involving both the preanalytical and postanalytical phases. A major contributor was the disuse of the APTL during the COVID-19 pandemic leading to the nonavailability of barcoded vacutainers. In addition, our HMIS had a major drawback in the form of specimen numbers being generated daily and not being linked to the date or CR number. The specimen number together with the patient CR number usually gives each specimen a unique identity in the laboratory.

Moreover, the HMIS was not bidirectionally functional, implying that specimen programming needed to be done manually and only data transfer in the form of results was possible from the autoanalyzer to the interfacing computer. This drawback prompted us to switch over to the use of the LIS because it has bidirectional data transfer—ie, the barcode labeled tubes can be read automatically by the autoanalyzer and also transfer the results generated from the machine to an interfacing computer in real time. The bidirectional functionality provides a near-complete assurance of freedom from preanalytical errors in the laboratory with respect to specimen misidentification.

Hence the customization of the HMIS or LIS as per the needs of the end user is mandatory. However, its establishment involves a good deal of effort and interaction with stakeholders. Significant time is needed to understand the functionality of the laboratory involved. The workflow related to the processing of laboratory specimens until reports are made available to the patient concerned varies from laboratory to laboratory despite the basic processes involved remaining the same. LISs have been established to augment communication between patients and healthcare professionals, thereby enabling patients to play a more dynamic role in their own treatment and self-management.[3] Hence it is of utmost importance that the system be flawless.

Monitoring quality indicators in daily work can reduce laboratory errors and risks to patient safety by identifying problems in all phases of laboratory processes and allowing their correction.[4] Apart from the recommended postanalytical quality indicators such as TAT, noting errors during transcription, and notification of critical results, a few other elements that may help identify errors in the postanalytical phase include a random choice of specimens already run for repeat testing without disclosing their identity or the reports obtained in the initial run and cross-checking the results with the ones obtained earlier and matching visually icteric or lipemic specimens with the values obtained for bilirubin or triglycerides in initial runs. Moreover, if 2 different specimens are obtained in different vacutainers from the same patient for routine clinical chemistry and immunoassay tests, a correlation of the values obtained from 2 different platforms for different tests should be requested to check for the integrity of the specimen run.

Finally, we note our delta checks. A delta check is a process of comparing a patient's result with his/her previous result for any analyte over a specified period of time. The difference, or delta, from pre-established rules may indicate a specimen mislabel or another preanalytical, analytical, or postanalytical error.[5] If for any reason the laboratory information software does not have a delta-check procedure for flagging, a good practice would be to check for the results of a specimen from the previous day or the past few days to check for any obvious discrepancy of results: ie, a manual delta check. Because a built-in auto–delta check process within an LIS can produce frequent alarms in hospitals with critically ill patients and delay TAT, our laboratory had not activated our delta check. The postanalytical phase requires more such concerted measures to do a final check before the results are released from the laboratories.

A human crisis like COVID-19 has caused a severe disruption of the healthcare sector globally. However, it has also created unique opportunities enabling researchers and clinicians to revisit healthcare delivery by rationalizing and optimizing the use of available resources.[6]

Takeaway Messages

i. Postanalytical quality indicators should include final measures to monitor the overall testing process before laboratory reports are released.
ii. The use of barcoded specimen containers capable of being read by autoanalyzers is a must to ensure

minimal error in laboratories; there is no alternative for good laboratory practices.

iii. The customization of the HMIS/LIS as per the needs of end users is mandatory.

iv. COVID-19 is a scientific, medical, and social challenge: We need to redefine our priorities in the days to come because SARS-CoV-2 is here to stay. **LM**

Acknowledgments

MM and MK researched the literature and conceived the study. MM and AB wrote the first draft of the manuscript, and SK edited the draft. All authors reviewed and edited the manuscript and approved the final version of the manuscript.

References

1. Wahls TL, Cram PM. The frequency of missed test results and associated treatment delays in a highly computerized health system. *BMC Fam Pract.* 2007;8:32.
2. Klovning A, Sandberg S. Searching the literature and relevant databases. In: Price CP, Christenson RH, eds. *Evidence Based Laboratory Medicine: From Principles to Outcomes.* Washington, DC: AACC Press; 2003: 93–114.
3. Jastania R. How laboratory information system improves patient safety. *Am J Lab Med.* 2019;4:97–100.
4. Sciacovelli L, Aita A, Padoan A, et al. Performance criteria and quality indicators for the post-analytical phase. *Clin Chem Lab Med.* 2016;54(7):1169–1176.
5. Randell EW, Yenice S. Delta checks in the clinical laboratory. *Crit Rev Clin Lab Sci.* 2019;56(2):75–97.
6. Iyengar K, Mabrouk A, Jain VK, Venkatesan A, Vaishya R. Learning opportunities from COVID-19 and future effects on health care system. *Diabetes Metab Syndr.* 2020;14(5):943–946.

Science

Performance Evaluation of the Siemens SARS-CoV-2 Total Antibody and IgG Antibody Test

Lisa Florin, Pharm D,[1,*] *Karel Maelegheer, MD,*[1] *Wouter Vandewal, MD,*[1] *Dirk Bernard, MD,*[1] *Johan Robbrecht, MD*[1]

Laboratory Medicine 2021;52:e147-e153

DOI: 10.1093/labmed/lmab027

ABSTRACT

Objective: In this study, the performance of 2 commercially available SARS-CoV-2 antibody assays is evaluated.

Methods: The Siemens SARS-CoV-2 Total (COV2T) and IgG (COV2G) antibody tests were evaluated on a Siemens Atellica IM1300 analyzer. Imprecision was assessed with the CLSI EP15 protocol using positive controls. Ninety control group specimens were analyzed for specificity, and 175 specimens from 58 patients with polymerase chain reaction–confirmed SARS-CoV-2 were measured for the sensitivity and kinetics of the antibody response.

Results: Within-run and total imprecision were acceptable for both assays. Both tests showed a specificity of 100%. Sensitivity earlier in the disease state was greater for the COV2T assay than for the COV2G assay, but sensitivity >14 days after onset of symptoms approached 100% for both. For all patients, antibody titers remained above the seroconversion cutoff for all follow-up specimens.

Conclusion: This study shows acceptable performance for both the Siemens COV2T and COV2G test, although seroconversion occurs earlier with the COV2T test.

Keywords: COVID-19, SARS-CoV-2, serology, antibody kinetics, performance evaluation, immunoassay

SARS-CoV-2, a novel coronavirus belonging to the beta-coronaviruses, emerged in December 2019 in the area of Wuhan, China, and spread rapidly all over the world thereafter. On March 11, 2020, the World Health Organization declared the spread of the virus as a pandemic.[1] COVID-19, the disease caused by SARS-CoV-2, may trigger a clinical spectrum of symptoms ranging from mild to life-threatening. Furthermore, many patients are asymptomatic and are unconsciously responsible for the further spread of the virus.[2] Therefore, timely and precise diagnosis is crucial for adequate treatment and for infection control. Diagnosis is commonly performed by reverse-transcription polymerase chain reaction (RT-PCR) of viral RNA in upper respiratory tract specimens.[3]

Abbreviations:

COV2T, SARS-CoV-2 Total; COV2G, SARS-CoV-2 IgG; RT-PCR, reverse-transcription polymerase chain reaction; ELISA, enzyme-linked immunosorbent assay; CLIA, chemiluminescent assay; S1-RBD, spike 1 protein receptor binding domain; CI, confidence interval.

[1]Department of Clinical Biology, AZ Sint-Lucas Brugge, Bruges, Belgium

*To whom correspondence should be addressed.
Lisa.florin@stlucas.be

Detection of specific SARS-CoV-2 IgM, IgA, and/or IgG antibodies in serum or plasma may be of added value in patients who present late after-symptom onset with a low viral load, causing the PCR test to be a false negative. In addition, antibody tests may be of use in epidemiological studies to determine antibody prevalence in the universal population or in specific settings, such as health care workers. Furthermore, large-scale vaccine studies are developing worldwide, and (serial) measurement of antibodies may be used for follow-up of vaccine effectiveness.[4-6] Previous studies have shown that antibodies typically appear starting 5 to 7 days after infection and are therefore not useful in detection of acute infection. Since the start of the spread of this disease, numerous antibody assays, mainly targeting the nucleocapsid (N) protein or spike (S) protein, have been developed. These assays are lateral flow assays, enzyme-linked immunosorbent assays (ELISAs), and electrochemiluminescent or chemiluminescent immunoassays (CLIAs), compatible with high-throughput analyzers.[7-13]

Siemens Healthineers developed two CLIA-based SARS-CoV-2 antibody tests directed against the spike 1 protein receptor binding domain (S1-RBD): a total antibody test (COV2T) detecting both IgM and IgG antibodies, and an

IgG antibody test (COV2G) detecting solely IgG antibodies. To date, 2 other studies have described the performance of the COV2T test, but no other studies have evaluated the COV2G antibody test.[9,14] It was the aim of this study to evaluate both antibody assays and to describe the kinetics of antibody response in patients with COVID-19 with specimens measured with both assays.

Materials and Methods

Patient Selection and Study Design

In this retrospective study, specificity was evaluated using residual pre-pandemic serum specimens from healthy volunteers (n = 34) and random patients (n = 22). In addition, specimens from patients with potential cross-reacting antibodies, including antinuclear antibodies (n = 5), rheumatoid factors (n = 5), Epstein-Barr virus (n = 5) and cytomegalovirus (n = 5) IgM-positive specimens, paraproteins (n = 5), and PCR-confirmed acute infections with other coronavirus strains (NL63: n = 3; HKU-1: n = 3; OC43: n = 3) were analyzed. For sensitivity, 175 follow-up routine serum specimens from 58 hospitalized patients (median age 80 years) with confirmed detection of SARS-CoV-2 RNA by RT-PCR on nasopharyngeal swab were measured. Specimens were drawn between 0 and 109 days after PCR positivity. Sensitivity was calculated for different time frames: day < 4, day 4–7, day 8–10, day 11–14 and day > 14, starting from the time to the first positive PCR result and starting from the time of symptom onset. Calculation of 95% confidence intervals (CI) was performed with MedCalc Statistical Software (MedCalc Software, Ostend, Belgium). Information about the start of symptoms was derived from the medical records.

For calculation of sensitivity compared to symptom onset, 18 specimens from 8 patients were excluded because these patients were asymptomatic. The median time between a positive PCR test or symptom onset and serum specimen collection was 8 days (interquartile range, 4–13 days) and 12 days (interquartile range, 6.5–18 days), respectively. With the same specimens, the kinetics of antibody response were assessed for both assays. A method comparison was performed against the Euroimmun Anti-SARS-CoV-2 IgG ELISA (Euroimmun AG, Luebeck, Germany), using specimens from health care workers (n = 194 for COV2T and n = 94 for COV2G) who either had a confirmed positive PCR result or who retrospectively reported symptoms suggestive of a SARS-CoV-2 infection but without a need for medical assistance during the period of illness. The study design occurred in accordance with the local ethics committee of the AZ Sint-Lucas hospital in Bruges, Belgium.

Analytical Performance

Intra- and interassay imprecision were assessed according to the CLSI EP15-A3 protocol with positive control material provided by the manufacturer by measurement of quintuplicates during 5 successive days.[15] An analysis of variance was used to calculate the repeatability and intermediate precision.

Laboratory Measurements

The COV2T test (Siemens Healthineers nr. 11206711, Munich, Germany)[16] is an automated 1-step antigen chemiluminescent sandwich immunoassay for total antibodies, and the COV2G (Siemens Healthineers nr. 11206997)[17] is an automated 2-step chemiluminescent sandwich immunoassay for IgG antibodies against the SARS-CoV-2 virus. Both assays target the S1-RBD. The COV2T assay is designed as a qualitative assay, whereas the COV2G test is used for the semi-quantitative detection of IgG antibodies. The performance of both assays was assessed on a Atellica IM1300 analyzer (Siemens Healthineers, Erlangen, Germany). Characteristics of these assays, as stated in the product leaflet,[16,17] are summarized in **Table 1**.

For the method comparison, the anti-SARS-CoV-2 ELISA IgG test (Euroimmun AG, nr. EL2606-9601G), targeted against the S1 protein, was carried out on a BEP 2000

Table 1. Characteristics of Siemens COV2T and COV2G, According to Manufacturer's Specifications

Assay	Detection	Sensitivity (d after PCR positivity)			Specificity	Measuring Interval (index value)
		< 6 d	7–13 d	> 13 d		
COV2T	IgM and IgG	60.7%	97.5%	100%	100%	0.05–10
COV2G	IgG	56.0%	92.2%	100%	100%	0.5–20

COV2T, SARS-CoV-2 Total antibody assay; COV2G, SARS-CoV-2 IgG antibody assay; PCR, polymerase chain reaction.

Advance system (Siemens Healthineers). All specimens were stored at –80°C until the time of analysis. Specimens were analyzed by trained laboratory staff in the general hospital AZ Sint-Lucas in Bruges, Belgium, in accordance with the manufacturer's protocol.

Results for COV2T and COV2G were reported as index values and considered as nonreactive (index < 1.0 for Siemens and index < 0.8 for Euroimmun), borderline (0.8 < index < 1.1 for Euroimmun) or reactive (index ≥ 1.0 for Siemens and index ≥ 1.1 for Euroimmun) according to the manufacturer's instructions. The measuring interval reported by the manufacturer was 0.05 to 10.00 for COV2T and 0.50 to 20.00 for COV2G.

Results

Results for imprecision are given in **Table 2**. Intra-assay imprecision for COV2T and COV2G assays revealed coefficients of variations of 2.81% and 2.35%, respectively, both lower than the manufacturer's claim of 10%. Total imprecision was 7.12% and 5.81%, respectively, also remaining below the manufacturer's claim of 12%.

Specificity, calculated on 90 specimens, was 100% for the COV2T assay and for the COV2G assay (95% CI, 96.4%–100.0%). There was no cross-reactivity found with possible interfering antibodies, including the specimens from other common-cold coronavirus strains.

Table 3 gives an overview of results for the sensitivity of both assays, calculated from the days since positive PCR result and days since symptom onset. Overall, calculated sensitivities were lower than the sensitivities stated in the product leaflets (**Table 1**). As expected, the sensitivity of both assays increased gradually with disease progression, reaching 100% (95% CI, 89.7%–100.0%) for the COV2T assay 14 days after PCR positivity. For the COV2G assay, sensitivity 14 days after PCR positivity was 97.1% (95% CI, 84.7%–100.0%) because of 1 specimen with a result just below the cutoff value. Sensitivity 14 days after disease onset was 94.6% (95% CI, 85.1–98.9) and 91.1% (95% CI, 80.4–97.0) for the COV2T and COV2G assay, respectively, because of 3 and 4 specimens (respectively) that remained seronegative after 14 days. However, follow-up specimens from these patients showed seroconversion later in the disease progression. Sensitivity in the different time frames was lower for COV2G than for COV2T. Sensitivities were lower when calculated for days after symptom onset because symptoms were typically already present a few days before PCR testing was performed.

The kinetics of antibody response on different days from symptom onset were evaluated on the same specimen set from hospitalized patients, with specimens taken up to 109 days after the start of symptoms. **Figures 1A and 1B** show the results for the COV2T and COV2G assays. The median time for seroconversion, after the start of

Table 2. Intra- and Interassay Imprecision of Siemens SARS-CoV-2 Antibody Assays, Assessed on Quality Control Material Provided by Manufacturer

Assay	Mean	Intra-Assay Imprecision		Total Imprecision	
		SD	CV (%)	SD	CV (%)
COV2T	2.44	0.07	2.81	0.17	7.12
COV2G	2.57	0.06	2.35	0.15	5.81

COV2T, SARS-CoV-2 Total antibody assay; COV2G, SARS-CoV-2 IgG antibody assay; CV, coefficient of variation; SD, standard deviation.

Table 3. Sensitivity of COV2T and COV2G Tests Calculated Against Day of Positive PCR Result and Day of Symptom Onset

	Days After PCR Positivity		Days After Symptom Onset	
	COV2T	COV2G	COV2T	COV2G
< 4 d	25.0% (10/40; 12.7–41.2)	17.5% (7/40; 7.3–32.8)	5.9% (1/17; 0.2–28.7)	5.9% (1/17; 0.2–28.7)
4–7 d	39.0% (16/41; 24.2–55.5)	31.7% (13/41; 18.1–48.1)	19.4% (6/31; 7.5–37.5)	12.9% (4/31; 3.63–29.8)
8–10 d	62.1% (18/29; 42.3–79.3)	44.8% (13/29; 26.5–64.3)	57.1% (12/21; 34.0–78.2)	38.1% (8/21; 18.1–61.6)
11–14 d	90.3% (28/31; 74.3–98.0)	64.5% (20/31; 45.4–80.8)	84.4% (27/32; 67.2–94.7)	56.3% (18/32; 37.7–73.6)
> 14 d	100.0% (34/34; 89.7–100.0)	97.1% (33/34; 84.7–100.0)	92.9% (53/56; 85.1–98.9)	91.1% (51/56; 80.4–97.0)

COV2T, SARS-CoV-2 Total antibody assay; COV2G, SARS-CoV-2 IgG antibody assay; PCR, polymerase chain reaction.
Numbers in parentheses are absolute specimen numbers, followed by calculated 95% confidence intervals for sensitivity.

Lab Medicine 2021;52;e147–e153 e149
DOI: 10.1093/labmed/lmab027

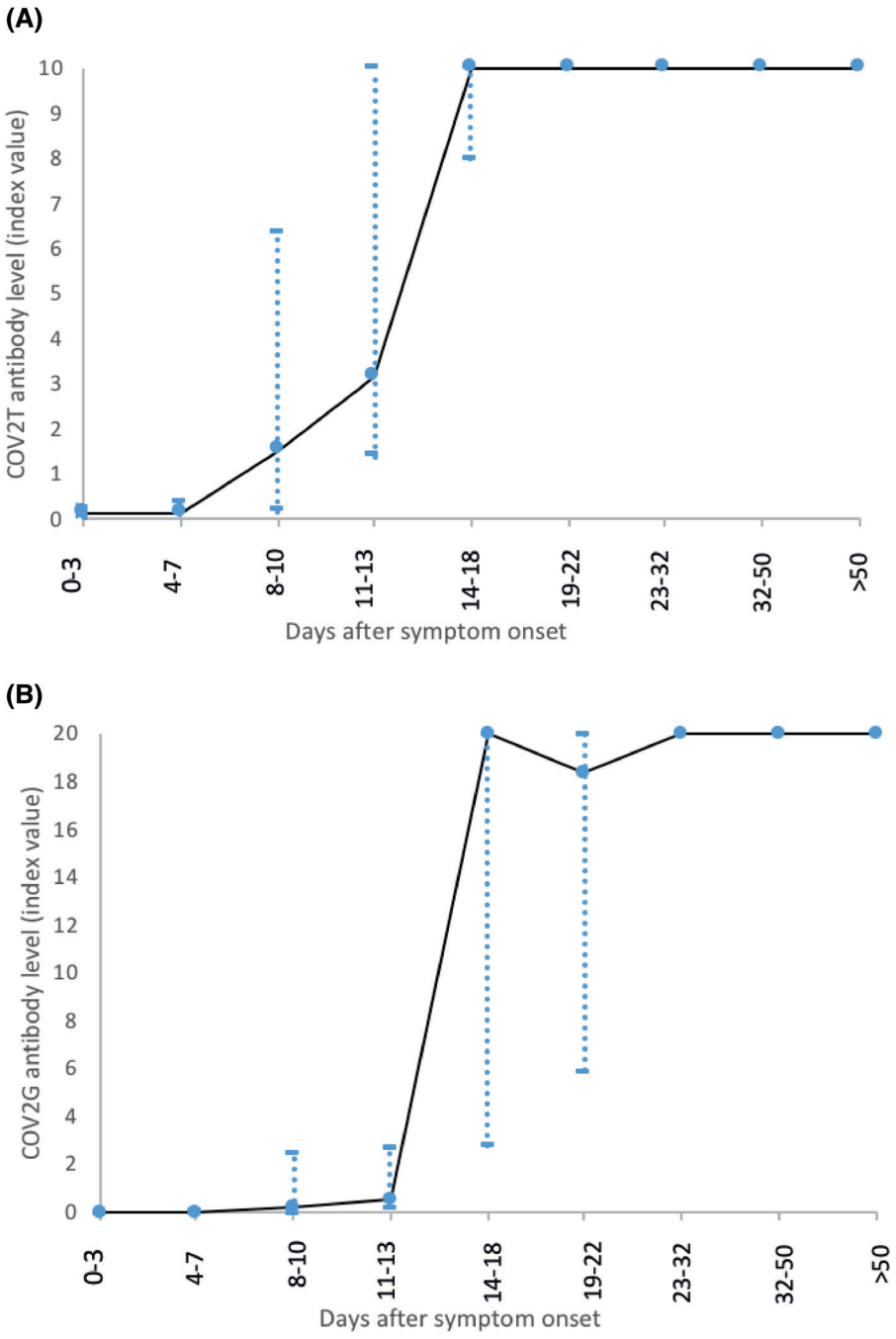

Figure 1

Kinetics of antibody response for the COV2T (**A**) and COV2G assay (**B**). Median values with interquartile range of antibody levels of all specimens are plotted against days after onset of symptoms. COV2T, SARS-CoV-2 Total antibody assay; COV2G, SARS-CoV-2 IgG antibody assay.

symptoms, was 11 days for the COV2T assay. For the COV2G assay, the median time to seroconversion was only 1 day later, at 12 days after symptom onset. The median antibody levels reached the upper limit of the manufacturers' measuring range 14 days and 16 days after symptom onset for the COV2T and COV2G assays, respectively. For

all but 2 patients, after reaching the maximum antibody levels, these levels were held with all further follow-up specimens. For those 2 patients, COV2T and COV2G antibody levels declined at 51 and 109 days, respectively, but values remained above the cutoff for seropositivity.

One hundred ninety-five specimens from health care workers working at the AZ Sint-Lucas hospital in Bruges, Belgium, and with presumptive or PCR-confirmed COVID-19 disease were analyzed with the Siemens COV2T assay and the Euroimmun IgG ELISA (**Table 4**). Twenty-four specimens were positive with the Siemens COV2T assay and negative with the Euroimmun assay, whereas 3 specimens were negative with the COV2T assay but positive or borderline with the Euroimmun ELISA. The results of this specimen set suggest a higher sensitivity of the Siemens COV2T assay compared to the Euroimmun ELISA. The percentage agreement between both assays, when borderline results were considered positive, was 86.2%. Only 94 of 195 specimens could be analyzed with the COV2G assay because of short specimen volume. The Euroimmun comparison with the Siemens COV2G assay showed that 22 specimens were positive or borderline with Euroimmun but negative with the Siemens IgG assay. This result hints at an increased sensitivity of the Euroimmun assay. The percentage agreement between these assays was only 76.6%. When these 94 specimens were compared to the COV2T test, 34 were found to be seropositive with COV2T but negative with COV2G, resulting in a sensitivity of 66% of the COV2G assay compared to COV2T.

Discussion

Serologic testing for SARS-CoV-2 may be of added value in the diagnosis of COVID-19. Furthermore, serologic assays can be used in epidemiological studies. However, it is not yet clear what the presence of anti-SARS-CoV-2 antibodies means for protection against reinfection. The International Federation of Clinical Chemistry recently published interim guidelines for the serologic testing of antibodies against SARS-CoV-2.[18] The guidelines make recommendations about clinical indications for serologic testing and suggest a framework for assay selection and verification protocols for commercially available assays. Fully automated assays permit rapid identification of the SARS-CoV-2 immune status. In this study, the COV2T and COV2G assays were evaluated. Imprecision, as tested by the CLSI EP15-A3 protocol, was found to be adequate. These results were in line with what was found earlier by Hörber et al,[14] who described an intra-assay imprecision of 3.4% and an interassay imprecision of 4.9%.

Specificity for COV2T and COV2G assays was both 100%. No cross-reaction was found for specimens with other infectious diseases, including the specimens from common-cold coronavirus strains. This finding is in line with the manufacturer claims and previous studies that found a specificity of 99.9% and 100% for the COV2T assay.[9,14] A drawback of this study was that no SARS-CoV specimens could be analyzed, but this missing information is of less importance because that virus is known to be eradicated. An excellent specificity is of great importance for assay performance because the positive predictive value of a test decreases greatly when the prevalence of the tested disease is low. The current SARS-CoV-2 seroprevalence is still relatively low—the latest numbers vary at approximately 10% seropositivity,[19-21] so a high specificity is required when conducting large population-scale studies.[22,23]

The sensitivity of a SARS-CoV-2 antibody assay depends on both the assay setup and the moment of testing in the disease course. Whereas assays that target the nucleocapsid protein are typically more sensitive earlier in the disease phase, antibodies targeting the spike protein are more specific and may have a neutralizing effect.[18]

Table 4. Method Comparison of COV2T and COV2G Assays Against Euroimmun SARS-CoV-2 IgG ELISA, Performed on Specimens from Health Care Workers

		COV2T			COV2G		
		+	–	Total	+	–	Total
Euroimmun	+	145	2	147	61	17	78
	±	16	1	17	1	5	6
	–	24	7	31	0	10	10
Total		185	10	195	62	32	94

COV2T, SARS-CoV-2 Total antibody assay; COV2G, SARS-CoV-2 IgG antibody assay; ELISA, enzyme-linked immunosorbent assay.

Lab Medicine 2021;52;e147–e153 e151
DOI: 10.1093/labmed/lmab027

Muecksch et al[24] found a significant correlation of the Siemens COV2T assay with neutralizing antibody levels, but this correlation was highest earlier in the disease state and declined thereafter. To date, an antibody cutoff for protective immunity has not yet been defined. In addition, the durability and nature of immunity conferred by these antibodies remains unclear. Moreover, because antibody titers tend to be associated with clinical severity, assay performance may depend on disease severity.[18] In this study, sensitivities calculated for timepoints < 14 days were lower than those claimed by the manufacturer. In general, clinical sensitivity in validation studies may be lower than stated in the product leaflet, whereas clinical specificity tends to be more stable.[18] The sensitivity for the COV2T assay found in this study earlier in the disease stage was lower than that found by Hörber et al,[14] who found a sensitivity of 56.5% 6 days after PCR positivity. For the later timepoints, sensitivity was comparable to the study of Hörber et al. This result was also in line with a study from the national SARS-CoV-2 serology assay evaluation group in the United Kingdom that found a sensitivity of 98.1% in specimens collected > 20 days postsymptom onset.[9]

The median time to seroconversion in this study was 8 days after PCR positivity for both assays and 11 and 12 days after symptom onset for the COV2T and COV2G assay, respectively. This median time may have lagged behind the true time to seroconversion because patients were not tested on a daily basis. Although the median time until seroconversion did not differ significantly for both assays, the sensitivity of the COV2T assay was higher compared to the COV2G assay in the different time frames up to 14 days after PCR positivity or disease onset. This finding may be explained by the complementary detection of IgM antibodies in the COV2T assay. However, contradictory studies have been published regarding the sensitivity of different antibody isotypes: Some studies have shown that the time to seropositivity for IgM or IgA is not significantly shorter than that for IgG, whereas others have reported a faster seroconversion for IgM and/or IgA.[18]

A drawback to this study was that this specimen set only included specimens from hospitalized patients and health care workers but none from outpatients, children, or asymptomatic patients. Because the antibody titer of almost all of the patients reached the upper limit of the dynamic range at a certain timepoint, no comparison could be made with regard to disease severity.

The kinetics of the antibody response were evaluated using the same specimen set. Only in 2 out of 50 patients did antibody levels decline, but the results remained above the seropositivity cutoff index. This decline started at 51 days for 1 patient and 109 days for the other. Earlier studies have shown that antibody titers may decline and that this decline also depends on the assay used. Muecksch et al[24] found that antibody titers globally decreased over time in a serologic Abbott assay, increased in the assays from manufacturers Roche and Diasorin, and remained constant in the Siemens COV2T assay.

The method comparison against the Euroimmun anti-SARS-CoV-2 IgG ELISA, performed on samples from health care workers, showed a lower sensitivity compared to the Siemens COV2T assay, but a greater sensitivity when compared to the COV2G assay. The improved sensitivity of the Siemens total antibody assay may be attributable to the concomitant detection of IgM (and possibly also IgA) antibodies. A possible explanation for the lower sensitivity of the COV2G assay compared to the Euroimmun IgG assay is that the latter assay detects antibodies directed against the full-length S1 protein, whereas the COV2G assay only detects antibodies against the S1-RBD. However, not all of the specimens were from health care workers who were confirmed PCR-positive, so these results must be interpreted with caution. More studies are necessary to confirm this observation. Hörber et al[14] showed that the Siemens COV2T assay was slightly more sensitive than the Euroimmun IgG ELISA and the Roche Elecsys anti-SARS-CoV-2 antibody assay, which targets total antibodies against the nucleocapsid protein. Diagnostic specificity was comparable for all 3 assays. In addition, in the study from the U.K. national SARS-CoV-2 serology assay evaluation group, the Siemens COV2T assay showed superior sensitivity compared to the other tested commercially available assays of Roche, DiaSorin, and Abbott.[9] Finally, the study by Muecksch et al[24] indicated a comparable performance of the Roche, Abbott, and Siemens assays, but only specimens starting from 21 days after a PCR-positive test were included.

Conclusion

The Siemens COV2T and COV2G assays for the detection of antibodies against SARS-CoV-2 are highly specific.

Sensitivity 14 days after COVID-19 symptom onset approaches 100%. The assays are reliable and accurate for routine clinical use. **LM**

Acknowledgments

The authors thank Siemens for kindly providing the COV2T and COV2G reagents for this study.

References

1. World Health Organization. WHO Virtual press conference on COVID-19. https://www.who.int/docs/default-source/coronaviruse/transcripts/who-audio-emergencies-coronavirus-press-conference-full-and-final-11mar2020.pdf?sfvrsn=cb432bb3_2. Accessed 6 September 2020.
2. Lauer SA, Grantz KH, Bi Q, et al. The incubation period of coronavirus disease 2019 (CoVID-19) from publicly reported confirmed cases: estimation and application. *Ann Intern Med.* 2020;172(9):577–582.
3. Pang J, Wang MX, Ang IYH, et al. Potential rapid diagnostics, vaccine and therapeutics for 2019 novel coronavirus (2019-nCoV): a systematic review. *J Clin Med.* 2020;9(3):623.
4. Vashist SK. In vitro diagnostic assays for COVID-19: recent advances and emerging trends. *Diagnostics (Basel)*. 2020;10(4):202.
5. Tang YW, Schmitz JE, Persing DH, Stratton CW. Laboratory diagnosis of COVID-19: current issues and challenges. *J Clin Med.* 2020;58(6):e00512-20.
6. Xu Y, Xiao M, Liu X, et al. Significance of serology testing to assist timely diagnosis of SARS-CoV-2 infections: implication from a family cluster. *Emerg Microbes Infect*. 2020;9(1):924–927.
7. Weidner L, Gänsdorfer S, Unterweger S, et al. Quantification of SARS-CoV-2 antibodies with eight commercially available immunoassays. *J Clin Virol.* 2020;129:104540.
8. Kohmer N, Westhaus S, Rühl C, Ciesek S, Rabenau HF. Brief clinical evaluation of six high-throughput SARS-CoV-2 IgG antibody assays. *J Clin Virol.* 2020;129:104480.
9. National SARS-CoV-2 Serology Assay Evaluation Group. Performance characteristics of five immunoassays for SARS-CoV-2: a head-to-head benchmark comparison. *Lancet Infect Dis.* 2020;20(12):1390–1400.
10. Liu W, Liu L, Kou G, et al. Evaluation of nucleocapsid and spike protein-based enzyme-linked immunosorbent assays for detecting antibodies against SARS-CoV-2. *J Clin Microbiol.* 2020;58(6):e00461-20.
11. Lippi G, Salvagno GL, Pegoraro M, et al. Assessment of immune response to SARS-CoV-2 with fully automated MAGLUMI 2019-nCoV IgG and IgM chemiluminescence immunoassays. *Clin Chem Lab Med.* 2020;58(7):1156–1159.
12. Soleimani R, Khourssaji M, Gruson D, et al. Clinical usefulness of fully automated chemiluminescent immunoassay for quantitative antibody measurements in COVID-19 patients. *J Med Virol.* 2021;93(3):1465–1477.
13. Theel ES, Harring J, Hilgart H, Granger D. Performance characteristics of four high-throughput immunoassays for detection of IgG antibodies against SARS-CoV-2. *J Clin Microbiol*. 2020;58:e01243-20.
14. Hörber S, Soldo J, Relker L, et al. Evaluation of three fully-automated SARS-CoV-2 antibody assays. *Clin Chem Lab Med.* 2020;58(12):2113–2120.
15. Neil Carey R, Paul Durham A, Hauck WW, et al. *EP15-A3 user verification of precision and estimation of bias: approved guideline—third edition*. Clin Lab Stand Inst. 2014;34(12):1–81.
16. Siemens. *Atellica: COV2T: Siemens Healthcare Diagnostics*; 2020; Rev. A.
17. Siemens. *Atellica: COV2G: Siemens Healthcare Diagnostics*; 2020; Rev. A.
18. Bohn MK, Loh TP, Wang CB, et al.; and the IFCC Taskforce on COVID-19. IFCC interim guidelines on serological testing of antibodies against SARS-CoV-2. *Clin Chem Lab Med.* 2020;58(12):2001–2008.
19. Pollán M, Pérez-Gómez B, Pastor-Barriuso R, et al. Prevalence of SARS-CoV-2 in Spain (ENE-COVID): a nationwide, population-based seroepidemiological study. *Lancet*. 2020;396(10250):535–544.
20. Slot E, Hogema BM, Reusken CBEM, et al. Low SARS-CoV-2 seroprevalence in blood donors in the early COVID-19 epidemic in the Netherlands. *Nat Commun.* 2020;11(1):5744.
21. Eckerle I, Meyer B. SARS-CoV-2 seroprevalence in COVID-19 hotspots. *Lancet*. 2020;396(10250):514–515.
22. Perkmann T, Perkmann-Nagele N, Breyer MK, et al. Side-by-side comparison of three fully automated SARS-CoV-2 antibody assays with a focus on specificity. *Clin Chem.* 2020;66(11):1405–1413.
23. Espejo AP, Akgun Y, Al Mana AF, et al. Review of current advances in serologic testing for COVID-19. *Am J Clin Pathol.* 2020;154(3):293–304.
24. Muecksch F, Wise H, Batchelor B, et al. Longitudinal analysis of clinical serology assay performance and neutralising antibody levels in COVID19 convalescents. *J Infect Dis*. 2021;223(3):389–398.

DOI: 10.1093/labmed/lmab027

Science

Utility of Antigen-Based Rapid Diagnostic Test for Detection of SARS-CoV-2 Virus in Routine Hospital Settings

Preeti Thakur, MD,[1] Sonal Saxena, MD,[1,] Vikas Manchanda, MD,[1] Neha Rana, MD,[1] Ruchi Goel, MS,[2] Ritu Arora, MS[2]*

Laboratory Medicine 2021;52:e154-e158

DOI: 10.1093/labmed/lmab033

ABSTRACT

Objective: This study aims to evaluate the performance of an antigen-based rapid diagnostic test (RDT) for the detection of the SARS-CoV-2 virus.

Methods: A cross-sectional study was conducted on 677 patients. Two nasopharyngeal swabs and 1 oropharyngeal swab were collected from patients. The RDT was performed onsite by a commercially available immune-chromatographic assay on the nasopharyngeal swab. The nasopharyngeal and oropharyngeal swabs were examined for SARS-CoV-2 RNA by real-time reverse-transcription quantitative polymerase chain reaction (RT-qPCR) assay.

Results: The overall sensitivity of the SARS-CoV-2 RDT was 34.5% and the specificity was 99.8%. The positive predictive value and negative predictive value of the test were 96.6% and 91.5%, respectively. The detection rate of RDT in RT-qPCR positive results was high (45%) for cycle threshold values <25.

Conclusion: The utility of RDT is in diagnosing symptomatic patients and may not be particularly suited as a screening tool for patients with low viral load. The low sensitivity of RDT does not qualify its use as a single test in patients who test negative; RT-qPCR continues to be the gold standard test.

Keywords: RDT, rapid antigen test, RT-qPCR, COVID-19

COVID-19 has influenced every life over the past year. The pandemic has resulted in worldwide lockdowns, bringing life to a standstill. The licensing of vaccines in many countries has brought hope. But until universal immunization is achieved, testing, tracking, and treating continue to be the only tools in our armamentarium to curb the community spread of SARS-CoV-2.[1] The current diagnostic method for SARS-CoV-2 infection is focused on the identification of viral genome targets in respiratory specimens by real-time reverse-transcription quantitative polymerase chain reaction (RT-qPCR).[2] The molecular tests are the most sensitive and specific methods for the detection of SARS-CoV-2, but the downside is that they are time-consuming and need specialized laboratories with skilled manpower.[3] The delay in reporting results can lead to the inadvertent spread of disease in the community. These conditions have prompted the development of antigen-based rapid diagnostic tests (RDTs). The advantage of RDT is the availability of test results within 30 minutes without running any specialized instrument, making it an acceptable point-of-care test that relieves the workload in diagnostic hospitals and laboratories.[4] However, the performance of these assays on the ground remains uncertain. The sensitivity of the RDT has been claimed to be between 30.2% and 81.8% across the world.[1,5,6] The World Health Organization strongly encourages research into the efficiency and potential diagnostic usefulness of RDT.[7]

The RDT is being used extensively to detect and trace patients with COVID-19. This study was undertaken to

Abbreviations:

RDT, rapid diagnostic test; RT-qPCR, reverse-transcription quantitative polymerase chain reaction; Ct, cycle threshold; NPS, nasopharyngeal swab; OPS, oropharyngeal swab; ICMR, Indian Council of Medical Research; PPV, positive predictive value; NPV, negative predictive value; ROC, receiver operating characteristic; CI, confidence interval.

[1]Department of Microbiology, Maulana Azad Medical College, New Delhi, India, [2]Department of Ophthalmology, Guru Nanak Eye Center, New Delhi, India

*To whom correspondence should be addressed.
sonalsaxena3@gmail.com

evaluate the performance of antigen-based RDT for the detection of SARS-CoV-2 virus in screening asymptomatic patients and to establish the association between the results of a positive RDT and cycle threshold (Ct) values of RT-qPCR. In addition, this study aimed to understand the Ct value at which the RDT would be able to detect true positives.

Methods

A cross-sectional study was conducted at the largest COVID-19-dedicated hospital (Delhi, India) after clearance from the institutional ethics committee. Adult preoperative or asymptomatic patients seeking health care in the ophthalmology department for eye ailments and who wished to get themselves tested for COVID-19 were included in the study.[8] Written informed consent was obtained from participants before enrollment. Two nasopharyngeal swabs (NPS) were collected from patients for testing (for RDT and RT-qPCR). An additional oropharyngeal swab (OPS) was collected from all patients for RT-qPCR. The NPS and OPS were placed together in a 3 mL tube of viral transport medium and were transported to a COVID-19 diagnostic laboratory in the department of microbiology at the same hospital within 4 hours of collection, maintaining the cold chain. The RDT was performed onsite by a trained technician as per the manufacturer's instructions.

The SARS-CoV-2 antigen was detected by commercially available immune-chromatographic lateral flow assay (PathoCatch/ACCUCARE, Lab Care Diagnostics Private Ltd., Sari Gam, India) approved by the Indian Council of Medical Research (ICMR). Briefly, the nasopharyngeal swab was inserted into a prefilled extraction buffer tube that was provided with the kit for antigen extraction. The swab was squeezed and then removed after 10 to 15 seconds. With the help of a nozzle cap, 2 to 3 drops of the extracted specimen were put on the sample port of the test device. The result was read after 20 to 30 minutes. The appearance of the control line and the detection line was interpreted as a positive result.

For RT-qPCR, the RNA was extracted with the MagNA Pure 96 System (Roche Molecular Systems Inc., Pleasanton, CA). The extracted RNA was examined for SARS-CoV-2 RNA by a COVID-19 real-time PCR assay using an ICMR-approved commercial assay (SD Biosensor Inc., Republic of Korea). This assay utilizes primers and probes for the detection of the *E* gene and the *RdRp* (*ORF1ab*) gene of the SARS-CoV-2 virus. Results were read and interpreted, and Ct values for both genes were recorded. A Ct value up to 32 was known to indicate a positive result for the *E*/*RdRp* gene as per validation performed in earlier research.[9]

The data collected were entered into a Microsoft Excel spreadsheet. The sensitivity, specificity, positive predictive value (PPV), and negative predictive value (NPV) were expressed as percentages. Cohen's kappa statistics were used for determining the agreement between the RDT and RT-qPCR while the association of antigen positivity and Ct values was assessed. A receiver operating characteristic (ROC) curve was built to estimate the Ct cutoff value for RDT-positive specimens. A P value <.05 was considered statistically significant. Confidentiality and privacy were ensured at all stages of the study. Results of RDT and RT-qPCR were provided to patients through the ICMR portal.

Results

Between October 27 and November 23, 2020, 677 patients were enrolled in the study. Among these patients, 372 (54.9%) were men and 305 (45.1%) were women. The mean age of study participants was 44.78 ± 16.35 years (range,18–89 years). Thirty patients tested positive by antigen-based RDT. Viral RNA was detected by RT-qPCR in NPS and OPS collected from 84 patients. Concordant results (RT-qPCR+/RDT+) were observed in 29 specimens, whereas discordant results (RT-qPCR+/RDT–) were observed in 55 specimens (**Table 1**).

Table 1. Comparison of Results of SARS-CoV-2 Antigen-Based RDT with RT-qPCR (n = 677)

RDT result	RT-qPCR Result		Total
	Negative	Positive	
Negative	592 (99.8%)	55 (65.5%)	647
Positive	1 (0.2%)	29 (34.5%)	30
Total	593	84	677

RDT, rapid diagnostic test; RT-qPCR, reverse-transcription quantitative polymerase chain reaction.

Lab Medicine 2021;52;e154–e158 e155
DOI: 10.1093/labmed/lmab033

The overall sensitivity of the SARS-CoV-2 antigen based RDT was 34.5% (95% confidence interval [CI], 24.5%–45.6%) and the specificity was 99.8% (95% CI, 99.1%–100.0%). The PPV and NPV of the test were 96.6% (95% CI, 80.0%–99.5%) and 91.5% (95% CI, 90.2%–92.6%), respectively. The diagnostic accuracy of the test was found to be 91.7% with moderate agreement between the 2 methods (Cohen's kappa index = 0.47).

Association of SARS-CoV-2 Antigen-Based RDT Results with Ct Values

For the 55 specimens that tested positive by RT-qPCR, the Ct values ranged between 10 and 32 (**Figure 1**). A significant negative association was observed between the RDT results and the Ct values: Lower Ct values were associated with RDT positivity, and vice versa (P <.001; **Table 2**). The detection rate of the RDT in RT-PCR positive specimens was high (45%) for Ct values <25 (**Table 3**).

Table 2. Association of Ct Values with RDT Results in Patients with Positive RT-PCR Results

	RDT-Negative (n = 55)	RDT-Positive (n = 29)	*P* Value
Ct value (*E* gene)	22.62 (21.20–24.04)	16.24 (14.40–18.08)	<.001*
Range	10–32	10–27	
Ct value (*RdRp* gene)	22.24 (20.76–23.71)	16.10 (14.36–17.84)	<.001*
Range	10–32	10–26	

*Ct, cycle threshold; RDT, rapid diagnostic test; RT-PCR, reverse-transcription polymerase chain reaction. *Significant at P <.05.*

Table 3. Detection Rate of RDT According to Ct Values in Patients with Positive RT-PCR Results

	Ct Value	RDT-Positive (n)	RDT Detection Rate (%)
1	<25 (n = 60)	27	45
2	25–29 (n = 21)	2	9.5
3	>30 (n = 3)	0	0

Ct, cycle threshold; RDT, rapid diagnostic test; RT-PCR, reverse-transcription polymerase chain reaction.

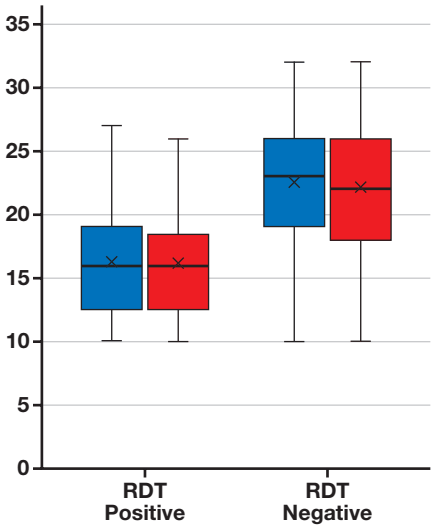

Figure 1

Association of Ct values with RTD results in positive RT-PCR results. Ct, cycle threshold; RTD, rapid diagnostic test; RT-PCR, reverse-transcription polymerase chain reaction.

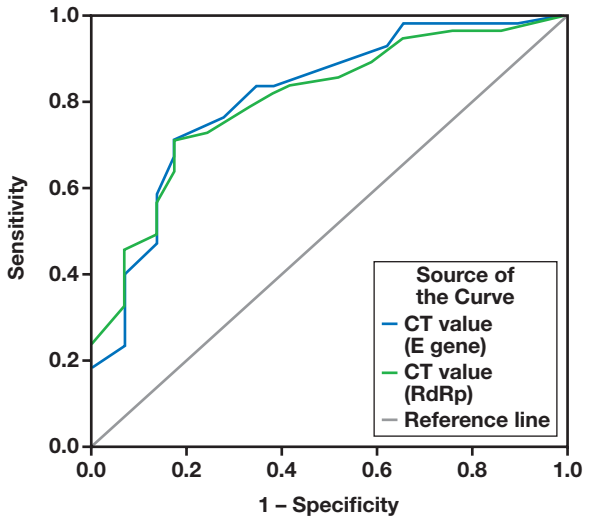

Figure 2

ROC curve using Ct values to estimate Ct cutoff value for RDT to detect SARS-CoV-2 antigen. Ct, cycle threshold; RDT, rapid diagnostic test; ROC, receiver operating characteristic.

Estimation of Ct Cutoff Value for RDT to Detect SARS-CoV-2 Antigen

An ROC curve analysis indicated that a Ct value (*E* gene and *RdRp* gene) <19.5 best discriminated between RT-qPCR+/RDT+ and RT-qPCR+/RDT– specimens, with a sensitivity and specificity of 70.9% and 82.8%. The area under the curve for the *E* gene and the *RdRp* gene were 0.81 (95% CI, 0.71–0.91) and 0.80 (95% CI, 0.71–0.89), respectively (**Figure 2**).

Discussion

The diagnostic performance of SARS-CoV-2 antigen-based RDT with RT-qPCR as the gold standard was evaluated in our health care setting. The sensitivity of RDT (34.5%) observed in our study was lower than that claimed by the manufacturer (84%). A low sensitivity of an antigen-based assay with false-negative results has been reported previously.[4,5,10] The Scohy et al[5] evaluation of RDT showed an overall sensitivity of 30.2% for SARS-CoV-2 RT-qPCR–positive specimens. Mak et al[4] evaluated RDT using different respiratory specimens such as nasopharyngeal aspirate, throat swab, saliva, and sputum. A very low positivity of RDT was observed in the sputum (11.1 %) of patients who were RT-qPCR–positive, whereas 45.7% of nasopharyngeal aspirate and throat swabs were positive.[4]

The Ct value indirectly indicates the initial virus concentration in the specimen, so it can be used as a substitute for the viral load. In this study, the lower Ct values were associated with a higher antigen detection rate. The Ct cutoff value for RDT positivity was 19.5, implying that RDT positivity occurred more in specimens with a high viral load. Therefore, there are more likely chances of missing positive specimens with a low viral load if only RDT is used for a diagnosis of COVID-19. Similar observations regarding the association of Ct value with RDT results were seen in previous studies.[1,4,11-13] It is understood that antigens are expressed only when the virus is actively replicating.[7] This may not be the scenario with patients in the presymptomatic phase or in those seeking routine health care, so the utility of rapid antigen tests is very limited in such patients. A similar situation is also a possibility in patients who are convalescing or asymptomatic. Further, the high sensitivity (70%) and specificity (95%) of RT-qPCR[14] enable the test to detect very low levels of the virus, which could be a reason for the detection of a greater number of infections by RT-PCR.

Diagnostics for COVID-19 can be used for the triage of symptomatic individuals in an epidemic or endemic setting, screening of at-risk asymptomatic and symptomatic individuals in an epidemic or endemic setting, confirmatory testing, and testing of patients with previous exposure to SARS-CoV-2.[15] Even with its less-than-optimal performance and limitations, the rapid test can still act as an adjunct to RT-qPCR testing.[16] It can also be useful in diagnosing symptomatic patients with a high viral load in resource-limited settings. Faster detection enables public health authorities in rapid contact tracing and isolation along with providing specific care.

In a hospital setting, there is a potential risk of disease exposure to health care workers, other uninfected patients, and attendants from an infected patient. The RDT is used as a point-of-care test providing rapid results. Aside from turnaround time, however, the diagnostic accuracy of the test is also paramount. A test with high sensitivity and specificity should be used in such scenarios. The high specificity of RDT offers a quick screening for COVID-19 positivity, especially in patients with a high viral load. The overall sensitivity of RDT in our study was low, so it can give false-negative results and may not be of much help in screening patients if used alone. The challenge is to explore other options and weigh their pros and cons. Cartridge-based nucleic acid amplification tests have a quick turnaround time (30–60 minutes), but these tests require expertise, reagents, and instruments. These tests are also limited by the maximum number of specimens that can be tested per day: 24 to 48 specimens only.

The performance of any test depends upon various epidemiological and technical factors such as clinical manifestations, duration of disease onset to testing, type of specimen, specimen quality, specimen handling and processing techniques, commercial kit, and the batch of the kit used.[7] Other factors that can affect the quality of testing are high patient load, fewer staff members, and limited resources. The training of technical staff involved in specimen collection and processing is also very essential and plays a key role in improving the quality of testing.

Conclusion

The high specificity of RDT warrants it as a diagnostic tool in patients with a positive result for SARS-CoV-2

DOI: 10.1093/labmed/lmab033

infection. However, its low sensitivity does not qualify its use as a standalone test, especially in asymptomatic or presymptomatic patients, for whom RT-qPCR continues to be the gold-standard test. The utility of RDT is in diagnosing symptomatic patients and may not be particularly suited as a screening tool for patients with a low viral load. **LM**

References

1. Albert E, Torres I, Bueno F, et al. Field evaluation of a rapid antigen test (Panbio™ COVID-19 Ag Rapid Test Device) for COVID-19 diagnosis in primary healthcare centres. *Clin Microbiol Infect.* 2021;27(3):472.e7–472.e10.
2. Goudouris ES. Laboratory diagnosis of COVID-19. *J Pediatr (Rio J).* 2021;97(1):7–12.
3. Tromberg BJ, Schwetz TA, Pérez-Stable EJ, et al. Rapid scaling up of Covid-19 diagnostic testing in the United States—the NIH RADx initiative. *N Engl J Med.* 2020;383(11):1071–1077.
4. Mak GC, Cheng PK, Lau SS, et al. Evaluation of rapid antigen test for detection of SARS-CoV-2 virus. *J Clin Virol.* 2020;129:104500.
5. Scohy A, Anantharajah A, Bodéus M, Kabamba-Mukadi B, Verroken A, Rodriguez-Villalobos H. Low performance of rapid antigen detection test as frontline testing for COVID-19 diagnosis. *J Clin Virol.* 2020;129:104455.
6. Gupta A, Khurana S, Das R, et al. Rapid chromatographic immunoassay-based evaluation of COVID-19: a cross-sectional, diagnostic test accuracy study and its implications for COVID-19 management in India. *Ind J Med Res.* Published online October 31, 2020. doi: 10.4103/ijmr.IJMR_3305_20.
7. World Health Organization. Advice on the use of point-of-care immunodiagnostic tests for COVID-19. Published April 8, 2020. https://www.who.int/news-room/commentaries/detail/advice-on-the-use-of-point-of-care-immunodiagnostic-tests-for-covid-19. Accessed March 31, 2021.
8. Indian Council of Medical Research. COVID-19: information of testing strategies. https://www.icmr.gov.in/cteststrat.html. Accessed March 31, 2021.
9. Siddiqui O, Manchanda V, Yadav A, et al. Comparison of two real-time polymerase chain reaction assays for the detection of severe acute respiratory syndrome-CoV-2 from combined nasopharyngeal-throat swabs. *Indian J Med Microbiol.* 2020;38(3–4):385–389.
10. Blairon L, Wilmet A, Beukinga I, Tré-Hardy M. Implementation of rapid SARS-CoV-2 antigenic testing in a laboratory without access to molecular methods: experiences of a general hospital. *J Clin Virol.* 2020;129:104472.
11. Cerutti F, Burdino E, Milia MG, et al. Urgent need of rapid tests for SARS CoV-2 antigen detection: evaluation of the SD-Biosensor antigen test for SARS-CoV-2. *J Clin Virol.* 2020;132:104654.
12. Lambert-Niclot S, Cuffel A, Le Pape S, et al. Evaluation of a rapid diagnostic assay for detection of SARS-CoV-2 antigen in nasopharyngeal swabs. *J Clin Microbiol.* 2020;58(8):e00977-20.
13. Nagura-Ikeda M, Imai K, Tabata S, et al. Clinical evaluation of self-collected saliva by quantitative reverse transcription-PCR (RT-qPCR), direct RT-qPCR, reverse transcription-loop-mediated isothermal amplification, and a rapid antigen test to diagnose COVID-19. *J Clin Microbiol.* 2020;58(9):e01438-20.
14. Watson J, Whiting PF, Brush JE. Interpreting a Covid-19 test result. *BMJ.* 2020;369:m1808.
15. Vandenberg O, Martiny D, Rochas O, van Belkum A, Kozlakidis Z. Considerations for diagnostic COVID-19 tests. *Nat Rev Microbiol.* 2021;19(3):171–183.
16. Chaimayo C, Kaewnaphan B, Tanlieng N, et al. Rapid SARS-CoV-2 antigen detection assay in comparison with real-time RT-PCR assay for laboratory diagnosis of COVID-19 in Thailand. *Virol J.* 2020;17(1):177.